Final Report

Advancing sustainable and technology driven apple orchard production systems

Project leader:

Dr Ian Goodwin

Delivery partner:

The Department of Energy, Environment and Climate Action

Project code:

AP19003

Project:

Advancing sustainable and technology driven apple orchard production systems (AP19003)

Disclaimer:

Funding statement:

This project has been funded by Hort Innovation, using the apple and pear research and development levy and contributions from the Australian Government. Hort Innovation is the grower-owned, not-for-profit research and development corporation for Australian horticulture.

Publishing details:

Published and distributed by: Hort Innovation

Level 7
141 Walker Street
North Sydney NSW 2060

Telephone: (02) 8295 2300

www.horticulture.com.au

Contents

Public summary

High costs of production threaten the future profitability of Australian apple orchards and the constraints on production are exacerbated by some adverse effects of climate change such as extreme heat events and erratic rainfalls and hailstorms. This project aimed to improve orchard design and crop load management in a variable climate by providing knowledge and tools to consistently deliver premium fruit that meets consumer expectations.

Physiological studies on chemical signalling, floral initiation, fruit quality and yield under different light environments, crop loads and rootstocks, and the calibration and validation of sensing technologies for estimates of productive performance and fruit quality were undertaken in the Sundial apple orchard at the Tatura SmartFarm and in commercial apple orchards. The technology was evaluated for its performance and suitability for the industry.

'ANABP 01' apples grown on M.26 and M.9 rootstocks achieved higher values of total tree light interception compared to Bud.9, and in turn intercepted light was positively correlated with yield. Fruit quality was best in Bud.9 but canopy vigour of trees grown on this rootstock may not be suitable to support higher crop loads and its sparseness may increase the risk of sunburn damage. Increasing light exposure led to improved fruit quality without significant sunburn, although the summer seasons in which the study was conducted were mild. Using UV-filter on fruit produced undesirable yellow-orange peel colouration indicating that UV light, in addition to visible light, is a key to the appealing dark-red colour development in this cultivar. Fruit from east – west rows of trees had the lowest overcolour and sweetness and were delayed in maturity.

in ‘Rosy Glow’, a crop load of 8 fruit per cm^2 of trunk cross-sectional area achieved the most consistent return bloom and fruit quality over five seasons. In ‘Ruby Matilda’, 6.5 – 7 fruit per cm^2 of trunk cross-sectional achieved return bloom and crop load consistency, while maintaining high yields and adequate fruit quality. In multileader trees, individual leaders should be used as management units—as opposed to whole trees—to reduce within-tree and -orchard spatial variability.

The spur bud metabolites hydroxycinnamates, coumarins, salicylates and flavanols were negatively affected by crop load in ‘Rosy Glow’. Cytokinin precursors and derivatives such as adenosine and inosine were positively correlated with crop load in ‘Ruby Matilda’ spur buds. Gibberellic acid differences were identified in fruitlet seeds from trees with different crop loads, linked to a negative regulation of flavanols via gibberellic acid.

Calibration and validation of a commercial platform for flower number, fruit number, fruit size and fruit colour prediction revealed prediction errors below 10 % (5 % on average) in commercial apple orchards. The platform could be efficiently used to extract data on canopy and crop parameter and to extrapolate orchard-specific relationships that can be used to limit spatial variability while maintaining high yields and fruit quality. Data zoning and integration with follow-up management technology is advised. The technology provided data quicker, more objectively and more reliably than if gathered by people on the ground. The use of technology such as the one used in this study is recommended for industry adoption in commercial orchards and for research application.

Keywords

apple; crop load; chemical signalling; flower detection; fruit colour; fruit detection; fruit size; mobile sensing; orchard technology; organic metabolites.

Introduction

Apple in the Australian environment

The profitability of Australian apple orchards is affected by high costs of production (e.g., labour) and by variable fruit quality. In the Australian apple growing regions, the constraints on production are exacerbated by some adverse effects of climate change such as extreme heat events and erratic rainfalls and hailstorms. Managing various inputs to optimise the production system (e.g., cultivar genetics, canopy training, water, rootstock, nutrients, light interception, soil) can improve the ability to meet market expectation for fruit quality and lead to higher prices and improved profitability. Modern horticulture is moving toward increased mechanisation, automation, robotics, and non-destructive sensing and monitoring.

Australia’s climate is characterised by relatively high temperatures and light. While high light intensity allows for high photosynthetic rates and consequently carbohydrate availability, when excessive and combined with high air temperature can cause sunburn, damage the leaf photosynthetic systems or induce stomata closure for long periods during the day thereby reducing carbohydrates. Light interception plays an important role in defining the optimal number

of fruit and the position of fruit within the canopy to meet market specification for fruit quality. Some aspects of internal and external apple fruit quality (e.g., red colour development, fruit size and sugar accumulation) rely on light to produce higher quality fruit.

Effects of crop load on fruit quality

High variability in fruit numbers translates into inconsistent fruit quality and reduced consumer satisfaction (Stefanelli et al., 2018). From previous studies on crop load (CL) management of an established cultivar ('Rosy Glow') and an emerging cultivar ('Nicoter') in projects AP15013 and AP15002, it was noticed that there is an inverse correlation between fruit number on trees and most aspects of fruit quality (size, soluble solids concentration, red colour), and a direct correlation with fruit maturity (Stefanelli et al., 2019). This study also observed that fruit from trees that had been forced into biennial bearing (artificially alternating high and low fruit numbers) had reduced quality traits in the subsequent season following a high fruit number.

High CL—expressed as number of fruit per cm^2 of trunk cross-sectional area (TCSA)—negatively affect return bloom, as shown in 'Rosy Glow' and 'Nicoter' (Stefanelli et al., 2018). Moreover, previous studies have unveiled some unfavourable effects of high CL on fruit quality characteristics in several apple cultivars.

Effects of crop load on chemical signalling

Biennial bearing is controlled at tree level from a combination of flowering genes and environment (carbohydrate availability) probably mediated by metabolites that act as chemical signals that either stimulate or inhibit gene activation, as suggested in recent studies (Guitton et al., 2012; Milyaev et al., 2022, 2018; Reddy et al., 2022). Previous projects AP15013 and AP15002 partially confirmed this by identifying clusters of candidate genes as well as several possible signalling metabolites. In AP15013 and AP15002, it was visually observed that tree sub-sections displayed biennial behaviour independent to the rest of the tree. The fact that flower induction in these zones was different from the rest of the tree suggested that there may be localised signalling pathways. Furthermore, the fruit in these zones showed the quality pattern of the rest of the tree.

Regulation of flowering was initially thought to be driven by nutritional competition between flower bud initiation and concurrent fruit formation. More recently, Milyaev et al. (2021) indicated that a combination of increased carbohydrates and activation of flower induction genes, likely mediated by phytohormones, either stimulated or inhibited flower induction. They found that thiamine, chlorogenic acid and an adenine derivative are involved in the metabolic pathway promoting early flower bud development in apples, and that increased levels of flavonoids such as kaempferol derivatives were also identified in low CL trees. Identifying localised signalling metabolites would be beneficial for the Australian apple industry.

Modern apple orchard systems and localised leader-dependent responses

Fruit of 'Cripps Pink' sports (marketed as Pink Lady®) are the dominant apples in the Australian market with a market share > 40 % recorded in 2020 and 2021. Modern apple orchard systems with increased tree density (4,000 – 6,000 trees per ha) such as the super spindle, improve light distribution and help maximise yields, although their return on investment is questionable due to high establishment costs. Training trees to multiple leaders (uprights) can reduce costs and achieve the same density of leaders per hectare as single-axis trees. In a recent study, it was observed that bi-axis apple trees are more efficient than single-axis trees (trained to spindle) in intercepting light, photosynthesising and for their light distribution. Although whole-tree effects of CL on trunk growth, return bloom, fruit quality and yield are well established in many apple cultivars, little is known about leader-dependency, and leader comparison to tree total relationships between CL, trunk growth, return bloom, yield and fruit quality.

Technology for accurate detection of crop parameters

The integration of technologies that are already adopted in other industries into horticulture systems aims to increase resource use efficiency—including labour—and make orchards more profitable. Several recent studies have focused on the application of machine learning algorithms to detect tree features (e.g., flowers, fruit, architecture) using proximal and remote sensing. Most of the state-of-the-art research has attempted to detect flower and fruit for yield determination, or for integration with automated harvesting machines applying image segmentation, deep learning and different Convolutional Neural Networks on RGB/RGB-D images. LiDAR sensors can be used to extract canopy architecture features such as height, width, area and density and have also been used to model canopy light interception.

Only limited studies have been carried out to estimate fruit size in orchards using machine vision systems, and even fewer

literature is available on fruit colour estimation. The CIELab / LCh colour space primarily expresses colour using five colour parameters—L*, a*, b*, C* and h°—and it has become a dominant colour scale in the fruit industries. In situ fruit colour captured by imaging sensors mounted on ground-based mobile platforms can be used to estimate fruit maturity or to map harvest readiness based on peel colour. The use of artificial intelligence to estimate fruit number and fruit size can improve the accuracy of yield estimates, where according to Anderson et al. (2021), a generally accepted error of yield estimations is 5 – 10 %.

Commercial services such as *Cartographer* (Green Atlas) use a combination of sensors (e.g., RGB cameras, LiDAR, GPS) to gather data while driving through orchard rows. *Cartographer* is currently available to estimate flower and fruit number, fruit size and colour in apples, and to measure canopy geometry parameters such as height, area and density, and canopy cross-sectional leaf area (CSLA) can be calculated as the product of canopy area and canopy density and acts as a proxy of leaf area in the scanned transect.

Aims of the project

The project aimed to investigate physiological mechanisms and develop management tools so that apple orchards can consistently produce high yields and fruit that meets market specification through uncertain climate. The project focused on:

- Investigating the dynamics of fruit position and light exposure on colour development, sunburn damage, fruit quality and floral initiation using the Sundial experimental orchard and technology such as LiDAR combined with solar position and light extinction models.
- Exploring the physiological mechanism (e.g., chemical signals) for observed impacts of high CL on floral initiation and flower development, and the subsequent season(s) fruit size, assimilation and translocation of carbohydrate to fruit.
- Developing a rapid orchard assessment tool using sensing technologies (e.g., proximal sensing of light interception, fruit number and fruit size) to determine CL for optimum fruit size in apple orchards.

Methodology

The experiment methods are described in the paragraphs below. Extension activities such as orchard walks, roadshows, presentations, videos and news interviews, user guidelines, factsheets and industry articles were coordinated with the help of the PIPS3 program coordinator and APAL facilitators (see output table for a full list).

Colour development, sunburn damage, fruit quality and floral initiation responses to fruit position and light exposure

This experimental activity was carried out in the Sundial orchard at the Tatura Smart Farm—a high-density orchard planted with the apple cultivar 'ANABP 01', commercialised as Bravo™. Trees are planted in a semicircle of the orchard following four different row orientations (i.e., N – S, NE – SW, E – W and SE – NW). Trees were grafted onto three rootstocks in a completely randomised design and planted on site in 2018. The tree rootstocks are Bud.9, M.9 and M.26. For a full description of the site, see paragraph 2.1.1. of Appendix A.

Effects of row orientation and rootstock

The effects of row orientation and rootstock and their interaction on (i) flower cluster number, (ii) and light interception, (iii) fruit quality, (iv) fruit maturity and (v) CL, yield and yield efficiency (YE), were evaluated in the Sundial orchard. Flower cluster numbers were estimated using the Green Atlas *Cartographer* and the algorithms obtained for apple flower cluster recognition. Canopy light interception was calculated in terms of effective area of shade (EAS) based on methods by Goodwin et al. (2006). EAS is a measure of total tree light interception and does not gauge light distribution in the tree and fruit exposure to sunlight. Tree geometry data—i.e., canopy height, canopy area, canopy density and CSLA—extracted from *Cartographer* were used to predict intercepted light. Detailed methodology on flower cluster number scanning, tree geometry and light interception estimates is presented in paragraph 2.1.2 of Appendix A and in the materials and method of published research (Scalisi et al., 2021). CL was expressed as the number of fruit per cm^2 trunk cross-sectional area (TCSA). YE was calculated as the number of kilograms yielded per cm^2 of TCSA.

Fruit in each plot were harvested and scanned with a commercial fruit grader equipped with optical sensors (Compac InVision 9000, Compac Sorting Equipment Ltd, Australia) to estimate skin colour (i.e., % of background and overcolour), soluble solids concentration (SSC), flesh firmness (FF), index of absorbance difference (I_{AD}), fruit diameter (FD) and fruit mass (FM). A batch of 10 fruit per plot was sampled for further non-destructive and destructive determinations. Fruit were classified into the following groups based on their external characteristics—overcolour on a scale from 1 to 5 based

on Figure 3a of Appendix A; background colour on a scale from 1 to 5 based on Figure 3b of Appendix A; and sunburn classes on a scale from 0 to 5 based on Figure 2 of Appendix B. SSC was determined with a digital refractometer (PR-1; ATAGO CO., LTD, Saitama, Japan), FF obtained with a penetrometer equipped with an 8 mm tip (FT327, FACCHINI srl, Alfonsine, Italy), I_{AD} measured with a DA-Meter (Model 53500, T.R. Turoni, Forli, Italy). Last, fruit were cut through the equator and sprayed with an iodine solution to determine the starch index (SI) based on the classification reported in Figure 4 of Appendix A.

Effects of fruit position, light exposure, photosynthesis and surface temperature on fruit quality

In 2020 – 21, one tree was selected from the middle of each of 36 experimental plots, spread evenly across the row orientations and rootstocks. Three fruit per tree were selected from three different canopy heights for a total of 108 fruit. Fruit position was determined using a static LiDAR 3D laser scanner (Leica BLK360, Leica Geosystems, Heerbrugg, Switzerland). X-, Y- and Z-coordinates were assigned to each fruit, with X representing horizontal shift across the row (X = 0 at the trunk), Y representing horizontal shift along the row (Y = 0 at the trunk) and Z representing vertical shift (Z = 0 at ground level). Fruit light exposure and proximal spur leaf conductance (g_l, mmol m^{-2} s^{-1}) were measured to determine whether reduced leaf stomatal aperture was triggered by position in the canopy and light environment. At harvest, the tagged fruit were assessed for red colour coverage percentage, L*, a*, b* C*, h°, sunburn damage, FD, SSC, FF and SI, and then put through the Compac InVision 9000 grader to measure the percentage coverage of dark red and light red colour. A peel colour development index (CDI_{dark}) was calculated from L*, a* and b* as shown in Equation 1 of Appendix C. This calculation was different from the standard CDI calculation derived from h° explained in a recent study (Scalisi et al., 2022), as 'ANABP 01' fruit become dark when they approach maturity. Due to the dark burgundy to black peel colour of mature 'ANABP 01' fruit, the resulting a* and h° values are not necessarily representative of better colour in this cultivar. The CDI calculated from Scalisi et al. (2022) performs well for fruit that go from green to yellow, orange, red, purple or blue, but its performance is deteriorated when fruit peel tends to black. This explains why we used L* (a measure of lightness of colour) to derive CDI_{dark}—ranging from zero (less developed colour) to one (more developed, desirable colour)—for 'ANABP 01'. For a detailed description of the methods see Appendix C.

Effects of shade and UV filtration on and fruit surface temperature and quality

The experiment was conducted in 2021 – 22 as a randomized complete block design. 25 sample fruit were chosen in each of three rows (n = 75). In total, five light exposure treatments were applied to five sample fruit in each block over two consecutive time periods. The treatments involved covering sample fruit with either aluminium umbrellas (SS1, SS2 and SS3, classified according to the time period) or a longpass ultraviolet filter (UVF), in addition to a fully exposed control. Timing and treatments are summarised in Table 1 of Appendix C. A sample of six fruit per treatment spread evenly across the three rows (n = 30) were monitored for fruit surface temperature (FST) from 1 February 2022 (110 days after full bloom, DAFB) until harvest. Fine-wire thermocouples (32 g copper-constantan; Type T, Tranzflo NZ Ltd., Palmerston North, New Zealand) were inserted on the face of the fruit expected to receive the most sun exposure. Sample fruit were monitored for peel colour parameters immediately prior to treatment application, when treatments were changed over on 17 February, and lastly at harvest. For detailed experiment methodology see Appendices B and C.

Impacts of crop load on return bloom, tree growth, yield, fruit quality and chemical signalling

This final report summarises findings on CL relationships obtained in experimental activities carried out at (i) a commercial 'Rosy Glow' orchard in the Yarra Valley (Sanders Apples, Three Bridges, Victoria) as part of project AP15013 (PIPS 2), and at (ii) a commercial 'Ruby Matilda' orchard in the Goulburn Valley (Plunkett Orchards, Ardmona, Victoria) as part of the current project AP19003 (PIPS 3). Methodologies are presented separately.

Long-term crop load effects in 'Rosy Glow'

The experiment was conducted in a commercial farm in Three Bridges, Yarra Valley, Victoria, Australia, over five years (from 2015 – 16 to 2019 – 20). Three-year old trees of the cultivar 'Rosy Glow' (marketed as Pink Lady®), trained on Open Tatura trellis, were used. Five CL treatments were first applied during the 2015 – 16 growing season with six single tree replicates (a total of 30 trees). CL treatments consisted of 1 %, 50 %, 100 %, 150 %, and 200 % of normal grower practice, based on TCSA. In 2016 – 17 and subsequent seasons, three replicates of each CL treatment maintained the same CL, and the other three replicates alternated between reciprocal low and high treatments. Treatments are summarised in Table 1 of Appendix D. Thinning strategies are outlined in Appendices D and E. From approximately 3 – 4 weeks before harvest, fruit physiological age was measured weekly as I_{AD}. At harvest, all fruit on the trees were counted and weighed to obtain total yield and average FM. A sample of 20 fruit per tree was randomly selected for laboratory analysis, which consisted

of FM, C* and h°, FF and SSC. Extensive methodology for CL effects on 'Rosy Glow' return bloom, yield and fruit quality is detailed in Appendices D and E.

To determine CL effects on chemical signalling, spur buds were collected after thinning in late spring and early summer of the 2018 – 19 growing season. Weekly collection of one bud per tree began 4 weeks after full bloom and continued for 8 weeks. Sample preparation and extraction for liquid chromatography-mass spectrometry (LCMS) analysis is detailed in the methods of Appendix F and in recently published research (Reddy et al., 2022).

Long-term crop load effects in 'Ruby Matilda'

The experiment was conducted in a commercial 'Ruby Matilda' apple—a 'Cripps Pink' sport marketed as Pink Lady®, previously known as 'Ruby Pink'—orchard (Plunkett Orchards, Ardmona, Victoria, Australia, 36° 22' 54.2" S and 145° 19' 36.0" E. 113 m a.s.l.) over three seasons—2020 – 21 (year 1), 2021 – 22 (year 2) and 2022 – 23 (year 3). Thirty trees were utilised for the experiment and were replicated in three blocks using a randomised block design, each consisting of 10 trees. The bi-axis trees were split into 'primary' (L1) and 'secondary' (L2) leaders. L1 leaders were selected based on the lowest difference from the TCSA mean in the whole experiment. The remaining leaders were classified as L2. The standard commercial thinning practice for the block at the start of the experiment was to achieve 120 fruit per leader—i.e., CL of ~ 4.4 fruit per cm^2 of TCSA—and it was used as a reference CL level for L1 (CL_{L1}). Four additional CL levels were imposed to L1. Concurrently, two extreme CL levels were applied to L2 (CL_{L2})—very low and very high. Experimental treatments are extensively described in the methodology of Appendix G.

The yearly relative growth rate (RGR, fractional) of TCSA was used as indicator of growth in the two leaders. Flower clusters on each leader were manually counted at full bloom and percent return bloom was obtained by relating flower cluster counts between seasons. Percent return CL was obtained by relating fruit counts at harvest in the current season and the pre-thinning fruitlet number in the following season. Fruit were harvested at commercial maturity, as determined by the orchard manager, counted and weighted to obtain fruit number, FM and yield. The CieLAB/Ch peel colour attributes L*, a*, b*, C*, and h°, I_{AD}, SSC, dry matter concentration (DMC, %) and FF were measured at harvest. CDI was calculated from h° using the original calculation (Scalisi et al., 2022) that is suited to 'Cripps Pink' sports. A detailed description of the methodology to estimate CL effects on yield, return bloom and tree growth in 'Ruby Matilda' is described in Appendix G.

For the analysis of bud chemicals in relation to CL, spur buds were collected from apple trees after thinning, at 70 DAFB, in late spring and early summer. Buds were then prepared for LCMS molecular analysis, as described in Appendices H, I, and J.

Validation of a mobile sensorised platform to measure fruit number, size and colour, and light interception

Calibrations and validations of the commercial platform *Cartographer* (Green Atlas) were carried out over the three seasons between 2020 – 21 and 2022 – 23. The platform was calibrated and validated in the Sundial orchard 'ANABP 01' apple trees and in two commercial orchards—the 'Ruby Matilda' orchard at Plunkett Orchards (Ardmona, Victoria) and the 'Perfect Pink' orchard at a Geoffrey Thompson Orchard (Coomboona, Victoria). The methodologies below are separated based on the orchards where they were carried out.

Sundial orchard

A smartphone interface was used to control logging on *Cartographer* and enter experimental metadata to aid retrospective identification of scan locations and note relevant scan or plot issues. *Cartographer* was driven at a constant speed of approximately 7 – 8 km h^{-1} for calibration scans, and at 20 km h^{-1} when mapping orchard blocks. Images were logged at a rate of 5 images per second. Images were collected in the entire orchard block to obtain uncalibrated predictions of flower and fruit counts and to assess tree geometry (i.e., canopy height, canopy area, canopy density and CSLA). Flower clusters and fruit count detections obtained from continuous mobile scans of all the measurement rows in the Sundial orchard were reprocessed using a calibration factor. Tree geometry data was used with no additional calibration. Data extraction and spatial mapping was done using QGIS (v.3.10, QGIS Development Team, 2021). EAS was compared to LiDAR-obtained tree geometry parameters canopy area, canopy density and CSLA. Flower cluster, fruit number and yield predictions were then related to CSLA to determine whether there was an effect of canopy size on productivity. For extended methodology see Appendices K and L and methodology section of a recently published paper (Scalisi et al., 2021).

FD and CDI estimates were validated in a sampled of tagged fruit. Ground-truth measurements were collected in situ and

Cartographer estimates of the tagged fruit were extracted from stationary images. *Cartographer* predictions of yield per tree were obtained by multiplying fruit number by average FM. Yield predictions were validated against the yield measured with the commercial grader at harvest. For detailed methodology see Appendices L and M.

Commercial orchards

Commercial orchards were scanned between 2020 – 21 and 2021 – 22 for flower cluster, fruitlet number, canopy geometry, FD and CDI. The regular calibration protocol described above for the Sundial orchard was carried out at the commercial sites. The 'Ruby Matilda' block was scanned for flower clusters at full bloom, for fruitlets before thinning and for full-size fruit before harvest. The 'Perfect Pink' block was scanned in 2021 – 22 for flower clusters at full bloom and for fruitlet number in December. Spatial maps of crop parameters were generated, and block averages and relative measures of spatial variability (coefficient of variation, percentage) were estimated. Detailed methodology is described in Appendix M.

Data points from the 'Ruby Matilda' orchard were subsequently overlaid with a grid of pseudo-plots (i.e., plots subjectively drawn with horizontal spacing equivalent to 2 × row spacing and vertical spacing equivalent to 5 × tree spacing, to obtain a number of experimental units for correlation purposes > 200). Medians of the measured variables were extracted from each pseudo-plot to derive orchard-specific correlations. Detailed methodology on deriving block-specific relationships can be found in a recently published paper (Scalisi et al., 2023).

Technology evaluation, utility, application for precision management and user guidelines

The Green Atlas *Cartographer* technology was evaluated at the end of the project by analysing prediction errors of absolute flower, fruitlet and fruit detections, FD and CDI in commercial orchards, and by assessing spatial maps and coefficients of variation (CV, %) in a block. End-user (commercial orchard manager) feedback and commercial uptake was part of the evaluation process to define the utility of the platform. The technology operation was described and its applications for precision management strategies (e.g., spatial zoning for variable rate management) were discussed at the end of the project, and user guidelines were drafted.

Results and discussion

Colour development, sunburn damage, fruit quality and floral initiation responses to fruit position and light exposure

Effects of row orientation and rootstock

The variation in 'ANABP 01' scion vigour between the three rootstocks was visually evident from orchard planting and early growth. Bare rooted Bud.9 trees were notably "weaker" in appearance. Bud.9 trees had consistently the lowest canopy geometry features (height, area, density and CSLA) compared to other trees, that in turn led to the lowest EAS over the three years of study. Canopy area, density, CSLA and EAS were statistically similar in M.9 and M.26, although M.26 trees were more variable. Canopy height was greater in M.26 than in M.9 and Bud.9 only in 2020 – 21, and then this difference disappeared likely because of trees being uniformly topped 20 cm above the last trellis wire, regardless of rootstock. In addition, TCSA was significantly the highest in M.26 trees. Tables 1 – 3 in Appendix N show the 3-year progression of intercepted light for each rootstock. Canopy geometry and light interception measured in 2022 – 23 were affected by extensive foliar damage resulting from a severe hailstorm which occurred on 22 December 2022. This caused non-significant differences in EAS between 2021 – 22 and 2022 – 23.

Fruit from Bud.9 trees showed improved background colour and overcolour, I_{AD} and higher SI compared to M.9 and M.26. This was likely to be the consequence of greater light exposure. No significant effects of rootstock were observed on sunburn susceptibility, FM, FF and SSC. A significantly negative correlation was discovered between EAS and overcolour, indicating that trees that fill more of the available space achieve less purple-burgundy colour development. The time taken by trees grown on Bud.9 to reach desired tree height and to fill out would be a drawback and could sacrifice early yields. CL was similar in the three rootstocks in 2020 – 21 but differed significantly between all rootstocks in the 2021 – 22 season, with M.9 and M.26 having the highest and lowest values, respectively. Fruit diameter was significantly higher in M.9 than in M.26 and Bud.9 in the 2020 – 21 season ($p < 0.001$), but a similar finding was not obtained in the following season despite differences in CL.

Rootstock affected yield in 2020 – 21 and 2021 – 22, with Bud.9 consistently producing between 5 and 10 t ha^{-1} less than M.9 and M.26. M.26 displayed a tendency towards biennial bearing based on its increase in canopy between the two

seasons with relatively little increase in yield. Yield efficiency was highest for M.9 rootstock in 2020 – 21 and 2021 – 22. Among the rootstocks, M.26 trees bore more flower clusters and fruit, and had the highest yield and tree height (Table 4). M9 trees had similar canopy area, canopy density, CSLA to M26 trees. Bud.9 trees were significantly smaller in terms of canopy area and CSLA, had lower density and intercepted less light than trees grafted on M9 and M26. Overall, among the trialled rootstocks, M.9 performed best in terms of productive performance.

Row orientation did not have significantly consistent (over 3 years) effect on sunburn susceptibility and individual fruit weight. Fruit from E – W trees had the lowest overcolour, SSC and SI, and the highest I_{AD}, indicating a delay in maturity, while maintaining a low FF.

Significant differences in CL between row orientations were evident in the 2020 – 21 and 2021 – 22 seasons, although no particular orientations were consistently the highest or lowest in both seasons. Thus, there is not a clear and consistent evidence that CL was affected by row orientation. This is further corroborated by the fact that TCSA, yield and YE were not significantly affected by row orientation in 2021 – 22. E – W trees had the smallest flower cluster number in both 2020 – 21 and 2021 – 22, although in the second season, harvest yields were similar to other row orientations, indicating that when flower scans were conducted, flowers in E – W were late in their full bloom time and thus not detected by the scanning platform *Cartographer*. Thus, the delay in fruit maturation that is likely to occur in E – W fruit may start in early phenological stages. Furthermore, row orientation displayed a significant effect on fruit diameter in the 2021 – 22 season, with E – W rows having the largest fruit but no effect in 2020 – 21. Fruit from E – W and N – S row orientations had consistently the lowest and the highest dark red coverage (%), respectively.

No interactions between rootstock and row orientation were found for CL, mean fruit diameter, yield and yield efficiency in either season. Detailed results and discussion for rootstock and row orientation effects on ‘ANABP 01’ are described in Appendices K, L, N, O, and in recently published research (Peavey et al., 2023; Scalisi et al., 2021).

Effects of fruit position, light exposure, photosynthesis and surface temperature on fruit quality

Fruit sampled from different parts of the canopy were well spatially spread for X, Y and Z and exposed to a wide range of light levels coordinates (Figure 3 of Appendix C). There was a highly significant positive correlation between light exposure and vertical position in the canopy (Z) but no correlation between light exposure and horizontal shift across (X) or along (Y) the row (Table 2 of Appendix C). In leaves near fruit at the top of canopies, g_l was significantly higher than in lower positions and increasing incoming light had a positive correlation with g_l, whereas X and Y had no significant effect on g_l (Slide 5 of Appendix P). Thus, in non-limiting irrigation conditions, leaves near the top of the canopy are expected to transpire more, and in turn are likely to exhibit increased photosynthetic activity.

Peel dark-red coverage was negatively correlated with horizontal shifts but did so positively with vertical shift. The opposite was the case with light red coverage, positively correlating with the horizontal shifts and negatively with the vertical shift. L* and b* positively correlated with the X- and Y-coordinates but negatively with the Z-coordinate. There was a highly significant positive correlation between a* and the Y-coordinate but a highly significant negative correlation between CDI_{dark} and the Y-coordinate. Sunburn damage severity was not affected by any spatial factor, although the summer in which this experiment was conducted was mild and overall sunburn incidence was poor. SSC showed a negative correlation with horizontal shift from the trunk across, but not along, the row. FF increased in high canopy positions. FD was not affected by X-, Y- and Z-coordinates.

Light exposure level had significant effects and positive correlations with dark red coverage and CDI_{dark} and significant negative correlations with light red coverage, L*, b* and FD. FF had a strong positive correlation with light exposure. The remaining parameters—a*, h°, sunburn damage severity, SSC and SI—were not significantly correlated with light exposure.

Total red colour coverage remained the same regardless of fruit position, but the ratio of dark to light red colour changed depending on the fruit position. This was also true in response to light exposure, with dark red increasing and light red decreasing, but the total red colour coverage also increased with increasing light exposure. In fact, out of the fruit position parameters only fruit height (Z) correlated positively with both light exposure and dark red coverage demonstrating the positive response of 'ANABP 01' colour development to light exposure. This is in line with findings outlined in recent research (Peavey et al., 2023) that noted increased dark red colour coverage in Bud.9 trees given to more open canopy that allowed better light penetration (Peavey et al., 2023). Detailed results and discussion are available in Appendix C.

Effects of shade and UV filtration on and fruit surface temperature and quality

Appendices B and C show that the SS2 treatment, which was initially shaded from direct sunlight and then exposed, had

the highest degree of sunburn damage severity and was significantly higher than the fully shaded SS1 treatment. The UVF treated fruit also had a high severity of sunburn damage but was not significantly different from any other treatment. Overall, in control fruit, peel redness decreased along with maturation generating the dark-burgundy peel that is a key feature of 'ANABP 01' fruit. Despite similar FST results to the control, the UVF fruit did not behave normally when it came to colour development and produced undesirable yellow-orange peel colouration. This indicates that UV light, in addition to visible light, is a key to the appealing dark-red colour development in this cultivar. Shaded fruit throughout the experiment had much lower FST, which were much closer to the ambient air temperature, although they retained some heat during the afternoon once the air temperature started to drop. Sun-exposed fruit consistently displayed significantly higher FST with UVF-treated fruit reaching the highest values, although not significantly different from the Control treatment. Night-time average FST was similar for all treatments. Visually, it was noted that the SS2 treatment was the only treatment to develop photo-oxidative sunburn damage. This clearly demonstrated the importance of "acclimation" — a physiological process whereby fruit adapt to gradual increases in solar radiation. Acclimation during fruit growth reduces its susceptibility to sunburn damage development during periods of excessive light and heat exposure. For effective acclimation, fruit need exposure to high (but not too high) levels of sunlight during development.

The progression of the fully exposed control treatment showed a slight increase in CDI_{dark} between 17 January and 17 February and then a large increase by harvest. At harvest, control and SS2 treatments had significantly higher CDI_{dark} than SS1 and SS3. CDI_{dark} of UVF fruit initially grouped with the shaded fruit on 17 February but then increased and became similar to SS2 at harvest. Control and UVF fruit had the highest SSC. Starch degradation was accelerated under the UVF treatment. There were no significant differences between treatment means for FD, FF and DMC although it was noted that UVF treated fruit had the highest values of FF and DMC.

Findings on the effects of shade and UV filtration could have implications for the use of pre-harvest defoliators on early season cultivars in a future climate where light and temperature levels, and extreme heat events, are likely to increase in the final stages of the growing season. Future developments in netting technology for apples should take into account light quality transmission and ensure that sufficient PAR and UV light reach the fruit, particularly for red and bi-coloured cultivars. Extended results and discussion on the effects of shade and UV filtration on FST and fruit quality are detailed in Appendices B and C.

Impacts of crop load on return bloom, tree growth, yield, fruit quality and chemical signalling

Long-term crop load effects in 'Rosy Glow'

The five-year study in the Yarra Valley showed that in 'Rosy Glow' CL was positively correlated with yield, and inversely correlated with fruit size, and return bloom the following season. On average, fruit from the higher CL treatments developed less colour intensity and matured approximately one week later than fruit from trees with a normal CL, whereas fruit from the lowest CL trees developed more colour intensity and reached maturity (as indicated by I_{AD}) almost two weeks earlier. There was a consistent strong negative correlation of SSC with CL, with fruit from the highest CL trees generally 2.5 – 3 °Brix lower than those from trees with the lowest CL. CL effects on FF were not significant in constant CL treatments, whereas there was a strong negative correlation of FF and CL in variable CL trees. Trees in a forced biennial bearing regime tended to produce fruit with lower FM and higher FF in the season following a high CL season, compared to trees with a consistent CL each season. This indicates there may be a carryover effect of the previous season's CL, and that consistent CL year to year is more likely to have consistent firmness. I_{AD} and SSC were not different in trees subjected to forced biennial bearing and trees with regular cropping. After several years of a forced biennial cropping regime, zonal effects within some trees were observed, where the distribution of flowers, and subsequently fruit, became unbalanced with the rest of the tree.

Overall, in 'Rosy Glow', among treatments imposed, the CL level of 8 fruit per cm^2 TCSA was achieved more consistent return bloom and fruit quality. This matched the optimal grower thinning strategy and led, on a 5-year average to: return bloom = 14 clusters per cm^2 TCSA, yield of 1.56 kg cm^{-2} TCSA, FM = 185 g, SSC = 14.3 °Brix, FF = 8.8 kg cm^{-2}, I_{AD} = 0.63, overcolour C* = 47.6, overcolour h° = 23.8, background colour C* = 39.9 and background colour h° = 80.5.

These results indicate that higher CL should not be used as a means of producing smaller fruit to meet market demands as this could instigate biennial bearing and will produce less attractive fruit with lower quality. Extended results and discussion regarding the long-term CL effects on yield, return bloom and fruit quality are detailed in Appendices D, E and Q.

Varying CL also affected flavonoid levels in 'Rosy Glow' buds and this class of components may be involved in regulation of flower bud induction. The biosynthesis of phenylpropanoid pathway intermediates, including hydroxycinnamates (e.g., chlorogenic acid, coumarates, ferulates), coumarins, salicylates and flavanols, increased in response to low CL. These

findings provide evidence that the PAL (phenylalanine ammonia-lyase) salicylic acid biosynthetic pathway was activated in response to an "OFF" year during a biennial bearing cycle. Although no significant changes were exhibited in salicylic acid, its biosynthetic derivatives exhibited distinct increases in "OFF" trees of 'Rosy Glow' apples. An additional mechanism of cytokinin involvement via histidine-aspartate phosphorelays, which is also known to activate a defence response in trees, was observed. This study for the first time identified the participation of the salicylate group of plant hormones in flower induction in apple. Extended results and discussion regarding the long-term CL effects on chemical signalling are detailed in Appendix F and published in a recent paper (Reddy et al., 2022).

Long-term crop load effects in 'Ruby Matilda'

The three-year study conducted in the Goulburn Valley showed a negative effect of CL on tree growth of 'Ruby Matilda' trees. To maintain yearly cross-sectional growth of ≥ 10 %, individual leaders or whole trees need to be thinned to CL ≤ 7.55 or 7.44 fruit per cm^2, respectively. In addition, flower induction was likely to be more localised within leader. Nevertheless, trees likely managed to share resources and information between leaders after full bloom so that fruit set and fruitlet drop can be adjusted based on the available resources. In fact, the effect of CL of secondary leaders was more robust on return CL of primary leaders than it was on their return bloom. Thus, the information on fruit set and fruitlet early drop in one leader may be subject to the CL of another leader. In the bi-axis 'Ruby Matilda' on M.26 trees monitored in this study, results suggest that consistent (100 %) return bloom and return CL can be achieved by fruit thinning to CL of ~ 6.5 and 7.1 fruit per cm^2 TCSA, for within-leader and whole-tree thinning strategies, respectively. These numbers are relatively similar to the CL level (6 fruit per cm^2) recommended by Embree et al. (2007) for achieving regular cropping in 'Honeycrisp' on M.26 trees with a similar age.

Yield and FM were similarly affected by CL within-leaders and in tree total. The CL of 6.5 and 7.1 fruit per cm^2 TCSA that are ideal for regular return bloom and CL, if imposed to individual leaders or tree total would lead to 31 kg per leader (118 t ha^{-1}) and 59 kg per tree (112 t ha^{-1}), respectively. These values represent only a 14 and a 7 % yield reduction, respectively, when compared to CL = 15 fruit per cm^2 TCSA, a CL level that would cause near-zero return bloom and return CL. A significant improvement of desirable peel colour features such as increased redness and colour intensity was achieved in leaders and trees with low CL. Additional indicators of fruit quality such as SSC and DMC significantly increased, while I_{AD} was lower, under decreasing CL within leaders and trees. The effects of CL on FF and SI were not consistent; thus, we believe that effects of CL on FF and SI are negligible and non-direct, as they may only be mediated by correlated variables such as SSC and DMC.

Noticeably, the CL of secondary leaders did not have a significant effect on fruit peel colour, I_{AD}, SSC and DMC in primary leaders, suggesting that pigment formation, maturity advancement and sugars and dry matter accumulation are more localised responses within an apple tree.

Trunk growth, yield and fruit quality parameters achievable by mature 'Ruby Matilda' trees on M.26, if managed to achieve regular CL of ~ 6.5 and ~7.1 fruit per cm^2 TCSA, for within-leader and whole-tree thinning strategies, respectively, are shown in Table 4 of Appendix G. Predicted variables related to peel colour, SSC, DMC and I_{AD} were likely influenced by early harvest in year 3, so their absolute values should be treated with caution. The relationships obtained in this study need to be used as guidelines and will need further validation on other scion-rootstock combinations. In multileader apple systems, CL manipulation is necessary to achieve the best balance between tree growth, productive and qualitative features. Return bloom and fruit quality appear to have reduced susceptibility to CL on separate leaders and are mostly affected by localised CL. Whereas trunk growth, yield and fruit size may be affected by CL in distant fruit bearing units. We recommend using individual leaders as management units for hand thinning both for simplicity and to achieve best performance in terms of growth and return bloom while maintaining high yield and fruit quality features. Our recommendation is to thin leaders to 6.5 fruit per cm^2 TCSA in trees with similar age, scion-rootstock characteristics, and in similar environments (soil and climate) to those used in our study. Detailed results and discussion of localised CL effects on 'Ruby Matilda' yield, return bloom, growth and fruit quality are highlighted in Appendix G.

The increased levels of compounds identified in the flower induction phase of buds collected from 'Ruby Matilda' trees with high return bloom could be candidates for improving return bloom via exogenous application. Current thinning agents utilised by the industry are thought to potentially induce return bloom when fruitlets are removed prior to floral induction or at the early stages of fruitlet development of 8 – 15 mm in size. For example, the synthetic derivative of the cytokinin thinning agent BA (6-Benzyladenine), is known to promote return bloom when application is performed during the critical floral induction period. Similarly, the natural phytohormone abscisic acid, has been known to be an effective thinning agent with some cultivars and increases return bloom only in combination with BA. This study provided evidence that cytokinins and ABA are directly involved in floral induction.

The primary and secondary leaders showed differences in altered metabolites in spur buds, suggesting unique metabolic

pathways utilized in the two branches. Despite differences in both pathways, flavanols were possible signalling molecules related to CL treatments. Metabolites in the p-coumaric acid pathway showed significant response to CL. There were some key pathways in the primary leader that included benzoic acid and 4-hydroxybenzoic acid intermediaries in the shikimic acid pathway and may be linked to epicatechin. In the secondary leader, ERI and its glycoside were among the most significantly altered metabolites. Appendix J details how 'Ruby Matilda' spur buds had marked cytokinin precursors and derivatives including adenosine, and its deaminated form, inosine. The compounds showed significant positive correlation with return bloom, both as localised signalling and as a whole-tree response.

The primary and secondary leaders showed differences in altered leaf metabolites and, like in buds, unique metabolic pathways could be utilized in the two branches. The metabolites detected in the leaves were a diverse range of aromatic compounds. The regulation of these compounds is not clear and may display a very complex response to biennial bearing. Only two compounds reminiscent of the apple buds were present in secondary leaders' leaves, including decreased levels of ERI and D-glucose. It is possible that CL in secondary leaders had more pronounced effects on leaf metabolites due to their large range (very low – very high). Leaves are known as promoters of flower induction and are also a major source of cytokinins. Therefore, additional metabolic profiling of leaves could improve the understanding of sink-source relationships in flower initiation. Detailed results and discussion on bud and leaf metabolites are highlighted in Appendices H and J.

Differences in levels of phenylpropanoid pathway members and a putatively identified phytohormone gibberellic acid (GA) were identified in fruitlet seeds of high and low CL treatments of 'Ruby Matilda'. The reported negative regulation of flavanols via GA signalling and the downstream effects of the phenylpropanoid pathway suggest that there is phytohormone and flavonoid signalling crosstalk in the regulation of biennial bearing cycle. The putatively identified GA derivative identified in this study could be a possible candidate for floral repression, but further LCMSMS mass spectrometry techniques of the individual compounds are required to confirm or identify unknowns. Detailed results and discussion on fruitlet seed metabolites are highlighted in Appendix I.

Validation of a mobile sensorised platform to measure fruit number, size and colour, and light interception

Sundial orchard

Results on the calibration and validation of flower clusters, fruit number, yield, tree geometry and light interception using the Green Atlas *Cartographer* sensorised platform in 2020 – 21 were published in scientific journal (Scalisi et al., 2021). Overall, results showed that predictions in 'ANABP 01' trees were very accurate after initial calibration. Flower cluster detections had root mean square errors (RMSE) of ~ 5 cluster per image. Fruit number and yield predictions needed independent calibration across rootstocks, but errors after validation on a separate dataset were small (RMSE = 5 fruit per tree, and RMSE = 1 kg per fruit, for fruit number and yield, respectively). Orchard errors for fruit number and yield estimations were lower than 5 %. Canopy area, canopy density and CSLA were all linearly related with EAS but CSLA had the most robust and stable relationship with EAS. Increasing CSLA led to higher flower cluster number, fruit number and yield. These results were considered very good compared to the generally accepted yield prediction error of 5 – 10 % reported by Anderson et al. (2021). Tree height predictions needed a preliminary calibration for the ground height. After calibration, tree height predictions were considered accurate and in line with manual observations. Although a calibration is needed to obtain accurate absolute predictions, in several circumstances, an uncalibrated, relative fruit number heatmap of the orchard is sufficient to support thinning management decisions (e.g., management of labour for thinning operations). The technology allowed to measure a significant positive correlation between CSLA and flower cluster number, fruit number and yield.

A technical report (Appendix M) described the reliability of fruit diameter and colour in 2020 – 21. The accuracy of fruit diameter estimates was very high (> 95 %) and overall fruit diameter prediction errors were deemed below 3 mm. Among the traditional CieLAB colour parameters tested, only h° was satisfactorily predicted by *Cartographer* (r_c = 0.84). CDI was also accurately predicted by *Cartographer*—as it is derived from h°—but its use is preferrable to simplify (i) interpretation of colour estimates both in a temporal and in a spatial scale, (ii) application in a higher number of fruit crops, and (iii) large-scale adoption in fruit industries. However, CDI predicted from *Cartographer* does not perform well for assessing maturity in 'ANABP 01' as it utilises the original calculation that works well with fruit turning red. CDI_{dark} was not calculated as it is likely to be not accurate if predicted from non-contact sensors such as RGB cameras, due to L* being strongly affected by external light. Thus, CDI_{dark} obtained from *Cartographer* would only likely work if scans were carried out in dark, standardised conditions such as before dawn and after dusk. Future experimental activities could be carried out to validate this hypothesis. Fruit diameter and fruit colour were associated to fruit number and amount of radiation

interception by tree canopies and the direction of the correlation (positive or negative) was in line with expectations. Overall, *Cartographer* demonstrated to be a valid tool to combine predictions of fruit diameter and fruit colour that added up to the previously validated predictions of other significant crop parameters (e.g., cross-sectional leaf area, flower number, fruit number) using a single platform.

Results on predictions of flower clusters, fruit number, yield, tree geometry and light interception, fruit diameter and CDI from the 2021 – 22, confirmed the high reliability of the platform. *Cartographer d*ata were used to rapidly determine the effects of row orientation and rootstock on 'ANABP 01' performance. A summary of crop performance and comparison between the two seasons (2020 – 21 and 2021 – 22) is detailed in a technical report (Appendix L). EAS estimates were more accurate when considering two seasons, as canopy developed with time and the data range of ground-truth measurements was larger. Crop performance results from 2022 – 23 are not shown due to two hail events that damaged > 95 % of the crop, although calibration errors of 6 % were generated for both flower cluster and fruitlet estimates carried out before the hail events. Extensive results and discussion of calibration and validation carried out in the Sundial orchard are detailed in Appendices L and M and in a recently published paper (Scalisi et al., 2021).

Commercial orchards

The reliability of crop estimates in commercial orchards was similar to that achieved in the Sundial orchard under controlled experimental conditions. The first results on fruit diameter and CDI estimates in the 'Ruby Matilda' block (Plunkett Orchards) obtained in 2020 – 21 were presented in a technical report (Appendix M). Results on flower cluster detections, fruit number, canopy geometry, fruit diameter, CDI and yield predictions were presented at the virtual 2021 APAL Technical Forum (Appendix P). Predictions of fruit number, CDI and fruit diameter had 8.3, 6.0 and 1.2 % errors, respectively. The following season, predictions of flower cluster number, fruitlet number, fruitlet diameter, fruit number, fruit diameter and CDI had 5.1, 7.8, 0.5, 7.3, 2.2 and 1.7 % errors, respectively. In 2021 – 22, scans of the 'Perfect Pink' block at full bloom and at fruitlet-size stage (i.e., December 2021) generated predictions of flower cluster number, fruitlet number and fruitlet diameter equal to 8.8, 9.5 and 2.6 %, respectively. Spatial maps were generated in the commercial orchards and shared as geo-referenced pdfs with orchard managers to visualise spatial variability.

As described in an industry article (Appendix AC), spatial maps allowed to identify hotspots with low CL and hinted that there was a tendency for positive and negative effect of canopy size on the fruit diameter and CDI of 'Ruby Matilda', respectively. This hypothesis was empirically demonstrated by a study on orchard-specific relationships between tree geometry, fruit number, fruit clustering, fruit size and fruit colour, presented at the International Horticultural congress in 2022 (Appendix AD). This study was then published in the Proceedings of the "III International Symposium on Mechanization, Precision Horticulture, and Robotics: Precision and Digital Horticulture in Field Environments" (Scalisi et al., 2023). In summary, the research revealed that when geo-referenced data points generated by *Cartographer* were grouped into spatial plots, underlying relationships between tree geometry, productive performance and fruit quality attributes could be determined. Thus, these have potential to be used to standardise trees by tailoring management and consistently produce high-quality fruit over the lifespan of modern apple and pear orchards.

Overall, prediction errors in commercial orchards remained below 10 % and had an average of 5 %. Prediction errors obtained in the two commercial orchards over the course of the project are summarised in Table 1 of Appendix T. These values are compatible with reliable technology uptake by the industry as they can support efficient management based on consistently accurate and objective data. A portfolio of geo-referenced maps obtained with *Cartographer* during the project is attached in Appendix U.

Evaluation of technology and management system and guidelines

A protocol for outdoor machine operation is described in Appendix V. Overall, a calibration process is required for fruit number estimates, but unnecessary for fruit size and colour. For management purposes, it is recommended to create spatial zones from data points, in order to simplify operations. The three zoning approaches described were (i) contouring, (ii) interpolation and (iii) gridding with pseudo-plots. Data can be summarised into management zones such as the pseudo-plots, and then extracted for each block to model relationships between CSLA, fruit number, size and colour that are specific for that block. These provide valuable support for determining the most appropriate CL that is needed to achieve harvest targets. The availability of technology that serves multiple purposes is of pivotal importance for industry growth, as it may potentially reduce production costs such as labour and provide long-term benefits such as the creation of historical databases that can help measure performance over many years and support business decisions. There was significant commercial uptake of the technology by the industry, as described in Appendix T. Accessing platform data via consultants who provide the service, as opposed to purchasing individual machines for each farm, may

be the best strategy for smaller growers with occasional data. On the other hand, large fruit growers may prefer to purchasing and using the technology in their routine operations throughout the crop cycle.

In conclusion, the Green Atlas *Cartographer* platform is relatively easy to operate for unskilled staff and, through AI, can generate accurate results of fruit number, fruit size and colour, while concomitantly measuring tree size and geometry features. If linked to canopy geometry estimates, fruit quality and productivity predictions become a powerful tool that empowers growers to tailor precise strategies to each orchard block. Additional spatial zoning within blocks is recommended to establish management zones that can reduce variability in an orchard. A factsheet on the use of the platform is available online in the APAL website (link).

Outputs

Table 1. Output summary

Output	Description	Detail
Industry articles	Project scope and outcomes were communicated to growers via AFG magazine and to international audience in two Italian magazines. AFG Audience: 960 in print, freely available online. Italian magazine articles subject to copyright.	– PIPS3 integrated R&D will build whole-of-system understanding on the benefits of sustainable production practices (AFG Summer 2020, Appendix W). – Advancing apple orchard production systems (AFG Autumn 2021, Appendix X). – Effects of crop load on fruit quality in 'Rosy Glow' apples (AFG Summer 2021, Appendix Q). – Rootstocks, canopy architecture and fruit quality of 'ANABP 01' apples (AFG Autumn 2022, Appendix O). – Unveiling apple block variability using Green Atlas *Cartographer* (AFG Winter 2022, Appendix R). – Turning off biennial bearing (AFG Spring 2022, Appendix AB). – Meleto: effetti di portinnesti e direzione filari (L'informatore Agrario, 27/2022). – Strumenti di precisione stimano il carico dei frutti in meleti e pereti (Frutticoltura, 8/10/22). – Understanding apple sunburn damage in response to sunlight (In press, Appendix B).
Scientific journal papers	4 papers were published and 3 draft scientific papers were produced.	Published papers (Peavey et al., 2023; Reddy et al., 2022; Scalisi et al., 2021a, 2023); draft papers in Appendices C, D, J. For full details see Refereed scientific publications.
Factsheets	5 Factsheet pdfs available in the APAL's website. A collection of PIPS3 Program resources is available here.	– Project AP19003 – Ground-based mobile sensing – Irrigation sensors – Dendrometer installation and maintenance – Colorimeter – Objective fruit colour assessments – Trunk dendrometers – Data interpretation
Technical videos	11 Videos were published on the APAL website and on Youtube. Metrics on current (5 July 2023) Youtube views are included. A collection of PIPS3 Program resources is available here.	– PIPS 3: Advancing sustainable and technology driven apple orchard production systems (21 Oct 2020, 690 views). – Green Atlas Cartographer™ Mobile sensing technology calibration and validation for apples and pears (27 Oct 2020, 593 views). – Commercial orchard crop load experiment (5 April 2021, no audience stats). – PIPS3 - Advancing sustainable & technology driven apple orchard production systems (7 Apr 2021, 492 views). – AP19003 project update (13 Oct 2021, 43 views). – AP19003 December 2021 update: Irrigation scheduling at Tatura SmartFarm (Dec 2021, 479 views). – Using tech and data for apple orchard management and optimal crop load (26 Jan 2022, 369 views). – Tech-driven fruit diameter and colour measurement (2 Feb 2022, 307 views). – Sensing technologies to improve predictions and management of crop load – a PIPS3 update (9 Nov 2022, 532 views). – Crop load management: Signalling compounds that induce flowering (13 Dec 2022, 154 views). – Managing orchard data with smartphone technology (21 Dec 2022, 385 views).
News and online articles	6 online articles related to the project are available on the APAL website. 2 WinNews and Country	– Illuminating the future orchard (5 Aug 2020). – PIPS 3: Green Atlas Cartographer (27 Oct 2020). – WINNEWS – Interview on Green Atlas Cartographer (2 Feb 2021). – Non-invasive maturity testing a step closer (15 Mar 2021). – Advancing sustainable and tech driven apple orchard systems (7 Apr 2021).

	News article on technology adoption are also linked.	– Netting and orchard adaptation for future climates (17 Aug 2021). – Country News article "Orchard robot charms crowd" (29 Nov 2021). – Turning off biennial bearing (12 Dec 2022).
Presentations at industry events	Presentations at various industry events were made during the project.	– Goodwin, I. (2021). Development of a rapid apple and pear orchard assessment tool using a ground-based mobile sensing platform Green Atlas *Cartographer*. Presentation at National Tree Crop Intensification in Horticulture Program (TCI Program- AS18000) Team Webinar "Indirect measurement in tree crops using advanced technologies", 14 April 2021 (Appendix Y). – Alessio Scalisi presented at the APAL technical forum on 1 June 2021: AP19003 project presentation 'Advancing sustainable and technology driven apple orchard production systems' (presentation in Appendix P). – Presentations to PIPS3 meeting, 8 and 9 March 2022 held at Tatura SmartFarm by Ian Goodwin (project overview) and Alessio Scalisi (*Cartographer* – in-field). – Alessio Scalisi presented *Cartographer* at a Launch Vic event on 25 March 2022). – Tim Plozza presented results from experiments studying the effects of crop load on biennial bearing and chemical signals at the APAL R&D Day (1 September 2022). – Alessio Scalisi and Ian Goodwin provided an update on the Green Atlas *Cartographer* system at the APAL Grower orchard tour (2 September 2022). – Ian Goodwin presented on 'How can I prepare my orchard for extreme conditions?' at Horticulture Field Day (23 March 2023). – Ian Goodwin presented at the roadshow in South Australia (Flavell's Packing Shed, Collins Hill Rd, Lenswood Adelaide Hills) on climate challenges, crop load effects on fruit quality and biennial bearing, and sensing technology to inform crop load and other orchard management decisions (30 May 2023, audience n = 36). – Ian Goodwin presented at the roadshow in Western Australia (T&C Fontanini Orchard, 647 Seven Day Rd, Manjimup) on climate challenges, crop load effects on fruit quality and biennial bearing, and sensing technology to inform crop load and other orchard management decisions (1 Jun 2023, audience n ~ 20). – Ian Goodwin presented at the Fruit Growers Tasmania Annual Conference (Country Club Tasmania, Launceston) on climate challenges, crop load effects on fruit quality and biennial bearing, and sensing technology to inform crop load and other orchard management decisions (15 – 16 June 2023, audience n = 150).
Orchard walks and visitors	The list is split between (i) orchard walks and visitors hosted at the Tatura SmartFarm, and (ii) field walks in commercial orchards.	i) Tatura SmartFarms walks and visits: – Jul 2020 – May 2021: 4 school groups, 18 industry and Government events, and one AgSTEM workshop were hosted. – June – Nov 2021: Dr Chen Chao (Director of Laboratory of Motion Generation and Analysis at Monash University), Don and Keith Bryant (Dookie community leader) and Tony Filippi (ANFIC), APAL Future Orchard walk (audience of ~ 40 growers and industry stakeholders). – Dec 2021 – Apr 2022: Ms Suzanna Sheed (MP for Shepparton), Assoc. Professor Eduardo Daly (Monash University), Year 12 high school science students from Assumption College and Thornbury visited, PIPS3 program scientists and technical staff, Kubota Australia delegation, Ripe Robotics team to discuss ongoing and future potential collaborations, Monash University robotics team, LaunchVic event (approximately 80 participants), Deputy Secretary DJPR Matt Lowe and Julie Simons (Acting Executive Director Agriculture Policy), Goulburn Broken CMA Board, CEO and staff, – May – Nov 2022: Karen Adair (Deputy Director-General, Agriculture & Investment Services) and Chris Rodwell (Executive Director, NZ Ministry for Primary Industries), visitors from QDAF, Plant and Food Research NZ and Australia, Melbourne University engineering students, Federation University, Ag Vic extension officers, World Bank Uzbekistan Agriculture, Chief Science Adviser and Director (Ministry for Primary Industries NZ). – On 23 March 2023, Agriculture Victoria and Fruit Growers Victoria co-hosted an orchard walk. PIPS3 research was on display. – Dec 2022 – May 2023, visitors from Washington State University, AgFirst NZ, APAL, Fruit Help, University of Melbourne, University of Nottingham, CSIRO, high school and university student, Agrivoltaics conference delegates, Ministry Primary Industries NZ, NEC Corporation, University of Horticulture & Forestry, India, Ag Vic extension officers, Inspired Ag, Goulburn-Murray Water, and a horticultural agronomist from Uruguay.

		– Jun – July 2023: visitors from FruitHelp, AgFirst NZ, Plant and Food Research NZ. ii) Field walks in commercial orchards: – Vernview Orchard (Launching Place, VIC, 2 Sep 2022). – Future orchards®—McNab Orchards (Ardmona, VIC, 17 Nov 2022). – Future orchards®—Benipal Orchards (Shepparton East, VIC, 22 Jun 2023).
Presentations at science conferences	Oral and poster presentations given at the International Horticultural Congress (France 2022).	– Oral presentation on utilising *Cartographer* for orchard-specific relationships (Appendix Z). – Poster presentation on the effects of rootstocks and row orientation on 'ANABP 01' (Appendix AA).
Technical and summary reports	10 technical and summary reports were produced during the project.	– Report summary on crop load results in 'Rosy Glow' (Appendix E). – Technical report on chemical signalling in 'Rosy Glow' (Appendix F). – Technical report on chemical signals in 'Ruby Matilda' (Appendix H). – Technical report on crop load effects on organic metabolites in 'Ruby Matilda' (Appendix I). – Technical report on sensing spatial distribution in 'ANABP-01' (Appendix K). – Technical report on *Cartographer* (Nov 22) (Appendix L). – Technical report on *Cartographer* (Nov 21) (Appendix M). – Report summary on light interception and rootstock effects in 'ANABP 01' (Appendix N). – Report on Evaluating the utility of sensors and platform (Appendix T). – Technical report describing new technology and management system (Appendix V).

Outcomes

Table 2. Outcome summary

Outcome	Alignment to fund outcome, strategy and KPI	Description	Evidence
Short term – Relationships established between fruit position and light exposure on colour development, sunburn damage, fruit quality and floral initiation.	**Outcome 1: Industry profitability and global competitiveness is improved by reducing the average cost per carton** SIP Strategy 1.1 Drive orchard reworking with emphasis on preparedness for increased mechanisation/automation/scale. SIP Strategy 1.4 Improve labour productivity through greater adoption of technology and leadership training. SIP Strategy 1.5 Research IT and data systems that enable better collection and connectivity of orchard and business data at every level of the supply chain **Outcome 2: The value of the average bin has risen, resulting in improved**	Research methodology to meet journal publication standards was documented and presented to scientific peers. Scientific results from data collected over 2-year period (hail impacted the third year) showed that fruit position and light exposure (including UV) are directly related to red colour development and sunburn damage. Rootstock-scion vigour and row orientation influenced light exposure.	Results of fruit position and light exposure were communicated to growers, consultants and the science community via industry articles, orchard walks, regional roadshow, webinars, science presentations and a draft scientific paper.
Short term – Chemical signals identified that determine the impact of high crop load on floral initiation and differentiation, and fruit size in the subsequent season.		Research methodology to meet journal publication standards was documented and presented to scientific peers. Metabolites involved in the return bloom and biennial bearing regulation in apple cultivars were identified in 'Rosy Glow' (predecessor project AP15013) and in 'Ruby Matilda' orchards.	Chemical signal results (including the predecessor project AP15013) were communicated to growers, consultants and the science community via industry articles, industry forums, video and scientific papers. Results build a better scientific understanding of potential chemicals that could be applied (or avoided) to enhance floral induction.
Short term – Commercial mobile sensing technology available to industry to measure in situ fruit and		Testing a mobile sensorised platform (Green Atlas *Cartographer*) via scanning and measurements in the Sundial Orchard at the Tatura SmartFarm and a crop load	Results communicated during the project via online videos and webinars, factsheets, technical reports, magazine articles, scientific papers and presentations

tree parameters and establish orchard-specific crop load relationships.	**industry profitability** SIP Strategy 3.1 Improve quality consistency and percentage of Class 1 fruit per hectare.	experiment at Plunkett Orchards showed high precision estimates of fruit and flower number, and high precision and accuracy in fruit size, fruit colour and tree size. Evaluation of *Cartographer* in two commercial orchards was undertaken at flowering and pre-harvest to demonstrate technology. Maps were provided to growers and consultant. Methodology to relate tree size, fruit size and fruit number from orchard scans was developed so the orchard-specific crop load could be determined.	at an industry roadshow and technical and science forums. A consultant (Nic Finger, FruitHelp) has leased a Green Atlas *Cartographer* and is currently using it to provide data-driven feedback to apple and pear (synergy with AP19005 project) growers in the Goulburn Valley and in the Yarra Valley. Technology is also now available to growers via consultant in Western Australia.
Long term – Orchard design to maximise fruit yield and quality and minimise the impact of extreme heat events.		Further interpretation of the results is being carried out to derive the best orchard design (e.g., row orientation, choice of rootstock, pruning) practices in apple to optimize fruit yield and quality while coping with climate change and heat events. Green Atlas *Cartographer* was validated as a tool to estimate tree light interception in apple orchards. A new project proposal was submitted to Hort Innovation to investigate the effects of netting systems on light, yield and fruit quality.	Draft scientific publication on relationships of fruit position, light exposure and fruit quality will be utilized to assist growers in orchard design. Published relationships will feed into management systems (e.g., netting design) to improve fruit quality consistency. TIA-AgVic project proposal submitted to Hort Innovation (in response to RFP AP22004).
Long term – Improved crop load management by providing knowledge and tools to deliver premium fruit that meets consumer expectations.		Optimum crop loads to maximise yield and fruit quality and minimise biennial bearing were identified for 'Rosy Glow' (relationships established using data from predecessor project AP15013) and 'Ruby Matilda' orchards. A new project proposal was submitted to Hort Innovation to investigate chemical signalling under a combination of crop load and light environment conditions.	Results of the effects of crop load on fruit quality and yield were communicated to growers, consultants and the science community via an industry article, industry technical forum, regional roadshow and a draft scientific paper. Draft scientific publication on the effects of crop load on yield, fruit quality and biennial bearing will be utilized to assist growers in setting crop load targets. Published results on relationship of spatial data collected by *Cartographer* provides the foundation for using tools to set crop load targets. TIA-AgVic project proposal submitted to Hort Innovation (in response to RFP AP22004).
Long term – Sensing technology used in apple orchards to assist growers to produce fruit to market specifications.		The utility of the sensorized mobile platform by the industry identified how it can be used for management purposes (e.g., spatial thinning, pruning and leaf blowing strategies, variable rate spraying, irrigation requirements, yield forecasting, pre-	Communication and feedback from growers and service providers via regional roadshow, field days, technical forums and PRG meeting. Published results in refereed

		harvest fruit size distribution, harvest logistics). A new project proposal was submitted to Hort Innovation to undertake an economic analysis of spatial crop load management using mobile sensorised platform.	journals will contribute to the ongoing rapid development in sensing technologies to reduce orchard input costs and increase resource use efficiency and productivity. TIA-AgVic project proposal submitted to Hort Innovation (in response to RFP AP22004).

Monitoring and evaluation

Table 3. Key Evaluation Questions

Key Evaluation Question	Project performance	Continuous improvement opportunities
EFFECTIVENESS: To what extent has the PIPS3 Program addressed the objectives, research agreement achievement criteria and identified outcomes/ outputs? To what extent has the project improved orchard design and crop load management in a variable climate by providing knowledge and tools to consistently deliver premium fruit that meets consumer expectations in domestic and export markets? To what extent has the project developed, calibrated, validated and evaluated sensor technology to measure flower number, tree size, fruit number, fruit size and fruit colour?	The project has published results and recommendations on the reliability of *Cartographer* and its evaluation as a tool for research and industry. Results were widely disseminated at industry events and scientific conferences as outlined in Table 1. Research on the effects of fruit position, rootstock and row orientation on light interception, yield and fruit quality was published and recommendations were produced and made available to industry. Results on crop load effects on fruit quality, return bloom, tree growth, yield and chemical signaling were published in industry articles and research papers, and presented in videos and at industry events. Respondents from the final project evaluation survey were very confident that the project achieved its objectives and activities were executed as expected. It was identified that some goals were ambitious (i.e., *Cartographer* assessment of crop load relationships with tree size and fruit diameter) and more time and seasonal stability was needed for elements of the work. Seasonal variability and Covid restrictions were identified as constraints. AP19003 effectiveness rating was 4.6 on a scale from 0 – 5 (see Appendix AD).	Increasing opportunity for accurate spatial mapping of fruit size is essential for reliable yield predictions. *Cartographer* can be used for further applications, and economic efficiency (costs and benefits) needs to be evaluated. Future research should attempt to encompass effects of crop load levels on productivity in combination with netting. Orchard-specific relationships between *Cartographer* estimates of cross-sectional leaf area, fruit number and fruit size to determine crop load will improve technology uptake.
RELEVANCE: How relevant was the sub-project to the needs of the identified stakeholders? Do identified stakeholders believe the project investment was worthwhile and would they invest in the project team and/or subject matter in the future?	Information regarding orchard design, crop load management and sensor technology has been provided to growers and frontline advisors via industry articles, online resources, industry magazine articles, presentations to industry forums and engagement at orchard walks. The project was considered strongly relevant to both growers and advisors who support them, particularly in relation to calibration and validation of the Green Atlas *Cartographer* and temperature effects on fruit colour development and quality. There were no comments in relation to chemical signalling influence on floral initiation, likely a reflection that the findings have a more indirect	Provide the industry with the financial advantages of using a mobile sensing platform for spatial management, yield forecasting (including fruit size distribution) and orchard-specific crop load relationships. Explore the concept of narrow row pedestrian orchards that are ag tech ready and maximise fruit quality by better light environment.

	rather than immediate benefit to industry. AP19003 relevance rating was 4.6 on a scale from 0 – 5.	
APPROPRIATENESS: To what extent was the PIPS3 Program Communications and Extension Plan appropriate and had an impact upon the target audience? No specific AP19003 within M&E plan.	The technology for sensing fruit parameters and tree geometry was showcased at different field walks. A local consultant now provides the service commercially. Grower's confidence in technology data has soared during the duration of the project, as research data clearly articulated results on reliability. The project has communicated the importance of orchard design (e.g., row orientation, rootstock choice) and effects of excessive light on fruit quality. The project was considered extremely strong in engaging with the industry. Respondents were impressed with the mix of engagement across digital, printed and field-based activities. While growers are seeking practical application of the research in communications, primarily through videos, advisors are looking for technical and data driven evidence in longer articles or publications. AP19003 appropriateness rating was 4.8 on a scale from 0 – 5 (see Appendix AD).	Future research projects should increase engagement with leading growers and consultants to facilitate information transfer and target growers from interstate production regions. Many growers are not currently in the position to adopt new management systems but will learn from the examples of leading growers if market conditions allow in future.
EFFICIENCY: What efforts did the PIPS3 Program partners make to improve efficiency? Did the projects efficiently manage shared resources and utilise skills and knowledge within other PIPS3 Program projects?	Project preschedule documents were shared with other projects. Staff and resources were shared with other PIPS3 projects, where possible. Strong connections with AP19005 were established from the start due to similar research lines and staff. A mid-term program meeting helped define a shared vision for the future PIPS 4 Profit program. The AP19003 respondents rated the PIPS3 Program as strong on its performance to deliver an efficient approach to research, and communication and extension of the research. There was constructive feedback provided on ways in which projects could improve their "whole-of-system" perspective on data collection, sharing, interpretation and management implications. AP19003 efficiency rating was 4.3 on a scale from 0 – 5 (see Appendix AD).	Future research will need to adopt a systems approach where soil, irrigation and pests and diseases management are considered.
LEGACY: Are there signs that the PIPS3 Program will influence apple and pear growers in the future? To what extent has the project resulted in greater confidence, intention to adopt, or adoption of new orchard design and the uptake of sensor technologies?	AP19003 was the only project to rate higher on the likelihood of adoption in the next ten years over delivering improved knowledge and understanding. There were indicators that some adoption was already occurring such as advisors providing *Cartographer* scanning of orchards and changes to orchard management for reduced heating and sunburn impacts AP19003 legacy rating was 4.5 on a scale from 0 – 5 (Improved knowledge & understanding of the concepts = 4.3 & Likelihood of adoption < 10 years = 4.7) (see Appendix AD).	Continued support for online information (e.g., short videos), endorsement of the Tatura SmartFarm as an extension resource, more regional showcases, and greater sharing of grower experiences through on-farm trials of ag tech.

Recommendations

The following agronomic recommendation for apple growers can be made because of the research that was undertaken in this project:

- Orchard productivity is threatened by frequent hailstorms and heat events. New orchards need to be netted.
- M.9 performs better than M.26 and Bud.9 for trees spaced at 1 and 3.5m within and between rows, respectively.
- Precise crop load strategies (i.e., 6 – 8 fruit per cm^2 TCSA in 'Cripps Pink' sports) need to be imposed to achieve consistent crop load and fruit quality.
- In multileader trees, the individual leaders (uprights) should be used as crop load management units to improve management and consistency.
- Reliable pre-harvest spatial measures of apple orchard productivity (flower and fruit number, fruit size and colour, and tree size) are now available to fruit growers and scientists through ground-based mobile sensing technologies (e.g., *Cartographer*).
- Mobile scans (e.g., from *Cartographer*) for peel colour are preferably done early in the morning or late in the afternoon, when external light is reduced.

The following future research for apples is recommended:

- Evaluate the utility of spatial data to provide orchard-specific crop load management rules based on tree size to target fruit size.
- Undertake an economic analysis of spatial management including fruit thinning, pruning and variable rate spraying.
- Determine labour use efficiency with traditional methods against using Ag Tech.
- Study the effects of a combination of crop load levels and light environment under netting on productivity.

Refereed scientific publications

Scalisi, A., McClymont, L., Underwood, J., Morton, P., Scheding, S. and Goodwin, I., 2021. Reliability of a commercial platform for estimating flower cluster and fruit number, yield, tree geometry and light interception in apple trees under different rootstocks and row orientations. Computers and Electronics in Agriculture, 191, 106519. https://doi.org/10.1016/j.compag.2021.106519

Reddy, P., Plozza, T., Ezernieks, V., Stefanelli, D., Scalisi, A., Goodwin, I. and Rochfort, S., 2022. Metabolic pathways for observed impacts of crop load on floral induction in apple. International Journal of Molecular Sciences, 23 (11), 6019. https://doi.org/10.3390/ijms23116019

Scalisi, A., McClymont, L., Peavey, M., Morton, P., Scheding, S., Underwood, J. and Goodwin, I., 2023. Using Green Atlas Cartographer to investigate orchard-specific relationships between tree geometry, fruit number, fruit clustering, fruit size and fruit colour in commercial apples and pears. Acta Horticulturae, 1360, 203–210. https://doi.org/10.17660/ActaHortic.2023.1360.25

Peavey, M., Scalisi, A., McClymont, L. and Goodwin, I., 2023. Light interception, productive performance and red colour coverage of 'ANABP 01' apple trees grown on different rootstocks in a multidirectional orchard. Acta Horticulturae, 1366, 103–110. https://doi.org/10.17660/ActaHortic.2023.1366.12

References

Anderson, N.T., Walsh, K.B., Wulfsohn, D., 2021. Technologies for Forecasting Tree Fruit Load and Harvest Timing—From Ground, Sky and Time. Agron. 2021, Vol. 11, Page 1409 11, 1409. https://doi.org/10.3390/AGRONOMY11071409

Embree, C.G., Myra, M.T.D., Nichols, D.S., Wright, A.H., 2007. Effect of blossom density and crop load on growth, fruit quality, and return bloom in "Honeycrisp" apple. HortScience 42, 1622–1625. https://doi.org/10.21273/hortsci.42.7.1622

Goodwin, I., Whitfield, D.M., Connor, D.J., 2006. Effects of tree size on water use of peach (Prunus persica L. Batsch). Irrig. Sci. 24, 59–68. https://doi.org/10.1007/s00271-005-0010-z

Guitton, B., Kelner, J.J., Velasco, R., Gardiner, S.E., Chagné, D., Costes, E., 2012. Genetic control of biennial bearing in apple. J. Exp. Bot. 63, 131–149. https://doi.org/10.1093/jxb/err261

Islam, M.S., Scalisi, A., O'Connell, M.G., Morton, P., Scheding, S., Underwood, J., Goodwin, I., 2022. A Ground-based Platform for Reliable Estimates of Fruit Number, Size, and Color in Stone Fruit Orchards. Horttechnology 32, 510–522. https://doi.org/10.21273/HORTTECH05098-22

Milyaev, A., Kofler, J., Klaiber, I., Czemmel, S., Pfannstiel, J., Flachowsky, H., Stefanelli, D., Hanke, M.V., Wünsche, J.N., 2021. Toward Systematic Understanding of Flower Bud Induction in Apple: A Multi-Omics Approach. Front. Plant Sci. 12, 286. https://doi.org/10.3389/fpls.2021.604810

Milyaev, A., Kofler, J., Moya, Y.A.T., Lempe, J., Stefanelli, D., Hanke, M.-V., Flachowsky, H., von Wirén, N., Wünsche, J.-N., 2022. Profiling of phytohormones in apple fruit and buds regarding their role as potential regulators of flower bud formation. Tree Physiol. 42, 2319–2335. https://doi.org/10.1093/TREEPHYS/TPAC083

Milyaev, A., Kofler, J., Pfannstiel, J., Stefanelli, D., Flachowsky, H., Hanke, M. V., Wünsche, J.N., 2018. Histological and proteomic approaches to study floral bud induction in relation to biennial bearing in apple. Acta Hortic. 1229, 277–283. https://doi.org/10.17660/ActaHortic.2018.1229.42

Peavey, M., Scalisi, A., McClymont, L., Goodwin, I., 2023. Light interception, productive performance and red colour coverage of 'ANABP 01' apple trees grown on different rootstocks in a multidirectional orchard. Acta Hortic. 1366, 103–110. https://doi.org/10.17660/ActaHortic.2023.1366.12

Reddy, P., Plozza, T., Ezernieks, V., Stefanelli, D., Scalisi, A., Goodwin, I., Rochfort, S., 2022. Metabolic Pathways for Observed Impacts of Crop Load on Floral Induction in Apple. Int. J. Mol. Sci. 23, 6019. https://doi.org/10.3390/IJMS23116019/S1

Scalisi, A., McClymont, L., Peavey, M., Morton, P., Scheding, S., Underwood, J., Goodwin, I., 2023. Using Green Atlas Cartographer to investigate orchard-specific relationships between tree geometry, fruit number, fruit clustering, fruit size and fruit colour in commercial apples and pears. Acta Hortic. 203–210. https://doi.org/10.17660/actahortic.2023.1360.25

Scalisi, A., McClymont, L., Underwood, J., Morton, P., Scheding, S., Goodwin, I., 2021. Reliability of a commercial platform for estimating flower cluster and fruit number, yield, tree geometry and light interception in apple trees under different rootstocks and row orientations. Comput. Electron. Agric. 191. https://doi.org/10.1016/j.compag.2021.106519

Scalisi, A., O'Connell, M.G., Islam, M.S., Goodwin, I., 2022. A Fruit Colour Development Index (CDI) to Support Harvest Time Decisions in Peach and Nectarine Orchards. Horticulturae 8. https://doi.org/10.3390/horticulturae8050459

Stefanelli, D., Plozza, T., Darbyshire, R., Flachowsky, H., Wünsche, J.N., 2019. Effects of crop load on apple fruit maturity. Australian Fruit Grower 13(1), 36–38. https://apal.org.au/news-and-resources/apal-publications/

Stefanelli, D., Plozza, T., Flachowsky, H., Wünsche, J.N., 2018. Young apple tree responses to crop load. Acta Hortic. 1229, 221–228. https://doi.org/10.17660/ACTAHORTIC.2018.1229.34

Intellectual property

No project IP or commercialisation to report. Effects of fruit position and sun exposure on fruit quality, identified potential chemical signals that effect floral initiation, crop load and fruit quality response functions from data collected in designed experiments, and field testing of sensors to measure crop parameters and generate orchard-specific tree-scale crop load targets were published and made widely available through Agriculture Victoria (DEECA) and APAL. No patent or copyright issues were identified during the project. Sensor testing was undertaken in agreement with the manufacturers.

Acknowledgements

The project leader and authors of this report would like to acknowledge the project reference group, Apple and Pear Australia Limited, PIPS3 program coordinator Marguerite White (ICD Project Services), Adrian Hunt (Hort Innovation) and Nic Finger for horticultural advice. We also gratefully acknowledge Jason Shields (Plunkett Orchards), Brent Reeve (Geoffrey Thompson) for granting access to commercial orchards. Technical support and assistance of Rajandeep Singh, Laura Phillips, Katerina Zissimos, Jyothi Bhandari, Asha Gould, Shrawan Poudel, Dave Haberfield, Jim Selman, Naveen Valluri, Susanna Turpin, Doris Ram, Subhash Chandra and Vilnis Ezernieks are gratefully acknowledged.

Appendices

Appendix A Methodology Preschedule

Appendix B Draft Industry article on radiation exposure and sunburn damage

Appendix C Draft paper on light and temperature effects on colour expression and bleaching

Appendix D Draft paper on forced biennial bearing effects in 'Rosy Glow'

Appendix E Report summary on crop load results in 'Rosy Glow'

Appendix F Chemical signalling report on 'Rosy Glow'

Appendix G Draft paper on crop load effects on yield and fruit quality in 'Ruby Matilda'

Appendix H Technical report on chemical signals in 'Ruby Matilda'

Appendix I Technical report on crop load effects on organic metabolites in 'Ruby Matilda'

Appendix J Draft paper on metabolites in 'Ruby Matilda'

Appendix K Technical report on sensing spatial distribution in 'ANABP-01'

Appendix L Technical report on *Cartographer* (Nov 22)

Appendix M Technical report on *Cartographer* (Nov 21)

Appendix N Report summary on light interception and rootstock effects in 'ANABP 01'

Appendix O Industry article on rootstock effects on canopy and fruit quality of 'ANABP 01'

Appendix P Presentation at the 2021 APAL Tech Forum

Appendix Q Industry article on crop load in 'Rosy Glow'

Appendix R Industry article on unveiling apple block variability using Green Atlas *Cartographer*

Appendix S IHC 2022 presentation on *Cartographer*

Appendix T Report on Evaluating the utility of sensors and platform

Appendix U Portfolio of Green Atlas spatial maps in commercial orchards

Appendix V Technical report describing new technology and management system

Appendix W Industry article on PIPS3

Appendix X Industry article on advancing apple orchard production systems

Appendix Y Presentation on indirect measurements in tree crops using advanced technologies

Appendix Z IHC oral presentation on utilising *Cartographer* for orchard-specific relationships

Appendix AA IHC poster presentation on effects of rootstocks and row orientation on 'ANABP 01'

Appendix AB Industry article on turning off biennial bearing

Appendix AC Consultant industry article on *Cartographer*

Appendix AD Monitoring and evaluation

RESEARCH PRE-SCHEDULE

Advancing sustainable and technology driven apple orchard production systems

AP19003

Ian Goodwin, Alessio Scalisi, Tim Plozza, Priyanka Reddy, Simone Rochfort, Lexie McClymont and James Underwood

RESEARCH PRE-SCHEDULE

Advancing sustainable and technology driven apple orchard production systems

Project Summary

The Australian apple industry, like many fruit production industries, is plagued by high cost of production and variable fruit quality that often does not meet consumer expectations. This can greatly reduce a grower's profitability. In the last ten years, apple production is yet to reach its full potential based on the area planted (10,000 ha) and the theoretical yield (~800,000 t). This is mostly due to variable crop load management, biennial bearing and inconsistent fruit quality.

Australia has a unique climate characterised by relatively high temperatures and light intensity compared to other apple production areas around the world. Light interception and consequent carbohydrate availability play an important role in defining the optimal number of fruit that a tree should hold to maximise consistent fruit quality for the life of the tree. Furthermore, light interception and carbohydrate supply are fundamental in influencing fruit quality in a variable climate of extreme heat events.

Apple is generally susceptible to biennial bearing which is the tendency to alternate years of high flower initiation followed by low initiation the subsequent year. From previous studies on crop load management of an established cultivar ('Rosy Glow') and emerging cultivar ('Nicoter'), it was noticed that there is an inverse correlation between fruit number on trees and most aspects of fruit quality (size, soluble solids concentration, colour), and a direct correlation with fruit maturity and flesh firmness (projects AP15013 and AP15002). These previous studies found that biennial bearing is controlled at tree level from a combination of genetics (flower induction genes) and environment (carbohydrate availability) probably mediated by metabolites that act as chemical signals that either stimulate or inhibit the activation of the genes.

Physiological studies and the development of sensing tools will be undertaken in the Sundial apple orchard at the Tatura SmartFarm and in a commercial orchard in the Yarra Valley to address the following three objectives as per the Hort Innovation RFP:

- Develop crop load, training systems, pruning and irrigation optimisation for yield, quality and labour efficiency in new and emerging apple cultivars.
- Develop orchard design techniques, tools and management practices that enhance the ability of orchards to manage climate variability and weather extremes.
- Communicate findings in a clear and practical format to growers and wider industry.

The intended outcome of this project is to improve crop load management in a variable climate by providing knowledge and tools to deliver premium fruit that meets consumer expectations in domestic and export markets.

1. Background

The Australian apple industry, like many fruit production industries, is plagued by some common problems. The most common are high cost of production and fruit quality that does not meet consumer expectation. These two problems combined can significantly reduce grower's profitability. Managing various inputs to optimise the production system (i.e. cultivar genetics, canopy training, water, rootstock, nutrients, light interception, soil) will improve a grower's ability to meet market specification/expectation for fruit quality and lead to higher prices and improved profitability. Modern horticulture is moving toward increased mechanization, automation, robotics, and non-destructive sensing and monitoring. The

integration of next generation technologies in horticulture systems should allow for increased resource use efficiency (including labour) and make orchards more profitable.

Australia has a unique climate characterised by relatively high temperatures and light intensity compared to other apple production areas around the world (Darbyshire et al, 2018). While high light intensity allows for high photosynthetic rates and consequently carbohydrate availability, when excessive and combined with high air temperature can cause sunburn, damage the leaf photosynthetic apparatus or induce stomata closure for long periods during the day thereby reducing carbohydrates. Light interception and consequent carbohydrate availability will play an important role in defining the optimal number of fruit and the position of fruit within the canopy to meet market specification for fruit quality. It is therefore preferable to identify the optimal light interception conditions within the tree canopy that will minimise sunburn and maximize carbohydrate availability rather than trying to harvest as much light as possible.

Apples are generally susceptible to biennial bearing which is the tendency to alternate years of high floral initiation followed by low initiation the subsequent year. This unbalancing creates high variability within and between trees and consequently the orchard, making crop load management even more difficult. The variability in fruit numbers translates to inconsistent fruit quality and reduced consumer satisfaction (Stefanelli et al, 2018). From previous studies on crop load management of an established cultivar ('Rosy Glow') and an emerging cultivar ('Nicoter') in projects AP15013 and AP15002, it was noticed that there is an inverse correlation between fruit number on trees and most aspects of fruit quality (size, soluble solids concentration, colour), and a direct correlation with fruit maturity and flesh firmness (Stefanelli et al, 2019). It was also noticeable that fruit from trees that had been forced into biennial bearing (artificially alternating high and low fruit numbers) had reduced quality traits compared to fruit from trees with constant fruit numbers (either high or low).

Biennial bearing is controlled at tree level from a combination of genetics (flower induction genes) and environment (carbohydrate availability) and most likely mediated by metabolites that act as chemical signals that either stimulate or inhibit the activation of the genes (Milyaev et al, 2018). Previous projects AP15013 and AP15002 partially confirmed this by identifying clusters of candidate genes as well as several possible signalling metabolites. The presence of these metabolites was further substantiated by the formation of zones within trees that showed biennial behaviour independent to the rest of the tree. These zones were generally branches or areas (i.e. treetops) that started with high flower numbers but became biennial while the rest of the tree showed relatively constant flower numbers. The fact that flower induction in these zones was different from the rest of the tree indicates a localised signal. Furthermore, the fruit in these zones showed the quality pattern of the rest of the tree suggesting that these zones are not autonomous with respect to carbohydrate utilisation. For example, small fruit with low °Brix in trees with a high crop load were found in zones where the number of fruit was very low. This was contrary to expectation due to the high local carbohydrate availability. It would be very beneficial for the apple industry to identify signalling metabolites than when utilised would stimulate the trees to balance flowering within the whole tree.

1.1 Objectives

Broadly, the objectives of AP19003 are to:

- Investigate the dynamics of fruit position and light exposure on colour development, sunburn damage, fruit quality and floral initiation using the Sundial experimental orchard and technology such as LiDAR combined with solar position and light extinction models.
- Explore the physiological mechanism (e.g. chemical signals) for observed impacts of high crop load on floral initiation and flower development, and the subsequent season(s) fruit size, assimilation and translocation of carbohydrate to fruit.

- Develop a rapid orchard assessment tool using sensing technologies (e.g. proximal sensing of light interception, fruit number and fruit size) to determine crop load for optimum fruit size in apple orchards.

2. Methodology

The project will deliver experimental research and provide demonstration to the apple industry by utilising the experimental Sundial orchard at the Tatura SmartFarm and commercial orchards in the Goulburn Valley.

The different row orientations combined with different rootstocks in the Sundial orchard will allow studies to be undertaken to investigate the ideal light exposure to maximise carbohydrate availability and crop load toward optimal yield and fruit quality in the emerging cultivar 'ANABP 01' (marketed as Bravo™). In addition, data generated by Sundial orchard will further benefit apple growers by identifying ideal row orientation to manage climate variability (e.g. reducing the risk of sunburn from an increase in the number of extreme heat events) and by identifying temperature thresholds for protective interventions (i.e. evaporative cooling).

Crop load treatments have been established in a commercial 'Ruby Pink' apple orchard in the Goulburn Valley to identify metabolites that influence biennial bearing. Trees are trained to a vertical two-leader system. Five crop loads (1, 6, 11, 16, or 21 fruit/cm^2 TCSA) have been applied to the 'primary' leader on each tree, and either a low (1 fruit/cm^2 TCSA) or high (21 fruit/cm^2 TCSA) crop load were applied to the 'secondary' leader. This will enable studies on the localised impact of crop load and the movement of signals from one leader to another.

The project will work with Green Atlas to calibrate and validate mobile platform sensor measurements of fruit number, fruit size, fruit colour and tree size. The calibrated sensors will be used to capture data across an orchard block and processed to establish an orchard-specific relationship between fruit number (per unit of radiation intercepted by the tree's foliage) and average fruit size. This relationship can then be used by an orchard manager in subsequent seasons to determine the tree-scale crop load depending on the target final fruit size. Two commercial orchard blocks will be scanned in the second season of the project to test the approach in a commercial orchard.

2.1 Row orientation, fruit position, light exposure and fruit quality

Experiment objectives

- Investigate the influence of row orientation and rootstock on (i) flower cluster number, (ii) light interception and leaf conductance as a measure of photosynthesis, (iii) fruit quality [i.e. skin colour, soluble solids concentration (SSC), flesh firmness (FF), sunburn damage, fruit diameter (FD) and fruit shape] and fruit maturity [i.e. starch and Index of absorbance difference (IAD)], and (iv) crop load, yield and yield efficiency.
- Investigate the effect of within-tree fruit position on fruit light exposure, fruit surface temperature, and fruit quality (i.e. skin colour, SSC, FF, sunburn damage, fruit diameter and fruit shape).

Hypotheses

- The first hypothesis of this study is that row orientation will affect light interception and in turn have an influence on crop characteristics such as fruit quality, maturity, crop load and yield.
- The second hypothesis is that different rootstocks will cause a change in tree architecture that will in turn influence intercepted light, and that rootstocks may delay or bring forward maturity and induce changes in fruit quality.
- The third hypothesis is that fruit position and light environment within the canopy will produce an effect on fruit quality parameters.

2.1.1 Treatments and experimental design

The Sundial orchard at the Tatura SmartFarm (36.437° S, 145.268° E; 114 m APSL) is a high-density (HD) circular orchard of approximately 1.3 ha and hosts the nectarine cultivar 'Majestic Pearl' and the apple cultivar 'ANABP 01' (commercialised as Bravo™). The nectarine and apple cultivars are each planted in a semicircle of the orchard following four different row orientations (i.e. N – S, NE – SW, E – W and SE – NW). The 'ANABP-01' trees are trained on a vertical trellis in a 2D system and at 1 m spacing. The row spacing is 3.5 m and there is a total of twenty rows — five rows per row orientation. Trees were grafted onto three different rootstocks in a completely randomised design and planted on site in 2018. The tree rootstocks are Bud9, M9 and M26. Each row is subdivided into three panels (i.e. experimental plots) separated by posts, one for each rootstock, which is in turn composed of 11 'ANABP-01' trees and one polleniser ('Granny Smith'). A representation of a plot is shown in Figure 1. 'ANABP-01' originated from a cross-pollination between 'Cripps Red' and 'Royal Gala'. The cultivar was bred by the Department of Agriculture and Food, State of Western Australia. Fruit have dark purple colouration and consistent cropping characteristics (Cripps, 2016).

The soil is a red-brown earth (Stace et al. 1968) or Red Sodosol (Isbell 2002) known locally as a Shepparton fine sandy loam (Skene and Poutsma 1962). The region has a temperate climate with average annual rainfall of approximately 480 mm. Annual average reference crop evapotranspiration (ETo, Allen et al., 1998) is approximately 1190 mm (22-year mean, http://www.longpaddock.qld.gov.au/silo/).

The different row orientations combined with different rootstocks in the Sundial orchard allow studies to be undertaken to investigate the ideal light exposure to maximise carbohydrate availability and crop load toward optimal yield and fruit quality in the emerging cultivar 'ANABP 01'. Data generated in the Sundial orchard will further benefit apple growers by identifying ideal row orientation to manage climate variability (e.g. reducing the risk of sunburn from an increase in the number of extreme heat events) and by identifying temperature thresholds for protective interventions (i.e. evaporative cooling).

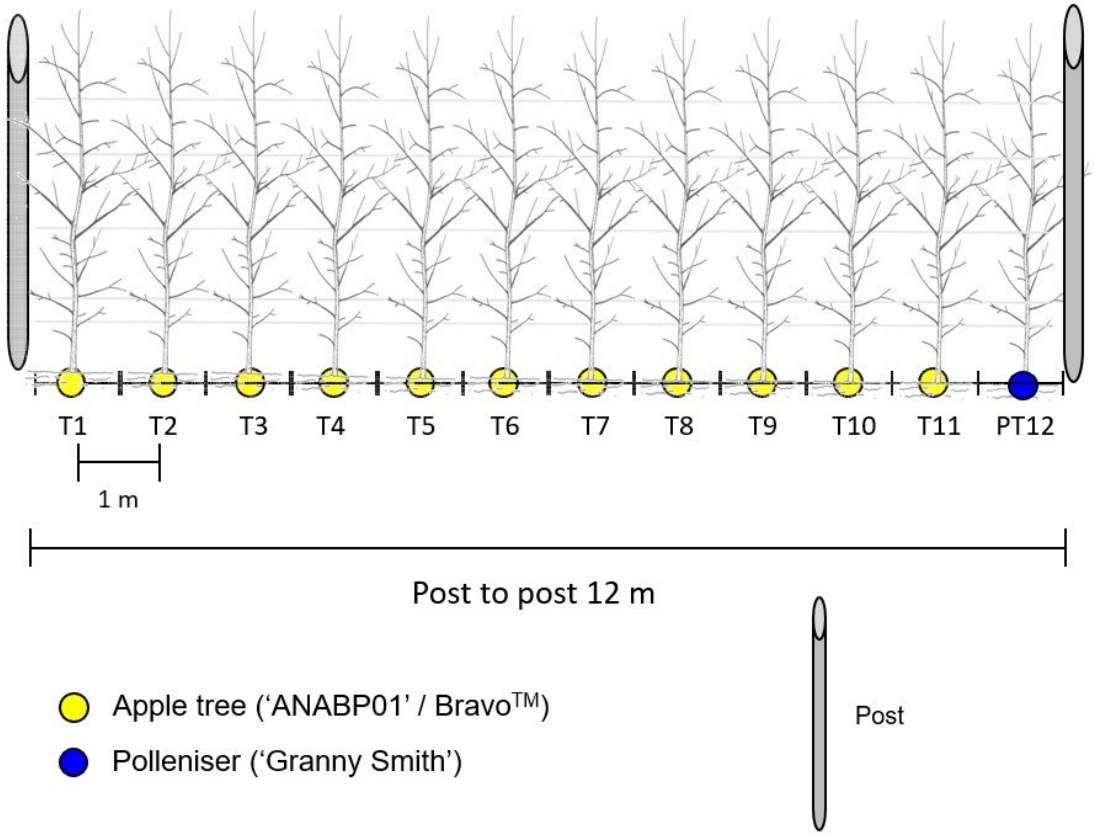

Figure 1. Plot structure in the Sundial orchard.

2.1.2 Effects of row orientation and rootstock

The effects of row orientation and rootstock and their interaction on (i) flower cluster number, (ii) leaf conductance and light interception, (iii) fruit quality and fruit maturity, and (iv) crop load, yield and yield efficiency, will be evaluated on 36 plots (shown in colours in Figure 2).

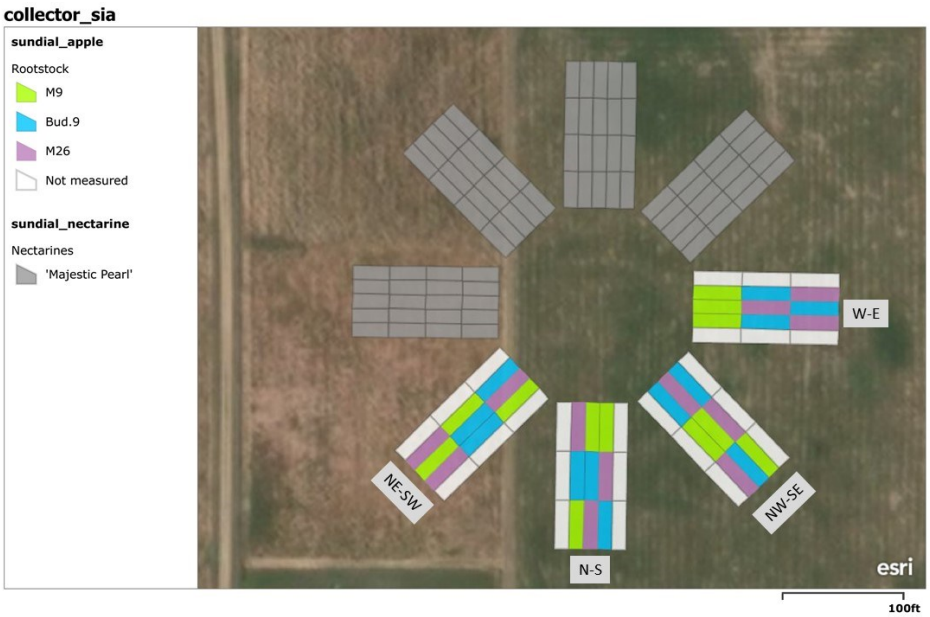

Figure 2. 'ANABP-01' apple plots in the Sundial orchard selected to test the effects of row orientation and rootstock on selected crop variables.

Flower cluster number

Flower cluster numbers will be estimated using the Green Atlas Cartographer™ and the algorithms obtained for apple flower cluster recognition. Sundial orchard plots will be scanned on both sides in systematic order, such that plots are always scanned in the same order and all plots within an experiment are scanned with only the left cameras. Mobile short scans will be collected in the plots shown in Figure 2. The posts will serve as markers to indicate the start and the end of each scanned section. Only if required, vertical pink flagging tape will be used to identify sub-sections (< 12 m) within each panel.

Continuous mobile scans of all the measurement rows in the Sundial orchard will be done to collect data that will be back processed when the high-resolution models will be obtained. The geographic precision of plot extraction from continuous scans using GIS shapefiles will be inspected with and without real-time kinematic (RTK) positioning.

Leaf conductance and light interception

Leaf conductance will be measured on three leaves per plot in the plots shown in Figure 2 — for a total of 106 leaves — in the mid-morning (1000 – 1100 h, AEST) of a summer, clear-sky day. A dynamic diffusion porometer (AP4, Delta-T Devices LTD, Cambridge, UK) will be used to determine leaf conductance (g_l).

Canopy photosynthetically active radiation (PAR) interception will be measured using a handheld ceptometer (Sunfleck Ceptometer; Decagon, Pullman, USA) and a light trolley (Tranzflo, New Zealand). The light trolley holds 24 PAR sensors at 0.125 m intervals along a 3 m bar, 0.4 m above ground-level on a wheeled base. A data logger (CR850, Campbell Scientific, Garbutt, Au) records measurements at 1 s intervals. Measurements of transmitted PAR (PAR_t) will be made over the planting square of the central trees in each plot at solar noon and three and a half hours before and after solar noon on a clear sky day. The ceptometer and light trolley sensors will be held horizontally below the canopy, perpendicular to the row direction, and moved at a slow walking speed with the ceptometer being used to measure PAR_t in those areas of the planting square not easily accessible to the light trolley. Unobstructed incoming PAR (PAR_i) will be measured at 1.5 m above ground level in an open area. Daily light intercepted by the trees (MJ/m2/day) will be estimated from effective area of shade (EAS), the standard parameter used as a reference of light interception at the Tatura SmartFarm, and total daily global radiation. EAS will be calculated from the average of the three fractional PAR interception measurements (i.e. solar noon, solar noon – 3.5 h and solar noon + 3.5 h) (Goodwin et al., 2006). EAS will be calculated in the plots shown in Figure 2.

Short mobile Cartographer™ scans will be collected on the same plots on the same day, with the former being preferably done near dawn or dusk. Tree geometry data (i.e. tree height, canopy area and canopy density) extracted from the Cartographer™ will be used as a measure of intercepted light.

Fruit quality and maturity

Fruit skin colour parameters (e.g. a* and H°) and fruit diameter will be estimated in situ prior to harvest using the Green Atlas Cartographer™ and algorithms previously calibrated and validated. The process will follow the methodology used for flower cluster scans.

Fruit in each plot will be harvested and scanned with a commercial fruit grader equipped with optical sensors (Compac InVision 9000, Compac Sorting Equipment Ltd, Australia) to estimate skin colour (i.e. % of background and overcolour), SSC, FF and FD. A batch of 10 fruit per plot will be sub-sampled for further non-destructive and destructive determinations. Fruit will be classified into the following groups based on their external characteristics:

- Shape: binary shape classification [0 = regular / obloid (Cripps, 2016); 1 = misshapen]

- Overcolour: on a scale from 1 to 5 based on Figure 3a.
- Background colour: on a scale from 1 to 5 based on Figure 3b.
- Sunburn classes: on a scale from 1 to 5 based on Figure 3c.

The same 10 fruit will be then scanned on two opposite cheeks with a DA-meter to determine the IAD and with a colourimeter (Rubens Technologies, Ltd) to determine colouration in the CieLAB space (i.e. a*, b*, C*, H° and L*). Then, fruit will be subjected to SSC determination with a digital refractometer (PR-1; ATAGO CO., LTD, Saitama, Japan) and FF determination with a penetrometer equipped with an 8 mm tip (FT327, FACCHINI srl, Alfonsine, Italy). Last, fruit will be cut through the equator and sprayed with the iodine solution. Starch degradation index will be determined based on the classification reported in Figure 4.

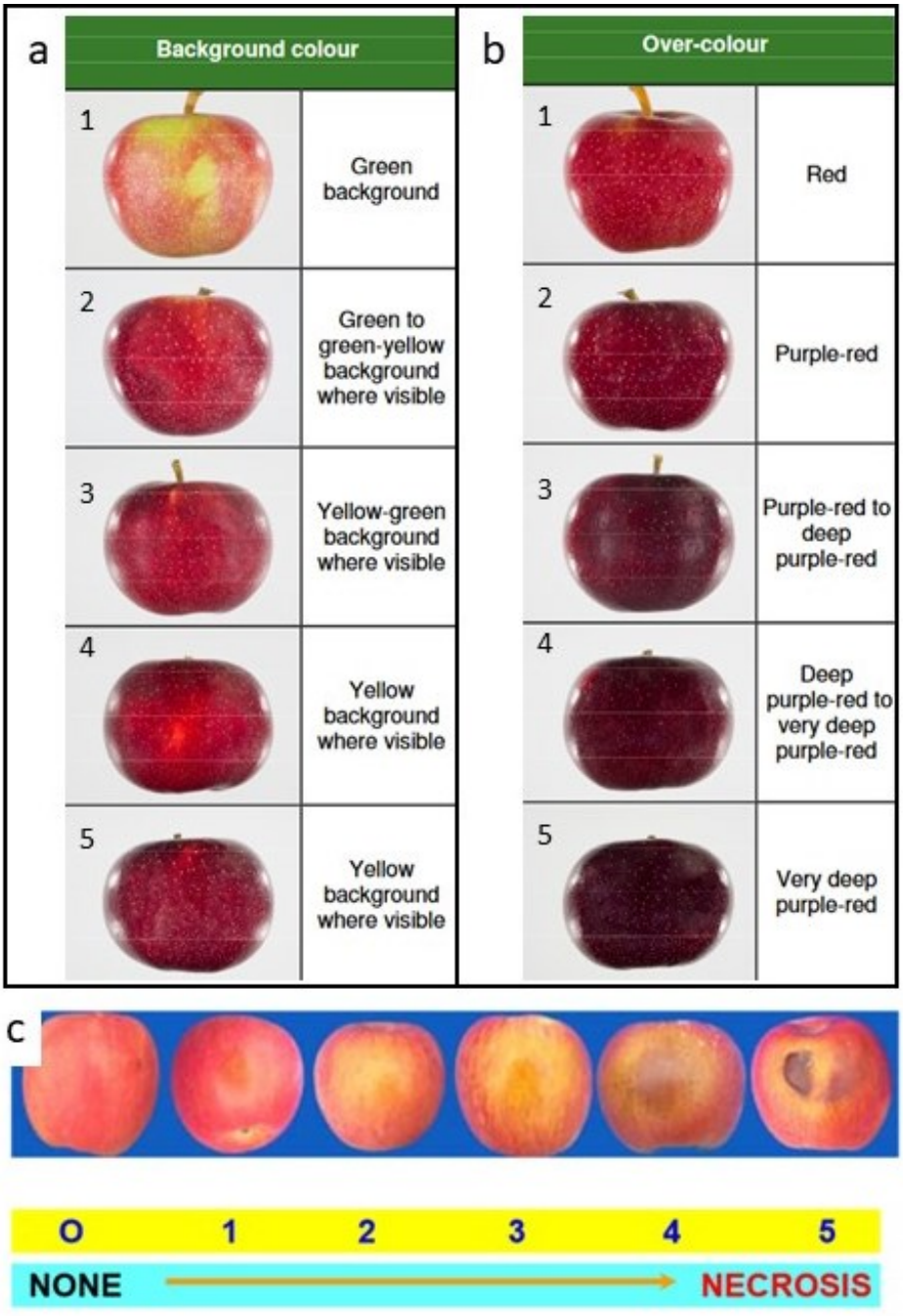

Figure 3. Background colour (a) overcolour (b) and sunburn (c) visual classifications. Modified from Steele et al. (2017) and Schrader et al. (2003).

Figure 4. Starch degradation classification. Modified from Steele et al. (2017).

Crop load and yield

Crop load and yield will be estimated in situ prior to harvest using the Green Atlas Cartographer™ and algorithms previously calibrated and validated. The process will follow the methodology used for flower cluster scans.

In addition, crop load and yield will also be determined after harvest using a commercial fruit grader equipped with optical sensors (Compac InVision 9000, Compac Sorting Equipment Ltd, Australia).

Yield efficiency will be expressed as kg of fruit per cm^2 of TCSA. TCSA measurements for each tree in the 36 plots (Figure 2) will be collected near harvest.

2.1.3 Effects of fruit position, light exposure and surface temperature on fruit quality

Individual fruit (≥9, i.e. 3 low, 3 medium and 3 high fruit) in each of the plots shown with colours in Figure 5 will be tagged with coloured tape. Where possible, a proportion of fruit showing colour degradation (bleaching, sunburn) or poor colour development (over-colour score 1) will be selected. Fruit will be selected from three different canopy heights (< 1 m, between 1 and 2 m and > 2 m). Fruit position will be determined using a static LiDAR 3D laser scanner (Leica BLK360). X and Y Coordinates will be assigned to each fruit, with x representing horizontal shift (x = 0 at the trunk) and Y representing vertical shift (y = 0 at the ground level).Considering that trees in the Sundial orchard are in a 2D setting, a Z (depth) coordinate will not be extrapolated. LiDAR measurements will be collected at two different points for each side of the selected plots and point cloud images will be stitched together using software.

Fruit light exposure

Fruit light exposure will be measured using a spot PAR reader (Rubens Technologies, Ltd) at three times of a clear-sky day (e.g. solar noon, solar noon – 3.5 h and solar noon + 3.5 h).

Fruit surface temperature

Fruit surface temperature will be measured continuously over a week prior to harvest using thermocouples wired to CR1000 data loggers. The thermocouples (type T, copper-constantan) will be gently inserted underneath the fruit peel and the data logger will be programmed to collect data at 5 min intervals. A weather station located in the BOM site nearby will provide continuous ambient temperature records.

Leaf conductance

A dynamic diffusion porometer (AP4, Delta-T Devices LTD, Cambridge, UK) will be used to determine leaf conductance (g_l) in the proximity of the tagged fruit, to determine whether reduced leaf stomatal aperture will be triggered by position in the canopy and light environment.

Fruit quality

At harvest, the tagged fruit will be assessed for skin colour (both visually using the scale in Fig. 3 and with a handheld colourimeter), FD, fruit shape, SSC, FF and sunburn damage. The methodology used to measure these parameters is reported in the previous section.

Figure 5. 'ANABP-01' apple plots in the Sundial orchard selected to test the effects of fruit positioning, light exposure, photosynthesis and surface temperature on fruit quality.

2.1.4 Statistical analysis

The effects of rootstock and row orientation on crop variables will be tested using general linear model (GLM) procedures.

Regression analysis techniques, linear mixed models and discriminant analyses will be conducted to verify relationships between fruit position, light exposure, photosynthesis and surface temperature and fruit quality parameters.

2.2 Physiological mechanism of crop load on floral initiation

Experiment objectives

- Explore the physiological mechanism (e.g. chemical signals) for observed impacts of high crop load on floral initiation and flower development, and the assimilation and translocation of carbohydrate within the tree, as evidenced by fruit size and quality attributes in the current and future growing seasons.

Hypothesis

- Metabolites produced by fruitlets, or as a response to the number of fruitlets on apple trees, act as chemical signalling compounds which either stimulate or inhibit the number of buds which become flowers in the subsequent season, and this effect is localised to individual branches within the tree.
- A low crop load zone within a tree where the rest of the tree has a high crop load will produce fruit of similar size and quality to the rest of the tree, and vice-versa.

2.2.1 Site, treatments and experimental design

The experiment will be conducted at the Plunkett Orchards, 255 Macisaac Rd, Ardmona (36.382° S, 145.326° E, 113 m a.s.l.) in the Goulburn Valley, Victoria, Australia. 'Ruby Pink' apple trees which have been trained into a two-leader vertical trellis configuration will be used for this experiment.

The experiment will utilise 30 trees occupying a single row in the orchard. There will be three replicates ('Blocks' in Figure 6), each consisting of 10 trees (two panels of five trees). One of five crop loads (20, 70, 120, 170 and 220 fruit per leader) will be applied to the 'Primary' leader on each tree, and one of two crop loads (Low (1 fruit/cm^2 TCSA) or High (21 fruit/cm^2 TCSA)) applied to the 'Secondary' leader. The randomised application of these treatments is shown in Table 1.

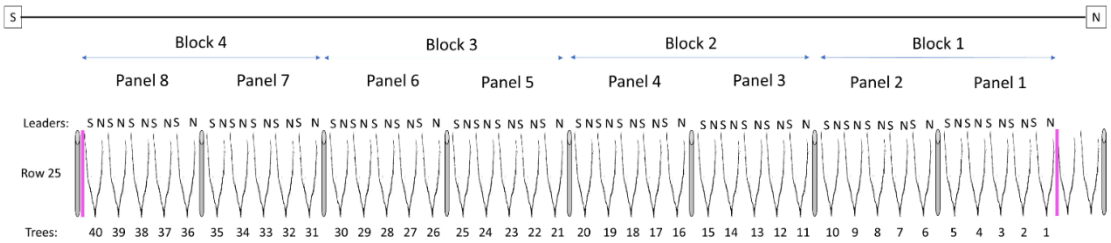

Figure 6: Layout of the 30 experimental trees within the row. N = North, S = South.

Table 1: Randomised application of crop load treatments for the Primary and Secondary leaders of the 'Ruby Pink' apple trees. Low = 20 fruit per leader, High = 220 fruit per leader.

		Crop load (fruit per leader)	
Block	Tree number	Primary leader	Secondary leader
1	1	170	Low
1	2	120	High
1	3	220	Low
1	4	20	Low
1	5	120	Low
1	6	70	Low
1	7	70	High
1	8	20	High
1	9	170	High
1	10	220	High
2	11	170	Low
2	12	220	Low
2	13	120	High
2	14	70	Low
2	15	20	Low
2	16	220	High
2	17	70	High
2	18	20	High
2	19	120	Low
2	20	170	High
3	21	70	Low
3	22	20	High
3	23	220	Low
3	24	120	High
3	25	170	High
3	26	70	High
3	27	220	High
3	28	20	Low

3	29	120	Low
3	30	170	Low

2.2.2 Tissue Sampling for chemical profiling

Bud and leaf material will be sampled in 2020 (bud set only), 2021 and 2022 at four stages of tree growth:

1. Dormancy (July – early August)
2. Bud break
3. After bloom (after petal fall)
4. Bud set (approximately 70 days after full bloom)

Three buds will be collected from each tree at each sampling time — one high on the Primary leader, one low on the Primary leader, and one at mid-level on the Secondary leader. Details of bud sample selection and preparation below.

A fully expanded leaf adjacent to each bud will also be sampled at the 'After bloom' and 'Bud set' stages.

Samples will be frozen in dry ice as soon as possible after collection and stored in a freezer at −80°C until analysis.

Bud sample selection and preparation in-field

Select buds on spurs growing on at least two-year old wood.

Choose spurs on lateral branches of the tree, not from the central leader or the top.

Choose only fruiting spurs with subtending bud (Figure 7a). If bourse shoot > 5 cm don`t sample spur.

Remove bud from tree by breaking it off the spur (Figure 7b).

Remove leaves from the bud (Figure 7c).

Using a scalpel, peel or slice away the brown scales on the bud to leave behind the growing tip with no/minimal brown material (Figure 7d).

Cut off the bud above the wooden part using a scalpel (no woody part should be in sample) (Figure 7e).

Place the prepared bud in an Eppendorf tube, close the cap and place in dry ice.

a. 

b. 

e. 

Figure 7: (a) fruiting spur with subtending bud, (b) bud removed from tree, (c) bud with leaves removed, (d) peeled bud, (e) growing tip removed from woody stem.

2.2.3 Fruit sampling

The index of absorbance difference (I_{AD}) of fruit on all trees will be monitored weekly from approximately 6 weeks before the first harvest for the purpose of predicting the ideal harvest time, which will be when the fruit on the control trees reach commercial maturity. At the first harvest, all suitably ripe fruit will be harvested. Harvested fruit will be counted and weighed to obtain total yield and average fruit weight. A subsample of 20 fruit will be randomly selected to determine fruit weight (FW) as a measure of fruit size, maturity (I_{AD}), colour (background and blush), flesh firmness (FF) and soluble solids concentration (SSC). A digital scale will be used to determine FW, a DA-meter (Turoni srl, Forlì, Italy) will be used to measure the I_{AD} and a colourimeter (Rubens Technologies, Ltd) will be used to scan background and blush colour and will be expressed in the CieLAB scale (i.e. a*, b*, C*, H° and L*). Subsequently, fruit will be subjected to destructive determination of SSC with a digital refractometer (PR-1, ATAGO CO., LTD, Saitama, Japan) and FF with a penetrometer equipped with an 8 mm tip (FT327, FACCHINI srl, Alfonsine, Italy).

2.2.4 Identification and quantification of potential chemical signaling compounds

Bud and leaf samples will be analysed using high-end liquid chromatography-mass spectrometry (LCMS) instruments to find and identify potential chemical signalling compounds related to crop load treatments and return bloom. Methods will include targeted analysis of compounds already identified as potential signalling compounds (from the previous AP15002 project), and untargeted analysis, which involves finding and identifying unknown compounds whose presence and concentration correlate with return bloom measurements.

Sample extraction

All specimens collected will be immediately snap-frozen in liquid nitrogen and stored at −80°C. Specimens from each biological replicate will be kept in separate safe-lock tubes. Apple buds will be ground in liquid nitrogen and metabolites extracted with 80% methanol overnight. Samples will be centrifuged, and the supernatant will be transferred into a microfuge tube and stored at −20°C until ready for analysis.

Targeted analysis: Compound library

The library of standards for the LCMS targeted analysis will include the phytohormones (gibberellins, salicylic acid, as well as cytokinin, auxin and abscisic derivatives). Table 2 provides an example of 20 different phytohormones within these groups.

Table 2: Example of the phytohormones for LCMS targeted analysis.

CLASSES	**DERIVATIVES**
CYTOKININ DERIVATIVES	Adenine, Adenosine, IPR, CZR, TZR, DZR, CZROG, TZROG
AUXIN DERIVATIVES	Indole-3-acetonitrile, Tryptamine, IAA, MeIAA, OXIAA, Tryptophan,
ABSCISIC ACID AND DERIVATIVES	ABA, 7-OH-ABA, Phaseic acid, Dihydroxiphaseic acid, ABAGlu
PHENOLCARBOXYLIC ACIDS	SA

Abbreviations: IPR - isopentenyl-adenine riboside, CZR – cis-zeatin riboside, TZR – trans-zeatin riboside, CZROG - cis-zeatin riboside-O-glucoside, TZROG - trans-zeatin riboside-O-glucoside, IAA – indole-3-acetic acid, MeIAA – methyl-indole-3-acetic acid, OxIAA - 2-oxindole-3-acetic acid, SA – salicylic acid, ABA – abscisic acid, 7-OH-ABA - 7’-hydroxy ABA, ABAGlu - abscisic acid glucosyl ester.

LCMS methods for targeted, untargeted analysis and compound identification

For untargeted and targeted metabolite profiling, a Vanquish Ultra-High Performance Liquid Chromatography (UHPLC) system (Thermo Fisher Scientific, Bremen) with a binary pump, autosampler and temperature-controlled column compartment coupled with a QExactive (QE) Plus mass spectrometer (Thermo Fisher, Waltham, MA, USA; Thermo, Bremen, Germany) detector will be used. The Thermo Fisher QExactive Plus mass spectrometer will be set at positive mode over a mass range of 70 – 1,200 amu with resolution set at 17,000. Nitrogen will be used as the sheath, auxiliary and sweep gas at a flow rate of 28, 15 and 4 L/min, respectively and spray voltage will be set at 3,600 V (positive). Sample injection volumes will range from 3 – 5 µL. Samples will be randomized, and blanks (80% methanol) injected every five samples. A PBQC will be run every 10 samples. Prior to data acquisition, the system will be calibrated with Pierce LTQ Velos ESI Positive and Negative Ion Calibration Solution (Thermo Fisher Scientific). Mass spectrometry data will be acquired using Thermo Xcalibur V. 2.1 (Thermo Fisher Scientific Inc., USA). Quantitative analysis will be conducted using LCQUAN™ Quantitative Software (Thermo Fisher Scientific).

For compound identification of untargeted analysis, a Agilent 1290 infinity High Performance Liquid Chromatography (HPLC) system equipped with a quaternary gradient pump and auto sampler with sample cooler (maintained at 4°C) (Agilent, Walbronn) will be coupled to a Thermo Scientific LTQ Orbitrap Velos ion trap MS system (Thermo Scientific, Waltham, MA, USA; Bremen, Germany), with a heated electrospray ionisation (ESI) source. Data-dependent MS/MS (MS2) spectra will be acquired on selected samples with normalised collision energy of 35 V and an ion max time of 50 microseconds. Source heater temperature will be maintained at 350°C and the heated capillary will be maintained at 320°C. The sheath, auxiliary and sweep gases will be 40, 15 and 8 units respectively, for both positive ion (ESI+) and negative ion (ESI−) mode. Source voltage will be set to 4.2 kV (positive) and 3.2 kV (negative) with a capillary voltage of −70 V. Sample injection volumes will range from 3 to 5 µL. Prior to data acquisition, the system will be calibrated with Pierce® LTQ Velos ESI Positive and Negative Ion Calibration Solution (Thermo Scientific). Spectra will be inspected in Thermo Xcalibur Qual Browser v.2.3.26 (Thermo Fisher Scientific™).

A Thermo Fisher Scientific Hypersil Gold 1.9 µm, 100 mm × 2.1 mm column with a gradient mobile phase, A (0.1% formic acid in H_2O) and B (0.1% formic acid in acetonitrile) at 0.3 mL/min with 98% to 0% A over 20 – 40 min will be explored.

Compounds targeted will be purchased from various sources such as Sigma-Aldrich (St. Louis, MO, USA) and method development steps will be conducted. These include the determination of LoD, LoQ and spike recovery tests. Assessment of peak retention time (RT) and ion extraction window (m/z) on Thermo Xcalibur Qual Browser v.2.3.26 (Thermo Fisher Scientific) will confirm the presence of the compounds.

Untargeted analysis: Compound identification

The data files obtained following LCMS analyses will be processed in the Refiner MS module of Genedata Expressionist® 12.0 optimising the; 1) chromatogram chemical noise subtraction, 2) intensity thresholding, 3) selection of positive mode data only, 4) chromatogram RT alignment, 5) chromatogram peak detection. Analyte identification of significant metabolites will be performed by searching experimental MS1 data through databases METLIN, ChemSpider

(http://www.chemspider.com) and MS/MS data will be searched on MzCloud (https://www.mzcloud.org) and MetFragment®.

To confirm the identification of the compounds, MS2 and MS3 will be performed on the targeted analytes for Level 2 identification. Compounds with significant effects will be purchased for Level 1 identification.

2.2.5 Statistical analysis

Fruit size and quality: The effects of reference leader's crop load and secondary leader's crop load on FW, I_{AD}, SSC and FF will be tested with linear mixed model procedures using JASP (v 0.14, JASP Team, University of Amsterdam, The Netherlands) or GenStat (v. 18.0, VSNI, Hemel Hempstead, UK).

Chemical profiling: Statistical analyses will be performed using the Analyst module of Genedata Expressionist® 12.0 or MatLab. A combination of linear and non-linear procedures will be tested (e.g. multiple regression analyses, partial least square regressions, principal component analyses).

2.3 Crop load assessment tool to maximise fruit size and yield using sensing data obtained from the Cartographer™

Experiment objectives

- Calibrate and validate in situ estimation of (i) flower cluster number (ii) fruit number and yield (iii) fruit size and colour and (iv) tree height and trunk cross-sectional area (TCSA) obtained with the Cartographer™ sensors in the Sundial orchard at the Tatura SmartFarm.
- Evaluate the utility of the Cartographer™ to map the spatial distribution of fruit number, fruit size and fruit colour in two commercial apple orchards.
- Examine the relationship of LiDAR-obtained tree geometry parameters (i.e. tree height, canopy area and canopy density) with reference light interception indices in the Sundial orchard at the Tatura SmartFarm.
- Develop an orchard-specific assessment tool to advise on the spatial distribution of crop load for optimum fruit size and yield from relationships between fruit number, fruit size and tree size (light interception) using data obtained from the Cartographer™.
- Analyse data from two commercial orchards to test and validate algorithms to derive orchard-specific crop load relationships between fruit number, fruit size and tree size (light interception).

Hypotheses

- The first hypothesis of this study is that the Cartographer™ can be trained to accurately predict flower cluster number, fruit number, fruit size and colour and tree height in the Sundial orchard.
- The second hypothesis is that the LiDAR can be a powerful tool for quick mobile light interception measurements in modern orchards.
- The third hypothesis is that relationships obtained from Cartographer™ data can be used in commercial orchards to determine the spatial distribution of crop load to maximise fruit size and yield.

2.3.1 Sites and selected cultivars

Tatura SmartFarm Sundial orchard

The Sundial orchard at the Tatura SmartFarm is a high-density (HD) circular orchard of approximately 1.3 ha and hosts the nectarine cultivar 'Majestic Pearl' and the apple cultivar 'ANABP 01' (commercialised as Bravo™). Both the nectarine and apple cultivars are planted each in a semicircle of the orchard following four different row orientations (i.e. N – S, NE –

SW, E – W and SE – NW). The 'ANABP-01' trees are trained on a vertical trellis in a 2D system at 1 m spacing. The row spacing is 3.5 m and there is a total of twenty rows — five rows per row orientation. Trees were grafted onto three different rootstocks in a completely randomised design and planted on site in 2018. The tree rootstocks are Bud.9, M9 and M26. Each row is subdivided into three panels (separated by posts), one for each rootstock, which is in turn composed of 11 'ANABP-01' trees and one polleniser ('Granny Smith').

'ANABP-01' originated from a cross-pollination between 'Cripps Red' and 'Royal Gala'. The cultivar was bred by the Department of Agriculture and Food, State of Western Australia. Fruit have dark purple colouration and consistent cropping characteristics (Cripps, 2016).

The different row orientations combined with different rootstocks in the Sundial orchard allow studies to be undertaken to investigate the ideal light exposure to maximise carbohydrate availability and crop load toward optimal yield and fruit quality in the emerging cultivar 'ANABP 01'. Data generated in the Sundial orchard will further benefit apple growers by identifying ideal row orientation to manage climate variability (e.g. reducing the risk of sunburn from an increase in the number of extreme heat events) and by identifying temperature thresholds for protective interventions (i.e. evaporative cooling).

Commercial orchards

The selected commercial orchards are located in the Goulburn Valley. Plunkett Orchards is located in Ardmona and the selected block is composed of six-year-old 'Ruby Pink' trees. 'Ruby Pink' was obtained as a limb sport mutation of 'Cripps Pink'. The fruit have an ellipsoid shape, firm flesh and are highly coloured (Staples and Staples, 2006). Trees are trained vertically and have two leaders. Tree spacing is 1.5 m (leaders are spaced at 0.75 m) and row spacing is 3.5 m.

2.3.2 Orchard scans

Protocols for orchard scans are described below. Depending on the data to be collected and subsequent use, scans will be 'mobile' or 'stationary'. Scans will be undertaken by Agriculture Victoria with the Green Atlas Cartographer™. The phone-interface will be used to control logging and enter file notes to aid retrospective identification of scan locations and note relevant scan or plot issues. The Cartographer™ will be driven at a constant speed of approximately 5 km/h. Logging will be switched on a few metres prior to the start of the measurement section and off a few metres past the end of the measurement section.

Mobile orchard scans

Short mobile scans will be conducted to calibrate and validate models for flower cluster number and fruit number and assess tree geometry (tree height, canopy area and canopy density). Plots will be scanned on both sides in systematic order, such that plots are always scanned in the same order and all plots within an experiment are scanned with only the left cameras.

In the Sundial apples, mobile short scans will be collected in the panels used for calibration and validation, using the existing post to post (panel) structure ~ 12m. Only if required, vertical pink flagging tape will be used to identify sub-sections (< 12 m) within each panel.

Continuous mobile scans of all the measurement rows in the Sundial orchard will be done to collect data that will be back processed when the high-resolution models are obtained. The geographic precision of plot extraction from continuous scans using GIS shapefiles will be investigated with and without real-time kinematic (RTK) positioning.

Stationary orchard scans

Stationary scans will be conducted for initial verification of the ability to assess fruit size and colour and TCSA. Images will be collected while Cartographer™ is stationary with cameras directly in front of pink tagged fruit and trunks. Tagged fruit and trunks will be scanned in

systematic order (e.g. west-side of Row 2 scanned N-S with left camera) with only one camera (left). Photographers' grey cards and tennis balls (or similar) will be hung from trellis wires as colour and size references, respectively, within each image.

Mobile scans of the same plots will provide data for the secondary analysis to determine if fruit size and colour can be assessed from scans when the Cartographer™ is in motion.

2.3.3 Calibration and validation of tree parameters in the Sundial orchard

Flower cluster number

A number of plots (≥ 3) in the Sundial orchard will be scanned with the Cartographer™ at ~ 50 – 70 % full bloom for cluster count calibration/validation. Visual assessments of the overall phenological stage of each plot will be made coincident with each scan. Short mobile scans will be conducted as described above. Ground-truth total cluster counts will be done on the day the scans were obtained. The number of clusters with open flowers (i.e. at least a fully open flower in the cluster) and closed clusters at pink balloon blossom stage will be counted.

The images collected by the Green Atlas Cartographer™ will be segmented and used to train a CNN model for flower cluster recognition. A linear regression model of counts obtained with the platform against the ground-truth counts will be used to calibrate the estimation. The robustness of the model will be validated on a separate set of plots (≥ 3). In these plots, ground-truth counts will be collected using the same approach used for calibration. The accuracy and prediction of the validation will be assessed using statistical procedures.

All the apple plots in the Sundial orchard will be scanned continuously at ~ 10%, ~ 50% and full bloom for the prediction of open flower clusters based on the calibration models.

Fruit number and yield

Fruit number will be determined at two stages: after thinning and at harvest. A number of plots (≥ 3) in the Sundial orchard will be scanned with the Cartographer™ after fruit thinning (i.e. end of November, start of December). Short mobile scans will be conducted as described above. Ground-truth fruit counts will be done on the day the scans were obtained.

The images collected by the Green Atlas Cartographer™ will be segmented and used to train a CNN model for fruit recognition. A linear regression model of counts obtained with the platform against the ground-truth counts will be used to calibrate the estimation. The robustness of the model will be validated on a separate set of plots (≥ 3).

All the apple plots in the Sundial orchard will be scanned continuously after thinning for the prediction of fruit number based on the calibration models.

Total yield and fruit number (i.e. crop load) will be determined by harvesting all fruit from the same plots used for fruit count calibration and validation. Fruit will be weighed and counted individually with a commercial fruit grader equipped with optical sensors (Compac InVision 9000, Compac Sorting Equipment Ltd, Australia) to obtain fruit number and yield. Short mobile scans of the same plots will be obtained prior to harvest. Next, all the apple plots in the Sundial orchard will be scanned continuously after thinning for the prediction of fruit number based on the calibration models.

Comparison of extracted (from Cartographer™ scans prior to harvest) and measured (with fruit grader at harvest) fruit numbers will be used for calibration and validation of the fruit recognition software for apples by Green Atlas. Calibration and validation modelling will follow the same protocol used for fruit counts.

Fruit size and colour

Three fruit in each plot — shown with colours in Figure 2 — with one fruit in each height zone ('Low' 0.5 – 1.2 m, 'Middle' 1.2 – 1.8 m and 'High' >1.8 m) in an approximately vertical line

(+/- 0.25 m horizontally) will be tagged with pink tape (plot n = 36, fruit n = 108). Fruit with variable fruit size and colour will be selected. Photographers' grey cards and tennis balls (or similar) will be hung from trellis wires as references within each image. Leaves obscuring the fruit will be removed prior to scanning. The size of tagged fruit and reference tennis ball will be measured with a Bluetooth calliper (OriginCal, iGAGING, San Clemente, California, USA) held parallel to the row direction (i.e. measuring the diameter seen by the cameras) and on the same day of orchard scans. The colour of tagged fruit and reference photographers' grey cards (on each of the three grey bands) will be measured with a portable spectrophotometer (Nix Pro, Nix Sensor Ltd., Hamilton, Ontario, Canada) with a 14 mm aperture, illuminant D65 (colour temperature 6504K, simulates daylight), and observer angle 2°, coincident with orchard scans. The Nix Pro outputs several colour scales, including RGB and CieLAB.

Fruit size and colour coverage will also be measured with the commercial Compac InVision 9000 grader on the same 108 fruits scanned at harvest and the latter will be expressed as percentage of cover colour.

Cartographer™ stationary scans will be collected on the 36 plots (Figure 2) within the Sundial orchard at two or three stages after fruit thinning (e.g. fruit diameter (FD) ~ 20 mm, FD ~ 40–50 mm, FD > 50 mm). Stationary images will be collected while the Cartographer™ is with the left cameras directly in front of the fruit. Mobile scans of all the plots in the sundial orchard will be obtained at the end of each measurement session. Fruit size and colour data corresponding to the tagged fruit will be extracted from stationary images by Green Atlas.

Calibration and validation modelling will be based on the 36 stationary scans

Tree height and trunk cross-sectional area

The same stationary scans collected for fruit size and colour estimation will be used for calibration and validation of tree height and TCSA. The tennis ball will be used as a reference of size for TCSA measurements. Tree height will be determined by the Cartographer™ using LiDAR images, whereas TCSA will be measured using RGB cameras. The ground-truth measurements will be collected with a measuring stick and a digital calliper for tree height and trunk diameter, respectively. Trunk diameter will then be converted into TCSA. The determination of tree height is expected to be already accurate and in line with ground-truth measurements; thus, its use without calibration will be tested with a simple linear regression analysis. If needed, tree height will be calibrated and then validated as done for all the other variables. Calibration and validation for TCSA will follow previous methodologies.

2.3.4 Light interception and tree size

Canopy light interception will be compared to LiDAR-obtained tree geometry parameters such as tree height, canopy area and canopy density. Individual geometry parameters or combinations will be related with the effective area of shade (EAS, Goodwin et al. 2006) — the mean of fractional canopy light interception measured at three times (solar noon, solar noon − 3.5 h and solar noon + 3.5 h) on a clear sky day. Photosynthetically active radiation (PAR) will be measured using a handheld ceptometer (Sunfleck Ceptometer; Decagon, Pullman, USA) and a light trolley (Tranzflo, New Zealand). The light trolley holds 24 light sensors at 0.125 m intervals along a 3 m bar, 0.4 m above ground-level on a wheeled base. A data logger (CR850, Campbell Scientific, Garbutt, Au) records measurements at 1 s intervals. Measurements of transmitted PAR (PAR_t) will be made over the planting square of the central trees in each plot. The ceptometer and light trolley sensors will be held horizontally below the canopy, perpendicular to the row direction, and moved at a slow walking speed with the ceptometer being used to measure PAR_t in those areas of the planting square not easily accessible to the

light trolley. Unobstructed incoming PAR (PAR_i) will be measured at 1.5 m above ground level in an open area.

Short mobile Cartographer™ scans will be collected on ≥ 3 plots (calibration) within the Sundial orchard at two or three stages after fruit set (e.g. fruit diameter (FD) < 20 mm, 20 < FD < 50 mm, FD > 50 mm) — matching different canopy development stages. Validation will be carried out on ≥ 3 plots. Mobile scans and ground-truth data will be collected on the same day, with the former being preferably done near dawn or dusk to minimise sunlight interference with LiDAR measures.

2.3.5 Effect of rootstock and row orientation

The effects of rootstock and row orientation on flower cluster number, crop load, fruit size, fruit colour, yield, TCSA and tree geometry (i.e. tree height, canopy area and canopy density) will be measured using the previously calibrated and validated models.

Short mobile scans will be collected using the Green Atlas Cartographer™ following the timeline reported in Table 3. Three replicates (plots) for each rootstock and row orientation combination will be scanned, for a total of 36 scans for each date (3 rootstocks * 4 row orientations * 3 reps). The selected plots are shown with colours in Figure 2.

Flower cluster number, crop load, fruit size, yield, fruit colour, TCSA, tree height and tree geometry will be extracted by Green Atlas using either the mobile scans, or the GIS shapefiles with treatment information.

If statistical procedures highlight significant effects of rootstocks and row orientations on the observed variables, specific relationships between the measured variables in each rootstock * row orientation setting will be investigated.

Table 3: Estimated dates of Cartographer™ scans in the plots shown in Figure 2.

Variable	**Dates of scan**			
Flower cluster number	~ 50 % bloom		Full bloom	
Crop load	FD < 20 mm	20 < FD < 50 mm	FD > 50 mm	At harvest (pre-grader)
Fruit size	FD < 20 mm	20 < FD < 50 mm	FD > 50 mm	At harvest (pre-grader)
Yield	FD < 20 mm	20 < FD < 50 mm	FD > 50 mm	At harvest (pre-grader)
Fruit colour	FD < 20 mm	20 < FD < 50 mm	FD > 50 mm	At harvest (pre-grader)
TCSA	Anytime between fruit thinning and harvest			
Tree geometry (tree height, canopy area and canopy density)	FD < 20 mm	20 < FD < 50 mm	FD > 50 mm	

2.3.6 Validation in commercial orchards

A validation of the models obtained in the Sundial orchard will be firstly attempted in the two commercial orchards. Based on one of the hypotheses of our study, different orchard features will lead to the inadequacy of models calibrated on the Sundial orchard unique conditions; thus, a re-calibration and re-validation may be necessary in commercial orchards as well. Calibration and validation approaches will follow identical methodologies to the ones used in the Sundial orchard. The only exception will be the marking strategy for short mobile scans – in commercial

orchards pink tape will be consistently used to mark the start and the end of each measured section.

2.3.7 Machine learning modelling and statistical analysis

Image segmentation and the CNN algorithms will be implemented by Green Atlas. Data obtained with the Cartographer™ will be processed and used for model calibration and validation for all the variables of interest.

Linear regression analyses will be conducted for calibration and validation purposes. The intercept of the linear regression model will be set to 0 and calibration will be based on the slope coefficient. Both the frequentist and Bayesian linear regression analyses will be evaluated. In the case of frequentist linear regression, the Lin's Concordance Correlation Coefficient (CCC) will be used to assess precision and accuracy of the validation (Lin, 1989). The root mean square error (RMSE) will be used to quantify the error. Alternatively, in the case of Bayesian regressions, the uncertainty of the model prediction will be assessed using credible intervals — a probabilistic measure. Statistical analyses will be carried out by Agriculture Victoria and Green Atlas.

The effects of rootstock and row orientation on crop variables will be tested using general linear model (GLM) procedures.

3. References

Bargoti, S., Underwood, J., 2017a. Deep fruit detection in orchards, in: Proceedings - IEEE International Conference on Robotics and Automation. Institute of Electrical and Electronics Engineers Inc., pp. 3626–3633. https://doi.org/10.1109/ICRA.2017.7989417

Bargoti, S., Underwood, J.P., 2017b. Image Segmentation for Fruit Detection and Yield Estimation in Apple Orchards. J. F. Robot. 34, 1039–1060. https://doi.org/10.1002/rob.21699

Bresilla, K., Perulli, G.D., Boini, A., Morandi, B., Corelli Grappadelli, L., Manfrini, L., 2019. Single-shot convolution neural networks for real-time fruit detection within the tree. Front. Plant Sci. 10, 611. https://doi.org/10.3389/fpls.2019.00611

Cripps, J.E., 2016. Apple tree named 'ANABP 01'. USPP27420P3.

Darbyshire, R., Goodwin, I., McClymont, L., Turpin, S., 2018. Addressing heat stress in pome fruit, in: Hermesch, S., Dominik, S. (Eds.), Breeding Focus 2018 - Reducing Heat Stress. Animal Genetics and Breeding Unit, University of New England, Armidale, NSW, Australia, pp. 81–97. http://agbu.une.edu.au/breedingfocus.html

Dias, P.A., Tabb, A., Medeiros, H., 2018a. Multispecies Fruit Flower Detection Using a Refined Semantic Segmentation Network. IEEE Robot. Autom. Lett. 3, 3003–3010. https://doi.org/10.1109/LRA.2018.2849498

Dias, P.A., Tabb, A., Medeiros, H., 2018b. Apple flower detection using deep convolutional networks. Comput. Ind. 99, 17–28. https://doi.org/10.1016/j.compind.2018.03.010

Goodwin, I., Whitfield, D.M., Connor, D.J., 2006. Effects of tree size on water use of peach (Prunus persica L. Batsch). Irrig. Sci. 24, 59–68. https://doi.org/10.1007/s00271-005-0010-z

Kang, H., Chen, C., 2020. Fast implementation of real-time fruit detection in apple orchards using deep learning. Comput. Electron. Agric. 168, 105108. https://doi.org/10.1016/j.compag.2019.105108

Kuznetsova, A., Maleva, T., Soloviev, V., 2020. Using YOLOv3 Algorithm with Pre- and Post-Processing for Apple Detection in Fruit-Harvesting Robot. Agronomy 10, 1016. https://doi.org/10.3390/agronomy10071016

Lin, L.I.-K., 1989. A Concordance Correlation Coefficient to Evaluate Reproducibility. Biometrics 45, 255–268. https://doi.org/10.2307/2532051

Milyaev, A., Kofler, J., Pfannstiel, J., Stefanelli, D., Flachowsky, H., Hanke, M.V., Wünsche, J.N., 2018. Histological and proteomic approaches to study floral bud induction in relation to biennial bearing in apple. Acta Horticulturae 1229, 277–283. https://doi.org/10.17660/ActaHortic.2018.1229.42

Örn, S., 2016. Estimating Light Interception of Orchard Trees Using LiDAR and Solar Models. Linköping University.

Schrader, L., Sun, J., Felicetti, D., Seo, J.-H., Jedlow, L., Zhang, J., 2003. Stress-induced disorders: Effects on apple fruit quality, in: Washington Tree Fruit Postharvest Conference.

Staples, M.R., Staples, J.R., 2006. Apple tree named 'Ruby Pink'. USOOPP16725P2.

Steele, J., Lacey, K., Sutton, J., 2017. Technical Information Dossier for Australia Apple Variety: ANABP 01.

Stefanelli D., Plozza t., Darbyshire R., Flachowsky H. and Wünsche J.N., 2019. Effects of crop load on apple fruit maturity. Australian Fruit Growers 13(Autumn 2019), 36–38.

Stefanelli, D., Plozza, T., Flachowsky, H., Wünsche, J.N., 2018. Young apple tree responses to crop load. Acta Horticulturae 1229, 221–228. https://doi.org/10.17660/ActaHortic.2018.1229.34

Underwood, J.P., Hung, C., Whelan, B., Sukkarieh, S., 2016. Mapping almond orchard canopy volume, flowers, fruit and yield using lidar and vision sensors. Comput. Electron. Agric. 130, 83–96. https://doi.org/10.1016/j.compag.2016.09.014

Underwood, J.P., Jagbrant, G., Nieto, J.I., Sukkarieh, S., 2015. Lidar-Based Tree Recognition and Platform Localization in Orchards. J. F. Robot. 32, 1056–1074. https://doi.org/10.1002/rob.21607

Wang, Z., Underwood, J., Walsh, K.B., 2018. Machine vision assessment of mango orchard flowering. Comput. Electron. Agric. 151, 501–511. https://doi.org/10.1016/j.compag.2018.06.040

Westling, F., Underwood, J., Örn, S., 2018. Light interception modelling using unstructured LiDAR data in avocado orchards. Comput. Electron. Agric. 153, 177–187. https://doi.org/10.1016/j.compag.2018.08.020

AP19003 Advancing sustainable and technology driven apple orchard production

Monitoring and evaluation

The PIPS3 Program Final Evaluation interview process was conducted in June and July 2023.

Overall, forty-three (43) telephone interviews were undertaken by the PIPS3 Program Coordinator, each interview averaging a 20 minute in duration. Eleven questions were asked, seven of these structured with a rating response required between 1 (most negative) and 5 (highly positive), with an opportunity to provide an extended comment to support the rating response. Most often, the respondents were highly motivated to expand upon the ratings provided. Four questions were open-ended to gain feedback and insight in a less formal and structured approach. These responses were particularly important in identifying areas for continuous improvement.

The stakeholder groups represented in the interviews were:

- Research team (n = 8)
- Growers (n = 20)
- Service Providers (n = 15)

The service provider stakeholder group included agency extension, commercial advisors, private advisors, and technical collaborators.

Some interviewees provided a response based upon their involvement across multiple projects of the program. This resulted in fifty-four (54) possible responses when quantifiably analysing results on a project basis. The following is a breakdown of possible responses per project:

- Whole-of-program relationship (n = 6)
- AP19002 (n = 10)
- AP19003 (n = 6; Researcher n = 2, Grower n = 2, Service Provider n = 2)
- AP19005 (n = 8)
- AP19006 (n = 24)

Although the spread of project respondents appears to be disproportionate, with AP19006 having 24 respondents, this reflects the large geographic spread of this project. The interviews conducted for this project ensured good representation across the regional areas in which both trial and demonstration activities were being conducted.

The interview process of both quantifiable and qualitative questions was used to evaluate **effectiveness**, **relevance**, **process appropriateness**, **efficiency** and **legacy** of the PIPS3 Program, and the specific program and project questions underpinning these (refer to the table below for questions that were specifically developed by the AP19003 project). The design of the questions enables analysis of responses at both a program and project level so that all users of the evaluation report can apply findings to both program and individual project level questions. A table of the interview questions used to assess performance of the program and projects against the key evaluation questions (KEQ) is provided in the final report for AP19007 (Independent Coordination).

AP19003 achieved a “Strong” performance rating across all KEQ from the final evaluation interview process.

Table 1. Stakeholder interview quantitative response ratings to determine final performance.

Stakeholder interview result	Evaluation criteria
Strong	Rating of between 3.8 to 5
Moderate	Rating of between 2.4 to 3.7

Weak	Rating of between 1 to 2.3

Table 2. AP19003 Key Evaluation Questions and performance results

AP19003 Key Evaluation Questions	Project performance	Example Feedback from interviewees.
EFFECTIVENESS: *To what extent has the PIPS3 Program addressed the objectives, research agreement achievement criteria and identified outcomes/ outputs?*		
• To what extent has the project improved orchard design and crop load management in a variable climate by providing knowledge and tools to consistently deliver premium fruit that meets consumer expectations in domestic and export markets? • To what extent has the project developed, calibrated, validated and evaluated sensor technology to measure in flower number, tree size, fruit number, fruit size and fruit colour?	**AP19003 effectiveness rating achieved:** 4.6 (n = 6) **Overall program effectiveness:** 4.3 (n = 43) Respondents were very confident that the project achieved its objectives and activities were executed as expected. It was identified that some goals were ambitious (i.e., *Cartographer* assessment of crop load relationships with tree size and fruit diameter) and more time and seasonal stability was needed for elements of the work. Seasonal variability and Covid restrictions were identified as constraints.	***Researcher*** *Our experimental design was strong, but years 2 & 3 were difficult due to seasonal conditions (e.g., fruit set & hailstorms) so longer-term projects are needed.* ***Grower*** *I think we achieved everything we were aiming for by using the Cartographer and what they came up with looked very real.* *The outcome of the different trials was good on heat and temperature effects on colour development.* ***Service Provider*** *They have done what we thought above and beyond at a high quality, and a good publication to come out of this work—Cartographer.*
RELEVANCE: *How relevant were the research outcomes/ outputs to the needs of apple and pear growers, advisors, and industry stakeholders?*		
• Do identified stakeholders believe the project investment was worthwhile and would they invest in the project team and/or subject matter in the future?	**AP19003 relevance rating achieved:** 4.6 (n = 6) **Overall program relevance:** 4.4 (n = 43) The project was considered strongly relevant to both growers and advisors who support them, particularly in relation to calibration and validation of the Green Atlas® *Cartographer* and temperature effects on fruit colour development and quality. There were no comments in relation to chemical signaling	***Researcher*** *PRG demonstrated they could see the importance of each component of the work at the final meeting.* *Utilisation of Cartographer—the pre-harvest sizing is so valuable to them in apples—the fruit size distribution prior to harvest, and colour also, we can do all this NOW. Can be used in planning and provide to the packing shed on pre-harvest pack-out and what they may be paying. It provides a transparency check.*

	influence on floral initiation, likely a reflection that the findings have a more indirect rather than immediate benefit to industry.	***Grower*** *We used the Cartographer for fruit size and crop load to find out how best to manage harvest decisions like what to pick first or harvest later.* ***Service Provider*** *Industries get swamped with new tech and hype (especially those with a big marketing budget). Having the independent validation & accuracy to prove it is important. Even if the farmers don't read the papers the evidence is there to give confidence.*
APPROPRIATENESS: *How well have intended audiences been engaged in the project?* *To what extent was the PIPS3 Program Communications and Extension Plan appropriate and had an impact upon the target audience?*		
No specific AP19003 within M&E plan	**AP19003 appropriateness rating achieved:** 4.8 (n = 6) **Overall program appropriateness:** 4.6 (n = 43) The project was considered extremely strong in engaging with the industry. Respondents were impressed with the mix of engagement across digital, printed and field-based activities. While growers are seeking practical application of the research in communications, primarily through videos, advisors are looking for technical and data driven evidence in longer articles or publications.	***Researcher*** *Talking live to the audience is always such good feedback for me. It's hard to know how well they are absorbing when it comes to articles and videos, but the advantage is that these [materials] are there for many years.* ***Grower*** *Knowledge on cooling has improved since listening to the researchers [at the Tatura Roadshow]. Encourages me to do some small trials at home.* *I see videos and have a quick look. Just makes me think and learn if there is anything new out there.* ***Service Provider*** *The publications have been important, but also the fact that articles are written for publications like AFG where growers can see the practical side. There is a lot of AgTech and this helps to demystify.*
EFFICIENCY: *What efforts did the PIPS3 Program partners make to improve efficiency?*		

• Did the project(s) efficiently manage shared resources and utilise skills and knowledge within other PIPS3 Program projects?	**AP19003 efficiency rating achieved:** 4.3 (n = 4) **Overall program efficiency:** 4.1 (n = 39) The AP19003 respondents rated the PIPS3 Program as strong on its performance to deliver an efficient approach to research, and communication and extension of the research. There was constructive feedback provided on ways in which projects could improve their "whole-of-system" perspective on data collection, sharing, interpretation and management implications.	***Researcher*** *But we can do some more connectivity across PIPS4 i.e., share data across the projects and have opportunities to prepare papers on integrated outcomes in orchards.* ***Grower (PRG Member)*** *The PRG has opened my eyes on the value of the projects working together. The only issue is that some projects are not as strong as others.* ***Service Provider*** *Benefits for the researchers which gives an indirect benefit to me. On the whole it has worked pretty well. Better than the past. Past knowledge is good. Ian Goodwin knowing what we have already done and not repeating.*
LEGACY: *Are there signs that the PIPS3 Program will influence apple and pear growers in the future?*		
• To what extent has the project resulted in greater confidence, intention to adopt, or adoption of new orchard design and the uptake of sensor technologies? *PROGRAM* • Is there evidence that outcomes and outputs of the PIPS3 Program will continue to be adopted by growers and front-line advisors? • To what extent do stakeholders believe that outcomes/ outputs of the PIPS3 Program are likely to become "usual grower practice" within the next ten years?	**AP19003 legacy rating achieved:** 4.5 (n = 6) (Improved knowledge & understanding of the concepts = 4.3 & Likelihood of adoption < 10 years = 4.7) **Overall program legacy:** 3.8 (n = 43) (Improved knowledge & understanding of the concepts = 4.0 & Likelihood of adoption < 10 years = 3.6) AP19003 was the only project to rate higher on the likelihood of adoption in the next ten years over delivering improved knowledge and understanding. There were indicators that some adoption was already occurring such as advisors providing *Cartographer* scanning of orchards and changes to orchard management for reduced heating and sunburn impacts.	***Researcher*** *They have had the opportunity but always difficult to gauge. We can get a good sense of this from face-to-face, that is why the roadshow was terrific. [Knowledge & Understanding}* *Highly likely as in what we do the service providers and resellers learn a lot from our projects. It is not necessarily about additional $. I am always surprised about what they take in. There are always some who will stick to their own beliefs. [Adoption]* ***Grower*** *There will be but will be in 5 – 10 years as always. 10% in 5 years, 30% in 10 years. It's a slow burn, only have one opportunity a year to make changes.* *For GV growers it's really relevant and the changes can be made easily. Growers need to just make the decision to make the change.*

		Service Provider *Those that are engaged have improved, but not everyone that has not been directly involved.*

Recommendations for continuous improvement

Comments from interviewees were grouped into the following areas for future research and communication of the results:

- Financial evaluation of new management systems including ag tech
    - *Financial and economic benefits for sure. Keep it simple though.*
    - *Communication using an economic approach at the same time as the other benefits. We need to respond to growers as they tell us what they want to learn about, profitability being part of this.*
    - *This time [was about] "potential value" but more "how they have had value" next time. ....it delivers us this value, and here are the tangible economic benefits. Content moves towards real use.*
- Long-term projects
    - *I take interest if I can see the end result—not just general information. Need the evidence over longer-term.*
- Communication of results
    - *Much more videos—these are the way forward. These are so succinct and engaging. Choosing the right questions has been done well.*
    - *Honestly got no idea. We seem to try everything.*
    - *Regular engagement through going to different states by working with TIA.*

Advancing sustainable and technology driven apple orchard production systems

Technical Report: Crop load relationships with return bloom, yield, fruit size, quality and tree zone in 'Rosy Glow'

Agriculture Victoria Research

May 2021

VICTORIA State Government | Jobs, Precincts and Regions

AGRICULTURE VICTORIA

Author: Tim Plozza

Project RDC Number: AP19003

Project CMI Number: 106472

Department of Jobs, Precincts and Regions
1 Spring Street Melbourne Victoria 3000
Telephone (03) 9651 9999

Contents

EXECUTIVE SUMMARY

The Australian apple industry is plagued by high cost of production and variable fruit quality that often does not meet consumer expectations, which can greatly reduce a grower's profitability. In addition to this, apple production in Australia is yet to reach its potential theoretical yield due to variable crop load management, biennial bearing, and inconsistent fruit quality.

Australia has a unique climate characterised by relatively high temperatures and light intensity compared to other apple production areas around the world. Light interception and consequent carbohydrate availability play an important role in defining the optimal number of fruit that a tree should hold to maximise consistent fruit quality for the life of the tree. However, care must be taken as apple trees have a tendency to biennial bearing, where an overabundance of flowers and subsequently fruit one season leads to suppression of flower initiation the following season, with low crop loads resulting. This has been estimated to account for approximately 20% decrease in potential yields (AP15002), as well as significantly increasing orchard management costs to manage fruit numbers.

This report presents data from a previous study on crop load management of an established cultivar ('Rosy Glow') (project AP15013). Crop load was found to have an inverse relationship with return bloom, fruit maturity, size, colour, and soluble solids concentration (SSC). Flesh firmness had an inverse relationship with crop load for trees with a variable crop load (alternating high and low year to year in a biennial-type pattern), but no relationship was found for trees with constant crop loads. The yield of fruit from each tree was found to be highly correlated with the crop load. In addition, after several years of a forced biennial cropping regime, zonal effects within some trees were observed, where the distribution of flowers, and subsequently fruit, became unbalanced with the rest of the tree.

This work shows the effects of a range of crop loads and cropping types (constant crop load from year to year, and variable — biennial-type — cropping behaviour) on tree yield and fruit quality. These results indicate that higher crop loads should not be used as a means of producing smaller fruit to meet market demands as this could instigate biennial bearing and will produce less attractive fruit with lower quality.

INTRODUCTION

This technical report is a deliverable for project AP19003 Advancing sustainable and technology driven apple orchard production systems. It summarizes the relationship between crop load and return bloom, yield, fruit size, quality and tree zone in the cultivar 'Rosy Glow' from field work undertaken in 2019-20 at Sanders' orchard at Three Bridges, Yarra Valley, Victoria, for project AP15013.

Project outcome

The intended outcome of this project is to improve crop load management in a variable climate by providing knowledge and tools to deliver premium fruit that meets consumer expectations in domestic and export markets.

Project background

The Australian apple industry, like many fruit production industries, is plagued by high cost of production and variable fruit quality that often does not meet consumer expectations. This can greatly reduce a grower's profitability. In the last ten years, apple production has increased but is yet to reach its full potential based on the area planted (10,000 ha) and the theoretical yield (~800,000 t). This is mostly due to variable crop load management, biennial bearing, and inconsistent fruit quality.

Australia has a unique climate characterised by relatively high temperatures and light intensity compared to other apple production areas around the world. Light interception and consequent carbohydrate availability play an important role in defining the optimal number of fruit that a tree should hold to maximise consistent fruit quality for the life of the tree. Furthermore, light interception and carbohydrate supply are fundamental in influencing fruit quality in a variable climate of extreme heat events.

Apple is generally susceptible to biennial bearing, which is the tendency to alternate years of high flower initiation followed by low initiation the subsequent year. From previous studies on crop load management of an established cultivar ('Rosy Glow') and emerging cultivar ('Nicoter') (projects AP15013 and AP15002), it was noticed that there is an inverse correlation between fruit number on trees and most aspects of fruit quality (size, colour, fruit maturity, flesh firmness and SSC). These previous studies found that biennial bearing is controlled at tree level from a combination of genetics (flower induction genes) and environment (carbohydrate availability) probably mediated by metabolites that act as chemical signals that either stimulate or inhibit the activation of the genes.

Project objectives

Physiological studies and the development of sensing tools are being undertaken in the Sundial apple orchard at the Tatura SmartFarm and in a commercial orchard in the Goulburn Valley to address the following three objectives as per the Hort Innovation RFP:

- Develop crop load, training systems, pruning and irrigation optimisation for yield, quality and labour efficiency in new and emerging apple cultivars.
- Develop orchard design techniques, tools and management practices that enhance the ability of orchards to tolerate climate variability and weather extremes.
- Communicate findings in a clear and practical format to growers and wider industry.

METHOD

The experiment was conducted in a commercial farm in Three Bridges, Yarra Valley, Victoria, Australia. Three-year old trees of the cultivar 'Rosy Glow' (marketed as Pink Lady®), trained on Open Tatura trellis, were used. Trees were managed according to the standard local practice and commercial operations. Five crop load treatments were first applied during the 2015-16 growing season with six single tree replicates (a total of 30 trees). Crop load treatments consisted of 1%, 50%, 100%, 150%, and 200% of normal grower practice, based on the tree's trunk cross sectional area (TCSA), which was measured 25 cm above the grafting union at the beginning of each growing season. In 2016-17 and subsequent seasons, three replicates of each crop load treatment maintained the same crop load, and the other three replicates alternated between reciprocal low and high treatments (e.g. 1% became 200%, 150% became 50%), thus forcing a biennial-type cropping behaviour on those trees (Table 1).

Table 1. Crop load level (% of normal grower practice and the approximate fruit number per cm^2 trunk cross sectional area in parenthesis) that was set for each treatment over the duration of the experiment.

Treatment	Crop load (% of normal grower practice)				
	2015-16	2016-17	2017-18	2018-19	2019-20
1	1 (1)	1 (1)	1 (1)	1 (1)	1 (1)
2	50 (4)	50 (4)	50 (4)	50 (4)	50 (4)
3	100 (8)	100 (8)	100 (8)	100 (8)	100 (8)
4	150 (12)	150 (12)	150 (12)	150 (12)	150 (12)
5	200 (16)	200 (16)	200 (16)	200 (16)	200 (16)
6	1 (1)	200 (16)	1 (1)	200 (16)	1 (1)
7	50 (4)	150 (12)	50 (4)	150 (12)	50 (4)
8	100 (8)	100 (8)	100 (8)	100 (8)	100 (8)
9	150 (12)	50 (4)	150 (12)	50 (4)	150 (12)
10	200 (16)	1 (1)	200 (16)	1 (1)	200 (16)

Each season at full bloom (80% open flowers), the number of flower clusters on each tree were counted manually to determine return bloom. Clusters were then thinned by hand to leave the required number of fruit per tree. Only one fruit per cluster was retained, except where insufficient clusters meant higher fruit numbers per cluster were needed to achieve the desired number of fruit per tree. Thinning was completed within 4 weeks of full bloom to minimize the chance of excess fruit affecting the following year's return bloom.

From approximately 3 – 4 weeks before harvest, fruit physiological age was measured weekly as Index of Absorbance Difference (I_{AD}) with a DA-Meter (Model 53500, T.R. Turoni, Forli, Italy). Correlation of I_{AD} with ethylene production at harvest allowed accurate prediction of the ideal harvest times for each cultivar and crop load treatment.

Two fruit harvests were conducted each season. The first occurred when the average maturity of the '100%' treatment trees reached the ideal value, determined by DA meter. At this harvest, all suitably ripe fruit were picked, or a minimum of 20 fruit per tree for comparative purposes. The second harvest occurred approximately two weeks later, when the remaining fruit had reached maturity. At harvest, all fruit on the trees were counted and weighed to obtain total yield and average fruit weight (AFW). A subsample of 20 fruit per tree was randomly selected for laboratory analysis, which consisted of fruit weight, colour measured with a colourimeter (Nix Mini, Nix Sensor, Hamilton, Canada), flesh firmness determined with a Food Texture Analyser (GS-15, FTA Guss, Strand, South Africa) and SSC measured with a digital refractometer (PAL-1 BLT/A+W, Atago, Tokyo, Japan).

RESULTS

Effect of crop load on return bloom

The number of flower clusters for each tree in a given growing season and the crop load of that tree in the previous growing season, shown in Figure 1, shows a decrease in flower clusters with increasing crop load. It also shows how the trees became unable to support the highest target crop loads in later seasons of the experiment due to insufficient flower clusters, which implies that the stress of overly high crop loads may be cumulative.

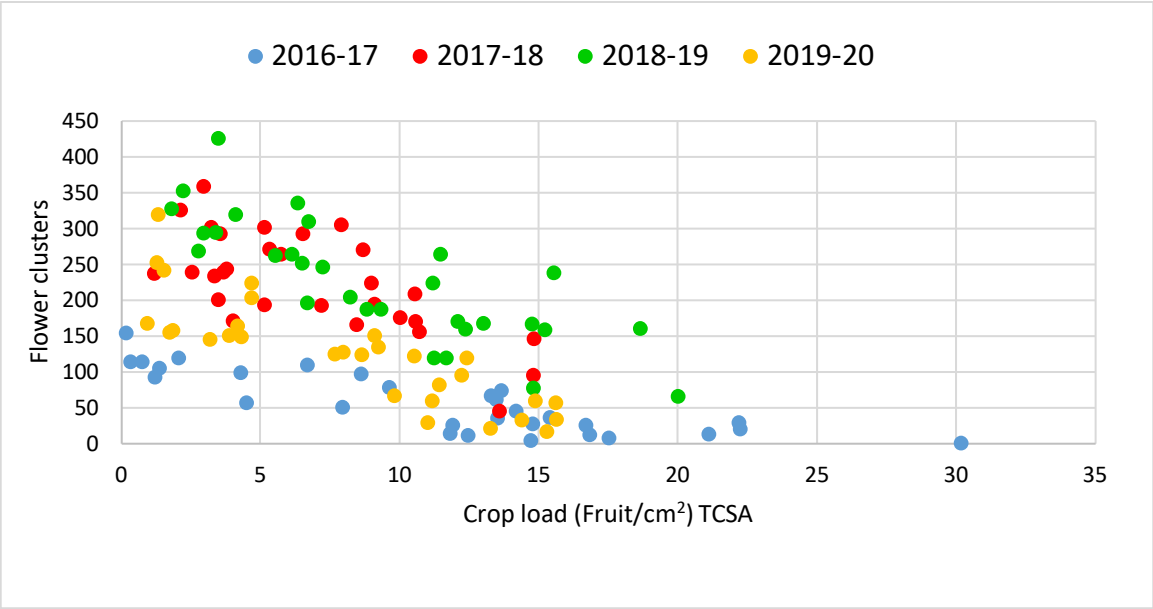

Figure 1: Number of flower clusters against the crop load of each 'Rosy Glow' tree during the preceding season, for each season of the experiment.

Effect of crop load on yield

The yield of fruit from each tree was found to be highly correlated with the crop load, as shown in Figure 2. Similar effects were observed for previous seasons of the experiment (see previous project AP15013 final report).

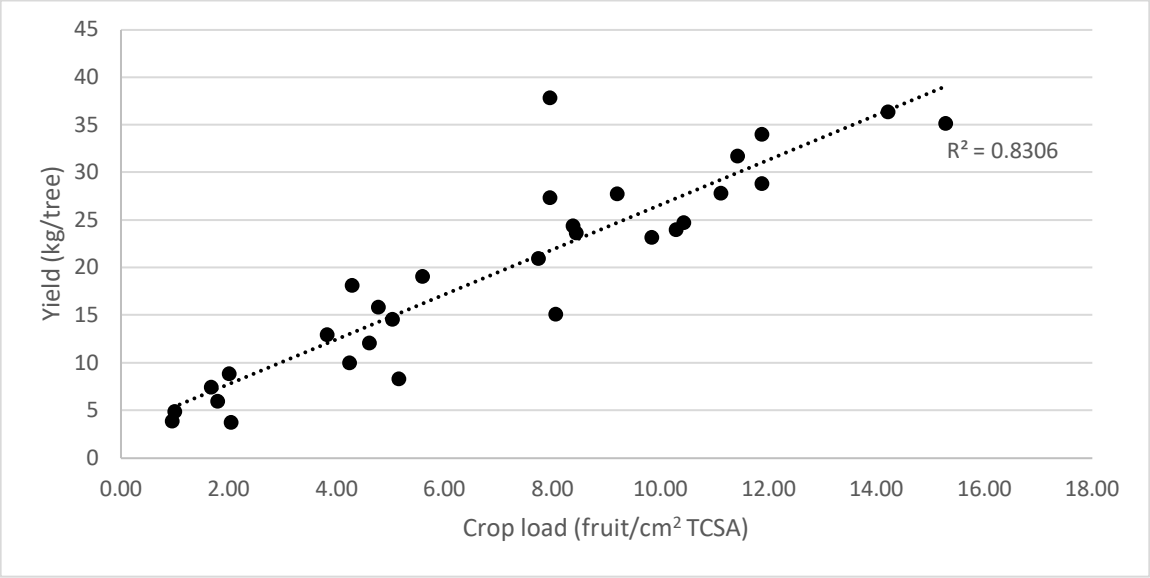

Figure 2: Relationship between fruit yield and the actual crop load (fruit/cm^2 TCSA) of each 'Rosy Glow' plot tree for the 2019/20 season.

Effects of crop load on maturity and fruit size

Fruit maturity, measured using DA meter, was affected by crop load, with fruit from trees with a lower crop load maturing earlier. There was generally approximately 2 weeks difference in date of maturity between the lowest and highest crop load treatments, depending on seasonal conditions.

In the 2019/20 season, as shown in Figure 3, fruit from all crop load treatments except the 1 fruit/cm^2 treatment, were at similar maturity levels 3 weeks before harvest, but then began to diverge as fruit from the lower crop load trees matured more quickly than fruit from the higher crop load trees. On average, fruit from trees thinned to 12 and 16 fruit/cm^2 matured at similar rates as, on average, these trees had similar crop loads in the 2019/20 season. In particular, this was due to the constant crop load trees in the 16 fruit/cm^2 group having insufficient return bloom to achieve the target crop load, plus self-thinning by these trees resulted in further reduced crop loads at harvest.

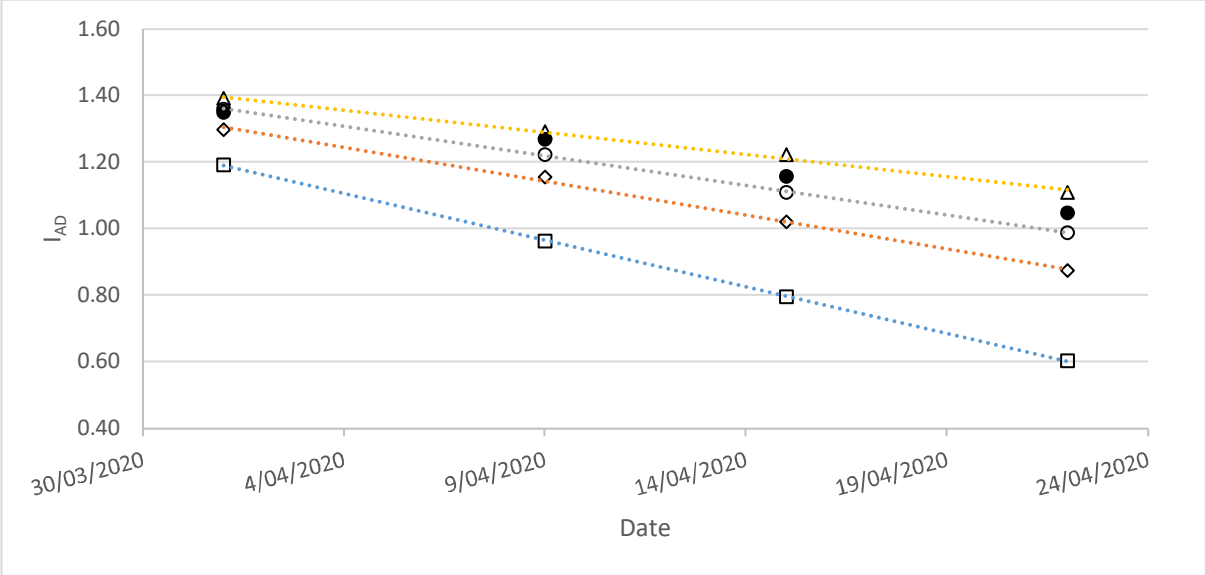

Figure 3: Index of absorbance difference (I_{AD}) for the various crop loads in at 3, 2, 1 weeks prior to and at harvest in the 2019/20 season. □ = 1 fruit/cm^2; ◇ = 4 fruit/cm^2; ○ = 8 fruit/cm^2; △ = 12 fruit/cm^2; ● = 16 fruit/cm^2. Similar effects were observed for previous seasons of the experiment.

Higher crop loads also resulted in smaller, lighter fruit, as shown in 2019/20 (Figure 4). Similar effects were observed for previous seasons of the experiment. This was expected as the tree's photosynthates must be distributed amongst a greater number of fruit, resulting in less carbohydrate per fruit. It was also noted that of the trees with the lowest crop load, the variable crop load trees (which had the highest crop load in the previous season) produced smaller fruit than the constant crop load trees, which suggests that there is a carry-over effect of overly high crop loads from one season to the next.

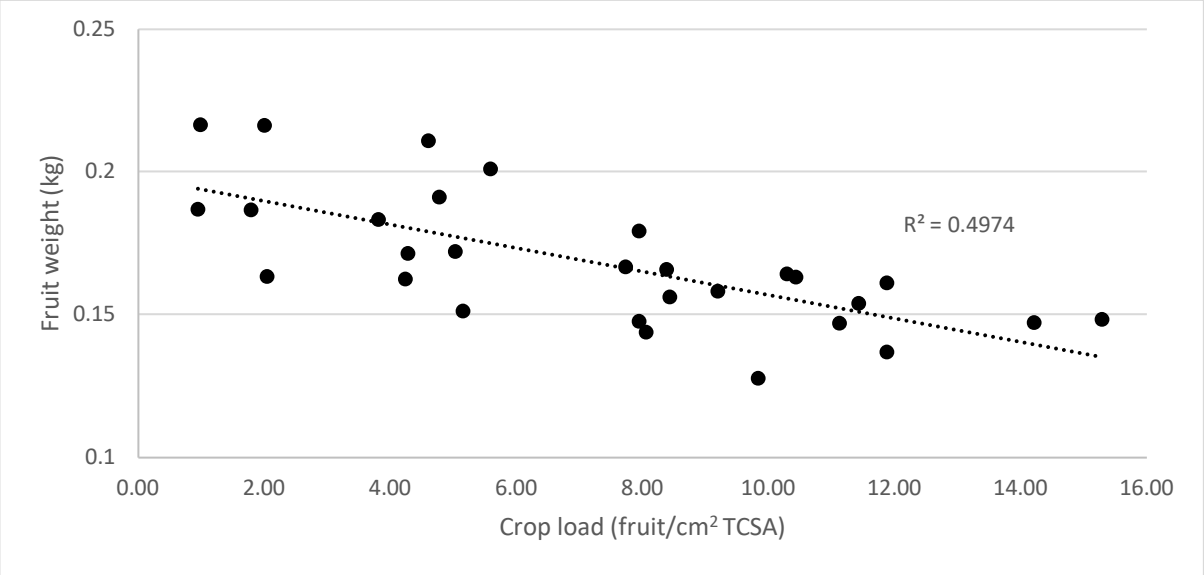

Figure 4: Relationship between average fruit weight and the actual crop load (fruit/cm^2 TCSA) of each 'Rosy Glow' plot tree at the first harvest for the 2019/20 season.

Effect of crop load on fruit quality

All fruit quality variables were found to have an inverse correlation with crop load. Fruit from higher crop load trees generally showed less intense colour (chroma), as shown in 2019/20 (Figure 5). Similar effects were observed for previous seasons of the experiment. However, it appears this may have been due to differences in maturity of the fruit, rather than a direct effect of crop load, as the colour intensity (chroma) was closely correlated with I_{AD} (R^2 = 0.83).

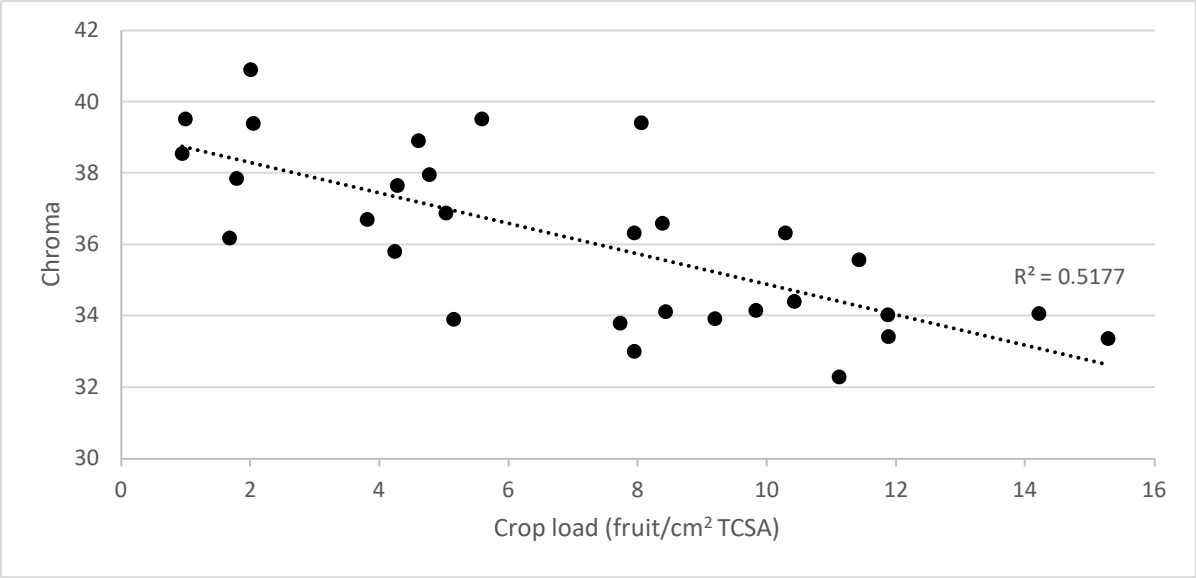

Figure 5: Relationship between fruit background chroma and the actual crop load (fruit/cm^2 TCSA) of each 'Rosy Glow' plot tree for the 2019/20 season.

The effect of crop load on flesh firmness varied depending on whether the trees had a constant or variable crop load treatment, as shown in Figure 6. Flesh firmness in the 2019/20 season was not correlated with crop load for the constant crop load treatments, whereas there was a strong inverse correlation of firmness and crop load for variable crop load trees.

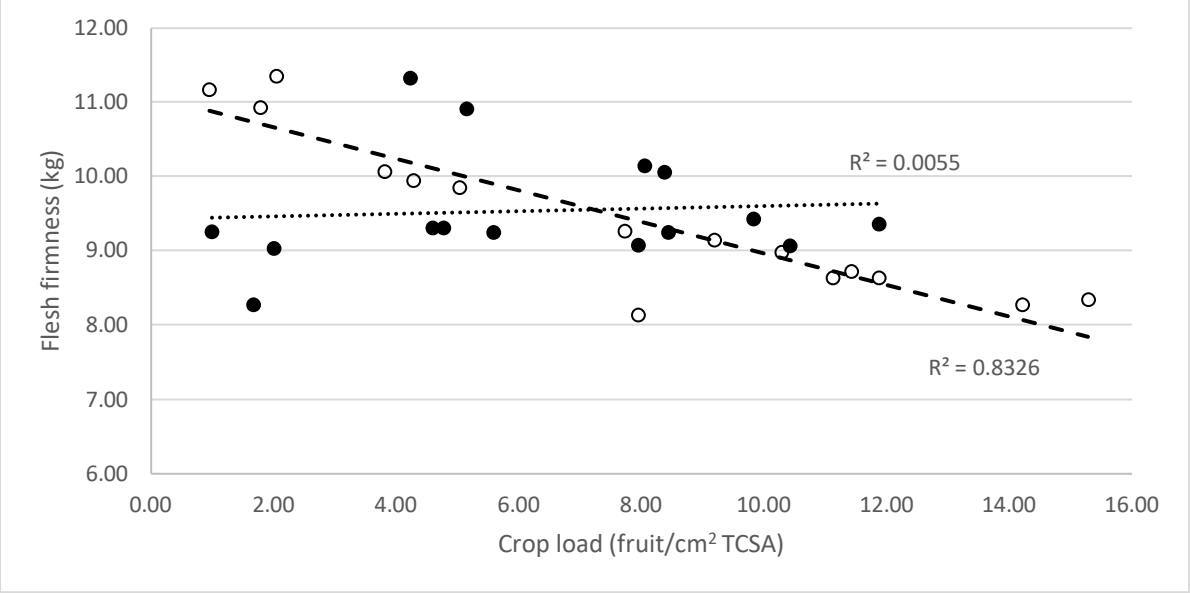

Figure 6: Relationship between average flesh firmness and the actual crop load (fruit/cm^2 TCSA) of each 'Rosy Glow' plot tree for the 2019/20 season. ● = Constant crop load treatments (dotted trendline), ○ = Variable crop load treatments (dashed trendline).

Fruit SSC was closely inversely correlated with crop load, as shown in 2019/20 (Figure 7). Similar effects were observed for previous seasons of the experiment. Similar to the effect of crop load on fruit size, this is due to the reduced carbohydrate availability in higher crop load trees.

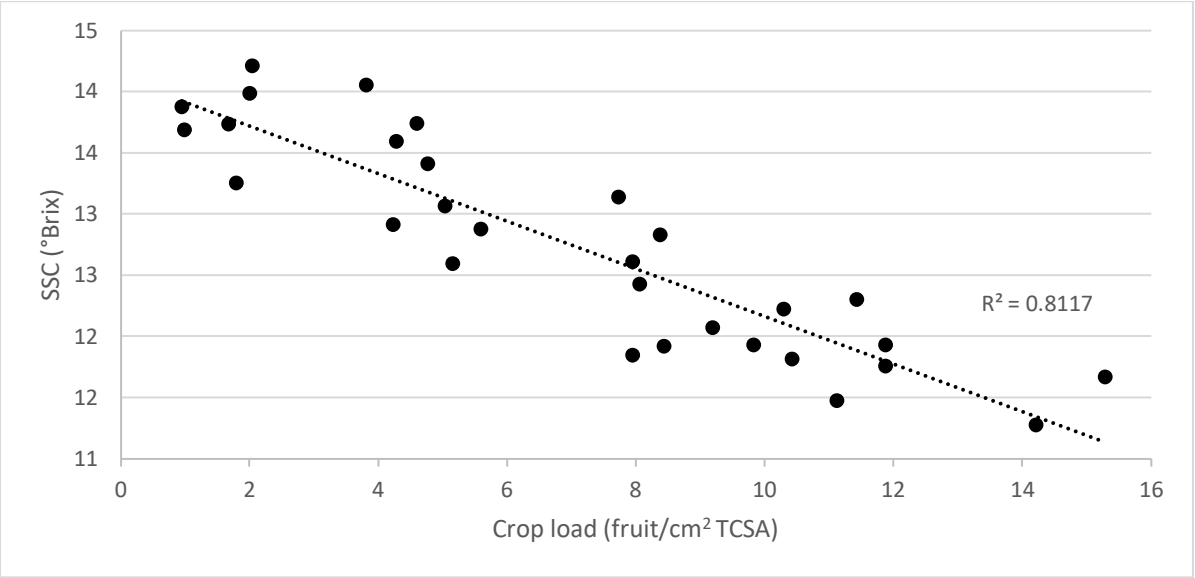

Figure 7: Relationship between soluble solids concentration (SSC) and actual crop load (fruit/cm^2 TCSA) of each 'Rosy Glow' plot tree for the 2019/20 season.

Zonal effects within trees due to biennial bearing

Some trees became severely unbalanced after several years of a forced biennial cropping regime. There were zones within trees that behaved in an opposite direction to the rest of the tree, such as a branch becoming biennial (having years on and off) independently of the crop load of the rest of the tree, indicating a localised chemical signal response. However, the fruit in these branches showed the pattern of the crop load the tree was having, for example, small fruit with low SSC typical of high crop load, even if in these branches the number of fruit was very low when compared with the rest of the tree. This suggests that, in contrast to the chemical response involved in flower initiation, carbohydrate utilization within the trees was not confined to autonomous zones.

CONCLUSION

The yield of fruit from each tree was found to be highly correlated with the crop load; however, crop load was found to have an inverse relationship with return bloom. This effect appeared to be cumulative, with trees repeatedly cropped at the highest crop load (16 fruit/cm^2 TCSA) becoming unable to support these very high fruit numbers in later years of the experiment.

Crop load was found to have an inverse relationship with fruit maturity, size, colour, and SSC. Flesh firmness had an inverse relationship with crop load for trees with a variable crop load (alternating high and low from year to year), but no relationship was found for trees with constant crop loads.

Several years of a forced biennial cropping regime resulted in zonal effects in some trees, where the distribution of flowers and subsequently fruit in these zones became unbalanced with the rest of the tree. This indicated a localised chemical signal response was responsible for flower induction, however the fruit in these zones was similar to those on the rest of the tree, suggesting carbohydrate utilization within the trees was not confined to autonomous zones.

RECOMMENDATIONS

Higher crop loads should not be used as a means of producing smaller fruit to meet market demands as this could instigate biennial bearing and will produce less attractive fruit with lower quality.

AP19003 Advancing sustainable and technology driven apple orchard production systems

Technical Report: Effect of crop load relationships on chemical signalling

Agriculture Victoria Research

April 2021

VICTORIA State Government | Jobs, Precincts and Regions

AGRICULTURE VICTORIA

Author: Priyanka Reddy, Tim Plozza, Vilnis Ezernieks, Simone Rochfort, Alessio Scalisi and Ian Goodwin

Project RDC Number: AP19003

Project CMI Number: 106472

Department of Jobs, Precincts and Regions
1 Spring Street Melbourne Victoria 3000
Telephone (03) 9651 9999

Contents

EXECUTIVE SUMMARY

The gross value of Australia's apple industry was $566 million in 2013, with Victoria representing approximately 30% of total Australian production. However, the value of this industry could be increased if more consistent crop loads were achieved for those apple cultivars which are susceptible to biennial bearing, a phenomenon characterised by "ON" and "OFF" years of flowering and, subsequently, fruit production. Biennial bearing costs growers and the Australian apple industry millions of dollars in additional labour and lost production due to inconsistent yields. Fruit growers usually remove excess flowers and fruitlets in "ON" years, using moderately effective horticultural practices, to increase fruit size in the current season and the amount of bloom in the subsequent season, but the methods are extremely time consuming and costly, and even with best thinning practice, yields can still be reduced by more than 20%.

Flower bud induction in "OFF" (i.e. low yield) years typically results from a poor flower bud formation due to a high crop load in the previous year (i.e. "ON"), suggesting that the fruit inhibits the concomitant development of the adjacent spur bud. The overall research goal of the current project was to reveal the largely unknown physiological and molecular mechanisms of biennial bearing in apple, thereby to better understand the underlying pathways and triggers of flower induction that might facilitate intervention opportunities for controlling apple crop load and thus ensuring stable apple production.

In this study, we report findings of metabolite regulation in apple buds and leaves in response to different crop load levels. Specifically, presented results are based on 1) buds collected from a previous experiment (AP15013) that utilised 'Rosy Glow' and 'Nicoter' apple cultivars in the Yarra Valley (from seven samples collected in late Spring — early Summer 2018 where, a range of crop loads were imposed on 'Rosy Glow' and 'Nicoter' apple trees over four seasons; 2) buds and leaves collected in the current crop load experiment (AP19003) which utilised 'Ruby Pink' apple trees subjected to crop load treatments established in October 2020. These treatments consisted of 5 crop load treatments (i.e. 20, 70, 120, 170 and 220 fruit per leader) in the primary leader as well as two crop load treatments (low and high) in the secondary leader of each tree.

Using non-targeted metabolomics profiling this study revealed that flavonoids in the buds were often affected by crop load levels and as such may play a role in regulating return bloom. Differences in expressed metabolites were found between the constant and variable crop load treatments (project AP15013). Samples from AP15013 varied in differentially expressed metabolites which could be related to constant crop loads showing a more pronounced effect due to equilibrated response over four seasons. Crop load effects were observed on flavanols such as kaempferol, naringenin and p-coumaric acid, which are consistent with physiological responses observed from bud samples taken and analysed in Germany for project AP15002 (Milyaev et al. 2021). Furthermore, crop load treatments showed larger effects on 'Nicoter' apple trees compared to 'Rosy Glow', which may be the consequence of a decreased susceptibility of 'Rosy Glow' to biennial bearing.

Results obtained on 'Nicoter' and 'Rosy Glow' trees were further corroborated by the findings in 'Ruby Pink' buds, where flavanols were also found as possible signalling molecules. Key pathways in the primary leader included benzoic acid and 4- hydroxybenzoic acid - intermediaries in the shikimic acid pathway linked to the flavanol epicatechin, one of the most abundant flavonoids in fruit such as apple, pear or grape. In the secondary leader, we found the flavanone eriodictyol (ERI) and its glycoside metabolites to be the most significantly altered metabolites.

Our study indicated possible candidates for potential signalling molecules for flower bud induction. However, plant metabolites identified in the non-targeted metabolomics analysis will require further identification using LCMS/MS mass spectrometry techniques. A further step towards systematic understanding of flower induction in apple will require determination of plant hormone profile by additional steps, such as using specific column chromatography techniques or extraction protocols specifically designed for the analyses of phytohormones (Farrow and Emery 2012; Urbanová et al. 2013), which we plan to perform in the near future.

INTRODUCTION

This technical report is a deliverable for project AP19003, "Advancing sustainable and technology driven apple orchard production systems". This work aims to explore the potential physiological mechanism (such as signalling compounds) for observed impacts of high crop load on floral initiation and flower development in apple trees. We report the results of molecular analysis of buds and leaves collected in December 2020 from 'Ruby Pink' apple trees from a commercial orchard in Ardmona, Victoria, as well as buds from the cultivars 'Nicoter' and 'Rosy Glow' collected from a commercial orchard at Three Bridges, Yarra Valley, Victoria, for project AP15013.

Project outcome

The intended outcome of this project is to improve crop load management in a variable climate by providing knowledge and tools to deliver premium fruit that meets consumer expectations in domestic and export markets.

Project background

The Australian apple industry, like many fruit production industries, is plagued by high cost of production and variable fruit quality that often does not meet consumer expectations. This can greatly reduce a grower's profitability. In the last ten years, apple production has increased but is yet to reach its full potential based on the area planted (10,000 ha) and the theoretical yield (~800,000 t). This is mostly due to variable crop load management, biennial bearing and inconsistent fruit quality.

Australia has a unique climate characterised by relatively high temperatures and light intensity compared to other apple production areas around the world. Light interception and consequent carbohydrate availability play an important role in defining the optimal number of fruit that a tree should hold to maximise consistent fruit quality for the life of the tree. Furthermore, light interception and carbohydrate supply are fundamental in influencing fruit quality in a variable climate of extreme heat events.

Apple is generally susceptible to biennial bearing, which is the tendency to alternate years of high flower initiation followed by low initiation the subsequent year. From previous studies on crop load management of an established cultivar ('Rosy Glow') and emerging cultivar ('Nicoter') (projects AP15013 and AP15002), it was noticed that there is an inverse correlation between fruit number on trees (i.e. crop load) and most aspects of fruit quality (size, colour, fruit maturity, flesh firmness and soluble solids concentration). These previous studies found that biennial bearing is controlled at tree level from a combination of genetics (flower induction genes) and environment (carbohydrate availability) probably mediated by metabolites that act as chemical signals that either stimulate or inhibit the activation of the genes.

Project objectives

Physiological studies and the development of sensing tools will be undertaken in the Sundial apple orchard at the Tatura SmartFarm and in a commercial orchard in the Goulburn Valley to address the following three objectives as per the Hort Innovation RFP:

- Develop crop load, training systems, pruning and irrigation optimisation for yield, quality and labour efficiency in new and emerging apple cultivars.
- Develop orchard design techniques, tools and management practices that enhance the ability of orchards to manage climate variability and weather extremes.
- Communicate findings in a clear and practical format to growers and wider industry.

METHOD

2018/2019 Bud Collection (AP15013)

The experiment was conducted in a commercial farm at Three Bridges, Yarra Valley, Victoria, Australia. Three-year old trees of the cultivars 'Nicoter' (marketed as Kanzi®) and 'Rosy Glow' (marketed as Pink Lady®), trained on Open Tatura trellis, were used. Trees were managed according to the standard local practice and commercial operations. Five crop load treatments were first applied during the 2015-16 growing season with six replicates, for a total of 30 trees per cultivar. Crop load treatments consisted of 1%, 50%, 100%, 150%, and 200% of normal grower practice, based on the tree's trunk cross sectional area (TCSA), which was measured at the beginning of each growing season. In 2016-17 and subsequent seasons, three replicates of each crop load treatment maintained the same crop load (NIC^{CON} = 'Nicoter' constant crop load; RG^{CON} = 'Rosy Glow' constant crop load), and the other three replicates alternated between corresponding low and high treatments (e.g. 1% became 200%, 150% became 50%), thus forcing a biennial-type cropping behaviour on those trees (NIC^{VAR} = 'Nicoter' Variable crop load; RG^{VAR} = 'Rosy Glow' Variable crop load).

Each season at full bloom (80% open flowers), flower clusters on each tree were counted manually to determine return bloom. Flower clusters were then thinned by hand to impose the required crop load level per tree. Only one fruit per cluster was retained, except where insufficient clusters meant higher fruit numbers per cluster were needed to achieve the desired number of fruit per tree. Thinning was completed within 4 weeks of full bloom to minimize the chance of excess fruit affecting the following year's return bloom.

In the 2018/19 season, beginning 4 weeks after full bloom, one bud per tree was collected weekly for eight weeks and prepared for molecular analysis by the Molecular Phenomics Group within Agriculture Victoria Research.

2020 Apple Bud Collection

The experiment was conducted at the Plunkett orchard, 255 Macisaac Rd, Ardmona (113 m a.s.l.) in the Goulburn Valley, Victoria, Australia. 'Ruby Pink' apple trees trained to a two leader vertical trellis configuration were used for this experiment, which began in the 2020/21 season. 30 trees occupying a single row in the orchard were utilized for the experiment and were replicated in three randomised blocks, each consisting of 10 trees (two panels of five trees). One of five crop loads (20, 70, 120, 170 or 220 fruit/leader) were applied to the 'Primary' leader on each tree in late October, and one of two crop loads (Low ~ 20 fruit/leader) or High (~220 fruit/leader)) applied to the 'Secondary' leader. The randomised application of these treatments is shown in Table 1. The selection of primary leaders was based on similar TCSA. At the beginning of the experiment, TCSA in primary leaders had a mean of 27.4 and a standard deviation of 6.3 cm^2, and secondary leaders had TCSA = 27.5 ± 12.4 cm^2.

Table 1. Randomised application of crop load levels to the Primary and Secondary leaders of the 'Ruby Pink' apple trees. Low = ~ 20 fruit/tree, High = ~ 220 fruit/tree.

Block	Tree number	Crop load of primary leader (n)	Crop load of secondary leader
1	1	170	Low
1	2	120	High
1	3	220	Low
1	4	20	Low
1	5	120	Low
1	6	70	Low
1	7	70	High
1	8	20	High
1	9	170	High
1	10	220	High
2	11	170	Low
2	12	220	Low
2	13	120	High
2	14	70	Low

2	15	20	Low
2	16	220	High
2	17	70	High
2	18	20	High
2	19	120	Low
2	20	170	High
3	22	70	Low
3	23	20	High
3	25	220	Low
3	26	120	High
3	29	170	High
3	30	70	High
3	31	220	High
3	32	20	Low
3	33	120	Low
3	34	170	Low

Buds and leaves were collected from the trees in December 2020, approximately 70 days after full bloom, which approximates the time at which buds transform from vegetative to reproductive, as documented in AP15002 final report. 3 buds per tree and 2 – 3 fully expanded leaves adjacent to each of these buds were collected and prepared for molecular analysis by the Molecular Phenomics Group within Agriculture Victoria Research. One bud each was collected from a low, mid and high location on each tree.

Samples were frozen on dry ice as soon as possible after collection and stored in a freezer at −80°C until analysis.

Bud and leaf sample selection and preparation

Buds were selected on spurs growing on at least 2-year-old wood.

Spurs on lateral branches of the tree were selected and not spurs from the central leader or the top.

Only fruiting spurs with subtending bud (figure 1 a) were chosen where possible, otherwise a bud close to a fruiting spur was chosen. If the bourse shoot was > 5 cm spur was not sampled.

Buds were removed from the trees by breaking them off the spur (figure 2 b).

Leaves were removed from the bud (figure 2 c) and for the 2020 sampling, 2 – 3 fully expanded leaves placed in a zip-lock bag and frozen in dry ice.

A scalpel was used to peel or slice away the brown scales on the bud to leave behind the growing tip with no/minimal brown material (figure 2 d).

The bud was cut off above the wooden part using a scalpel (no woody part was kept on the sample) (figure 2 e).

The prepared bud was placed in a pre-weighed Eppendorf tube, weighed and then placed on dry ice.

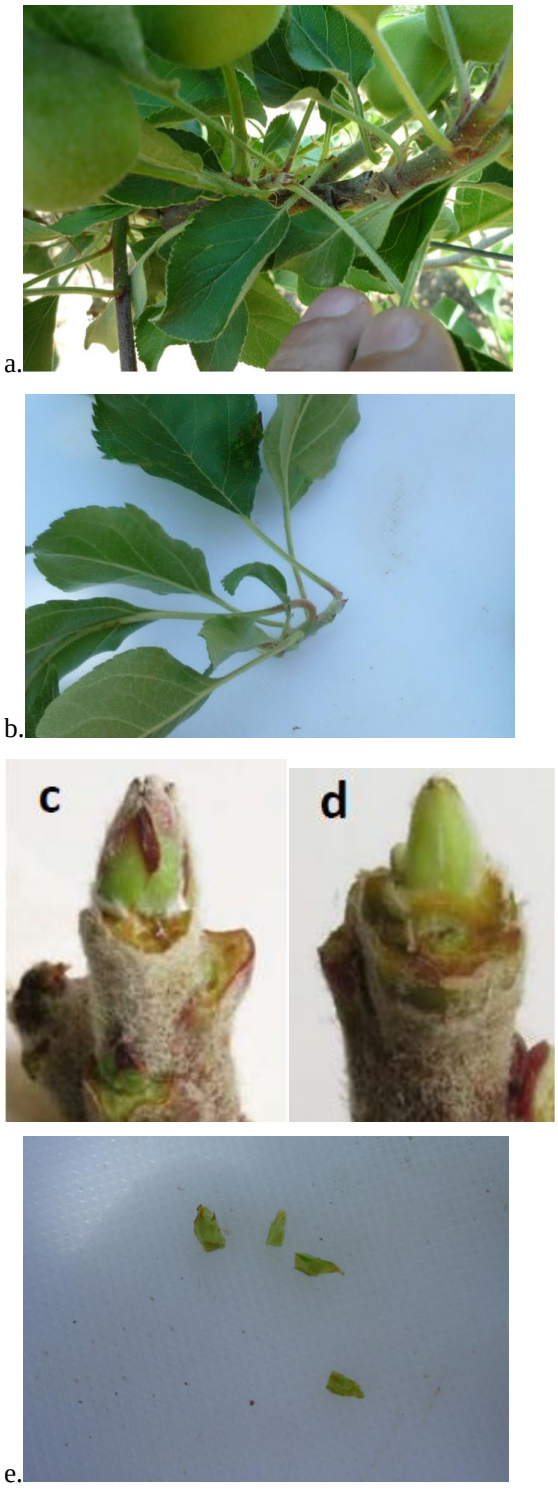

Figure 1. Fruiting spur with (a) subtending bud, (b) bud removed from tree, (c) bud with leaves removed, (d) peeled bud and (e) growing tip removed from woody stem.

Identification and relative quantitation of potential chemical signalling compounds

Metabolites were extracted from bud and leaf samples and analysed using high resolution, accurate mass liquid chromatography-mass spectrometry (LCMS) instruments to find and identify potential chemical signalling compounds related to crop load treatments and return bloom. Methods included untargeted analysis, which involved finding and identifying unknown compounds whose presence and concentration correlated with return bloom measurements.

Sample Extraction of 2020 Bud collection

All specimens collected were immediately snap-frozen in liquid nitrogen and stored at −80°C. Specimens from each biological replicate were kept in separate safe-lock tubes. Subsequent to apple buds being lyophilized, two ceramic beads (2.8 – 3.2 mm YTZP (yttria zirconia beads)) were placed in the 1.5 mL Eppendorf tubes for the ('Ruby Pink') 2020 collection, that contained one apple bud per tube. Three apple buds per tube were collected into a 2 mL Eppendorf for the 2018 collection ('Nicoter' and 'Rosy Glow') and thus 1 large (3.5 – 4.1 mm YTZP) and 2 small beads (2.8 – 3.2 mm YTZP) were added. Samples were placed in 24 well cryo-blocks on the Geno/Grinder 2010 (SPEX Sample Prep, Metuchen, NJ, USA) and the buds were ground at 1,200 rpm for 1 min. The samples were extracted with 80% methanol/water (v/v), with extraction volumes adjusted proportionally to the weight of the lyophilized bud. Samples were centrifuged at 13,000 rpm for 2 min and 200 µL of the supernatant was transferred into a HPLC tube and stored at −20°C until ready for LCMS analysis.

LCMS Methods for Untargeted Analysis and Compound Identification

For untargeted metabolite profiling, a Vanquish Ultra-High Performance Liquid Chromatography (UHPLC) system (Thermo Fisher Scientific, Bremen) with a binary pump, autosampler and temperature-controlled column compartment coupled with a QExactive (QE) Plus mass spectrometer (Thermo, Bremen, Germany) detector was used. An electrospray ionization (ESI) probe operating in the positive and negative ionization modes and the mass spectrometer captured data over a range of 80 – 1,200 m/z, with mass resolution set at 17,000. Nitrogen was used as the sheath, auxiliary and sweep gases at flow rates of 28, 15 and 4 L/min, respectively. Spray voltage was set at 4,000 V (positive and negative). A 3 µL sample injection volume was used. Samples were randomized, and blanks (80% methanol) injected every five samples. A pooled biological quality control (PBQC) was run every 10 samples. Prior to data acquisition, the system was calibrated with Pierce LTQ Velos ESI Positive and Negative Ion Calibration Solution (Thermo Fisher Scientific). Mass spectrometry data was acquired using Thermo Xcalibur V. 2.1 (Thermo Fisher Scientific Inc., USA). Quantitative analysis was conducted using LCQUAN™ Quantitative Software (Thermo Fisher Scientific).

A Thermo Fisher Scientific Hypersil Gold 1.9 µm, 100 mm × 2.1 mm column with a gradient mobile phase consisting of 0.1% formic acid in H_2O (A) and 0.1% formic acid in acetonitrile (B), at a flow rate of 0.3 mL/min was used. The gradient began at 2% B, increasing to 100% B over 11 min; followed by 4 min at 100% B before a 5 min equilibration with 2% B.

Untargeted Analysis: Putative Compound Identification

The data files obtained following LCMS analyses were processed in the Refiner MS module of Genedata Expressionist® 12.0 optimising the; 1) chromatogram chemical noise subtraction, 2) intensity thresholding, 3) selection of positive mode data only, 4) chromatogram RT alignment, 5) chromatogram peak detection. Analyte identification of significant metabolites were performed by searching experimental MS1 data through databases METLIN, ChemSpider (http://www.chemspider.com) and MS/MS data was searched on MzCloud (https://www.mzcloud.org) and MetFragment®.

Statistics

Data processing and statistical analyses

The data files obtained following LCMS analyses were processed in the Refiner MS module of Genedata Expressionist® 12.0 with the following parameters: 1) chromatogram chemical noise subtraction with removal of peaks with less than 4 scans, chromatogram smoothing using moving average estimator over 5 scans, and 30% quantile over 151 scans for noise subtraction, 2) intensity thresholding using a clipping method and a threshold of 100,000, 3) selection of positive mode data only, 4) chromatogram RT alignment using a pairwise alignment based tree and a maximum RT shift of 1 min, 5) chromatogram peak detection using a 5 scans summation window, a minimum peak size of 0.1 min, a maximum merge distance of 0.05 Da, a boundary merge strategy, a maximum gap/peak ratio of 70% with moving average smoothing over 10 scans for peak RT splitting 6) chromatogram isotope clustering using RT and m/z tolerance of 0.05 min and 0.05 Dalton respectively with a maximum charge of 2, 7) adduct detection using mainly M+H and allowable adducts (M+2H, M+K, M+Na, M-H_2O+H).

Statistical analyses were performed using the Analyst module of Genedata Expressionist® 12.0. Principal component analyses (PCA) were performed to identify tissue and treatment differences. Overlay of the PBQC and samples allowed for the validation of the high-quality dataset by ensuring that RT variation, mass error and sensitivity changes throughout

the run were consistent. Linear procedures were used (e.g. regression analysis, principal component analysis) to test treatment effects on the regulation of metabolites. In this study, final linear regression p-values were reported ($p < 0.01$), with metabolite (y) responses to the fixed effects of crop load treatments (x).

Identification of metabolites was performed by searching experimental MS[1] data through the following databases: Plant Metabolic Network (PMN) https://plantcyc.org/; Human Metabolome DataBase (HMDB) (http://hmdb.ca); ChemSpider (http://chemspider.com); and Lipid Maps®(http://www.lipidmaps.org); .

RESULTS AND DISCUSSION

2018/2019 Bud collection

PCA plots of 'Rosy Glow' and 'Nicoter' apple bud extracts revealed separation of the two cultivars (Figure 2 a). The metabolome of the individual cultivars was distinct. Although, crop load effects are thought to occur irrespective of cultivar (Milyaev, Kofler et al. 2021) the PCA model indicates that the pathways between the two cultivars may have differences and were thus explored individually. Furthermore, there may be differences in stress induced pathways associated with apple trees treated with a constant and a variable/biennial crop load.

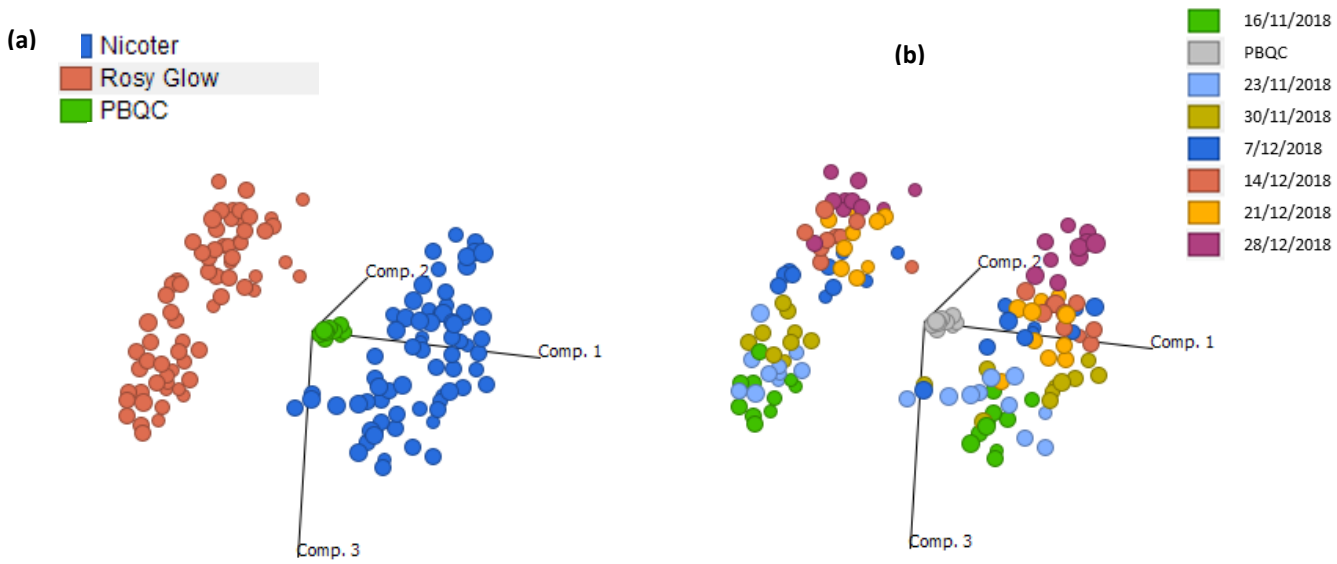

Figure 2. PCA scores plot showing (a) positive ion ESI LCMS of the metabolome (908 metabolites) categorised by variety and (b) by collection date.

A total of 908 compounds in positive ionisation mode and 634 compounds in negative ionization mode were detected from apple spur bud samples in NIC^{CON}, NIC^{VAR}, RG^{CON} and RG^{VAR}. Putative (Level 3) identification of 436 metabolites in positive mode and 265 in negative mode, provided valuable information on the complex composition of the apple bud, including plant hormones, lipids, amino acids, vitamins and phenols. However, it is important to note that further confirmation of metabolites (Level 1 and 2 compound identification) requires in-house standards, or MS2 fragmentation spectra matched to a database/journal publication (Viant et al. 2017).

Metabolite responses (y) against crop load (x) revealed significant metabolite changes ($p < 0.01$) in response to constant and variable crop load treatment effects in 'Nicoter' and 'Rosy Glow' (Figure 3).

In NIC^{CON} the flavonoids (afzelechin 7-apioside, quercetin, kaempferide, kaempferol and naringenin) showed increasing levels with higher crop load trees ("ON") (Table 1). Kaempferol and its precursor naringenin are important biomarkers as previous reports have identified derivatives of its biosynthetic intermediate, p-coumaryl COA in "ON" trees (Milyaev, Kofler et al. 2021). Moreover, the transcriptome and proteome of apple buds have shown enzymatic activity of enzymatic reaction EC:2.3.1.133 that metabolizes at least 3 derivatives of p-coumaric acid including p-coumaroyl CoA and caffeoyl shikimic acid, precursors of the kaempferol and chlorogenic acid pathway (Milyaev et al. 2021). Nuclear localisation of flavonoids has been reported in many plant species, suggesting that flavonoids may function in transcriptional regulation of endogenous gene expression (Peer and Murphy 2006). Naringenin chalcone and apigenin also may influence flavonoid biosynthesis by regulating transcription of flavonoid biosynthetic enzymes (Pelletier et al., 1999).

In NIC^{CON} decreased levels of amino acids L-asparagine and L-arginine and the peptide aspartyl-glutamine were observed in "ON" trees (Table 1), corroborating the findings on arginine levels obtained by Milyaev et al. (2021) . Amino acids serve as protein building blocks and reduced levels could suggest increased competition for resources/nutrients in high crop load trees. Arginine also serves as a nitrogen storage in plants and enables fine-tuning of the production of nitric oxide, polyamines and potentially proline (Winter et al. 2015).

Similar to NIC^{CON}, the RG^{CON} showed decreased levels of asparagine (Table 2); however, the perturbation in metabolites in RG^{CON} is limited to 5 metabolites compared to 22 metabolites in NIC^{CON}, this could be related to RG having less susceptibility to biennial bearing (AP15013) which could also explain the uneven trends in the RG^{VAR} (Table 4).

Table 1. Significant metabolites (P < 0.01) identified in spur buds of 'Nicoter' trees subjected to constant crop load.

Compound ID	Ionisation mode	Observed Mass	RT (min)	Putative identification[1]	P-Values	Regulation in "ON" trees
Group_012	pos	132.0534	1.2	L-Asparagine	5.1E-	DOWN
Group_013	pos	133.0505	1.2	Unknown amino	4.8E-	DOWN
Group_014	pos	133.0568	1.2	Unknown amino	4.4E-	DOWN
Group_030	pos	178.084	1.3	2-O-Methyl-L-	6.5E-	UP
Group_055	pos	261.0958	1.2	Aspartyl-	8.3E-	DOWN
Group_061	pos	280.0629	1.3	Sulfametopyrazine	7.3E-	UP
Group_092	pos	406.1263	5.6	Afzelechin 7-	2.3E-	UP
Group_094	pos	418.0897	5.2	Kaempferol 3-O-	3.3E-	UP
Group_096	pos	434.0844	4.9	Fukinolic acid	3.7E-	UP
Group_101	pos	462.1157	5.3	kaempferide 3-O-	6.8E-	UP
Group_113	pos	562.1469	3.7	Epifisetinidol-	9.4E-	UP
Group_246	pos	174.1115	1.2	L-Arginine	3.1E-	DOWN
Group_362	pos	272.0684	5.4	Naringenin	9.1E-	UP
Group_395	pos	286.0474	5.2	Luteolin	8.8E-	UP
Group_428	pos	302.0422	4.9	Quercetin	5.8E-	UP
Group_447	pos	314.1321	1.2	-	1.4E-	DOWN
Group_452	pos	398.9028	1.1	-	3.5E-	UP
Group_587	pos	425.0996	5.6	-	2.6E-	UP
Group_634	pos	451.1477	3.9	5-O-	1.0E-	DOWN
Group_663	pos	470.0822	5.2	-	6.2E-	UP
Group_722	pos	529.1285	5.0	-	2.5E-	DOWN
Group_786	pos	628.1628	5.6	-	6.0E-	UP

Table 2. Significant changes of metabolites (P < 0.01) identified in spur buds of 'Rosy Glow' trees subjected to constant crop load.

Compound ID	Ionisation	Observed	RT	Putative	P-Values	Regulation in
Group_690	pos	497.8984	1.1	-	6.4E-03	UP

Group_136	pos	81.00689	1.1	-	6.7E-03	UP
Group_137	pos	82.00765	1.1	-	7.1E-03	UP
Group_012	pos	132.0534	1.2	L-Asparagine	8.5E-03	DOWN
Group_532	pos	383.9176	1.1	-	8.9E-03	UP

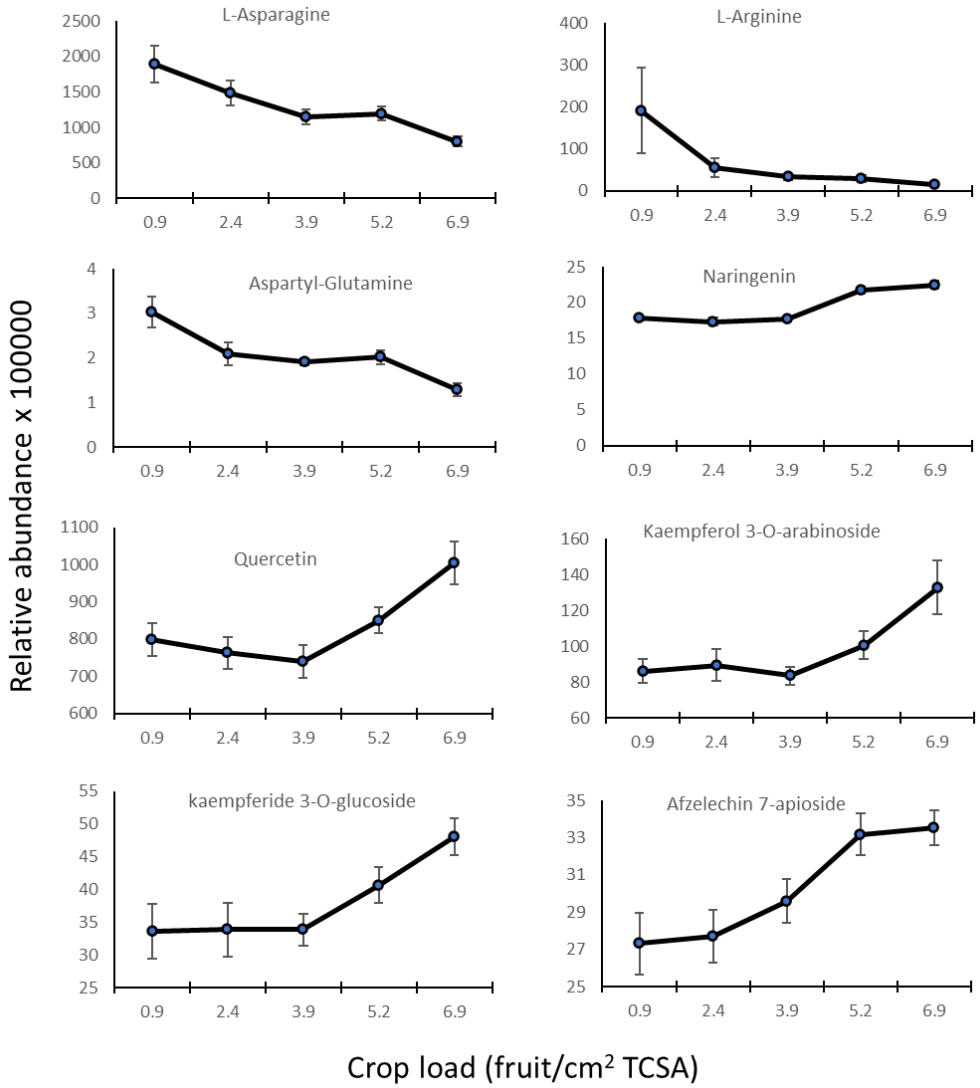

Figure 3. Relative abundance of selected amino acids and flavanols ($P < 0.01$) identified in spur buds of 'Nicoter' trees subjected to different crop load treatments.

NIC^{CON} and NIC^{VAR} crop load treatment effects showed little similarity in metabolite pathways. Most altered metabolites in the variable treatments eluted at 1.1 min, which suggests effects on primary metabolites such as sugars, amino acids, organic acids and nucleic acids (Table 3). These could be explained by the increased resources required for "ON" trees. The metabolites in the constant crop load trees may have reached an equilibrated state, making the effects more pronounced.

Table 3. Significant changes of identified metabolites (P < 0.01) in spur buds of 'Nicoter' trees subjected to variable crop load.

Compound ID	Ionisation mode	Observed Mass	RT (min)	Putative Identification	P-Values: Crop	Regulation in "ON" trees
Group_138	pos	82.0306	1.1	-	8.8E-	UP
Group_136	pos	81.0069	1.1	-	9.5E-	UP
Group_137	pos	82.0077	1.1	-	1.0E-	UP
Group_318	pos	240.1475	2.4	-	1.9E-	UP*
Group_613	pos	438.1502	4.3	7-Hydroxy-5-(4-hydroxy-2-oxopentyl)-2-methylchromone 7-glucoside	2.4E-03	UP
Group_185	pos	122.0332	1.1		2.6E-	UP
Group_045	pos	219.1107	3.0	Pantothenic acid	2.7E-	UP
Group_197	pos	127.0120	1.1	-	3.4E-	UP
Group_135	pos	81.0044	1.1	-	3.5E-	*
Group_421	pos	297.9324	1.1	-	3.7E-	UP
Group_308	pos	228.1473	1.9	L-isoleucyl-L-	3.8E-	UP*
Group_321	pos	241.9932	1.1	-	4.0E-	UP
Group_351	pos	266.0055	1.1	-	4.1E-	UP
Group_358	pos	269.9375	1.1	-	4.5E-	UP
Group_744	pos	572.4805	10.1	Dieporeticenin	4.7E-	UP
Group_056	pos	264.0079	1.1	-	4.7E-	UP
Group_320	pos	240.9921	1.1	-	5.0E-	UP
Group_200	pos	129.5147	1.1	-	6.1E-	UP
Group_021	pos	150.0279	1.1	-	6.4E-	UP
Group_046	pos	224.9792	1.1	-	6.4E-	UP
Group_088	pos	382.0874	1.2	-	6.7E-	UP*
Group_297	pos	217.9762	1.1	-	7.0E-	UP
Group_532	pos	383.9176	1.1	-	7.2E-	UP
Group_856	pos	832.5095	10.1	-	7.4E-	*
Group_134	pos	79.5328	1.1	-	7.7E-	UP
Group_586	pos	424.9444	1.1	-	8.1E-	UP
Group_441	pos	308.9670	1.1	-	8.3E-	UP
Group_226	pos	152.0254	1.1	-	8.5E-	UP
Group_418	pos	296.9361	1.1	-	8.6E-	UP
Group_364	pos	273.0552	1.4	-	8.8E-	UP
Group_173	pos	109.0016	1.1	-	8.9E-	UP
Group_302	pos	222.9816	1.1	-	9.0E-	UP
Group_599	pos	433.1945	4.3	-	9.0E-	UP
Group_049	pos	242.9896	1.1	-	1.0E-	UP

* not a clear treatment-response effect.

Table 4. Significant changes of metabolites (P < 0.01) identified in spur buds of 'Rosy Glow' trees subjected to variable crop load.

Row	Mass	RT	Putative identification	P-Values <0.01: Crop load effect	Regulation in "ON" trees
Group_673	478.3054	12.0	-	9.2E-03	UP*
Group_864	864.1890	4.7	Epicatechin-(4beta->6)-epicatechin-(2beta->7,4beta->8)-epicatechin	8.3E-03	UP*
Group_353	267.0229	4.6		7.0E-03	UP*
Group_706	512.1530	4.7	3-(4-Hydroxy-3-methoxyphenyl)-1,2-propanediol 2-O-(galloyl-glucoside)	5.9E-03	UP*
Group_571	412.0304	1.4	-	4.9E-03	DOWN*
Group_614	438.3133	12.0	-	3.2E-03	DOWN*
Group_151	89.0843	1.2	Dimethylethanolamine	8.8E-04	DOWN*

* not a clear treatment-response effect.

This study suggested that amino acids and flavonoids play a role in metabolic pathways associated with varying crop loads, and thus may be involved in regulating return bloom. The constant and variable (artificially alternating high and low fruit numbers) crop loads treatments varied in differentially expressed metabolites which could be related to constant crop loads showing a more pronounced response due to equilibration over four seasons. The increased levels of polar metabolites in the variable treatment could be related to increased demands of resources required for "ON" trees that could mask any phytohormone signalling pathways. Stefanelli et al. (2018) observed that fruit harvested from the trees with variable treatments had reduced quality traits compared to the fruit from trees with constant crop load treatments (either high or low). Thus, the response for these two treatments (variable and constant) showed clear evidence of distinct differences in the physiological mechanisms employed. It was also observed that NIC^{CON} (Table 1) and NIC^{VAR} (Table 2) showed more significantly affected metabolites compared to RG^{CON} (Table 2) and RG^{VAR} (Table 4), which could be related to the genetic disposition of RG being less susceptible to biennial bearing.

2020 'Ruby Pink' apple spur bud collection in Tatura

A total of 781 compounds in positive ionisation mode and 535 compounds in negative ionisation mode were detected in 'Ruby Pink' apple spur bud samples. Putative (Level 3) identification of 375 metabolites in positive mode and 227 in negative mode provided similar composition information to the apple buds in the 2018 apple bud collection (AP15013). Metabolite responses (y) against crop load (x) revealed significant metabolite changes (P < 0.01) in response to crop load treatment effects in the primary and secondary leaders (Table 5) and graphs of a few selected metabolites are shown in Figure 4. Most metabolites plateaued at high crop load.

The primary and secondary leaders showed differences in altered metabolites, suggesting unique metabolic pathways utilized in the two branches. Despite differences in both pathways, flavanols were possible signalling molecules. There were some key pathways in the primary leader that included benzoic acid and 4- hydroxybenzoic acid intermediaries in the shikimic acid pathway, and the similarity of the profiles in Figure 4 suggests that they are linked to epicatechin. In the secondary leader, ERI and its glycoside were among the most significantly altered metabolites. Recent studies demonstrated that ERI could efficiently promote fibre development, with genome-wide RNA profiling data indicating that various regulatory pathways like auxin biosynthesis, auxin signalling and transportation, along with the reactive oxygen species (ROS) homeostasis contribute to the enhanced fibre growth in response to ERI treatment (Khan et al. 2019).

Table 5. Significant changes of metabolites (P < 0.01) identified in spur buds of 'Ruby Pink' trees subjected to five crop load treatments on the 'Primary' leader and two crop loads on the 'Secondary' leader.

Row	Mass	Leader	Ionisation mode	RT	Name	P<0.01	Regulation in "ON"
Group_031	200.0332	primary	Pos	1.2	4-Fumarylacetoacetic acid	6.6E-	UP

Group_051	290.0785	primary	Pos	4.0	Epicatechin	9.2E-	DOWN
Group_146	122.0367	primary	Pos	4.0	Benzoic acid	4.5E-	DOWN
Group_160	138.0315	primary	Pos	4.0	4-Hydroxybenzoic acid	7.1E-	DOWN
Group_186	164.0471	primary	Pos	3.8	Phenylpyruvic acid	7.2E-	DOWN
Group_228	209.0382	primary	Pos	1.2	-	2.1E-	UP
Group_232	209.5398	primary	Pos	1.2	-	1.4E-	UP
Group_289	259.0365	primary	Pos	5.0	Glucosamine 6-sulfate	5.9E-	UP
Group_326	280.4721	primary	Pos	1.1	-	7.1E-	DOWN
Group_347	290.0616	primary	Pos	4.0	Dedimethylchlorpromazine	3.4E-	DOWN
Group_370	300.0777	primary	Pos	1.2	Carboxytolbutamide	4.8E-	UP
Group_650	560.1497	primary	Pos	5.1	Apimaysin	2.8E-	DOWN
Group_654	562.1472	primary	Pos	5.8	Epifisetinidol-(4beta->8)-catechin	8.4E-03	UP
Group_663	582.8853	primary	Pos	1.1	-	5.7E-	DOWN
Group_681	611.8793	primary	Pos	1.1	-	8.6E-	DOWN
Group_010	244.0356	primary	Neg	1.2	Fucose 1-phosphate	2.1E-	DOWN
Group_111	244.0744	primary	Neg	4.0	3,3',4'5-Tetrahydroxystilbene	8.2E-03	DOWN
Group_155	306.1328	primary	Neg	4.4	-	4.1E-	DOWN
Group_177	330.0392	primary	Neg	6.0	Blighinone	6.3E-	UP
Group_179	334.0700	primary	Neg	4.0	Xanthotoxol arabinoside	8.1E-	DOWN
Group_213	360.1565	primary	Neg	8.1	Quassinol	8.0E-	DOWN
Group_224	376.1748	primary	Neg	4.4	-	5.5E-	UP
Group_380	548.3371	primary	Neg	7.0	-	7.6E-	UP
Group_428	634.1523	primary	Neg	5.0	-	4.6E-	DOWN
Group_475	786.8641	primary	Neg	1.1	-	1.0E-	DOWN
Group_476	787.3643	primary	Neg	1.1	-	9.5E-	DOWN
Group_514	942.2081	primary	Neg	4.6	-	7.7E-	DOWN*
Group_531	1134.3454	primary	Neg	4.9	-	5.0E-	DOWN
Group_040	232.0555	secondary	Pos	1.3	(2E,11Z)-5-[5-(Methylthio)-4-penten-2-ynyl]-2-	3.6E-03	DOWN
Group_486	386.1393	secondary	Pos	1.2	Edultin	7.8E-	DOWN
Group_339	288.0634	secondary	Pos	3.0	Eriodictyol	2.2E-	DOWN
Group_666	594.1578	secondary	Pos	4.7	Isovitexin 2''-O-glucoside	6.9E-	DOWN
Group_551	450.1161	secondary	Pos	4.7	Eriodictyol-7-O-glucoside	5.2E-	DOWN
Group_211	190.0020	secondary	Pos	1.3	-	8.9E-	DOWN
Group_368	298.9335	secondary	Pos	1.1	-	8.8E-	DOWN
Group_440	338.9589	secondary	Pos	1.1	-	8.1E-	DOWN
Group_631	525.8942	secondary	Pos	1.1	-	2.0E-	DOWN
Group_695	639.8751	secondary	Pos	1.1	-	5.3E-	DOWN
Group_081	152.0112	secondary	Neg	3.0	-	4.2E-	DOWN
Group_437	664.1427	secondary	Neg	6.5	-	5.5E-	DOWN

* not a clear treatment-response effect.

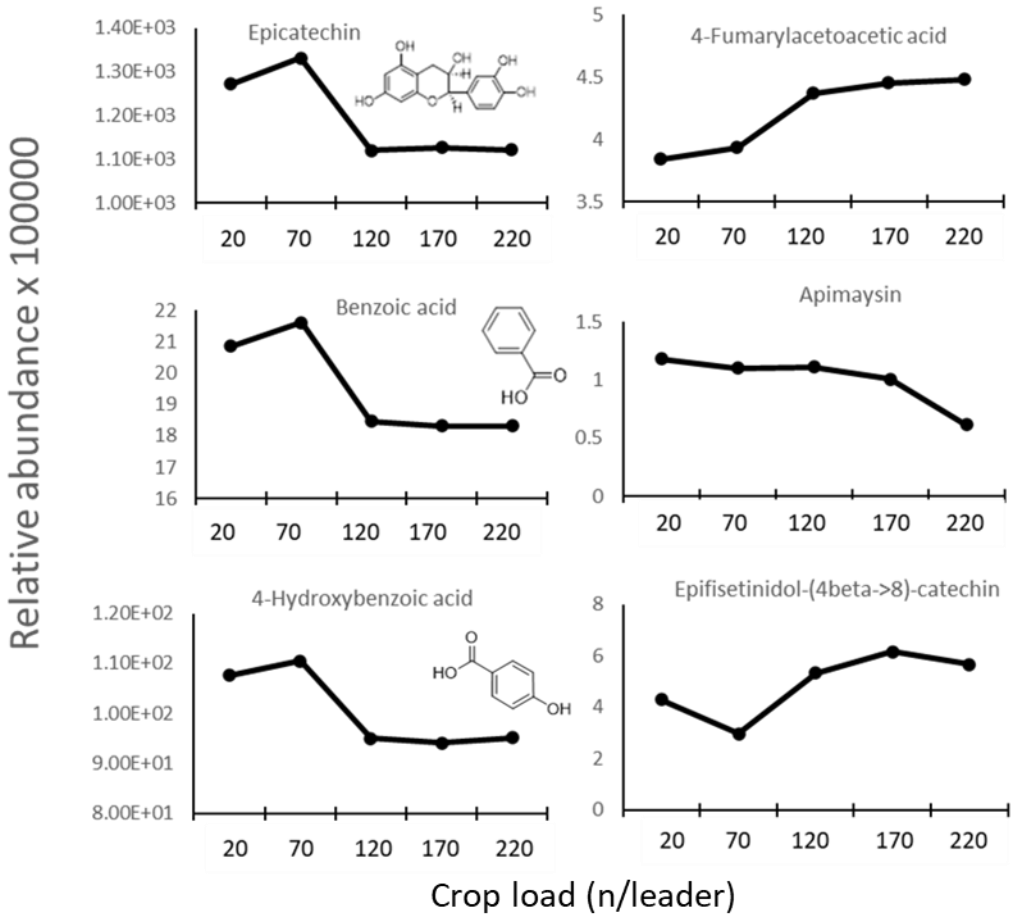

Figure 4. Metabolites Identified in spur buds of 'Ruby Pink' trees with significant changes ($P < 0.01$) in response to five crop load treatments on the 'Primary' leader.

To increase the statistical power of the experiment, the leaders were treated as replicates and a linear model was applied to the whole dataset, with the results shown in Table 6 and some examples in Figure 5. Similar to the 2018 bud samples, metabolites in the p- coumaric acid pathway showed significant response to crop load.

Similar to the flavanol response, the amino acid levels, L-aspartic acid, shows increased levels in "ON" trees which is an inverse response (Figure 5) compared to previous studies (AP15002) (Milyaev et al. 2021) and the AP15013 apple bud collection studies, previously mentioned.

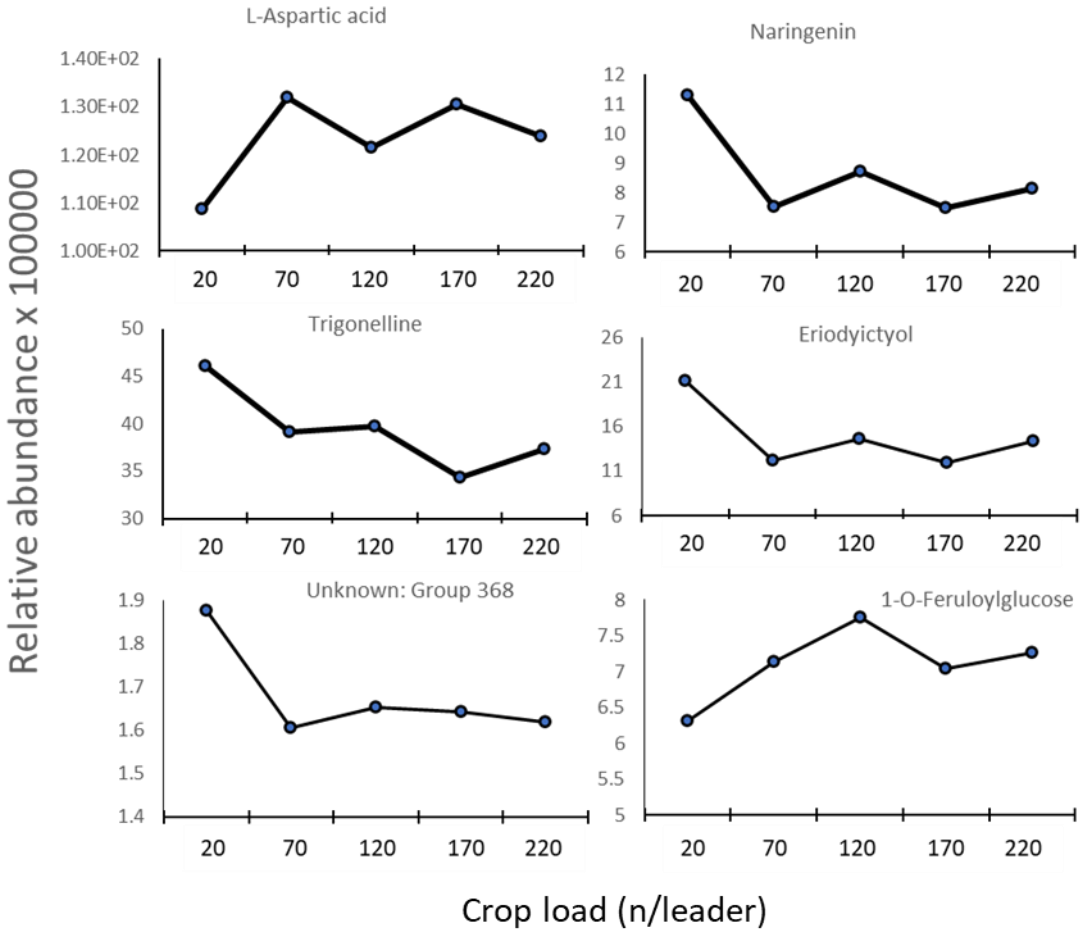

Figure 5. Compounds with significant changes (P < 0.01) associated with crop load in spur buds of 'Ruby Pink' trees, irrespective of leader.

Table 6. Metabolites with significant changes under different crop loads (P < 0.01) identified in spur buds of 'Ruby Pink' trees, irrespective of leader, with five crop load treatments on the 'Primary' leader and two crop loads on the 'Secondary' leader.

Compound ID	Observed Mass		RT (min)	Putative Identification	P-Values: Cropload	Regulation in "ON" trees
Group_011	133.0373	Pos	1.2	L-Aspartic acid	3.5E-03	UP
Group_013	137.0475	Pos	1.3	Trigonelline	7.1E-03	DOWN
Group_308	272.0683	Pos	3.4	Naringenin	4.4E-03	DOWN
Group_339	288.0634	Pos	3.0	Eriodictyol	8.7E-04	DOWN
Group_368	298.9335	Pos	1.1	-	4.0E-03	DOWN
Group_453	356.1103	Pos	4.2	1-O-Feruloylglucose	7.7E-03	UP
Group_529	431.4282	Pos	1.1	-	1.4E-03	DOWN
Group_531	1134.3454	Neg	4.9	-	1.1E-03	*
Group_475	786.8641	Neg	1.1	-	1.6E-03	*
Group_081	152.0112	Neg	3.0	-	2.0E-03	DOWN
Group_155	306.1328	Neg	4.4	-	2.3E-03	*

Group_010	244.0356	Neg	1.2	Fucose 1-phosphate	3.2E-03	DOWN
Group_465	730.3737	Neg	1.1	-	4.6E-03	DOWN
Group_167	326.1016	Neg	3.5	trans-o-Coumaric acid 2-glucoside	4.9E-03	DOWN
Group_486	840.2495	Neg	5.6	-	5.6E-03	DOWN
Group_119	270.0543	Neg	6.4	Apigenin	6.5E-03	DOWN

* not a clear treatment-response effect.

This study demonstrated that flavonoids were affected by varying crop loads, and as such may play a role as signalling molecules within the trees. This is backed up by a recent review which summarized compelling evidence that flavonoids mediate phytohormone signalling and growth responses in plants (Brunetti et al. 2018) . Flavonoids have long been considered as primarily synthesized to constitute an effective shield against the penetration of UV-B radiation to sensitive leaf tissues, and greatly involved in protecting plants challenged by the depletion of stratospheric ozone layer (Bais et al. 2018). However, there is evidence indicating that flavonoids may exert complex functions in both animal and plant cell metabolism, going well-beyond the mere chemical quenching of ROS. Certain flavonoids, especially but not limited to quercetin derivatives, have the ability to modulate signalling cascades that regulate cell growth and differentiation (Jacobs and Rubery, 1988; Stafford, 1991),

2020 'Ruby Pink' apple spur leaves collection in Tatura

A total of 2,811 compounds in positive ionisation mode, and 1,688 compounds in negative ionisation mode were detected in 'Ruby Pink' leaf samples. Putative (Level 3) identification of 1,225 metabolites in positive mode and 614 in negative mode indicated a richer and more complex composition compared to buds. Linear models revealed significant metabolites correlating to crop load treatment effects in the primary and secondary leaders of 'Ruby Pink' (Table 7).

The primary and secondary leaders showed differences in altered metabolites and, like in buds, unique metabolic pathways could be utilized in the two branches. The metabolites detected in the leaves were a diverse range of aromatic compounds. The regulation of these compounds is not clear and may display a very complex response to biennial bearing. Only two compounds reminiscent of the apple buds were present in the secondary leader, including decreased levels of ERI and D-glucose. It is possible that the secondary leader had more pronounced effects due to the large difference in crop load treatments.

Table 7. Metabolites with significant changes under different crop loads (P < 0.01) identified in spur leaves of 'Ruby Pink' trees subjected to five crop load treatments on the 'Primary' leader and two crop loads on the 'Secondary' leader.

Row	Mass	Leader	Ionisation mode	RT	Putative Identification	P-Values <0.01	Regulation of "ON" trees
Group_0036	192.078	Primary	pos	4.6	(R)-Shinanolone	4.3E-03	UP*
Group_0060	235.951	Primary	pos	1.1	-	9.3E-03	DOWN
Group_0139	372.176	Primary	pos	3.6	-	1.4E-03	UP
Group_0312	690.434	Primary	pos	11.	-	6.9E-03	UP
Group_0378	80.2632	Primary	pos	11.	-	4.6E-03	UP
Group_0386	88.0013	Primary	pos	1.1	-	8.8E-03	DOWN
Group_0408	106.042	Primary	pos	6.5	Benzaldehyde	3.8E-03	UP
Group_0437	125.995	Primary	pos	1.1	-	2.6E-03	DOWN*
Group_0478	148.052	Primary	pos	6.5	Cinnamic acid	3.9E-03	UP
Group_0485	152.120	Primary	pos	4.8	(-)-trans-Carveol	2.0E-04	UP
Group_0516	166.005	Primary	pos	1.1	-	7.3E-03	DOWN
Group_0624	214.044	Primary	pos	4.0	fluorobenzoylpropionic acid	2.1E-03	DOWN
Group_0658	225.023	Primary	pos	4.3	-	2.0E-04	UP

Group_0821	274.083	Primary	pos	11.	Phloretin	8.5E-03	DOWN*
Group_0908	294.060	Primary	pos	6.5	-	1.1E-03	UP*
Group_1065	336.035	Primary	pos	1.8	-	1.9E-04	DOWN*
Group_1124	354.146	Primary	pos	9.6	1-Methoxyphaseollidin	5.8E-04	UP
Group_1125	354.146	Primary	pos	8.8	1-Methoxyphaseollidin	7.2E-03	UP*
Group_1158	367.090	Primary	pos	2.9	Xanthurenate-8-O-beta-D-	3.2E-03	UP*
Group_1162	368.110	Primary	pos	4.6	3-O-Feruloylquinic acid	3.5E-03	UP*
Group_1182	372.157	Primary	pos	8.4	Tetrahydrocurcumin	4.7E-03	UP*
Group_1316	408.103	Primary	pos	4.6	-	1.5E-03	UP*
Group_1363	419.126	Primary	pos	5.0	Fenvalerate	8.2E-03	UP*
Group_1474	445.173	Primary	pos	6.2	Narceine	4.9E-03	DOWN**
Group_1609	486.207	Primary	pos	4.8	Glucosylgalactosyl	7.5E-04	UP*
Group_1837	566.412	Primary	pos	11.	3'-Hydroxy-e,e-caroten-3-one	3.6E-03	UP*
Group_1875	582.111	Primary	pos	6.3	5'-Methoxybilobetin	2.9E-03	UP*
Group_1893	586.114	Primary	pos	6.5	-	7.4E-04	UP
Group_1997	618.522	Primary	pos	12.	DG(14:1(9Z)/22:2(13Z,16Z)/0:0	7.7E-03	UP*
Group_2005	620.263	Primary	pos	10.	-	7.4E-03	UP**
Group_2031	626.274	Primary	pos	9.2	-	3.9E-03	UP*
Group_2216	702.395	Primary	pos	11.	-	6.3E-03	UP*
Group_2247	714.395	Primary	pos	11.	-	6.7E-03	UP*
Group_2273	722.460	Primary	pos	11.	-	1.0E-02	UP*
Group_2290	730.426	Primary	pos	11.	-	4.8E-03	UP
Group_2375	762.452	Primary	pos	11.	-	9.0E-03	UP
Group_2410	775.225	Primary	pos	14.	-	3.0E-03	DOWN*
Group_2715	983.258	Primary	pos	3.4	-	4.9E-03	DOWN
Group_0086	528.147	Primary	neg	4.4	-	5.9E-04	UP
Group_0130	622.132	Primary	neg	6.6	-	9.3E-03	UP
Group_0143	662.384	Primary	neg	10.	-	3.4E-03	UP
Group_0305	294.220	Primary	neg	9.8	13-OxoODE	6.3E-03	DOWN
Group_0351	326.101	Primary	neg	4.1	trans-o-Coumaric acid 2-	5.8E-03	UP
Group_0356	328.096	Primary	neg	7.0	Zapotinin	3.2E-03	UP
Group_0379	344.075	Primary	neg	2.7	Theogallin	5.5E-03	*
Group_0459	384.107	Primary	neg	4.6	Eleutheroside B1	1.0E-04	UP*
Group_0630	461.163	Primary	neg	4.4	-	7.3E-05	UP*
Group_0634	462.211	Primary	neg	4.8	-	1.0E-03	UP*
Group_0665	474.160	Primary	neg	1.3	D-Galactopyranosyl-(1->3)-D-	1.8E-03	UP*
Group_0713	496.156	Primary	neg	5.0	Musabalbisiane A	3.4E-03	UP
Group_0750	508.217	Primary	neg	4.8	6-O-Oleuropeoylsucrose	1.7E-03	UP
Group_0889	576.204	Primary	neg	4.5	-	1.9E-03	UP
Group_1178	718.251	Primary	neg	11.	Diisodityrosine	6.9E-04	UP*
Group_1183	719.484	Primary	neg	10.	-	4.4E-03	DOWN
Group_1350	794.520	Primary	neg	14.	1,2-Di-O-palmitoyl-3-O-(6-	1.1E-03	*
Group_1407	823.540	Primary	neg	11.	-	7.4E-03	*
Group_1463	862.507	Primary	neg	14.	-	6.9E-03	*
Group_1542	921.222	Primary	neg	4.8	3-oxo-(2S)-Methylisocapryloyl-	7.7E-04	*
Group_0116	348.118	Secondary	pos	5.5		7.5E-03	DOWN
Group_0219	495.332	Secondary	pos	10.	LysoPC(16:0)	5.7E-03	DOWN
Group_0229	519.332	Secondary	pos	10.	LysoPC(18:2(9Z,12Z))	1.2E-03	DOWN

Group_0545	177.023	Secondary	pos	1.4	Brassicanal A	9.1E-03	DOWN
Group_0698	235.068	Secondary	pos	5.0	6-Succinoaminopurine	1.8E-03	UP
Group_0731	249.052	Secondary	pos	4.2	Cysteinyl-Glutamate	2.0E-04	DOWN
Group_0885	288.063	Secondary	pos	3.0	Eriodictyol	3.4E-03	DOWN
Group_0918	297.066	Secondary	pos	1.4	-	4.0E-03	DOWN
Group_1462	442.129	Secondary	pos	1.4	-	1.6E-04	DOWN
Group_1503	455.314	Secondary	pos	10.	-	4.4E-03	UP
Group_0004	180.063	Secondary	neg	1.2	D-Glucose	1.8E-03	DOWN
Group_0008	226.069	Secondary	neg	1.2	5-Acetylamino-6-formylamino-	1.8E-03	DOWN
Group_0017	320.056	Secondary	neg	1.3	-	5.5E-03	DOWN
Group_0429	370.127	Secondary	neg	5.5	Linusitamarin	1.6E-03	DOWN
Group_0447	378.151	Secondary	neg	12.	-	4.3E-03	DOWN
Group_0740	504.149	Secondary	neg	4.2	6-Caffeoylsucrose	3.1E-04	DOWN
Group_0810	539.323	Secondary	neg	10.	-	6.8E-03	DOWN
Group_1024	633.402	Secondary	neg	11.	-	5.2E-03	DOWN
Group_1102	678.378	Secondary	neg	9.1	Gingerglycolipid B	5.9E-03	DOWN
Group_1233	740.463	Secondary	neg	9.5	-	8.3E-03	DOWN

* not a clear treatment-response effect.

Metabolites in 'Ruby Pink' spur leaves were not clearly affected by crop load and this could be due to the complexity of the tissue as a result of its many functions. However, spur leaves in the secondary leader expressed a significant down regulation of ERI and an energy shift indicated with changes in D-glucose. It is possible that strong, significant metabolite regulation can only be observed in the leaves if the crop load levels are distinct such as the case of the secondary leader.

CONCLUSION

Our study indicated that flavonoid levels in apple buds are affected by varying crop loads, and as such may be involved in regulation of flower bud induction. The constant crop load experiments showed the most consistent findings with previous metabolomics studies (AP15002), these include significant effects on cholorogenic and kaempferol pathway and the amino acid L-arginine. In our study, the flavonoids were the most significantly affected class of compounds in apple buds and some of these, for example ERI, are associated with tissue growth and development. At transcriptomic and proteomic levels, in apple spur buds collected from OFF-trees, metabolic pathways associated with tissue growth and development were detected that potentially result in a promoting effect on early flower bud development. The transcriptomic and proteomic levels in spur buds collected on ON-trees showed that the plant hormone signal transduction pathway was enriched, suggesting the involvement of hormonal metabolites in determining the fate of the apple bud meristem. A further step towards systematic understanding of flower induction in apple will require the determination of plant hormone profile by additional analysis and using extraction protocols specifically designed for the analyses of phytohormones and polar metabolites (Farrow and Emery 2012; Urbanová et al. 2013), which we plan to perform in the near future.

In this study, it must be noted that the plant metabolites identified will require further identification using LCMSMS techniques and/or library confirmation.

RECOMMENDATIONS

It is recommended that further LCMS analysis of bud extracts be undertaken to provide better confidence in the identity of the compounds putatively identified so far, and to attempt to identify the unknown compounds which have shown good correlation with crop load.

It is also recommended that a LCMS column and gradient conditions more amenable to the separation of the more polar compounds be investigated for future work, to allow for easier detection and better confidence in the identity of these early eluting compounds.

REFERENCES

Brunetti, C., et al. (2018). "Modulation of Phytohormone Signaling: A Primary Function of Flavonoids in Plant-Environment Interactions." Frontiers in Plant Science **9**: 1042-1042.

Khan, A. Q., et al. (2019). "Eriodictyol can modulate cellular auxin gradients to efficiently promote in vitro cotton fibre development." BMC Plant Biology **19**(1): 443.

Milyaev, A., et al. (2021). "Toward Systematic Understanding of Flower Bud Induction in Apple: A Multi-Omics Approach." Frontiers in Plant Science **12**(286).

Peer, W. A. and A. S. Murphy (2006). Flavonoids as signal molecules: Targets of flavonoid action. The Science of Flavonoids**:** 239-268.

Viant, M. R., et al. (2017). "How close are we to complete annotation of metabolomes?" Current Opinion in Chemical Biology **36**: 64-69.

Stefanelli D, Plozza T, Flachowsky H, Wünsche JN (2018) Young apple tree responses to crop load. In: Acta Horticulturae, pp 221-228.

Milyaev A, Kofler J, Pfannstiel J, Stefanelli D, Flachowsky H, Hanke MV, Wünsche JN (2018) Histological and proteomic approaches to study floral bud induction in relation to biennial bearing in apple. In: Acta Horticulturae, pp 277-283.

APPENDICES

Appendix A:

Supplementary Table 1. Metabolites with significant changes in response to different crop loads identified in spur leaves of 'Ruby Pink' trees, irrespective of leader, with five crop load treatments on the 'Primary' leader and two crop loads on the 'Secondary' leader. Metabolites identified using (ESI+)- LCMS profiling.

Row	Mass		RT	Putative Identification	P-Values <0.01	Regulation in "ON" trees
Group_0049	215.9433	pos	1.1	-	9.2E-03	DOWN*
Group_0116	348.1185	pos	5.5	-	7.0E-03	DOWN
Group_0403	103.0963	pos	1.2	-	6.3E-03	UP*
Group_0461	142.9895	pos	1.1	-	8.2E-03	DOWN*
Group_0478	148.0524	pos	6.5	Cinnamic acid	8.7E-03	UP*
Group_0516	166.0055	pos	1.1	-	8.7E-03	DOWN*
Group_0698	235.0682	pos	5.0	6-Succinoaminopurine	6.7E-03	UP**
Group_0731	249.0524	pos	4.2	Cysteinyl-Glutamate	2.0E-03	DOWN
Group_0746	255.1081	pos	3.8	-	9.4E-03	DOWN*
Group_0753	256.9697	pos	1.1	-	3.8E-03	DOWN*
Group_0835	275.5843	pos	5.2	-	7.8E-03	DOWN*
Group_0908	294.0606	pos	6.5	-	1.1E-03	UP*
Group_0912	294.2194	pos	10.0	13-OxoODE	8.1E-03	DOWN
Group_0918	297.0663	pos	1.4	-	2.3E-03	DOWN*
Group_1124	354.1469	pos	9.6	1-Methoxyphaseollidin	5.1E-03	UP*
Group_1158	367.0903	pos	2.9	Xanthurenate-8-O-beta-D-glucoside	7.5E-04	UP**
Group_1182	372.1572	pos	8.4	Tetrahydrocurcumin	1.0E-02	UP*
Group_1296	402.1499	pos	3.8	Benzyl beta-primeveroside	6.7E-03	UP*
Group_1326	408.3751	pos	14.3	-	9.7E-03	UP*
Group_1334	410.3183	pos	10.6	Gamma-Tocotrienol	9.4E-03	UP*
Group_1462	442.1298	pos	1.4	-	1.2E-04	DOWN*
Group_1474	445.1731	pos	6.2	Narceine	4.9E-03	DOWN(NA

Group_1523	462.0817	pos	4.9	Oxazepam glucuronide	9.9E-03	UP*
Group_1578	475.2052	pos	5.2	-	2.3E-03	DOWN
Group_1630	494.1555	pos	6.7	-	8.7E-03	DOWN
Group_1788	545.1610	pos	5.7	-	4.5E-03	DOWN
Group_1837	566.4121	pos	11.5	3'-Hydroxy-e,e-caroten-3-one	9.1E-03	UP*
Group_1875	582.1115	pos	6.3	5'-Methoxybilobetin	4.6E-04	UP*
Group_1893	586.1147	pos	6.5	-	1.4E-03	UP*
Group_1949	606.2080	pos	6.2	-	1.2E-03	DOWN*
Group_2257	718.3913	pos	9.2	-	5.9E-03	*
Group_2306	737.4438	pos	8.8	-	6.6E-03	DOWN(NA
Group_2715	983.2584	pos	3.4	-	4.1E-03	DOWN
Group_0885	288.0635	pos	3.0	Eriodictyol*	3.6E-02	*
Group_2417	777.5307	pos	9.6	PC(14:0/22:6(4Z,7Z,10Z,13Z,16Z,19Z))	4.6E-02	*
Group_0004	180.0638	ne	1.2	D-Glucose	4.9E-03	*
Group_0008	226.0697	ne	1.2	5-Acetylamino-6-formylamino-3-	6.2E-03	*
Group_0213	128.9546	ne	1.2	-	5.2E-03	*
Group_0456	382.1388	ne	1.3	Licoricone	1.1E-03	*
Group_1178	718.2516	ne	11.1	Diisodityrosine	9.7E-04	*
Group_1620	1006.312	ne	4.9	-	6.2E-04	*
Group_1662	1122.454	ne	6.0	-	2.6E-03	*

° > 1.5 effect size and good general linear trend for L1 and L2 (P<0.05)

*Unclear metabolite direction

Supplementary Table 2. Metabolites with significant changes in response to different crop loads identified in spur leaves of 'Ruby Pink' trees, irrespective of leader, with five crop load treatments on the 'Primary' leader and two crop loads on the 'Secondary' leader. Metabolites identified using (-ve) LCMS profiling.

Compound ID	**Observed Mass**		**RT (min)**	**Putative Identification**	**P-Values: Cropload**	**Regulation in "ON" trees**
Group_0004	180.0638	Neg	1.2	D-Glucose	4.9E-03	DOWN
Group_0008	226.0697	Neg	1.2	5-Acetylamino-6-formylamino-3-methyluracil	6.2E-03	DOWN
Group_0213	128.9546	Neg	1.2		5.2E-03	*
Group_0456	382.1388	Neg	1.3	Licoricone	1.1E-03	DOWN
Group_1178	718.2516	Neg	11.1	Diisodityrosine	9.7E-04	*
Group_1620	1006.3120	Neg	4.9		6.2E-04	*
Group_1662	1122.4541	Neg	6.0		2.6E-03	*

*Unclear metabolite direction

AP19003 Advancing sustainable and technology driven apple orchard production systems

Technical Report: Effect of crop load relationships on chemical signalling

Agriculture Victoria Research

April 2021

VICTORIA State Government | Jobs, Precincts and Regions

AGRICULTURE VICTORIA

Author: Priyanka Reddy, Tim Plozza, Vilnis Ezernieks, Simone Rochfort, Alessio Scalisi and Ian Goodwin

Project RDC Number: AP19003

Project CMI Number: 106472

Department of Jobs, Precincts and Regions
1 Spring Street Melbourne Victoria 3000
Telephone (03) 9651 9999

Contents

EXECUTIVE SUMMARY

The gross value of Australia's apple industry was $566 million in 2013, with Victoria representing approximately 30% of total Australian production. However, the value of this industry could be increased if more consistent crop loads were achieved for those apple cultivars which are susceptible to biennial bearing, a phenomenon characterised by "ON" and "OFF" years of flowering and, subsequently, fruit production. Biennial bearing costs growers and the Australian apple industry millions of dollars in additional labour and lost production due to inconsistent yields. Fruit growers usually remove excess flowers and fruitlets in "ON" years, using moderately effective horticultural practices, to increase fruit size in the current season and the amount of bloom in the subsequent season, but the methods are extremely time consuming and costly, and even with best thinning practice, yields can still be reduced by more than 20%.

Flower bud induction in "OFF" (i.e. low yield) years typically results from a poor flower bud formation due to a high crop load in the previous year (i.e. "ON"), suggesting that the fruit inhibits the concomitant development of the adjacent spur bud. The overall research goal of the current project was to reveal the largely unknown physiological and molecular mechanisms of biennial bearing in apple, thereby to better understand the underlying pathways and triggers of flower induction that might facilitate intervention opportunities for controlling apple crop load and thus ensuring stable apple production.

In this study, we report findings of metabolite regulation in apple buds and leaves in response to different crop load levels. Specifically, presented results are based on 1) buds collected from a previous experiment (AP15013) that utilised 'Rosy Glow' and 'Nicoter' apple cultivars in the Yarra Valley (from seven samples collected in late Spring — early Summer 2018 where, a range of crop loads were imposed on 'Rosy Glow' and 'Nicoter' apple trees over four seasons; 2) buds and leaves collected in the current crop load experiment (AP19003) which utilised 'Ruby Pink' apple trees subjected to crop load treatments established in October 2020. These treatments consisted of 5 crop load treatments (i.e. 20, 70, 120, 170 and 220 fruit per leader) in the primary leader as well as two crop load treatments (low and high) in the secondary leader of each tree.

Using non-targeted metabolomics profiling this study revealed that flavonoids in the buds were often affected by crop load levels and as such may play a role in regulating return bloom. Differences in expressed metabolites were found between the constant and variable crop load treatments (project AP15013). Samples from AP15013 varied in differentially expressed metabolites which could be related to constant crop loads showing a more pronounced effect due to equilibrated response over four seasons. Crop load effects were observed on flavanols such as kaempferol, naringenin and p-coumaric acid, which are consistent with physiological responses observed from bud samples taken and analysed in Germany for project AP15002 (Milyaev et al. 2021). Furthermore, crop load treatments showed larger effects on 'Nicoter' apple trees compared to 'Rosy Glow', which may be the consequence of a decreased susceptibility of 'Rosy Glow' to biennial bearing.

Results obtained on 'Nicoter' and 'Rosy Glow' trees were further corroborated by the findings in 'Ruby Pink' buds, where flavanols were also found as possible signalling molecules. Key pathways in the primary leader included benzoic acid and 4- hydroxybenzoic acid - intermediaries in the shikimic acid pathway linked to the flavanol epicatechin, one of the most abundant flavonoids in fruit such as apple, pear or grape. In the secondary leader, we found the flavanone eriodictyol (ERI) and its glycoside metabolites to be the most significantly altered metabolites.

Our study indicated possible candidates for potential signalling molecules for flower bud induction. However, plant metabolites identified in the non-targeted metabolomics analysis will require further identification using LCMS/MS mass spectrometry techniques. A further step towards systematic understanding of flower induction in apple will require determination of plant hormone profile by additional steps, such as using specific column chromatography techniques or extraction protocols specifically designed for the analyses of phytohormones (Farrow and Emery 2012; Urbanová et al. 2013), which we plan to perform in the near future.

INTRODUCTION

This technical report is a deliverable for project AP19003, "Advancing sustainable and technology driven apple orchard production systems". This work aims to explore the potential physiological mechanism (such as signalling compounds) for observed impacts of high crop load on floral initiation and flower development in apple trees. We report the results of molecular analysis of buds and leaves collected in December 2020 from 'Ruby Pink' apple trees from a commercial orchard in Ardmona, Victoria, as well as buds from the cultivars 'Nicoter' and 'Rosy Glow' collected from a commercial orchard at Three Bridges, Yarra Valley, Victoria, for project AP15013.

Project outcome

The intended outcome of this project is to improve crop load management in a variable climate by providing knowledge and tools to deliver premium fruit that meets consumer expectations in domestic and export markets.

Project background

The Australian apple industry, like many fruit production industries, is plagued by high cost of production and variable fruit quality that often does not meet consumer expectations. This can greatly reduce a grower's profitability. In the last ten years, apple production has increased but is yet to reach its full potential based on the area planted (10,000 ha) and the theoretical yield (~800,000 t). This is mostly due to variable crop load management, biennial bearing and inconsistent fruit quality.

Australia has a unique climate characterised by relatively high temperatures and light intensity compared to other apple production areas around the world. Light interception and consequent carbohydrate availability play an important role in defining the optimal number of fruit that a tree should hold to maximise consistent fruit quality for the life of the tree. Furthermore, light interception and carbohydrate supply are fundamental in influencing fruit quality in a variable climate of extreme heat events.

Apple is generally susceptible to biennial bearing, which is the tendency to alternate years of high flower initiation followed by low initiation the subsequent year. From previous studies on crop load management of an established cultivar ('Rosy Glow') and emerging cultivar ('Nicoter') (projects AP15013 and AP15002), it was noticed that there is an inverse correlation between fruit number on trees (i.e. crop load) and most aspects of fruit quality (size, colour, fruit maturity, flesh firmness and soluble solids concentration). These previous studies found that biennial bearing is controlled at tree level from a combination of genetics (flower induction genes) and environment (carbohydrate availability) probably mediated by metabolites that act as chemical signals that either stimulate or inhibit the activation of the genes.

Project objectives

Physiological studies and the development of sensing tools will be undertaken in the Sundial apple orchard at the Tatura SmartFarm and in a commercial orchard in the Goulburn Valley to address the following three objectives as per the Hort Innovation RFP:

- Develop crop load, training systems, pruning and irrigation optimisation for yield, quality and labour efficiency in new and emerging apple cultivars.
- Develop orchard design techniques, tools and management practices that enhance the ability of orchards to manage climate variability and weather extremes.
- Communicate findings in a clear and practical format to growers and wider industry.

METHOD

2018/2019 Bud Collection (AP15013)

The experiment was conducted in a commercial farm at Three Bridges, Yarra Valley, Victoria, Australia. Three-year old trees of the cultivars 'Nicoter' (marketed as Kanzi®) and 'Rosy Glow' (marketed as Pink Lady®), trained on Open Tatura trellis, were used. Trees were managed according to the standard local practice and commercial operations. Five crop load treatments were first applied during the 2015-16 growing season with six replicates, for a total of 30 trees per cultivar. Crop load treatments consisted of 1%, 50%, 100%, 150%, and 200% of normal grower practice, based on the tree's trunk cross sectional area (TCSA), which was measured at the beginning of each growing season. In 2016-17 and subsequent seasons, three replicates of each crop load treatment maintained the same crop load (NIC^{CON} = 'Nicoter' constant crop load; RG^{CON} = 'Rosy Glow' constant crop load), and the other three replicates alternated between corresponding low and high treatments (e.g. 1% became 200%, 150% became 50%), thus forcing a biennial-type cropping behaviour on those trees (NIC^{VAR} = 'Nicoter' Variable crop load; RG^{VAR} = 'Rosy Glow' Variable crop load).

Each season at full bloom (80% open flowers), flower clusters on each tree were counted manually to determine return bloom. Flower clusters were then thinned by hand to impose the required crop load level per tree. Only one fruit per cluster was retained, except where insufficient clusters meant higher fruit numbers per cluster were needed to achieve the desired number of fruit per tree. Thinning was completed within 4 weeks of full bloom to minimize the chance of excess fruit affecting the following year's return bloom.

In the 2018/19 season, beginning 4 weeks after full bloom, one bud per tree was collected weekly for eight weeks and prepared for molecular analysis by the Molecular Phenomics Group within Agriculture Victoria Research.

2020 Apple Bud Collection

The experiment was conducted at the Plunkett orchard, 255 Macisaac Rd, Ardmona (113 m a.s.l.) in the Goulburn Valley, Victoria, Australia. 'Ruby Pink' apple trees trained to a two leader vertical trellis configuration were used for this experiment, which began in the 2020/21 season. 30 trees occupying a single row in the orchard were utilized for the experiment and were replicated in three randomised blocks, each consisting of 10 trees (two panels of five trees). One of five crop loads (20, 70, 120, 170 or 220 fruit/leader) were applied to the 'Primary' leader on each tree in late October, and one of two crop loads (Low ~ 20 fruit/leader) or High (~220 fruit/leader)) applied to the 'Secondary' leader. The randomised application of these treatments is shown in Table 1. The selection of primary leaders was based on similar TCSA. At the beginning of the experiment, TCSA in primary leaders had a mean of 27.4 and a standard deviation of 6.3 cm^2, and secondary leaders had TCSA = 27.5 ± 12.4 cm^2.

Table 1. Randomised application of crop load levels to the Primary and Secondary leaders of the 'Ruby Pink' apple trees. Low = ~ 20 fruit/tree, High = ~ 220 fruit/tree.

Block	Tree number	Crop load of primary leader (n)	Crop load of secondary leader
1	1	170	Low
1	2	120	High
1	3	220	Low
1	4	20	Low
1	5	120	Low
1	6	70	Low
1	7	70	High
1	8	20	High
1	9	170	High
1	10	220	High
2	11	170	Low
2	12	220	Low
2	13	120	High
2	14	70	Low

2	15	20	Low
2	16	220	High
2	17	70	High
2	18	20	High
2	19	120	Low
2	20	170	High
3	22	70	Low
3	23	20	High
3	25	220	Low
3	26	120	High
3	29	170	High
3	30	70	High
3	31	220	High
3	32	20	Low
3	33	120	Low
3	34	170	Low

Buds and leaves were collected from the trees in December 2020, approximately 70 days after full bloom, which approximates the time at which buds transform from vegetative to reproductive, as documented in AP15002 final report. 3 buds per tree and 2 – 3 fully expanded leaves adjacent to each of these buds were collected and prepared for molecular analysis by the Molecular Phenomics Group within Agriculture Victoria Research. One bud each was collected from a low, mid and high location on each tree.

Samples were frozen on dry ice as soon as possible after collection and stored in a freezer at −80°C until analysis.

Bud and leaf sample selection and preparation

Buds were selected on spurs growing on at least 2-year-old wood.

Spurs on lateral branches of the tree were selected and not spurs from the central leader or the top.

Only fruiting spurs with subtending bud (figure 1 a) were chosen where possible, otherwise a bud close to a fruiting spur was chosen. If the bourse shoot was > 5 cm spur was not sampled.

Buds were removed from the trees by breaking them off the spur (figure 2 b).

Leaves were removed from the bud (figure 2 c) and for the 2020 sampling, 2 – 3 fully expanded leaves placed in a zip-lock bag and frozen in dry ice.

A scalpel was used to peel or slice away the brown scales on the bud to leave behind the growing tip with no/minimal brown material (figure 2 d).

The bud was cut off above the wooden part using a scalpel (no woody part was kept on the sample) (figure 2 e).

The prepared bud was placed in a pre-weighed Eppendorf tube, weighed and then placed on dry ice.

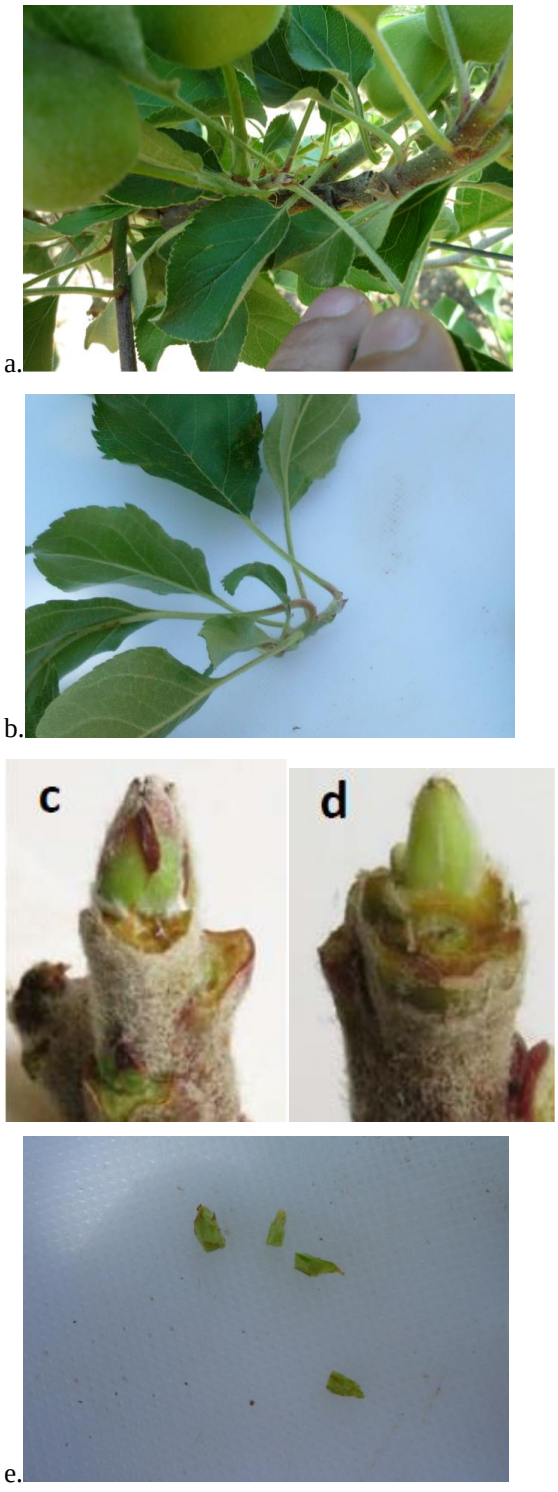

Figure 1. Fruiting spur with (a) subtending bud, (b) bud removed from tree, (c) bud with leaves removed, (d) peeled bud and (e) growing tip removed from woody stem.

Identification and relative quantitation of potential chemical signalling compounds

Metabolites were extracted from bud and leaf samples and analysed using high resolution, accurate mass liquid chromatography-mass spectrometry (LCMS) instruments to find and identify potential chemical signalling compounds related to crop load treatments and return bloom. Methods included untargeted analysis, which involved finding and identifying unknown compounds whose presence and concentration correlated with return bloom measurements.

Sample Extraction of 2020 Bud collection

All specimens collected were immediately snap-frozen in liquid nitrogen and stored at −80°C. Specimens from each biological replicate were kept in separate safe-lock tubes. Subsequent to apple buds being lyophilized, two ceramic beads (2.8 – 3.2 mm YTZP (yttria zirconia beads)) were placed in the 1.5 mL Eppendorf tubes for the ('Ruby Pink') 2020 collection, that contained one apple bud per tube. Three apple buds per tube were collected into a 2 mL Eppendorf for the 2018 collection ('Nicoter' and 'Rosy Glow') and thus 1 large (3.5 – 4.1 mm YTZP) and 2 small beads (2.8 – 3.2 mm YTZP) were added. Samples were placed in 24 well cryo-blocks on the Geno/Grinder 2010 (SPEX Sample Prep, Metuchen, NJ, USA) and the buds were ground at 1,200 rpm for 1 min. The samples were extracted with 80% methanol/water (v/v), with extraction volumes adjusted proportionally to the weight of the lyophilized bud. Samples were centrifuged at 13,000 rpm for 2 min and 200 µL of the supernatant was transferred into a HPLC tube and stored at −20°C until ready for LCMS analysis.

LCMS Methods for Untargeted Analysis and Compound Identification

For untargeted metabolite profiling, a Vanquish Ultra-High Performance Liquid Chromatography (UHPLC) system (Thermo Fisher Scientific, Bremen) with a binary pump, autosampler and temperature-controlled column compartment coupled with a QExactive (QE) Plus mass spectrometer (Thermo, Bremen, Germany) detector was used. An electrospray ionization (ESI) probe operating in the positive and negative ionization modes and the mass spectrometer captured data over a range of 80 – 1,200 m/z, with mass resolution set at 17,000. Nitrogen was used as the sheath, auxiliary and sweep gases at flow rates of 28, 15 and 4 L/min, respectively. Spray voltage was set at 4,000 V (positive and negative). A 3 µL sample injection volume was used. Samples were randomized, and blanks (80% methanol) injected every five samples. A pooled biological quality control (PBQC) was run every 10 samples. Prior to data acquisition, the system was calibrated with Pierce LTQ Velos ESI Positive and Negative Ion Calibration Solution (Thermo Fisher Scientific). Mass spectrometry data was acquired using Thermo Xcalibur V. 2.1 (Thermo Fisher Scientific Inc., USA). Quantitative analysis was conducted using LCQUAN™ Quantitative Software (Thermo Fisher Scientific).

A Thermo Fisher Scientific Hypersil Gold 1.9 µm, 100 mm × 2.1 mm column with a gradient mobile phase consisting of 0.1% formic acid in H_2O (A) and 0.1% formic acid in acetonitrile (B), at a flow rate of 0.3 mL/min was used. The gradient began at 2% B, increasing to 100% B over 11 min; followed by 4 min at 100% B before a 5 min equilibration with 2% B.

Untargeted Analysis: Putative Compound Identification

The data files obtained following LCMS analyses were processed in the Refiner MS module of Genedata Expressionist® 12.0 optimising the; 1) chromatogram chemical noise subtraction, 2) intensity thresholding, 3) selection of positive mode data only, 4) chromatogram RT alignment, 5) chromatogram peak detection. Analyte identification of significant metabolites were performed by searching experimental MS1 data through databases METLIN, ChemSpider (http://www.chemspider.com) and MS/MS data was searched on MzCloud (https://www.mzcloud.org) and MetFragment®.

Statistics

Data processing and statistical analyses

The data files obtained following LCMS analyses were processed in the Refiner MS module of Genedata Expressionist® 12.0 with the following parameters: 1) chromatogram chemical noise subtraction with removal of peaks with less than 4 scans, chromatogram smoothing using moving average estimator over 5 scans, and 30% quantile over 151 scans for noise subtraction, 2) intensity thresholding using a clipping method and a threshold of 100,000, 3) selection of positive mode data only, 4) chromatogram RT alignment using a pairwise alignment based tree and a maximum RT shift of 1 min, 5) chromatogram peak detection using a 5 scans summation window, a minimum peak size of 0.1 min, a maximum merge distance of 0.05 Da, a boundary merge strategy, a maximum gap/peak ratio of 70% with moving average smoothing over 10 scans for peak RT splitting 6) chromatogram isotope clustering using RT and m/z tolerance of 0.05 min and 0.05 Dalton respectively with a maximum charge of 2, 7) adduct detection using mainly M+H and allowable adducts (M+2H, M+K, M+Na, M-H_2O+H).

Statistical analyses were performed using the Analyst module of Genedata Expressionist® 12.0. Principal component analyses (PCA) were performed to identify tissue and treatment differences. Overlay of the PBQC and samples allowed for the validation of the high-quality dataset by ensuring that RT variation, mass error and sensitivity changes throughout

the run were consistent. Linear procedures were used (e.g. regression analysis, principal component analysis) to test treatment effects on the regulation of metabolites. In this study, final linear regression p-values were reported ($p < 0.01$), with metabolite (y) responses to the fixed effects of crop load treatments (x).

Identification of metabolites was performed by searching experimental MS[1] data through the following databases: Plant Metabolic Network (PMN) https://plantcyc.org/; Human Metabolome DataBase (HMDB) (http://hmdb.ca); ChemSpider (http://chemspider.com); and Lipid Maps®(http://www.lipidmaps.org); .

RESULTS AND DISCUSSION

2018/2019 Bud collection

PCA plots of 'Rosy Glow' and 'Nicoter' apple bud extracts revealed separation of the two cultivars (Figure 2 a). The metabolome of the individual cultivars was distinct. Although, crop load effects are thought to occur irrespective of cultivar (Milyaev, Kofler et al. 2021) the PCA model indicates that the pathways between the two cultivars may have differences and were thus explored individually. Furthermore, there may be differences in stress induced pathways associated with apple trees treated with a constant and a variable/biennial crop load.

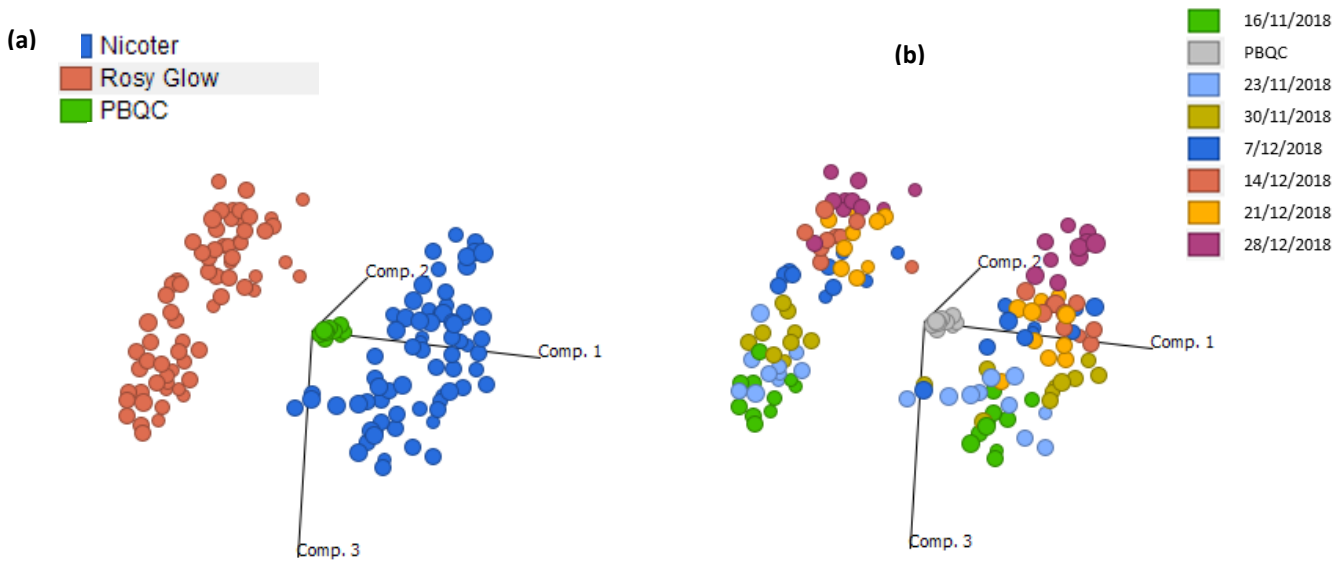

Figure 2. PCA scores plot showing (a) positive ion ESI LCMS of the metabolome (908 metabolites) categorised by variety and (b) by collection date.

A total of 908 compounds in positive ionisation mode and 634 compounds in negative ionization mode were detected from apple spur bud samples in NIC^{CON}, NIC^{VAR}, RG^{CON} and RG^{VAR}. Putative (Level 3) identification of 436 metabolites in positive mode and 265 in negative mode, provided valuable information on the complex composition of the apple bud, including plant hormones, lipids, amino acids, vitamins and phenols. However, it is important to note that further confirmation of metabolites (Level 1 and 2 compound identification) requires in-house standards, or MS2 fragmentation spectra matched to a database/journal publication (Viant et al. 2017).

Metabolite responses (y) against crop load (x) revealed significant metabolite changes ($p < 0.01$) in response to constant and variable crop load treatment effects in 'Nicoter' and 'Rosy Glow' (Figure 3).

In NIC^{CON} the flavonoids (afzelechin 7-apioside, quercetin, kaempferide, kaempferol and naringenin) showed increasing levels with higher crop load trees ("ON") (Table 1). Kaempferol and its precursor naringenin are important biomarkers as previous reports have identified derivatives of its biosynthetic intermediate, p-coumaryl COA in "ON" trees (Milyaev, Kofler et al. 2021). Moreover, the transcriptome and proteome of apple buds have shown enzymatic activity of enzymatic reaction EC:2.3.1.133 that metabolizes at least 3 derivatives of p-coumaric acid including p-coumaroyl CoA and caffeoyl shikimic acid, precursors of the kaempferol and chlorogenic acid pathway (Milyaev et al. 2021). Nuclear localisation of flavonoids has been reported in many plant species, suggesting that flavonoids may function in transcriptional regulation of endogenous gene expression (Peer and Murphy 2006). Naringenin chalcone and apigenin also may influence flavonoid biosynthesis by regulating transcription of flavonoid biosynthetic enzymes (Pelletier et al., 1999).

In NIC^{CON} decreased levels of amino acids L-asparagine and L-arginine and the peptide aspartyl-glutamine were observed in "ON" trees (Table 1), corroborating the findings on arginine levels obtained by Milyaev et al. (2021) . Amino acids serve as protein building blocks and reduced levels could suggest increased competition for resources/nutrients in high crop load trees. Arginine also serves as a nitrogen storage in plants and enables fine-tuning of the production of nitric oxide, polyamines and potentially proline (Winter et al. 2015).

Similar to NIC^{CON}, the RG^{CON} showed decreased levels of asparagine (Table 2); however, the perturbation in metabolites in RG^{CON} is limited to 5 metabolites compared to 22 metabolites in NIC^{CON}, this could be related to RG having less susceptibility to biennial bearing (AP15013) which could also explain the uneven trends in the RG^{VAR} (Table 4).

Table 1. Significant metabolites (P < 0.01) identified in spur buds of 'Nicoter' trees subjected to constant crop load.

Compound ID	Ionisation mode	Observed Mass	RT (min)	Putative identification[1]	P-Values	Regulation in "ON" trees
Group_012	pos	132.0534	1.2	L-Asparagine	5.1E-	DOWN
Group_013	pos	133.0505	1.2	Unknown amino	4.8E-	DOWN
Group_014	pos	133.0568	1.2	Unknown amino	4.4E-	DOWN
Group_030	pos	178.084	1.3	2-O-Methyl-L-	6.5E-	UP
Group_055	pos	261.0958	1.2	Aspartyl-	8.3E-	DOWN
Group_061	pos	280.0629	1.3	Sulfametopyrazine	7.3E-	UP
Group_092	pos	406.1263	5.6	Afzelechin 7-	2.3E-	UP
Group_094	pos	418.0897	5.2	Kaempferol 3-O-	3.3E-	UP
Group_096	pos	434.0844	4.9	Fukinolic acid	3.7E-	UP
Group_101	pos	462.1157	5.3	kaempferide 3-O-	6.8E-	UP
Group_113	pos	562.1469	3.7	Epifisetinidol-	9.4E-	UP
Group_246	pos	174.1115	1.2	L-Arginine	3.1E-	DOWN
Group_362	pos	272.0684	5.4	Naringenin	9.1E-	UP
Group_395	pos	286.0474	5.2	Luteolin	8.8E-	UP
Group_428	pos	302.0422	4.9	Quercetin	5.8E-	UP
Group_447	pos	314.1321	1.2	-	1.4E-	DOWN
Group_452	pos	398.9028	1.1	-	3.5E-	UP
Group_587	pos	425.0996	5.6	-	2.6E-	UP
Group_634	pos	451.1477	3.9	5-O-	1.0E-	DOWN
Group_663	pos	470.0822	5.2	-	6.2E-	UP
Group_722	pos	529.1285	5.0	-	2.5E-	DOWN
Group_786	pos	628.1628	5.6	-	6.0E-	UP

Table 2. Significant changes of metabolites (P < 0.01) identified in spur buds of 'Rosy Glow' trees subjected to constant crop load.

Compound ID	Ionisation	Observed	RT	Putative	P-Values	Regulation in
Group_690	pos	497.8984	1.1	-	6.4E-03	UP

Group_136	pos	81.00689	1.1	-	6.7E-03	UP
Group_137	pos	82.00765	1.1	-	7.1E-03	UP
Group_012	pos	132.0534	1.2	L-Asparagine	8.5E-03	DOWN
Group_532	pos	383.9176	1.1	-	8.9E-03	UP

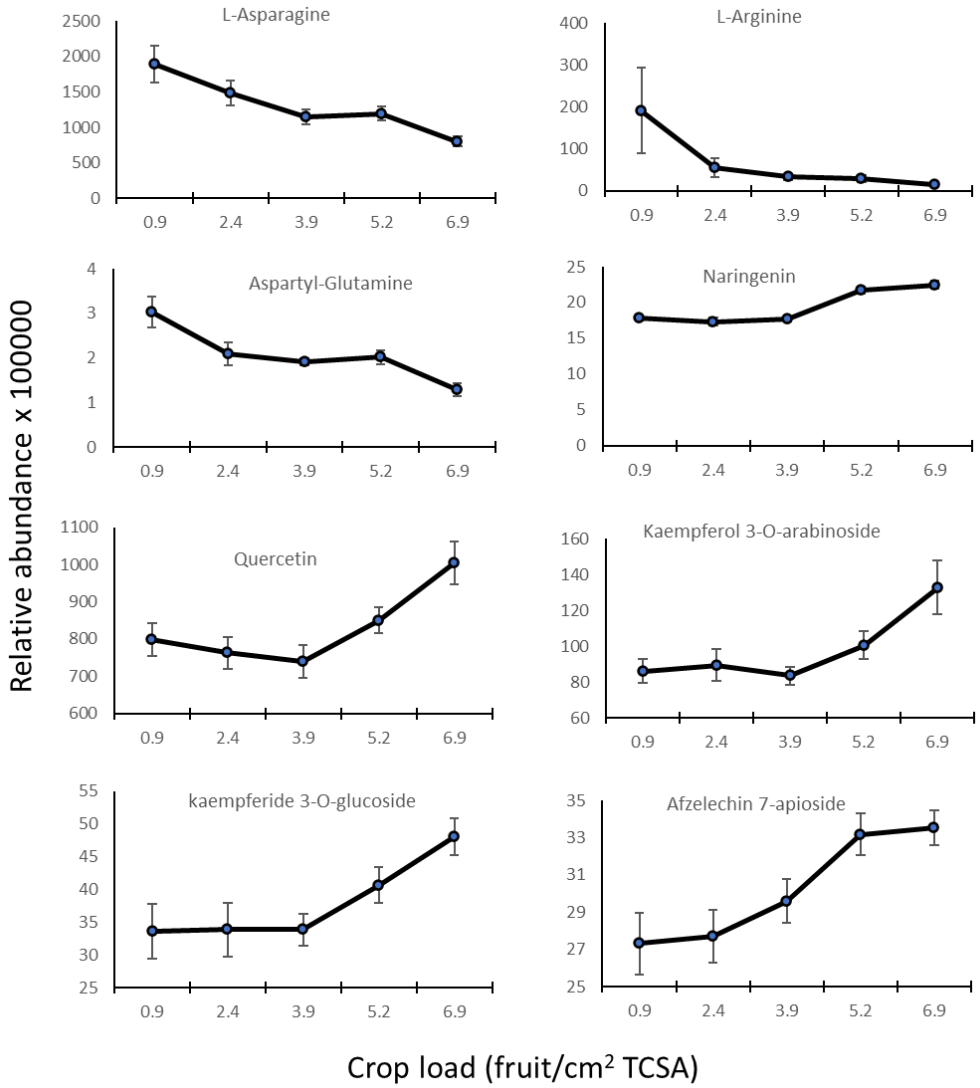

Figure 3. Relative abundance of selected amino acids and flavanols ($P < 0.01$) identified in spur buds of 'Nicoter' trees subjected to different crop load treatments.

NIC^{CON} and NIC^{VAR} crop load treatment effects showed little similarity in metabolite pathways. Most altered metabolites in the variable treatments eluted at 1.1 min, which suggests effects on primary metabolites such as sugars, amino acids, organic acids and nucleic acids (Table 3). These could be explained by the increased resources required for "ON" trees. The metabolites in the constant crop load trees may have reached an equilibrated state, making the effects more pronounced.

Table 3. Significant changes of identified metabolites (P < 0.01) in spur buds of 'Nicoter' trees subjected to variable crop load.

Compound ID	Ionisation mode	Observed Mass	RT (min)	Putative Identification	P-Values: Crop	Regulation in "ON" trees
Group_138	pos	82.0306	1.1	-	8.8E-	UP
Group_136	pos	81.0069	1.1	-	9.5E-	UP
Group_137	pos	82.0077	1.1	-	1.0E-	UP
Group_318	pos	240.1475	2.4	-	1.9E-	UP*
Group_613	pos	438.1502	4.3	7-Hydroxy-5-(4-hydroxy-2-oxopentyl)-2-methylchromone 7-glucoside	2.4E-03	UP
Group_185	pos	122.0332	1.1		2.6E-	UP
Group_045	pos	219.1107	3.0	Pantothenic acid	2.7E-	UP
Group_197	pos	127.0120	1.1	-	3.4E-	UP
Group_135	pos	81.0044	1.1	-	3.5E-	*
Group_421	pos	297.9324	1.1	-	3.7E-	UP
Group_308	pos	228.1473	1.9	L-isoleucyl-L-	3.8E-	UP*
Group_321	pos	241.9932	1.1	-	4.0E-	UP
Group_351	pos	266.0055	1.1	-	4.1E-	UP
Group_358	pos	269.9375	1.1	-	4.5E-	UP
Group_744	pos	572.4805	10.1	Dieporeticenin	4.7E-	UP
Group_056	pos	264.0079	1.1	-	4.7E-	UP
Group_320	pos	240.9921	1.1	-	5.0E-	UP
Group_200	pos	129.5147	1.1	-	6.1E-	UP
Group_021	pos	150.0279	1.1	-	6.4E-	UP
Group_046	pos	224.9792	1.1	-	6.4E-	UP
Group_088	pos	382.0874	1.2	-	6.7E-	UP*
Group_297	pos	217.9762	1.1	-	7.0E-	UP
Group_532	pos	383.9176	1.1	-	7.2E-	UP
Group_856	pos	832.5095	10.1	-	7.4E-	*
Group_134	pos	79.5328	1.1	-	7.7E-	UP
Group_586	pos	424.9444	1.1	-	8.1E-	UP
Group_441	pos	308.9670	1.1	-	8.3E-	UP
Group_226	pos	152.0254	1.1	-	8.5E-	UP
Group_418	pos	296.9361	1.1	-	8.6E-	UP
Group_364	pos	273.0552	1.4	-	8.8E-	UP
Group_173	pos	109.0016	1.1	-	8.9E-	UP
Group_302	pos	222.9816	1.1	-	9.0E-	UP
Group_599	pos	433.1945	4.3	-	9.0E-	UP
Group_049	pos	242.9896	1.1	-	1.0E-	UP

* not a clear treatment-response effect.

Table 4. Significant changes of metabolites (P < 0.01) identified in spur buds of 'Rosy Glow' trees subjected to variable crop load.

Row	Mass	RT	Putative identification	P-Values <0.01: Crop load effect	Regulation in "ON" trees
Group_673	478.3054	12.0	-	9.2E-03	UP*
Group_864	864.1890	4.7	Epicatechin-(4beta->6)-epicatechin-(2beta->7,4beta->8)-epicatechin	8.3E-03	UP*
Group_353	267.0229	4.6		7.0E-03	UP*
Group_706	512.1530	4.7	3-(4-Hydroxy-3-methoxyphenyl)-1,2-propanediol 2-O-(galloyl-glucoside)	5.9E-03	UP*
Group_571	412.0304	1.4	-	4.9E-03	DOWN*
Group_614	438.3133	12.0	-	3.2E-03	DOWN*
Group_151	89.0843	1.2	Dimethylethanolamine	8.8E-04	DOWN*

* not a clear treatment-response effect.

This study suggested that amino acids and flavonoids play a role in metabolic pathways associated with varying crop loads, and thus may be involved in regulating return bloom. The constant and variable (artificially alternating high and low fruit numbers) crop loads treatments varied in differentially expressed metabolites which could be related to constant crop loads showing a more pronounced response due to equilibration over four seasons. The increased levels of polar metabolites in the variable treatment could be related to increased demands of resources required for "ON" trees that could mask any phytohormone signalling pathways. Stefanelli et al. (2018) observed that fruit harvested from the trees with variable treatments had reduced quality traits compared to the fruit from trees with constant crop load treatments (either high or low). Thus, the response for these two treatments (variable and constant) showed clear evidence of distinct differences in the physiological mechanisms employed. It was also observed that NIC^{CON} (Table 1) and NIC^{VAR} (Table 2) showed more significantly affected metabolites compared to RG^{CON} (Table 2) and RG^{VAR} (Table 4), which could be related to the genetic disposition of RG being less susceptible to biennial bearing.

2020 'Ruby Pink' apple spur bud collection in Tatura

A total of 781 compounds in positive ionisation mode and 535 compounds in negative ionisation mode were detected in 'Ruby Pink' apple spur bud samples. Putative (Level 3) identification of 375 metabolites in positive mode and 227 in negative mode provided similar composition information to the apple buds in the 2018 apple bud collection (AP15013). Metabolite responses (y) against crop load (x) revealed significant metabolite changes (P < 0.01) in response to crop load treatment effects in the primary and secondary leaders (Table 5) and graphs of a few selected metabolites are shown in Figure 4. Most metabolites plateaued at high crop load.

The primary and secondary leaders showed differences in altered metabolites, suggesting unique metabolic pathways utilized in the two branches. Despite differences in both pathways, flavanols were possible signalling molecules. There were some key pathways in the primary leader that included benzoic acid and 4- hydroxybenzoic acid intermediaries in the shikimic acid pathway, and the similarity of the profiles in Figure 4 suggests that they are linked to epicatechin. In the secondary leader, ERI and its glycoside were among the most significantly altered metabolites. Recent studies demonstrated that ERI could efficiently promote fibre development, with genome-wide RNA profiling data indicating that various regulatory pathways like auxin biosynthesis, auxin signalling and transportation, along with the reactive oxygen species (ROS) homeostasis contribute to the enhanced fibre growth in response to ERI treatment (Khan et al. 2019).

Table 5. Significant changes of metabolites (P < 0.01) identified in spur buds of 'Ruby Pink' trees subjected to five crop load treatments on the 'Primary' leader and two crop loads on the 'Secondary' leader.

Row	Mass	Leader	Ionisation mode	RT	Name	P<0.01	Regulation in "ON"
Group_031	200.0332	primary	Pos	1.2	4-Fumarylacetoacetic acid	6.6E-	UP

Group_051	290.0785	primary	Pos	4.0	Epicatechin	9.2E-	DOWN
Group_146	122.0367	primary	Pos	4.0	Benzoic acid	4.5E-	DOWN
Group_160	138.0315	primary	Pos	4.0	4-Hydroxybenzoic acid	7.1E-	DOWN
Group_186	164.0471	primary	Pos	3.8	Phenylpyruvic acid	7.2E-	DOWN
Group_228	209.0382	primary	Pos	1.2	-	2.1E-	UP
Group_232	209.5398	primary	Pos	1.2	-	1.4E-	UP
Group_289	259.0365	primary	Pos	5.0	Glucosamine 6-sulfate	5.9E-	UP
Group_326	280.4721	primary	Pos	1.1	-	7.1E-	DOWN
Group_347	290.0616	primary	Pos	4.0	Dedimethylchlorpromazine	3.4E-	DOWN
Group_370	300.0777	primary	Pos	1.2	Carboxytolbutamide	4.8E-	UP
Group_650	560.1497	primary	Pos	5.1	Apimaysin	2.8E-	DOWN
Group_654	562.1472	primary	Pos	5.8	Epifisetinidol-(4beta->8)-catechin	8.4E-03	UP
Group_663	582.8853	primary	Pos	1.1	-	5.7E-	DOWN
Group_681	611.8793	primary	Pos	1.1	-	8.6E-	DOWN
Group_010	244.0356	primary	Neg	1.2	Fucose 1-phosphate	2.1E-	DOWN
Group_111	244.0744	primary	Neg	4.0	3,3',4'5-Tetrahydroxystilbene	8.2E-03	DOWN
Group_155	306.1328	primary	Neg	4.4	-	4.1E-	DOWN
Group_177	330.0392	primary	Neg	6.0	Blighinone	6.3E-	UP
Group_179	334.0700	primary	Neg	4.0	Xanthotoxol arabinoside	8.1E-	DOWN
Group_213	360.1565	primary	Neg	8.1	Quassinol	8.0E-	DOWN
Group_224	376.1748	primary	Neg	4.4	-	5.5E-	UP
Group_380	548.3371	primary	Neg	7.0	-	7.6E-	UP
Group_428	634.1523	primary	Neg	5.0	-	4.6E-	DOWN
Group_475	786.8641	primary	Neg	1.1	-	1.0E-	DOWN
Group_476	787.3643	primary	Neg	1.1	-	9.5E-	DOWN
Group_514	942.2081	primary	Neg	4.6	-	7.7E-	DOWN*
Group_531	1134.3454	primary	Neg	4.9	-	5.0E-	DOWN
Group_040	232.0555	secondary	Pos	1.3	(2E,11Z)-5-[5-(Methylthio)-4-penten-2-ynyl]-2-	3.6E-03	DOWN
Group_486	386.1393	secondary	Pos	1.2	Edultin	7.8E-	DOWN
Group_339	288.0634	secondary	Pos	3.0	Eriodictyol	2.2E-	DOWN
Group_666	594.1578	secondary	Pos	4.7	Isovitexin 2''-O-glucoside	6.9E-	DOWN
Group_551	450.1161	secondary	Pos	4.7	Eriodictyol-7-O-glucoside	5.2E-	DOWN
Group_211	190.0020	secondary	Pos	1.3	-	8.9E-	DOWN
Group_368	298.9335	secondary	Pos	1.1	-	8.8E-	DOWN
Group_440	338.9589	secondary	Pos	1.1	-	8.1E-	DOWN
Group_631	525.8942	secondary	Pos	1.1	-	2.0E-	DOWN
Group_695	639.8751	secondary	Pos	1.1	-	5.3E-	DOWN
Group_081	152.0112	secondary	Neg	3.0	-	4.2E-	DOWN
Group_437	664.1427	secondary	Neg	6.5	-	5.5E-	DOWN

* not a clear treatment-response effect.

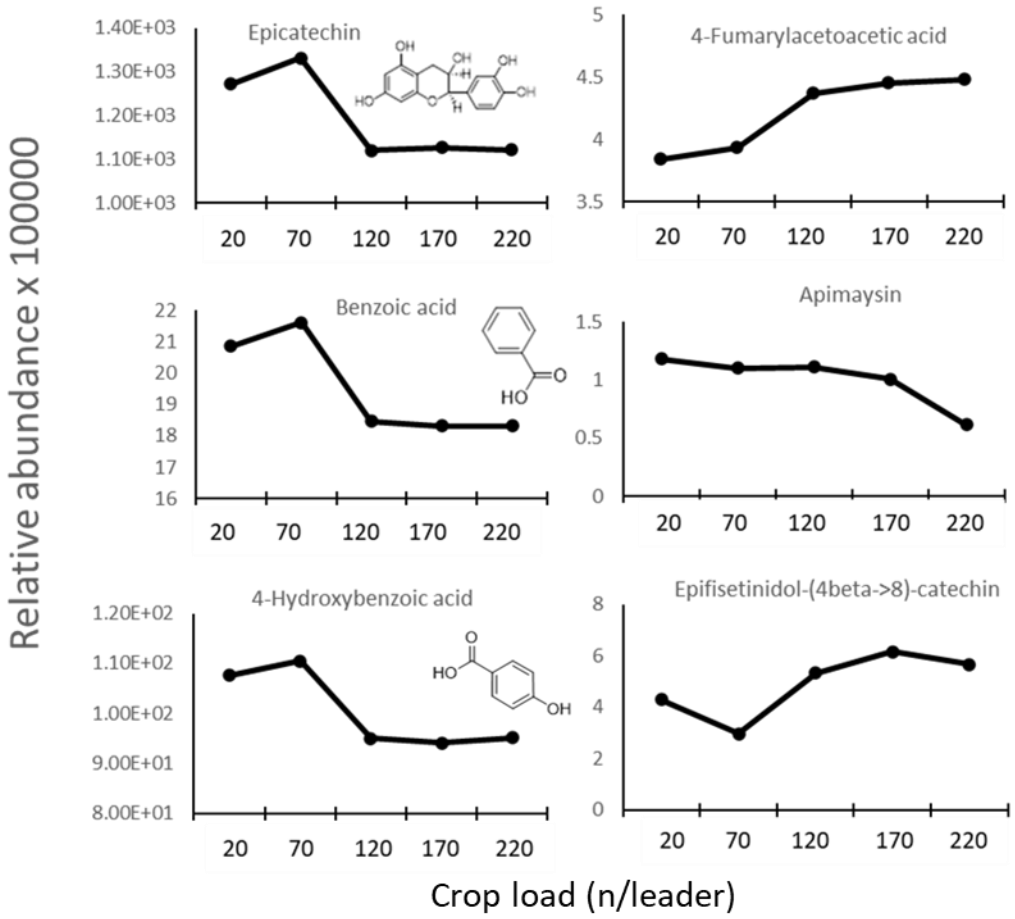

Figure 4. Metabolites Identified in spur buds of 'Ruby Pink' trees with significant changes ($P < 0.01$) in response to five crop load treatments on the 'Primary' leader.

To increase the statistical power of the experiment, the leaders were treated as replicates and a linear model was applied to the whole dataset, with the results shown in Table 6 and some examples in Figure 5. Similar to the 2018 bud samples, metabolites in the p- coumaric acid pathway showed significant response to crop load.

Similar to the flavanol response, the amino acid levels, L-aspartic acid, shows increased levels in "ON" trees which is an inverse response (Figure 5) compared to previous studies (AP15002) (Milyaev et al. 2021) and the AP15013 apple bud collection studies, previously mentioned.

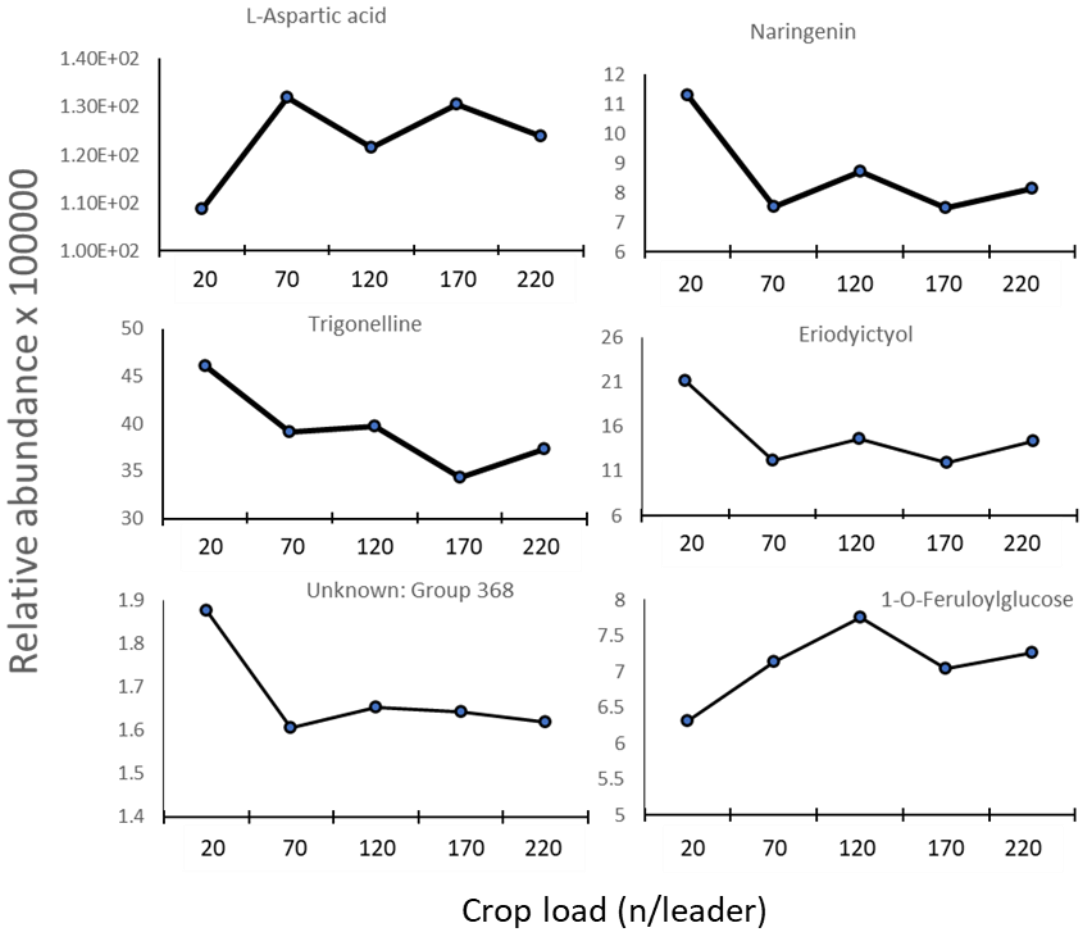

Figure 5. Compounds with significant changes (P < 0.01) associated with crop load in spur buds of 'Ruby Pink' trees, irrespective of leader.

Table 6. Metabolites with significant changes under different crop loads (P < 0.01) identified in spur buds of 'Ruby Pink' trees, irrespective of leader, with five crop load treatments on the 'Primary' leader and two crop loads on the 'Secondary' leader.

Compound ID	Observed Mass		RT (min)	Putative Identification	P-Values: Cropload	Regulation in "ON" trees
Group_011	133.0373	Pos	1.2	L-Aspartic acid	3.5E-03	UP
Group_013	137.0475	Pos	1.3	Trigonelline	7.1E-03	DOWN
Group_308	272.0683	Pos	3.4	Naringenin	4.4E-03	DOWN
Group_339	288.0634	Pos	3.0	Eriodictyol	8.7E-04	DOWN
Group_368	298.9335	Pos	1.1	-	4.0E-03	DOWN
Group_453	356.1103	Pos	4.2	1-O-Feruloylglucose	7.7E-03	UP
Group_529	431.4282	Pos	1.1	-	1.4E-03	DOWN
Group_531	1134.3454	Neg	4.9	-	1.1E-03	*
Group_475	786.8641	Neg	1.1	-	1.6E-03	*
Group_081	152.0112	Neg	3.0	-	2.0E-03	DOWN
Group_155	306.1328	Neg	4.4	-	2.3E-03	*

Group_010	244.0356	Neg	1.2	Fucose 1-phosphate	3.2E-03	DOWN
Group_465	730.3737	Neg	1.1	-	4.6E-03	DOWN
Group_167	326.1016	Neg	3.5	trans-o-Coumaric acid 2-glucoside	4.9E-03	DOWN
Group_486	840.2495	Neg	5.6	-	5.6E-03	DOWN
Group_119	270.0543	Neg	6.4	Apigenin	6.5E-03	DOWN

* not a clear treatment-response effect.

This study demonstrated that flavonoids were affected by varying crop loads, and as such may play a role as signalling molecules within the trees. This is backed up by a recent review which summarized compelling evidence that flavonoids mediate phytohormone signalling and growth responses in plants (Brunetti et al. 2018) . Flavonoids have long been considered as primarily synthesized to constitute an effective shield against the penetration of UV-B radiation to sensitive leaf tissues, and greatly involved in protecting plants challenged by the depletion of stratospheric ozone layer (Bais et al. 2018). However, there is evidence indicating that flavonoids may exert complex functions in both animal and plant cell metabolism, going well-beyond the mere chemical quenching of ROS. Certain flavonoids, especially but not limited to quercetin derivatives, have the ability to modulate signalling cascades that regulate cell growth and differentiation (Jacobs and Rubery, 1988; Stafford, 1991),

2020 'Ruby Pink' apple spur leaves collection in Tatura

A total of 2,811 compounds in positive ionisation mode, and 1,688 compounds in negative ionisation mode were detected in 'Ruby Pink' leaf samples. Putative (Level 3) identification of 1,225 metabolites in positive mode and 614 in negative mode indicated a richer and more complex composition compared to buds. Linear models revealed significant metabolites correlating to crop load treatment effects in the primary and secondary leaders of 'Ruby Pink' (Table 7).

The primary and secondary leaders showed differences in altered metabolites and, like in buds, unique metabolic pathways could be utilized in the two branches. The metabolites detected in the leaves were a diverse range of aromatic compounds. The regulation of these compounds is not clear and may display a very complex response to biennial bearing. Only two compounds reminiscent of the apple buds were present in the secondary leader, including decreased levels of ERI and D-glucose. It is possible that the secondary leader had more pronounced effects due to the large difference in crop load treatments.

Table 7. Metabolites with significant changes under different crop loads (P < 0.01) identified in spur leaves of 'Ruby Pink' trees subjected to five crop load treatments on the 'Primary' leader and two crop loads on the 'Secondary' leader.

Row	Mass	Leader	Ionisation mode	RT	Putative Identification	P-Values <0.01	Regulation of "ON" trees
Group_0036	192.078	Primary	pos	4.6	(R)-Shinanolone	4.3E-03	UP*
Group_0060	235.951	Primary	pos	1.1	-	9.3E-03	DOWN
Group_0139	372.176	Primary	pos	3.6	-	1.4E-03	UP
Group_0312	690.434	Primary	pos	11.	-	6.9E-03	UP
Group_0378	80.2632	Primary	pos	11.	-	4.6E-03	UP
Group_0386	88.0013	Primary	pos	1.1	-	8.8E-03	DOWN
Group_0408	106.042	Primary	pos	6.5	Benzaldehyde	3.8E-03	UP
Group_0437	125.995	Primary	pos	1.1	-	2.6E-03	DOWN*
Group_0478	148.052	Primary	pos	6.5	Cinnamic acid	3.9E-03	UP
Group_0485	152.120	Primary	pos	4.8	(-)-trans-Carveol	2.0E-04	UP
Group_0516	166.005	Primary	pos	1.1	-	7.3E-03	DOWN
Group_0624	214.044	Primary	pos	4.0	fluorobenzoylpropionic acid	2.1E-03	DOWN
Group_0658	225.023	Primary	pos	4.3	-	2.0E-04	UP

Group_0821	274.083	Primary	pos	11.	Phloretin	8.5E-03	DOWN*
Group_0908	294.060	Primary	pos	6.5	-	1.1E-03	UP*
Group_1065	336.035	Primary	pos	1.8	-	1.9E-04	DOWN*
Group_1124	354.146	Primary	pos	9.6	1-Methoxyphaseollidin	5.8E-04	UP
Group_1125	354.146	Primary	pos	8.8	1-Methoxyphaseollidin	7.2E-03	UP*
Group_1158	367.090	Primary	pos	2.9	Xanthurenate-8-O-beta-D-	3.2E-03	UP*
Group_1162	368.110	Primary	pos	4.6	3-O-Feruloylquinic acid	3.5E-03	UP*
Group_1182	372.157	Primary	pos	8.4	Tetrahydrocurcumin	4.7E-03	UP*
Group_1316	408.103	Primary	pos	4.6	-	1.5E-03	UP*
Group_1363	419.126	Primary	pos	5.0	Fenvalerate	8.2E-03	UP*
Group_1474	445.173	Primary	pos	6.2	Narceine	4.9E-03	DOWN**
Group_1609	486.207	Primary	pos	4.8	Glucosylgalactosyl	7.5E-04	UP*
Group_1837	566.412	Primary	pos	11.	3'-Hydroxy-e,e-caroten-3-one	3.6E-03	UP*
Group_1875	582.111	Primary	pos	6.3	5'-Methoxybilobetin	2.9E-03	UP*
Group_1893	586.114	Primary	pos	6.5	-	7.4E-04	UP
Group_1997	618.522	Primary	pos	12.	DG(14:1(9Z)/22:2(13Z,16Z)/0:0	7.7E-03	UP*
Group_2005	620.263	Primary	pos	10.	-	7.4E-03	UP**
Group_2031	626.274	Primary	pos	9.2	-	3.9E-03	UP*
Group_2216	702.395	Primary	pos	11.	-	6.3E-03	UP*
Group_2247	714.395	Primary	pos	11.	-	6.7E-03	UP*
Group_2273	722.460	Primary	pos	11.	-	1.0E-02	UP*
Group_2290	730.426	Primary	pos	11.	-	4.8E-03	UP
Group_2375	762.452	Primary	pos	11.	-	9.0E-03	UP
Group_2410	775.225	Primary	pos	14.	-	3.0E-03	DOWN*
Group_2715	983.258	Primary	pos	3.4	-	4.9E-03	DOWN
Group_0086	528.147	Primary	neg	4.4	-	5.9E-04	UP
Group_0130	622.132	Primary	neg	6.6	-	9.3E-03	UP
Group_0143	662.384	Primary	neg	10.	-	3.4E-03	UP
Group_0305	294.220	Primary	neg	9.8	13-OxoODE	6.3E-03	DOWN
Group_0351	326.101	Primary	neg	4.1	trans-o-Coumaric acid 2-	5.8E-03	UP
Group_0356	328.096	Primary	neg	7.0	Zapotinin	3.2E-03	UP
Group_0379	344.075	Primary	neg	2.7	Theogallin	5.5E-03	*
Group_0459	384.107	Primary	neg	4.6	Eleutheroside B1	1.0E-04	UP*
Group_0630	461.163	Primary	neg	4.4	-	7.3E-05	UP*
Group_0634	462.211	Primary	neg	4.8	-	1.0E-03	UP*
Group_0665	474.160	Primary	neg	1.3	D-Galactopyranosyl-(1->3)-D-	1.8E-03	UP*
Group_0713	496.156	Primary	neg	5.0	Musabalbisiane A	3.4E-03	UP
Group_0750	508.217	Primary	neg	4.8	6-O-Oleuropeoylsucrose	1.7E-03	UP
Group_0889	576.204	Primary	neg	4.5	-	1.9E-03	UP
Group_1178	718.251	Primary	neg	11.	Diisodityrosine	6.9E-04	UP*
Group_1183	719.484	Primary	neg	10.	-	4.4E-03	DOWN
Group_1350	794.520	Primary	neg	14.	1,2-Di-O-palmitoyl-3-O-(6-	1.1E-03	*
Group_1407	823.540	Primary	neg	11.	-	7.4E-03	*
Group_1463	862.507	Primary	neg	14.	-	6.9E-03	*
Group_1542	921.222	Primary	neg	4.8	3-oxo-(2S)-Methylisocapryloyl-	7.7E-04	*
Group_0116	348.118	Secondary	pos	5.5		7.5E-03	DOWN
Group_0219	495.332	Secondary	pos	10.	LysoPC(16:0)	5.7E-03	DOWN
Group_0229	519.332	Secondary	pos	10.	LysoPC(18:2(9Z,12Z))	1.2E-03	DOWN

Group_0545	177.023	Secondary	pos	1.4	Brassicanal A	9.1E-03	DOWN
Group_0698	235.068	Secondary	pos	5.0	6-Succinoaminopurine	1.8E-03	UP
Group_0731	249.052	Secondary	pos	4.2	Cysteinyl-Glutamate	2.0E-04	DOWN
Group_0885	288.063	Secondary	pos	3.0	Eriodictyol	3.4E-03	DOWN
Group_0918	297.066	Secondary	pos	1.4	-	4.0E-03	DOWN
Group_1462	442.129	Secondary	pos	1.4	-	1.6E-04	DOWN
Group_1503	455.314	Secondary	pos	10.	-	4.4E-03	UP
Group_0004	180.063	Secondary	neg	1.2	D-Glucose	1.8E-03	DOWN
Group_0008	226.069	Secondary	neg	1.2	5-Acetylamino-6-formylamino-	1.8E-03	DOWN
Group_0017	320.056	Secondary	neg	1.3	-	5.5E-03	DOWN
Group_0429	370.127	Secondary	neg	5.5	Linusitamarin	1.6E-03	DOWN
Group_0447	378.151	Secondary	neg	12.	-	4.3E-03	DOWN
Group_0740	504.149	Secondary	neg	4.2	6-Caffeoylsucrose	3.1E-04	DOWN
Group_0810	539.323	Secondary	neg	10.	-	6.8E-03	DOWN
Group_1024	633.402	Secondary	neg	11.	-	5.2E-03	DOWN
Group_1102	678.378	Secondary	neg	9.1	Gingerglycolipid B	5.9E-03	DOWN
Group_1233	740.463	Secondary	neg	9.5	-	8.3E-03	DOWN

* not a clear treatment-response effect.

Metabolites in 'Ruby Pink' spur leaves were not clearly affected by crop load and this could be due to the complexity of the tissue as a result of its many functions. However, spur leaves in the secondary leader expressed a significant down regulation of ERI and an energy shift indicated with changes in D-glucose. It is possible that strong, significant metabolite regulation can only be observed in the leaves if the crop load levels are distinct such as the case of the secondary leader.

CONCLUSION

Our study indicated that flavonoid levels in apple buds are affected by varying crop loads, and as such may be involved in regulation of flower bud induction. The constant crop load experiments showed the most consistent findings with previous metabolomics studies (AP15002), these include significant effects on cholorogenic and kaempferol pathway and the amino acid L-arginine. In our study, the flavonoids were the most significantly affected class of compounds in apple buds and some of these, for example ERI, are associated with tissue growth and development. At transcriptomic and proteomic levels, in apple spur buds collected from OFF-trees, metabolic pathways associated with tissue growth and development were detected that potentially result in a promoting effect on early flower bud development. The transcriptomic and proteomic levels in spur buds collected on ON-trees showed that the plant hormone signal transduction pathway was enriched, suggesting the involvement of hormonal metabolites in determining the fate of the apple bud meristem. A further step towards systematic understanding of flower induction in apple will require the determination of plant hormone profile by additional analysis and using extraction protocols specifically designed for the analyses of phytohormones and polar metabolites (Farrow and Emery 2012; Urbanová et al. 2013), which we plan to perform in the near future.

In this study, it must be noted that the plant metabolites identified will require further identification using LCMSMS techniques and/or library confirmation.

RECOMMENDATIONS

It is recommended that further LCMS analysis of bud extracts be undertaken to provide better confidence in the identity of the compounds putatively identified so far, and to attempt to identify the unknown compounds which have shown good correlation with crop load.

It is also recommended that a LCMS column and gradient conditions more amenable to the separation of the more polar compounds be investigated for future work, to allow for easier detection and better confidence in the identity of these early eluting compounds.

REFERENCES

Brunetti, C., et al. (2018). "Modulation of Phytohormone Signaling: A Primary Function of Flavonoids in Plant-Environment Interactions." Frontiers in Plant Science **9**: 1042-1042.

Khan, A. Q., et al. (2019). "Eriodictyol can modulate cellular auxin gradients to efficiently promote in vitro cotton fibre development." BMC Plant Biology **19**(1): 443.

Milyaev, A., et al. (2021). "Toward Systematic Understanding of Flower Bud Induction in Apple: A Multi-Omics Approach." Frontiers in Plant Science **12**(286).

Peer, W. A. and A. S. Murphy (2006). Flavonoids as signal molecules: Targets of flavonoid action. The Science of Flavonoids**:** 239-268.

Viant, M. R., et al. (2017). "How close are we to complete annotation of metabolomes?" Current Opinion in Chemical Biology **36**: 64-69.

Stefanelli D, Plozza T, Flachowsky H, Wünsche JN (2018) Young apple tree responses to crop load. In: Acta Horticulturae, pp 221-228.

Milyaev A, Kofler J, Pfannstiel J, Stefanelli D, Flachowsky H, Hanke MV, Wünsche JN (2018) Histological and proteomic approaches to study floral bud induction in relation to biennial bearing in apple. In: Acta Horticulturae, pp 277-283.

APPENDICES

Appendix A:

Supplementary Table 1. Metabolites with significant changes in response to different crop loads identified in spur leaves of 'Ruby Pink' trees, irrespective of leader, with five crop load treatments on the 'Primary' leader and two crop loads on the 'Secondary' leader. Metabolites identified using (ESI+)- LCMS profiling.

Row	Mass		RT	Putative Identification	P-Values <0.01	Regulation in "ON" trees
Group_0049	215.9433	pos	1.1	-	9.2E-03	DOWN*
Group_0116	348.1185	pos	5.5	-	7.0E-03	DOWN
Group_0403	103.0963	pos	1.2	-	6.3E-03	UP*
Group_0461	142.9895	pos	1.1	-	8.2E-03	DOWN*
Group_0478	148.0524	pos	6.5	Cinnamic acid	8.7E-03	UP*
Group_0516	166.0055	pos	1.1	-	8.7E-03	DOWN*
Group_0698	235.0682	pos	5.0	6-Succinoaminopurine	6.7E-03	UP**
Group_0731	249.0524	pos	4.2	Cysteinyl-Glutamate	2.0E-03	DOWN
Group_0746	255.1081	pos	3.8	-	9.4E-03	DOWN*
Group_0753	256.9697	pos	1.1	-	3.8E-03	DOWN*
Group_0835	275.5843	pos	5.2	-	7.8E-03	DOWN*
Group_0908	294.0606	pos	6.5	-	1.1E-03	UP*
Group_0912	294.2194	pos	10.0	13-OxoODE	8.1E-03	DOWN
Group_0918	297.0663	pos	1.4	-	2.3E-03	DOWN*
Group_1124	354.1469	pos	9.6	1-Methoxyphaseollidin	5.1E-03	UP*
Group_1158	367.0903	pos	2.9	Xanthurenate-8-O-beta-D-glucoside	7.5E-04	UP**
Group_1182	372.1572	pos	8.4	Tetrahydrocurcumin	1.0E-02	UP*
Group_1296	402.1499	pos	3.8	Benzyl beta-primeveroside	6.7E-03	UP*
Group_1326	408.3751	pos	14.3	-	9.7E-03	UP*
Group_1334	410.3183	pos	10.6	Gamma-Tocotrienol	9.4E-03	UP*
Group_1462	442.1298	pos	1.4	-	1.2E-04	DOWN*
Group_1474	445.1731	pos	6.2	Narceine	4.9E-03	DOWN(NA

Group_1523	462.0817	pos	4.9	Oxazepam glucuronide	9.9E-03	UP*
Group_1578	475.2052	pos	5.2	-	2.3E-03	DOWN
Group_1630	494.1555	pos	6.7	-	8.7E-03	DOWN
Group_1788	545.1610	pos	5.7	-	4.5E-03	DOWN
Group_1837	566.4121	pos	11.5	3'-Hydroxy-e,e-caroten-3-one	9.1E-03	UP*
Group_1875	582.1115	pos	6.3	5'-Methoxybilobetin	4.6E-04	UP*
Group_1893	586.1147	pos	6.5	-	1.4E-03	UP*
Group_1949	606.2080	pos	6.2	-	1.2E-03	DOWN*
Group_2257	718.3913	pos	9.2	-	5.9E-03	*
Group_2306	737.4438	pos	8.8	-	6.6E-03	DOWN(NA
Group_2715	983.2584	pos	3.4	-	4.1E-03	DOWN
Group_0885	288.0635	pos	3.0	Eriodictyol*	3.6E-02	*
Group_2417	777.5307	pos	9.6	PC(14:0/22:6(4Z,7Z,10Z,13Z,16Z,19Z))	4.6E-02	*
Group_0004	180.0638	ne	1.2	D-Glucose	4.9E-03	*
Group_0008	226.0697	ne	1.2	5-Acetylamino-6-formylamino-3-	6.2E-03	*
Group_0213	128.9546	ne	1.2	-	5.2E-03	*
Group_0456	382.1388	ne	1.3	Licoricone	1.1E-03	*
Group_1178	718.2516	ne	11.1	Diisodityrosine	9.7E-04	*
Group_1620	1006.312	ne	4.9	-	6.2E-04	*
Group_1662	1122.454	ne	6.0	-	2.6E-03	*

° > 1.5 effect size and good general linear trend for L1 and L2 (P<0.05)

*Unclear metabolite direction

Supplementary Table 2. Metabolites with significant changes in response to different crop loads identified in spur leaves of 'Ruby Pink' trees, irrespective of leader, with five crop load treatments on the 'Primary' leader and two crop loads on the 'Secondary' leader. Metabolites identified using (-ve) LCMS profiling.

Compound ID	**Observed Mass**		**RT (min)**	**Putative Identification**	**P-Values: Cropload**	**Regulation in "ON" trees**
Group_0004	180.0638	Neg	1.2	D-Glucose	4.9E-03	DOWN
Group_0008	226.0697	Neg	1.2	5-Acetylamino-6-formylamino-3-methyluracil	6.2E-03	DOWN
Group_0213	128.9546	Neg	1.2		5.2E-03	*
Group_0456	382.1388	Neg	1.3	Licoricone	1.1E-03	DOWN
Group_1178	718.2516	Neg	11.1	Diisodityrosine	9.7E-04	*
Group_1620	1006.3120	Neg	4.9		6.2E-04	*
Group_1662	1122.4541	Neg	6.0		2.6E-03	*

*Unclear metabolite direction

AP19003 Advancing sustainable and technology driven apple orchard production systems

Technical Report: Effect of crop load relationships on chemical signalling

Agriculture Victoria Research

May 2022

VICTORIA State Government | Jobs, Precincts and Regions

AGRICULTURE VICTORIA

Author: Priyanka Reddy, Tim Plozza, Alessio Scalisi, Simone Rochfort and Ian Goodwin

Project RDC Number: AP19003

Project RCM Number: 6472

Department of Jobs, Precincts and Regions
1 Spring Street Melbourne Victoria 3000
Telephone (03) 9651 9999

Contents

EXECUTIVE SUMMARY

Flower bud induction in "off" years typically results from a poor flower bud formation due to a high crop load in the previous year, suggesting that the fruit inhibits the concomitant development of the adjacent spur bud. The overall research goal of the current project was to reveal the largely unknown physiological and molecular mechanisms of biennial bearing in apple, thereby to better understand the underlying pathways and triggers of flower induction that might facilitate intervention opportunities for controlling apple crop load and thus ensuring stable apple production.

This report presents findings from a preliminary investigation of potential signalling compounds originating from fruitlet seeds collected from a study on crop load management of an established cultivar ('Ruby Pink') at a commercial orchard in the Goulburn Valley. Seeds were collected fortnightly from early Nov (fruitlet thinning) to early Dec 2021, which is thought to be the critical period during which the signalling compounds may promote or inhibit the induction of flowering buds for the following growing season.

Differences in levels of phenylpropanoid pathway members and a putatively identified phytohormone gibberellic acid (GA) was identified in high and low crop load treatments of 'Ruby Pink'. The reported negative regulation of flavanols via GA signalling and the downstream effects of the phenylpropanoid pathway suggest that there is phytohormone and flavonoid signalling crosstalk in the regulation of biennial bearing cycle. Previous reports and a recently submitted scientific journal paper on the metabolic effects of high and low crop load treatments indicate that increased levels of downstream phenylpropanoid pathway metabolites likely belonging to the phenylalanine ammonia lyase (PAL) biosynthesis of salicylic acid are responsible for floral induction.

The putatively identified GA derivative identified in this study could be a possible candidate for floral repression. Moreover, further elucidation of the unknown compounds could lead to the identification of novel candidates for floral induction and/or repression. However, LCMSMS mass spectrometry techniques of the individual compounds are required to confirm or identify unknowns.

INTRODUCTION

This technical report is a deliverable for project AP19003 "Advancing sustainable and technology driven apple orchard production systems". This work aims to explore the potential physiological mechanism (such as signalling compounds) for observed impacts of high crop load on floral initiation and flower development in apple trees. We report the results of molecular analysis of fruitlet seeds collected in November and December 2021 from 'Ruby Pink' apple trees from a commercial orchard in Ardmona, Victoria.

Project outcome

The intended outcome of this project is to improve crop load management in a variable climate by providing knowledge and tools to deliver premium fruit that meets consumer expectations in domestic and export markets.

Project background

The gross value of Australia's apple industry was $566 million in 2013, with Victoria representing approximately 30% of total Australian production. However, the value of this industry could be increased if more consistent crop loads were achieved for those apple cultivars which are susceptible to biennial bearing, a phenomenon characterised by "on" and "off" years of flowering and, subsequently, fruit production. Biennial bearing costs growers and the Australian apple industry millions of dollars in additional labour and lost production due to inconsistent yields. Fruit growers usually remove excess flowers and fruitlets in "on" years, using moderately effective horticultural practices, to increase fruit size in the current season and the amount of bloom in the subsequent season, but the methods are extremely time consuming and costly, and even with best thinning practice, yields can still be reduced by more than 20%.

The Australian apple industry, like many fruit production industries, is plagued by high cost of production and variable fruit quality that often does not meet consumer expectations. This can greatly reduce a grower's profitability. In the last ten years, apple production has increased but is yet to reach its full potential based on the area planted (10,000 ha) and the theoretical yield (~800,000 t). This is mostly due to variable crop load management, biennial bearing and inconsistent fruit quality.

Australia has a unique climate characterised by relatively high temperatures and light intensity compared to other apple production areas around the world. Light interception and consequent carbohydrate availability play an important role in defining the optimal number of fruit that a tree should hold to maximise consistent fruit quality for the life of the tree. Furthermore, light interception and carbohydrate supply are fundamental in influencing fruit quality in a variable climate of extreme heat events.

Apple is generally susceptible to biennial bearing, which is the tendency to alternate years of high flower initiation followed by low initiation the subsequent year. From previous studies on crop load management of an established cultivar ('Rosy Glow') and emerging cultivar ('Nicoter') (projects AP15013 and AP15002), it was noticed that there is an inverse correlation between fruit number on trees and most aspects of fruit quality (size, colour, fruit maturity, flesh firmness and soluble solids concentration). These previous studies found that biennial bearing is controlled at tree level from a combination of genetics (flower induction genes) and environment (carbohydrate availability) probably mediated by metabolites that act as chemical signals that either stimulate or inhibit the activation of the genes.

Project objectives

Physiological studies and the development of sensing tools will be undertaken in the Sundial apple orchard at the Tatura SmartFarm and in a commercial orchard in the Goulburn Valley to address the following three objectives as per the Hort Innovation RFP:

- Develop crop load, training systems, pruning and irrigation optimisation for yield, quality and labour efficiency in new and emerging apple cultivars.
- Develop orchard design techniques, tools and management practices that enhance the ability of orchards to manage climate variability and weather extremes.

- Communicate findings in a clear and practical format to growers and wider industry.

METHOD

2021 Sample Collection

The experiment was conducted at a commercial orchard (Plunkett Orchards, 255 Macisaac Rd, Ardmona) in the Goulburn Valley, Victoria, Australia. Mature 'Ruby Pink' apple trees, trained into a two leader, vertical trellis configuration, were used for this experiment, which began in the 2020–21 season. Thirty trees occupying a single row in the orchard were utilized for the experiment and were grouped into three blocks, each consisting of 10 trees. The two leaders on each tree were classified into 'Primary' leader based on similar leader trunk cross sectional areas (TCSA, average = 27.4 cm^2) and 'Secondary' leaders. Five crop load treatments (20, 70, 120, 170 and 220 fruit per leader) were applied to the 'Primary' leaders on each tree in late October, and two crop load treatments (Low, in which the attempt was to achieve a number of approximately 20 fruit per leader, and High, aiming to 220 fruit per leader) were applied to the 'Secondary' leaders. The grower standard practice is to achieve a number of 120 fruit per leader. The randomised complete block design (CRBD) application of these 10 treatments (5 primary leader crop load x 2 secondary leader crop load) is shown in Table 1. The same treatments were applied again in the 2021–22 season; however, poor return bloom for the higher crop load treatment leaders (170 and 220 fruit per leader on primary leaders, and 'High' on secondary leaders) meant that this was not possible in many cases.

Table 1. Completely randomised block design application of crop load treatments for the primary and secondary leaders of the 'Ruby Pink' apple trees. Low = ~ 20 fruit per leader, High = ~ 220 fruit per leader.

Block	Tree number	Crop load of primary leader (fruit/leader)	Crop load of secondary leader
1	1	170	Low
1	2	120	High
1	3	220	Low
1	4	20	Low
1	5	120	Low
1	6	70	Low
1	7	70	High
1	8	20	High
1	9	170	High
1	10	220	High
2	11	170	Low
2	12	220	Low
2	13	120	High
2	14	70	Low
2	15	20	Low
2	16	220	High
2	17	70	High
2	18	20	High
2	19	120	Low
2	20	170	High
3	22	70	Low
3	23	20	High
3	25	220	Low
3	26	120	High
3	29	170	High

3	30	70	High
3	31	220	High
3	32	20	Low
3	33	120	Low
3	34	170	Low

Buds, fruitlets and leaves were collected from the trees on 9 November, 23 November and 10 December 2021, equating to 43, 57 and 74 days after full bloom, which approximates the time at which buds transform from vegetative to reproductive, as documented in the AP15002 final report. One bud per leader and 2–3 fully expanded leaves adjacent to each of these buds were collected. A total of 36 fruitlets were harvested and all fruitlet seeds were individually collected for each leader and collection time point (n = 108) from a subset of trees in Table 1 that only included the lowest, the mid and the highest crop load treatments. Crop loads obtained at harvest were expressed per unit of TCSA and classified as high (4.0–14.6 fruit / cm^2), mid (2.1–3.7 fruit / cm^2) and low (0.6–2.0 fruit / cm^2) treatments. Samples were frozen on dry ice as soon as possible after collection and stored in a freezer at −80°C until analysis. All samples were prepared for molecular analysis by the Molecular Phenomics Group within Agriculture Victoria Research.

For the purposes of this report only the fruitlet seed samples were evaluated.

Identification and relative quantitation of potential chemical signalling compounds

Metabolites were extracted from seed samples and analysed using high resolution, accurate mass liquid chromatography-mass spectrometry (LCMS) instruments to find and identify potential chemical signalling compounds related to crop load treatments and return bloom. Methods included untargeted analysis, which involved finding and identifying unknown compounds whose presence and concentration correlated with crop load treatments.

Sample Extraction of 2021 fruitlet seed collection

Seeds from each fruitlet belonging to a leader were kept in separate safe-lock tubes. Samples were placed in 24 well cryo-blocks on the Geno/Grinder 2010 (SPEX Sample Prep, Metuchen, NJ, USA) and the fruitlet seeds were ground at 1,200 rpm for 1 min. The fine powder was weighed (20 ± 0.1 mg) in 2 mL microcentrifuge tubes (Eppendorf Safelock) and extracted with 1 mL of 80% methanol/water (v/v). Samples were centrifuged at 13,000 rpm for 2 min and 200 µL of the supernatant was transferred into a HPLC tube and stored at −20°C until ready for LCMS analysis.

LCMS Methods for Untargeted Analysis and Compound Identification

For untargeted metabolite profiling, a Vanquish Ultra-High Performance Liquid Chromatography (UHPLC) system (Thermo Fisher Scientific, Bremen) with a binary pump, autosampler and temperature-controlled column compartment coupled with a QExactive (QE) Plus mass spectrometer (Thermo, Bremen, Germany) detector was used. An electrospray ionization (ESI) probe operating in the positive and negative ionization modes and the mass spectrometer captured data over a range of 80–1,200 m/z, with mass resolution set at 17,000. Nitrogen was used as the sheath, auxiliary and sweep gases at flow rates of 28, 15 and 4 L/min, respectively. Spray voltage was set at 4,000 V (positive and negative). A 3 µL sample injection volume was used. Samples were randomized, and blanks (80% methanol) injected every five samples. A pooled biological quality control (PBQC) was run every 10 samples. Prior to data acquisition, the system was calibrated with Pierce LTQ Velos ESI Positive and Negative Ion Calibration Solution (Thermo Fisher Scientific). Mass spectrometry data was acquired using Thermo Xcalibur V. 2.1 (Thermo Fisher Scientific Inc., USA). Quantitative analysis was conducted using LCQUAN™ Quantitative Software (Thermo Fisher Scientific).

A Thermo Fisher Scientific Hypersil Gold 1.9 µm, 100 mm × 2.1 mm column with a gradient mobile phase consisting of 0.1% formic acid in H_2O (A) and 0.1% formic acid in acetonitrile (B), at a flow rate of 0.3 mL/min was used. The gradient began at 2% B, increasing to 100% B over 11 min; followed by 4 min at 100% B before a 5 min equilibration with 2% B.

Untargeted Analysis: Putative Compound Identification

The data files obtained following LCMS analyses were processed in the Refiner MS module of Genedata Expressionist® 12.0 optimising the; 1) chromatogram chemical noise subtraction, 2) intensity thresholding, 3) selection of positive and negative mode data, 4) chromatogram RT alignment, 5) chromatogram peak detection. Analyte identification of significant metabolites were performed by searching experimental MS1 data through databases METLIN, ChemSpider (http://www.chemspider.com) and MS/MS data was searched on MzCloud (https://www.mzcloud.org) and MetFragment®.

Statistics

Data processing and statistical analyses

The data files obtained following LCMS analyses were processed in the Refiner MS module of Genedata Expressionist® 12.0 with the following parameters: 1) chromatogram chemical noise subtraction with removal of peaks with less than 4 scans, chromatogram smoothing using moving average estimator over 5 scans, and 30% quantile over 151 scans for noise subtraction, 2) intensity thresholding using a clipping method and a threshold of 100,000, 3) selection of positive mode data only, 4) chromatogram RT alignment using a pairwise alignment based tree and a maximum RT shift of 1 min, 5) chromatogram peak detection using a 5 scans summation window, a minimum peak size of 0.1 min, a maximum merge distance of 0.05 Da, a boundary merge strategy, a maximum gap/peak ratio of 70% with moving average smoothing over 10 scans for peak RT splitting 6) chromatogram isotope clustering using RT and m/z tolerance of 0.05 min and 0.05 Dalton respectively with a maximum charge of 2, and 7) adduct detection using mainly M+H and allowable adducts (M+2H, M+K, M+Na, M-H_2O+H) or (M+FA-H).

Statistical analyses were performed using the Analyst module of Genedata Expressionist® 12.0. Principal component analyses (PCA) were performed to identify tissue and treatment differences. Overlay of the PBQC and samples allowed for the validation of the high-quality dataset by ensuring that RT variation, mass error and sensitivity changes throughout the run were consistent. In this study, final p-values were reported ($p<0.01$) using linear regression, with metabolite (y) response predicting crop load treatments (y~cropload) and N-WAY ANOVA ($p<0.05$). The effect size was calculated by obtaining the ratio of average relative abundance of metabolites. Crop load results at harvest were expressed as fruit / cm^2 TCSA.

Putative analyte identification of metabolites was performed by searching experimental MS^1 data through the following databases: Plant Metabolic Network (PMN) https://plantcyc.org/; Human Metabolome DataBase (HMDB) (http://hmdb.ca); ChemSpider (http://chemspider.com); and Lipid Maps®(http://www.lipidmaps.org).

RESULTS AND DISCUSSION

2021–2022 Fruitlet seed collection

Heavy crop loads are known to induce alternate bearing in apple trees and the removal of fruitlets at 3–18 mm in size, through thinning practices has been shown to lead to a more consistent flower formation (return bloom) for the following season (Guitton, Kelner et al. 2012, Arseneault 2016, Kviklys and Samuolienė 2020). Previous research has postulated the involvement of phytohormones present in seed as the controlling signal for apple flower induction and the dominant cause of biennial bearing (Chan and Cain 1967). Thus, in the present study LCMS profiling of fruitlet seeds harvested from high and low crop load trees at key time points was investigated to better understand the metabolic pathways involved in repression of floral induction.

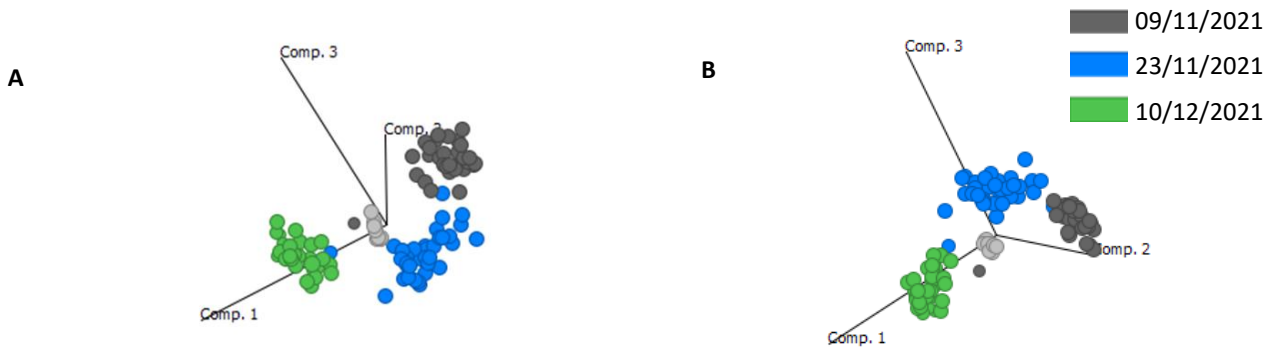

Figure 1. PCA scores plot showing A) positive ion and B) negative ion ESI-LCMS of the metabolome (1,344 metabolites) categorised by collection date.

A total of 1,344 compounds in positive ionization mode and 686 compounds in negative ionization mode were detected from apple fruitlet seed samples in 'Ruby Pink'. Putative (Level 3) identification of 380 metabolites in positive mode and 380 in negative mode, providing valuable information on the complex composition of the apple seeds, including plant hormones, lipids, amino acids, vitamins, phenols and secondary metabolites. However, it is important to note that further confirmation of metabolite identity (Level 1 and 2 compound identification) requires in-house standards, or MS2 fragmentation spectra matched to a database/journal publication (Viant et al. 2017). PCA score plots of the

individual collections were generated (Figure 1). PCA plots showed clear separation of samples collected on the 23/11/2021 and 10/12/2021 and all subsequent statistical analyses were conducted individually on those time points.

A linear model (y (metabolite response) ~ crop load) was applied to the whole dataset and N-WAY ANOVA was applied to the very high (6.6–14.7 fruit / cm^2 TCSA) and very low (0.4–0.7 fruit / cm^2 TCSA) crop loads. PCA plots were generated with all compounds in Tables 2 and 3 in the respective ionization mode and revealed separation of the high and low treatments (Figure 2).

The compounds associated with treatment effects were further statistically analysed for temporal changes across the collection period. Time and treatment effects resulted in 59 and 36 compounds significantly altered on 10 December and 23 November, respectively. The disruption in compounds such as those shown in Figures 3 and 4 and together with the temporal profile, suggest their possible involvement in floral induction and/or repression as shown in Tables 2 and 3. Selected metabolites with significant increase over time are represented in bar charts in Figures 5 and 6. Other compounds that reduced over time are shown in Tables 2 and 3.

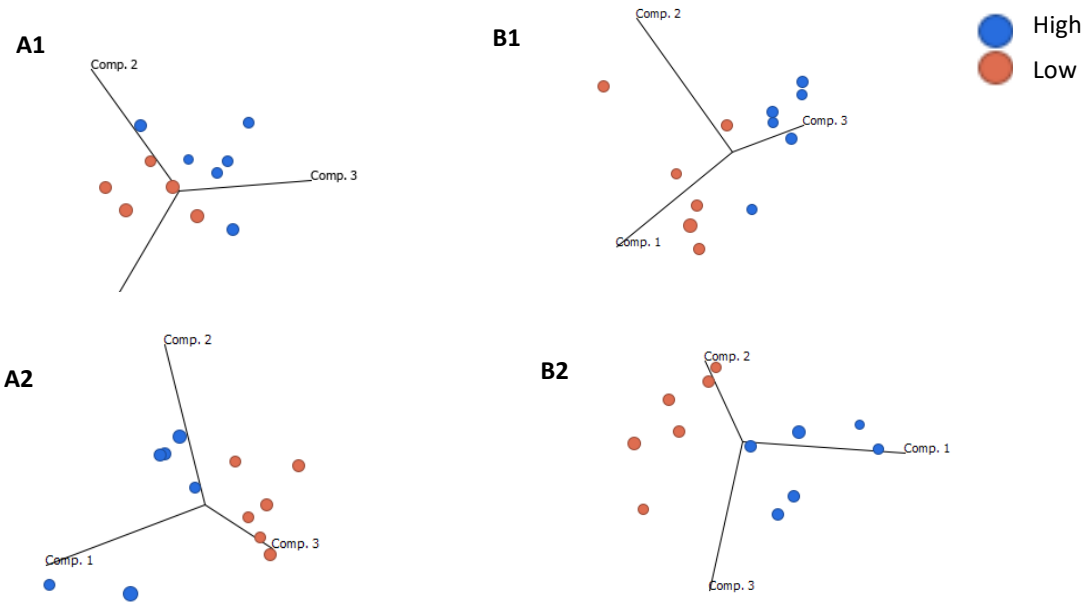

Figure 2. PCA scores plot of A) ESI positive ionization and B) ESI negative ionization data showing separation of high (n = 6) and low crop load treatments (n = 6) based on significant molecules identified from N-WAY ANOVA and a linear model based on crop load treatments. A1 and B1 show results from 10 December samples and A2 and B2 show results from 23 November samples.

A significant change in concentration of metabolites associated with crop load as per linear model and N-WAY ANOVA was identified on 23 November and 10 December. These compounds were also significantly altered over the course of the collection period. The putatively identified metabolites predominantly belonged to the phenylpropanoid biosynthesis pathway. These include benzoates: 2-formylbenzoate, benzoic acid, benzoic acid, 2-(acetyloxy)-5-amino-, and the related derivatives 6- gingesulfonic acid, sinapaldehyde, dehydrodiconiferyl acid as well as coumarines: scoparone and 4-coumaroyl-diketides and flavonoids (Group_0941), and quercetin derivatives (Group_459 and Group_460), eriodictyol, dihydrokaempferol as well as phenolics such as diarylhepatonoids and 1,3-Dicaffeoylquinic acid. Nuclear localization of flavonoids has been reported in many plant species, suggesting that flavonoids may function in transcriptional regulation of endogenous gene expression (Peer and Murphy 2006).

On 10 December 2021, tree phenology was at 74 days after full bloom (DAFB) — i.e., within the key timeframe associated with floral induction, as previously reported in AP15002. Significantly decreased levels of the putatively identified diterpene and phytohormone gibberellic acid (GA) derivative were associated with the high crop load treatment and with the disruption of the monoterpene dihydrovaltrate. Both these compounds showed an overall significant increase over the collection period.

High crop load treatments are known to repress return bloom in the following season. Exogenous GA has inhibitory effects on flowering (Dennis and Neilsen 1999). In this study, an overall increase of GA was identified over the collection period. Since more fruit were present in high crop load trees, it is possible that they produced higher total GA per tree which then translocated to the bourse shoots and buds (Dennis and Neilsen 1999). Increased GA may in turn lead to return bloom repression in adjacent buds the following season. Literature on the effects of GA on reducing return bloom is predominant (Luckwill and Silva 1979; Lenhahan et al. 2006; Schmidt et al. 2009 and 2010; Muñoz-Fambuena et al. 2012), although other studies suggested that GA-related compounds promote return bloom (Looney, Pharis et al. 1985; Zang et al. 2016). The role of GA derivatives detected in the present study is unclear; thus, more investigation on the transport of these compounds would be beneficial, as flowering signals are unlikely to determine the fate of the buds if they don't move to the buds (Bangerth 1998).

In this study, the phenylpropanoids pathway metabolites and GA were found to be likely involved in the signalling pathways associated with alternate bearing. Gibberellins are reported to negatively regulate flavonoid biosynthesis through GA-mediated signalling pathways in leaves (Sun et al. 2021). It is possible that GA could be controlling floral induction and repression via translocation from seeds. There are many compounds related to GA that have not been fully elucidated, thus it is possible that the GA derivative identified in our study could be a novel analogue.

Table 2. Significant metabolites in 'Ruby Pink' fruitlet seeds from apple trees based on varying crop load using linear model (P<0.05); N-WAY ANOVA (P<0.05) for collection on 10 December 2021 and significant effect over the collection period.

Row	Mass	Ionization mode	RT	Putative name (Level3)	N-Way ANOVA: *P* values	Linear Model Crop load (n cm²): *P* values	Effect size High and low	*
Group_0026	130.0628	positive	1.31	Methyl levulinate	0.45	0.03	1.08	↓
Group_0050	189.0632	positive	1.40	N-acetyl-L-glutamate	0.005	0.08	-	↑
Group_0174	642.1941	positive	6.42	-	0.04	0.05	3.05	↑
Group_0300	150.0317	positive	3.07	2-formylbenzoate	0.10	0.02	-	↓
Group_0310	156.9666	positive	1.74	-	0.04	0.09	1.22	↑
Group_0361	187.0907	positive	3.61	-	0.45	0.04	-	↓
Group_0370	192.0785	positive	4.73	coumaryl acetate	0.05	0.03	2.07	↑
Group_0376	195.0529	positive	1.31	Benzoic acid, 2-(acetyloxy)-5-amino-	-	0.02	-	↓
Group_0391	206.0577	positive	6.42	Scoparone	0.04	0.04	2.77	↑
Group_0394	206.0578	positive	5.14	4-coumaroyl-diketide	0.04	0.03	2.24	↑
Group_0397	208.0733	positive	5.52	sinapaldehyde	0.02	0.02	2.34	
Group_0425	219.4878	positive	1.88	-	0.01	0.05	1.19	↑
Group_0460	232.1419	positive	1.39	-	0.34	0.02	-	↓
Group_0577	278.1628	positive	4.69	-	0.29	0.04	-	↓
Group_0597	286.9724	positive	1.89	-	0.04	0.59	-	↑
Group_0625	295.0736	positive	5.03	-	0.11	0.02	1.69	↑
Group_0645	301.8892	positive	1.08	-	0.01	0.46	-	↓
Group_0655	304.0638	positive	3.97	(5-hydroxy-7-methoxy-2,2-dimethyl-3,4-dihydro-2H-1-benzopyran-4-yl) oxidanesulfonic acid	0.09	0.01	1.29	↑
Group_0674	311.9123	positive	1.07	-	0.19	0.04	1.38	↓
Group_0710	327.116	positive	1.33	-	0.03	0.02	-	↓

Group_0786	358.1482	positive	1.31	6-Gingesulfonic acid	-	0.02	-	↓
Group_0788	359.1936	positive	2.97	-	0.10	0.04	-	↓
Group_0801	365.0797	positive	3.74	-	0.23	0.04	1.41	↑
Group_0807	368.11	positive	6.42	-	0.04	0.04	3.03	↑
Group_0819	372.1207	positive	3.98	dehydrodiconiferyl acid	0.02	0.01	-	↓
Group_0826	375.3105	positive	12.43	Adrenoyl ethanolamide	0.02	0.12	-	↓
Group_0900	414.2039	positive	8.75	-	0.29	0.04	1.15	↓
Group_0918	424.207	positive	11.14	Dihydrovaltrate	0.13	0.04	1.95	↑
Group_0941	436.1855	positive	8.75	2-(2,4-dihydroxy-5-methoxyphenyl)-3-(3,7-dimethylocta-2,6-dien-1-yl)-7-hydroxy-4H-chromen-4-one	0.30	0.04	1.19	↓
Group_1009	476.1322	positive	3.97	Orientin 7,3'-dimethyl ether	0.03	0.06	1.18	↑
Group_1018	484.1166	positive	3.97	-	0.03	0.29	-	↑
Group_1019	484.6181	positive	3.97	-	0.02	0.27	-	↑
Group_1053	520.1939	positive	3.95	(7'S,8'S)-4,7'-Epoxy-3,8'-bilign-7-ene-3',5-dimethoxy-4',9,9'-triol 4'-glucoside	0.02	0.22	-	↓
Group_1075	542.1263	positive	3.74	6-{[3,7-dihydroxy-2-(1-hydroxy-3-methoxy-4-oxocyclohexyl)-6-methoxy-4-oxo-4H-chromen-5-yl]oxy}-3,4,5-trihydroxyoxane-2-carboxylic acid	0.16	0.04	1.53	↑
Group_1076	542.6275	positive	3.74	-	0.13	0.04	1.57	↑
Group_1104	579.1617	positive	5.01	-	0.14	0.04	1.75	↑
Group_1110	584.2567	positive	3.73	-	0.02	0.09	-	↓
Group_1138	607.188	positive	3.68	-	0.62	0.05	-	↓
Group_1219	719.1729	positive	3.74	-	0.13	0.03	1.51	↑
Group_1272	805.555	positive	11.59	Lactosylceramide (d18:1/12:0)	0.01	0.38	-	↓
Group_1277	810.2995	positive	8.08	-	0.04	0.07	-	↑
Group_1294	894.2471	positive	5.41	-	0.16	0.04	1.34	↑
Group_1333	1116.202	positive	3.73	-	0.04	0.23	-	↓
Group_1334	1136.356	positive	5.01	-	0.03	0.35	-	↓
Group_016	310.1017	negative	1.22	-	0.44	0.04	1.16	↓
Group_040	642.1959	negative	6.42	-	0.04	0.04	-	↑
Group_042	710.1833	negative	6.42	-	0.04	0.04	-	↑
Group_070	131.0208	negative	1.24	Iminoaspartic acid	-	0.05	-	↓
Group_106	196.0941	negative	1.32	1-(2-Thienyl)-1-heptanone	0.16	0.01	1.28	↓
Group_180	289.9442	negative	1.07	-	0.16	0.03	1.11	↓
Group_242	330.0957	negative	4.23	1-O-vanilloyl-β-D-glucose	0.11	0.03	2.04	↓
Group_261	346.1423	negative	6.82	Gibberellin derivative (gibberellin A29-catabolite, gibberellin A6, gibberellin A34-catabolite)	0.03	0.19	1.24	↑

Group_347	432.1791	negative	8.09	(2S,4S,6S)-2-[2-(4-Hydroxy-3-meyhoxyphenyl)ethyl]tetrahydro-6-(4,5-dihydroxy-3-methoxyphenyl)-2H-pyran-4-yl 4-acetate	0.05	0.19	1.05	↑
Group_394	471.1591	negative	1.40	-	0.04	0.75	1.01	↑
Group_444	516.1269	negative	5.04	1,3-Dicaffeoylquinic acid	0.15	0.05	1.11	↓
Group_459	536.154	negative	5.15	3,7,3',4'-tetramethylquercetin 2'-O-β-D-glucoside	0.04	0.03	-	↑
Group_460	536.154	negative	5.92	3,6,7,4'-tetramethylquercetagetin 3'-O-β-D-glucoside	0.07	0.05	-	↑
Group_567	682.4589	negative	11.77	-	-	0.00	-	↑
Group_621	816.2863	negative	1.28	-	0.01	0.64	1.14	↑

*Temporal change from first collection (9 November 2021), ↓ = downregulation; ↑ = upregulation.

Table 3. Significant metabolites in 'Ruby Pink' fruitlet seeds from apple trees based on varying crop load using linear model (P<0.05); N-WAY ANOVA (P<0.05) for collection on 23 November 2021 and tested significance over the collection period.

Row	Mass	Ionisation mode	RT	Putative name	N-Way Anova: *P* values	Linear Model *P* values	Effect size	*
Group_0012	110.0368	positive	1.31	Catechol	0.00	0.28	1.13	↓
Group_0031	143.9493	positive	1.07	(2S)-eriodictyol	0.17	0.00	1.46	↑
Group_0038	159.0891	positive	1.28	2-Methylbutyrylglycine	0.06	0.00	1.15	↓
Group_0096	288.0628	positive	4.18	(+)-dihydrokaempferol/eriodyctyol	0.13	0.01	1.26	↓
Group_0152	457.1576	positive	3.97	Amygdalin	0.02	0.06	-	↑
Group_0357	186.1002	positive	2.46	Alanyl-Proline	0.01	0.69	-	↓
Group_0456	231.1663	positive	3.50	-	0.01	0.23	3.23	↓
Group_0482	240.1470	positive	2.42	Pirbuterol	0.10	0.01	1.18	↓
Group_0567	275.9399	positive	1.07	-	0.19	0.00	1.40	↑
Group_0655	304.0638	positive	3.97	(5-hydroxy-7-methoxy-2,2-dimethyl-3,4-dihydro-2H-1-benzopyran-4-yl) oxidanesulfonic acid	0.01	0.10	-	↑
Group_0732	336.0837	positive	4.26	5-O-caffeoylshikimate	0.10	0.01	1.35	↓
Group_0751	341.1667	positive	3.74	-	0.00	0.00	1.68	↑
Group_0789	359.2050	positive	4.63	-	0.00	0.12	2.48	↓
Group_0829	376.2581	positive	11.71	9'-Carboxy-gamma-chromanol	0.23	0.01	1.50	↑
Group_0867	395.1324	positive	3.37	-	0.02	0.28	-	↓
Group_0889	407.3002	positive	12.66	-	0.13	0.00	1.14	-
Group_0933	433.1077	positive	1.22	-	0.04	0.01	-	↑
Group_1047	512.1506	positive	4.08	3-(4-Hydroxy-3-methoxyphenyl)-1,2-propanediol 2-O-(galloyl-glucoside)	0.02	0.35	-	

Group_1115	589.2108	positive	2.48	-	0.00	0.42	-	↑
Group_1170	634.1991	positive	3.70	-	0.02	0.51	-	↓
Group_1251	781.5599	positive	11.14	1-α-linolenoyl-2-linoleoyl-phosphatidylcholine	0.42	0.01	1.52	↓
Group_041	684.233139	negative	1.28	Citbismine C	0.10	0.01	1.30	↑
Group_120	222.1003864	negative	3.22	Glycyl-Phenylalanine	0.05	0.26	-	↓
Group_181	289.9729634	negative	2.29	-	0.01	0.00	1.65	↓
Group_191	294.122019	negative	3.03	gamma-Glutamylphenylalanine	0.03	0.17	-	↓
Group_202	301.0331174	negative	4.99	-	0.03	0.50	1.09	↑
Group_214	308.9150237	negative	1.07	-	0.16	0.00	1.41	↑
Group_222	315.11782	negative	1.21	-	0.03	0.11	1.21	↓
Group_366	440.0923141	negative	1.28	3,5-Dihydroxyphenyl 1-O-(6-O-galloyl-beta-D-glucopyranoside)	0.06	0.01	1.42	↓
Group_392	469.1220848	negative	5.68	-	0.18	0.01	1.24	↓
Group_476	554.2267669	negative	4.11	23-Hydroxyphysalolactone	0.05	0.01	-	↓
Group_479	557.0840995	negative	3.98	-	0.03	0.01	-	↑
Group_500	575.0958025	negative	3.98	-	0.03	0.17	-	↑
Group_583	707.5707779	negative	3.74	-	0.03	0.38	1.45	↓
Group_618	811.2543812	negative	3.97	-	0.02	0.15	-	↑
Group_648	872.4497489	negative	5.37	-	0.04	0.04	1.16	↓
Group_674	1084.308204	negative	5.02	-	0.05	0.23	1.32	↓

*Temporal change from first collection (9 November2021), ↓ = downregulation; ↑ = upregulation.

A

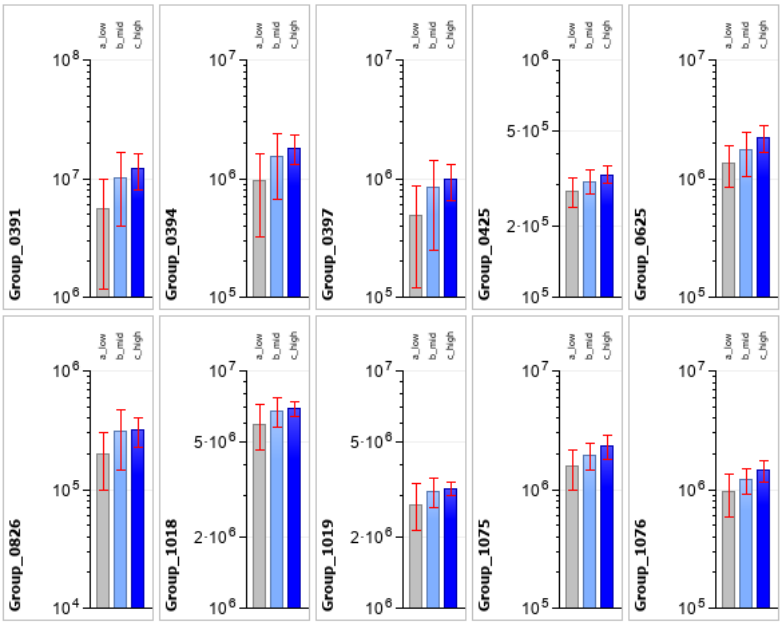

B

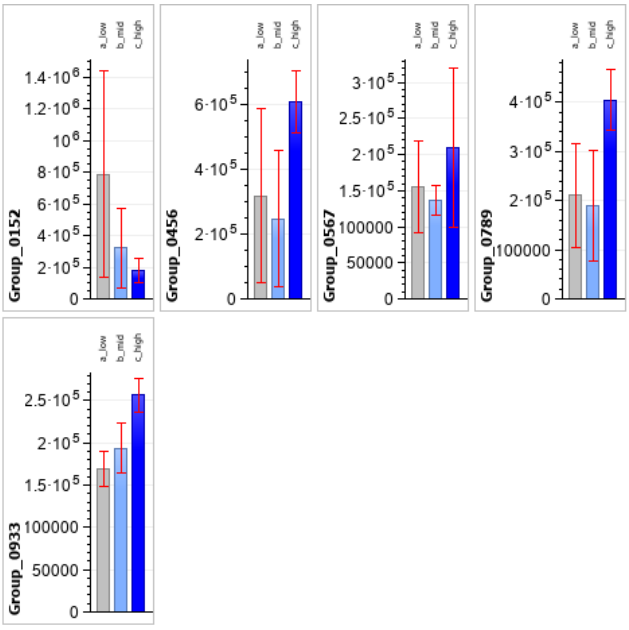

Figure 3. Relative abundances (log transformed) of selected compounds in fruitlet seeds of high (4.0–14.6 n cm^{-2} TCSA), mid (2.1–3.7 n cm^{-2} TCSA) and low (0.6–2.0 n cm^{-2} TCSA) crop load treatments imposed on 'Ruby Pink' leaders. Compounds identified in positive ionisation mode ($p<0.05$) in A) 10 December 2021 and B) 23 November 2021 samples.

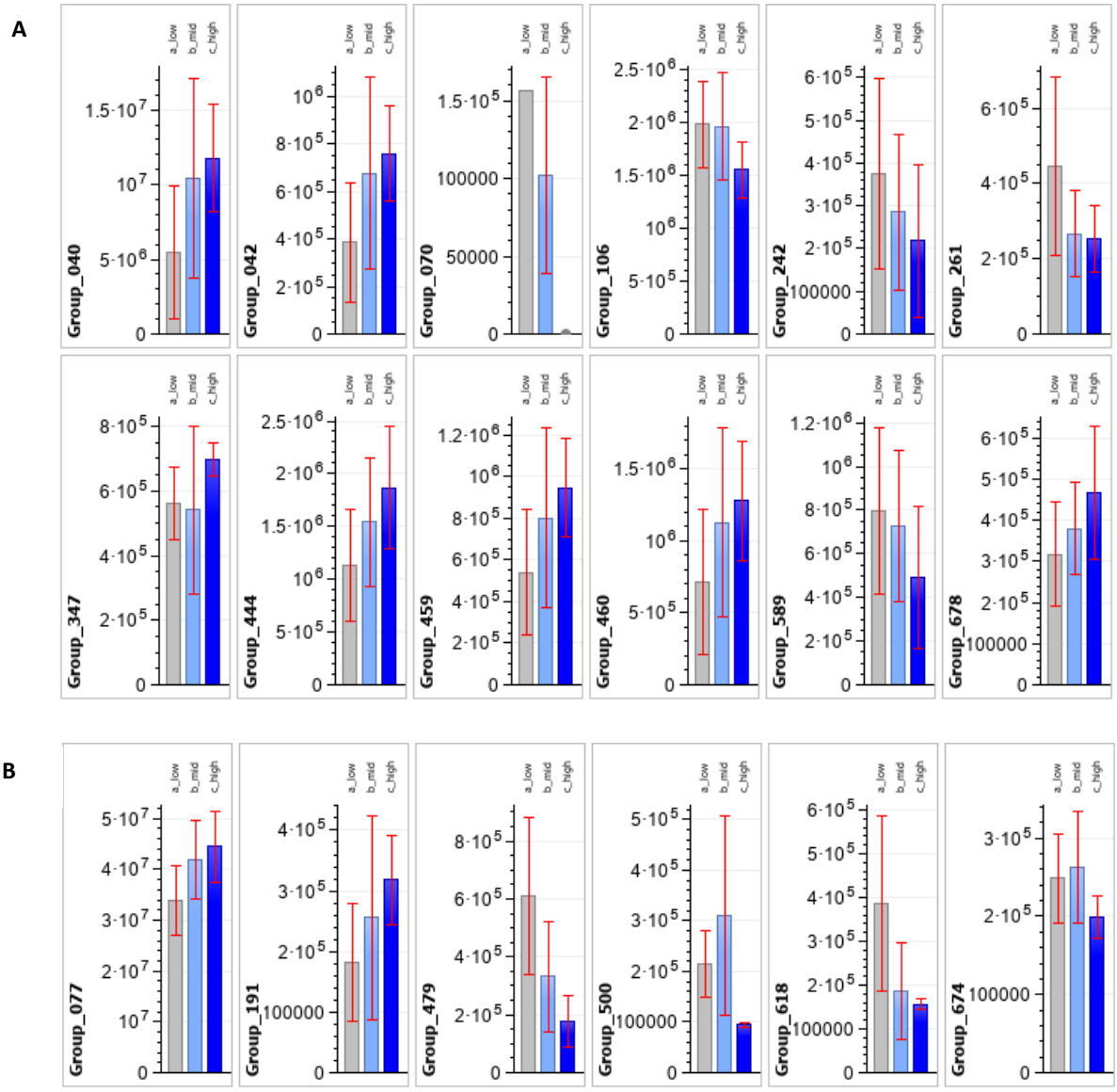

Figure 4. Relative abundances (log transformed) of selected compounds in fruitlet seeds of high (4.0–14.6 n cm^{-2} TCSA), mid (2.1–3.7 n cm^{-2} TCSA) and low (0.6–2.0 n cm^{-2} TCSA) crop load treatments imposed on 'Ruby Pink' leaders. Compounds identified in negative ionization mode ($p<0.05$) in A) 10 December 2021 and B) 23 November 2021 samples.

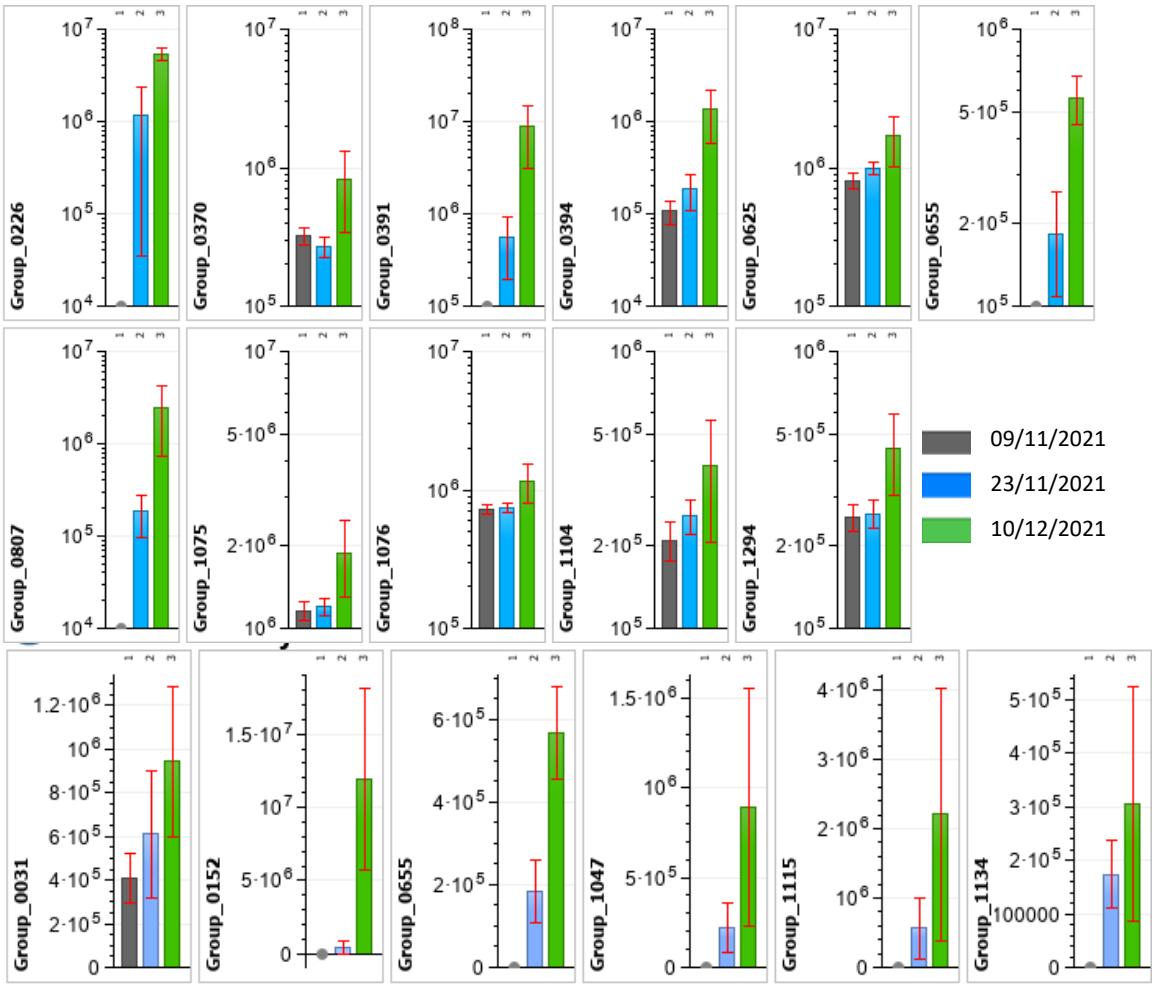

Figure 5. Relative abundance (log transformed) of selected compounds in fruitlet seeds collected from 'Ruby Pink' at three sampling dates. Compounds identified in positive ionisation mode with significant ($p<0.01$) temporal effect.

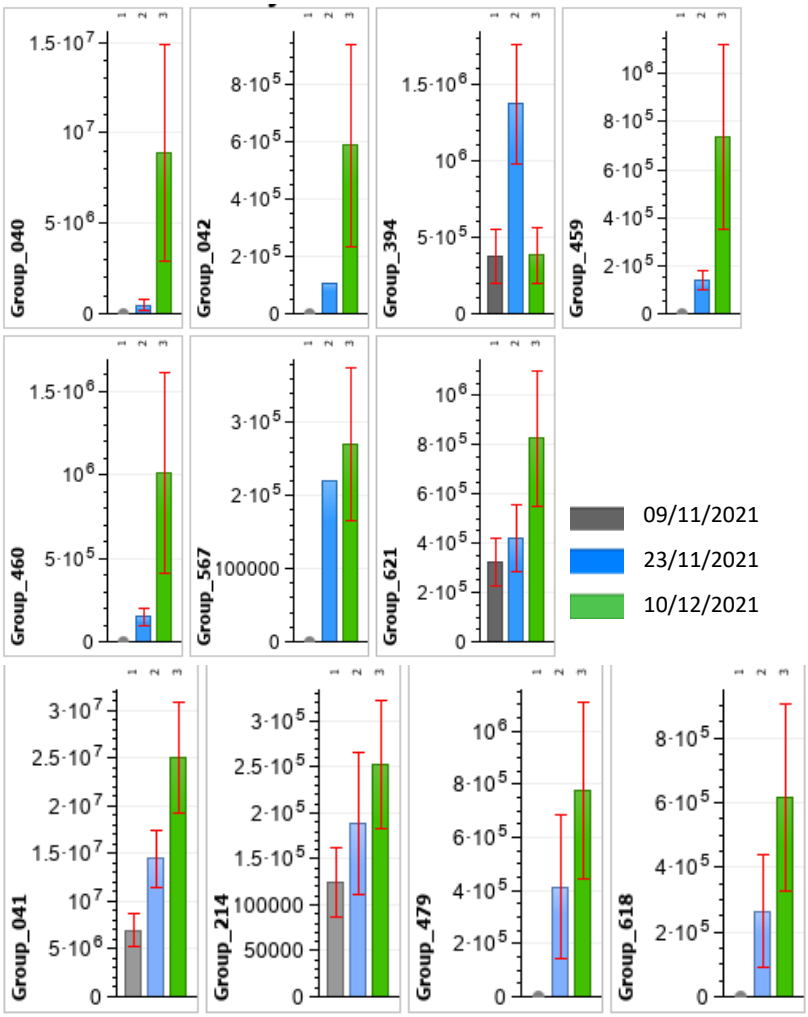

Figure 6. Relative abundance (log transformed) of selected compounds in fruitlet seeds collected from 'Ruby Pink' at three sampling dates. Compounds identified in negative ionisation mode with significant ($p<0.01$) temporal effect.

CONCLUSION

Our study indicated that the levels of phenylpropanoid pathway metabolites and a putatively identified phytohormone GA derivative are significantly altered in high and low crop load treatments. However, it is noteworthy that there was an increase in abundance of GA over the duration of the collection period. Thus, the total amount of GA in high crop load trees would be much higher and thus would explain the increased repression of return bloom in the following season. Fruitlet seeds are rich in gibberellins, and it is likely that these compounds move out of the fruit into other regions to induce floral repression. There are many GA-like compounds and the GA derivative identified in this study could be novel. Thus, it is likely that there are other unknown and novel phytohormones that could be elucidated with further LCMSMS mass spectrometry techniques and/or library confirmation. Further investigation into the identification of the compounds would be beneficial as these compounds are potential signalling molecules for floral repression.

RECOMMENDATIONS

The preliminary investigation on the fruitlet seed shows promising results and it is recommended that a complete investigation be undertaken to seek metabolites associated with floral repression. Further, more replicates in the high and low treatments would be required to elucidate small metabolic changes exerted by the treatment. LCMSMS analysis of fruitlet seed extracts will need to be undertaken to provide better confidence in the identity of the compounds putatively identified so far, and to attempt to identify the unknown compounds which have shown good correlation with crop load.

ACKNOWLEDGEMENTS

This technical report is part of the apple and pear industry's PIPS3 (Productivity, Irrigation, Pests and Soils) program of research and development. The project is funded by Hort Innovation, using the Hort Innovation Apple and Pear research and development levy, contributions from the Australian Government and co-investment from Agriculture Victoria. Hort Innovation is the grower-owned, not-for-profit research and development corporation for Australian horticulture

REFERENCES

Arseneault, M. H. (2016). Crop load management of apple by chemical fruitlet thinning, preharvest drop management, and investigation of abscission physiology.

Bangerth, F. K. (1998). Can regulatory mechanism in fruit growth and development be elucidated through the study of endogenous hormone concentrations? Acta Horticulturae. 463: 77-87.

Chan, B.G., Cain, J.C. (1967) The effect of seed formation on subsequent flowering in apple. Proc. Am. Soc. Hort. Sci. 91, 63–67

Dennis, F. G. and J. C. Neilsen (1999). "Physiological factors affecting biennial bearing in tree fruit: the role of seeds in apple." HortTechnology 9(3): 317-322.

Guitton, B., J. J. Kelner, R. Velasco, S. E. Gardiner, D. Chagné and E. Costes (2012). "Genetic control of biennial bearing in apple." Journal of Experimental Botany 63(1): 131-149.

Kviklys, D. and G. Samuolienė (2020). "Relationships among the rootstock, crop load, and sugar hormone signalling of apple tree, and their effects on biennial bearing." Frontiers in Plant Science 11.

Lenahan, O. M., Whiting, M. D., & Elfving, D. C. (2006). Gibberellic acid inhibits floral bud induction and improvesBing'sweet cherry fruit quality. HortScience, 41(3), 654-659.

Looney, N. E., R. P. Pharis and M. Noma (1985). "Promotion of flowering in apple trees with gibberellin A4 and C-3 epi-gibberellin A4." Planta 165(2): 292-294.

Luckwill, L. C., & Silva, J. M. (1979). The effects of daminozide and gibberellic acid on flower initiation, growth and fruiting of apple cv Golden Delicious. Journal of Horticultural Science, 54(3), 217-223. https://doi.org/10.1080/00221589.1979.11514873

Muñoz-Fambuena, N., Mesejo, C., González-Mas, M. C., Iglesias, D. J., Primo-Millo, E., & Agustí, M. (2012). Gibberellic acid reduces flowering intensity in sweet orange [Citrus sinensis (L.) Osbeck] by repressing CiFT gene expression. Journal of Plant Growth Regulation, 31(4), 529-536.

Peer, W. A. and A. S. Murphy (2006). Flavonoids as signal molecules: Targets of flavonoid action. The Science of Flavonoids: 239-268.

Schmidt, T., Elfving, D. C., McFerson, J. R., & Whiting, M. D. (2009). Crop load overwhelms effects of gibberellic acid and ethephon on floral initiation in apple. HortScience, 44(7), 1900-1906. https://doi.org/10.21273/HORTSCI.44.7.1900

Schmidt, T., McFerson, J., Elfving, D.C. and Whiting, M. (2010). PRACTICAL GIBBERELLIC ACID PROGRAMS FOR MITIGATION OF BIENNIAL BEARING IN APPLE. Acta Hortic. 884, 663-670. https://doi.org/10.17660/ActaHortic.2010.884.89

Sun, H., H. Cui, J. Zhang, J. Kang, Z. Wang, M. Li, F. Yi, Q. Yang and R. Long (2021). "Gibberellins Inhibit Flavonoid Biosynthesis and Promote Nitrogen Metabolism in Medicago truncatula." International Journal of Molecular Sciences 22(17): 9291.

Stefanelli D, Plozza T, Flachowsky H, Wünsche JN (2018b) Young apple tree responses to crop load. In: Acta Horticulturae, pp 221-228.

Zang, Y. X., Chun, I. J., Zhang, L. L., Hong, S. B., Zheng, W. W., & Xu, K. (2016). Effect of gibberellic acid application on plant growth attributes, return bloom, and fruit quality of rabbiteye blueberry. Scientia Horticulturae, 200, 13-18. https://doi.org/10.1016/j.scienta.2015.12.057

Viant, M. R., I. J. Kurland, M. R. Jones and W. B. Dunn (2017). "How close are we to complete annotation of metabolomes?" Current Opinion in Chemical Biology 36: 64-69.

Advancing sustainable and technology driven apple orchard production systems

Technical Report:

Testing and calibration of Green Atlas *Cartographer* for spatial distribution of flowering, tree size and fruit setting in relation to light interception in 'ANABP-01'

Agriculture Victoria Research

May 2022

VICTORIA State Government | Jobs, Precincts and Regions

AGRICULTURE VICTORIA

Author: Alessio Scalisi and Ian Goodwin

Project RDC Number: AP19003

Project RCM Number: 6472

Department of Jobs, Precincts and Regions
1 Spring Street Melbourne Victoria 3000
Telephone (03) 9651 9999

Contents

EXECUTIVE SUMMARY

Modern horticulture is moving toward increased mechanisation, automation, robotics, and non-destructive sensing and monitoring. This technical report presents the second year of data for the initial calibration and validation of a sensorised platform (Green Atlas *Cartographer*) for the prediction of flower cluster number, fruit number and yield in 'ANABP-01' apples. In addition, this work modelled the relationships between tree geometry and light interception and the effects of light interception (i.e., effective area of shade, EAS) on flowers, fruit and yield. Results showed that predictions were very accurate after initial calibration and orchard errors for crop load and yield were lower than 5 %. Canopy height, canopy area, canopy density and cross-sectional leaf area (CSLA) were all linearly related with EAS, but the latter was the most stable single predictor of intercepted light. A combination of canopy geometry (density, height and predicted width) and row spacing appeared to be the best predictor of EAS. The orchard heatmaps generated after data validation proved very useful to support orchard management decisions. Increasing EAS led to improved yield, particularly in N – S oriented trees. N – S trees had the best fraction of intercepted light per unit of CSLA and achieved the top yield efficiency. On the other hand, E – W had the poorest performance. Yield efficiency was also improved in trees grafted onto M9 compared to M26 and B9. Overall, *Cartographer* demonstrated to be a valid tool to combine predictions of several important fruit crop parameters (i.e., flower cluster number, crop load, yield, tree size and geometry, and light interception) in one single platform and its use can be beneficial both for growers and scientists to collect large amounts of meaningful data and replace labour-intensive operations.

INTRODUCTION

This technical report is a deliverable for the milestone 105 of the project 'Advancing sustainable and technology driven apple orchard production systems' (AP19003). The report details the second year of a study on the initial testing and calibration of the Green Atlas *Cartographer* (i.e., a mobile platform with multiple sensors) for spatial distribution of flowering, crop load and tree size in relation to light interception in 'ANABP 01' apples. This report contributes towards meeting the project objectives by providing scientifically sound validations of the mobile platform's predictions of flower clusters, tree size, fruit number and yield to manage crop load and achieve premium fruit for domestic and export markets. The results presented in this report reflect a joint effort of Agriculture Victoria and Green Atlas staff.

Project outcome

The intended outcome of this project is to improve crop load management in a variable climate by providing knowledge and tools to deliver premium fruit that meets consumer expectations in domestic and export markets.

Project background

In Australia, apple production is yet to reach its full potential based on the area planted (10,000 ha) and the theoretical yield (~ 800,000 t). This is mostly due to variable crop load management, biennial bearing and inconsistent fruit quality. Australia has a unique climate characterised by relatively high temperatures and light intensity compared to other apple production areas around the world (Darbyshire et al., 2018). Light interception and carbohydrate availability play an important role not only in defining the optimal crop load to maximise consistent fruit quality for the life of the tree, but also in floral initiation and biennial bearing. While high light intensity generally leads to increasing photosynthetic rates and consequently carbohydrate availability, when excessive and/or combined with high air temperature can cause sunburn, photoinhibition (i.e., damage the leaf photosynthetic apparatus) or induce stomata closure for long periods during the day, reducing water loss but generating undesired reductions in photoassimilates. Therefore, an optimal regulation of the light harvested by tree canopies by canopy architecture, rootstock selection and planting design is paramount to minimise external inputs (e.g., water, thinning chemicals, reflective mulches, biostimulants) and maintain or even improve fruit quality characteristics such as skin colouration and fruit size.

Modern horticulture is moving toward increased mechanisation, automation, robotics, and non-destructive sensing and monitoring. The integration of technologies that are already adopted in other industries into horticulture systems aims to increase resource use efficiency — including labour — and make orchards more profitable. For this purpose, several recent studies have focused on the application of machine learning algorithms to detect tree structures (e.g., flowers, fruit, architecture) using sensorised robots or platforms. Most of the state-of-the-art research has attempted to detect apple fruit for crop load or yield determination, or for integration with automated harvesting machines using image segmentation, deep learning and different Convolutional Neural Networks (CNN) (Bargoti and Underwood, 2017a, 2017b; Bresilla et al., 2019; Kang and Chen, 2020; Kuznetsova et al., 2020) on images typically collected by RGB / RGB-D cameras. Underwood et al. (2016), Dias et al. (2018a, 2018b) and Wang et al. (2018) used similar machine vision approaches for almond, apple and mango flower recognition, respectively. In the case of almond, the machine image recognition was supported by LiDAR cloud points to reconstruct tree structure and assign tree geo-references when combined with GPS (Underwood et al., 2016). LiDAR sensors are a powerful tool to quickly determine canopy architecture parameters such as tree height, canopy size and density and have the potential to recognise tree location, alone or combined with GPS (Underwood et al., 2015). LiDAR cloud points have also been used to model light interception, as demonstrated by Örn (2016). The same idea was applied to estimate a solar-geometric model for light interception estimation in avocado trees (Westling et al., 2018).

Commercial services such as the Green Atlas *Cartographer* use a combination of sensors (e.g., RGB cameras, LiDAR, GPS, thermal sensors), mounted on a platform on an electric vehicle, to gather data while driving through orchard rows. The Cartographer is currently available to measure the spatial distribution of crop load in apples and to measure tree geometry parameters such as canopy area, canopy density and cross-sectional leaf area (CSLA). Canopy area (m^2) represents the area of the polygon drawn around the LiDAR-generated points in the scanned transect, excluding the trunk. Canopy density represents the ratio between the number of light beams generated by the LiDAR that bounces back to the light source and the total number of emitted light beams. CSLA is the area of the points (comparable to leaves) within the canopy area polygon. The Green Atlas Cartographer is rapidly expanding its capability and aims to achieve good predictions of flower cluster number and fruit size and colour.

The results of the first year of study in the Sundial orchard are published in the high-impact factor, peer-reviewed journal *Computers and Electronics in Agriculture* (Scalisi et al., 2021).

Project objectives

The overall goal of this project is to investigate physiological mechanisms and develop management tools so that apple orchards can consistently produce high yields and fruit that meet market specifications through variable climatic conditions and extreme heat events. The work presented in this report aimed to develop a rapid orchard assessment tool using proximal sensing technologies to determine several crop parameters that are typically manually measured in apple orchards. Specifically, this work aimed to: (i) evaluate relationships between ground-truth and Green Atlas *Cartographer* predictions of flower cluster number, crop load and yield in 'ANABP-01' apple trees; (ii) evaluate the relationship of LiDAR-obtained tree geometry parameters (i.e., canopy height, canopy area, canopy density and cross-sectional leaf area (CSLA) with reference light interception; (iii) determine the effect of light interception on flower, fruit number and yield.

METHOD

The study was conducted in the Sundial orchard at the Tatura SmartFarm, Victoria, Australia during 2021 – 2022 The experimental design was similar to that used in the first season (2020 – 21). The Sundial orchard is a high-density (HD, ~ 2857 trees / ha) circular orchard of approximately 1.3 ha. 'ANABP-01' apple trees were planted in a semicircle of the orchard following four different row orientations (i.e., N – S, NE – SW, E – W and SE – NW). Trees are grafted onto three different rootstocks (i.e., Bud.9, M9 and M26) in a completely randomised design and were planted on site in 2018 but not considered separately in this study. 'ANABP-01' trees are trained to spindles on vertical trellises at 1 m spacing. The row spacing is 3.5 m and there is a total of twenty rows, five rows per row orientation, and 60 experimental plots. Each experimental plot is composed of eleven 'ANABP-01' trees and one polleniser ('Granny Smith'). The experiment was conducted on trees at their 4th leaf. Figure 1 shows the spatial layout of the Sundial orchard used for this experiment.

'ANABP-01' originated from a cross-pollination between 'Cripps Red' and 'Royal Gala'. The cultivar was bred by the Department of Agriculture and Food, State of Western Australia.

The methodology used in 2021 – 2022 reflected the methodology used in 2020 – 21 and is fully reported in Appendix D of MS 103.

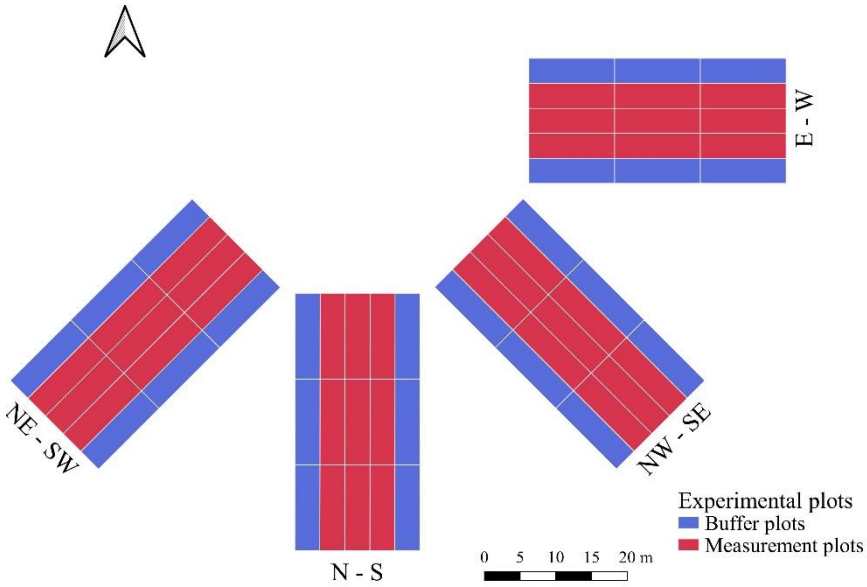

Figure 1. Layout of the 60 experimental plots (36 measurement plots) of 'ANABP-01' in the Sundial orchard at the Tatura SmartFarm. Row orientations: northeast–southwest (NE – SW), north–south (N – S), northwest–southeast (NW – SE) and east–west (E – W).

RESULTS

Predictions of tree parameters

Flower cluster number

Figure 2 shows the relationship between *Cartographer* predictions and observed values of flower clusters at full bloom. Predicted data was tightly associated with observations and the linear regression model returned a low prediction error (% standard error = 4.3%). The calibration factor (slope of the linear regression) was used to transform detections per image to flower clusters per tree. The spatial map suggested that plots in the E – W row orientation had the lowest return bloom.

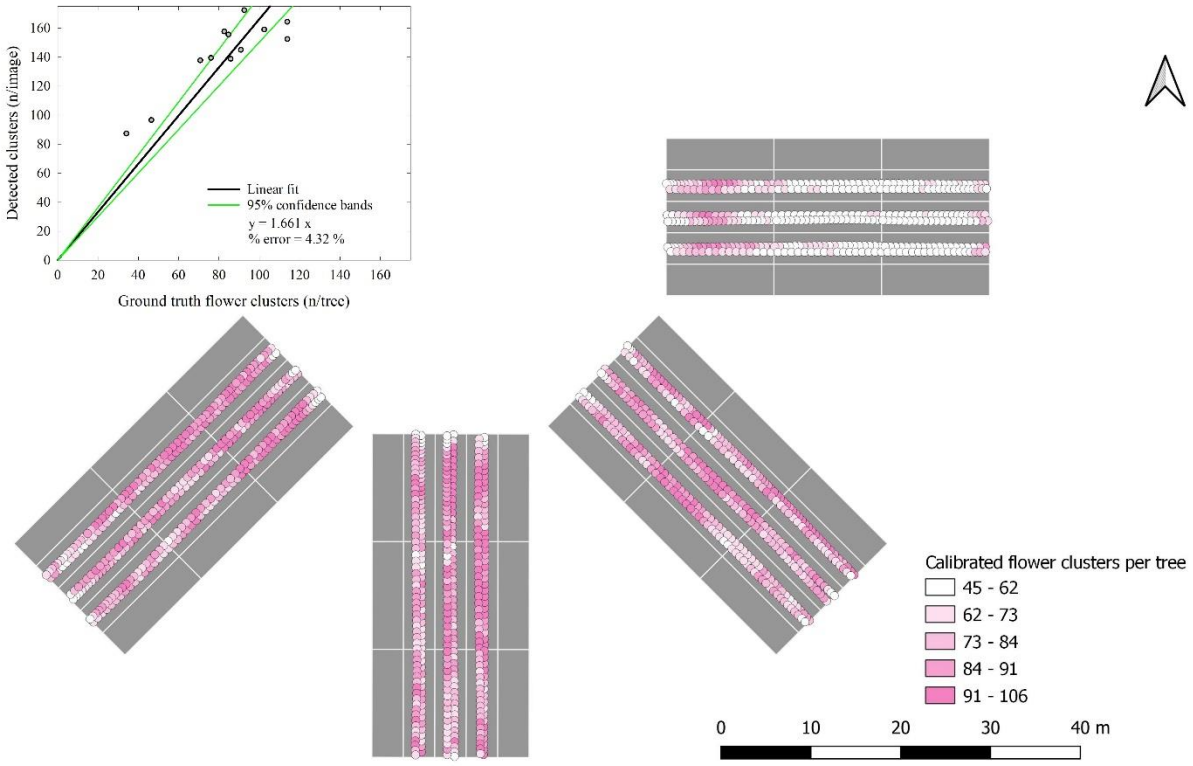

Figure 2. Heatmap of calibrated flower cluster counts (n/tree) in the 36 experimental measurement plots of 'ANABP-01' apples. Data collected at full bloom (1 October 2021). The graph in the top left of the image shows calibration equation and % standard error, and the black and green lines represent linear regression fits and 95% confidence interval bands, respectively.

Crop load and yield

The calibration relationship between fruit detections per image and ground truth fruit number on 1 April 2022 was similar to the relationship obtained in 2020-21, and the model had an error < 5% (Figure 3). The calibrated spatial map shows the position of pollenisers (white colour, no fruit) that were harvested a week prior to scanning the orchard. No significant differences between calibration factors in different rootstocks were detected in 2021 – 22, as opposed to 2020 – 21, and this is likely due to an improvement to the detection algorithm deployed by Green Atlas between the two seasons.

Yield (t ha^{-1}) predicted using the calibrated fruit number per tree and estimated fruit diameters converted to fruit weights showed good association with the ground truth yield obtained with a commercial grader (Lin's concordance correlation coefficient (r_c) = 0.66) (Figure 4). The yield obtained with a commercial grader in the experimental plots was 43.15 t ha^{-1}. *Cartographer* estimated a yield of 42.18 t ha^{-1}, which was equivalent to an overall error (underestimation) of < 1 t ha^{-1} or 2.2%.

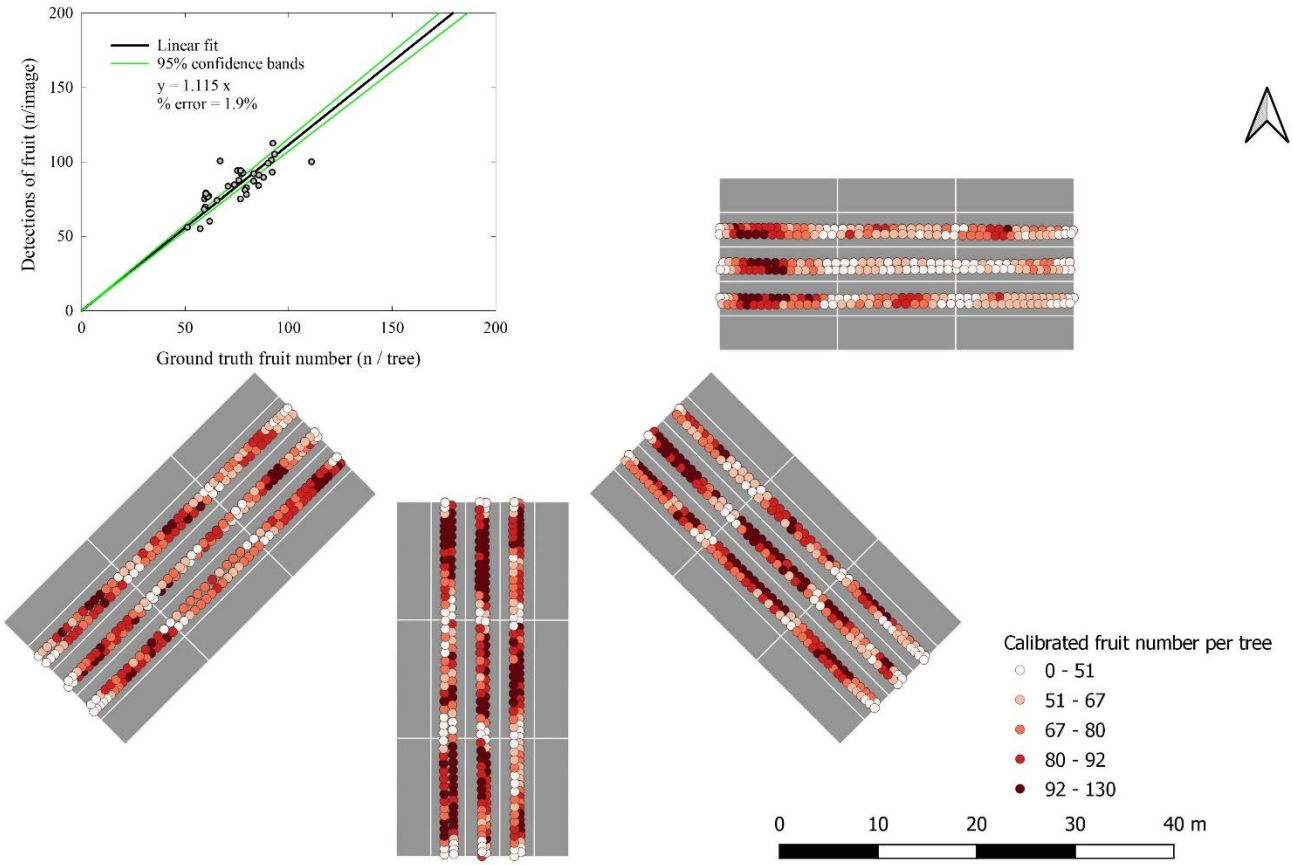

Figure 3. Heatmap of calibrated crop load in the 36 experimental measurement plots of 'ANABP-01' apples. Data collected at harvest (1 April 2022). The graph in the top left of the image shows calibration equation and % standard error, and the black and green lines represent linear regression fits and 95% confidence interval bands, respectively.

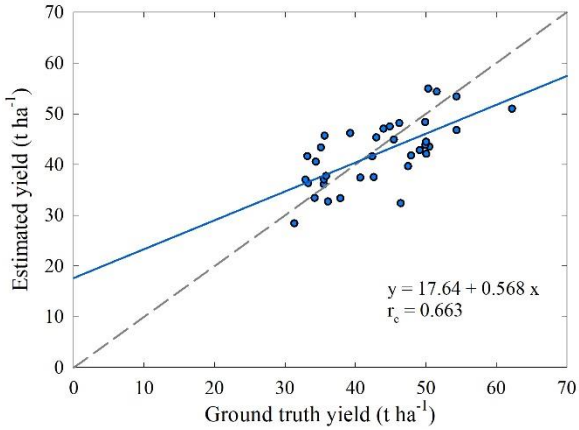

Figure 4. Validation of *Cartographer* estimated yield against yield measured by a commercial grader. Blue lines: linear regression fit; grey dashed lines: y = x fit. Lin's concordance correlation coefficient (r_c) reported as a measure of reliability.

Relationship between light interception and tree geometry

The four canopy geometry parameters output by *Cartographer* were all significantly linearly relate to EAS (Figure 5). Cross-sectional leaf area (CSLA) had the best relationship with EAS (R^2 = 0.53). Nevertheless, this was a generalised linear model obtained by pooling together the different row orientations. When row orientation relationships were separated, the linear equations were considered independently to evaluate the efficiency of intercepted light per unit of foliage. The relationships between EAS and CSLA in N – S and E – W trees had the most robust fits (Figure 6 and Table 1). Figure 6 shows a visual separation of row orientations, with a steeper slope in N – S trees, suggesting an improved light use efficiency per unit of foliage in this row orientation. The visual inference was supported by statistical findings, where no

significant difference was detected between the intercept values in the four row orientation equations (Table 1), whereas the slope coefficient was significantly higher in N – S than in E – W and NW – SE. These findings support the idea that N – S are the most efficient row orientation for fruit production.

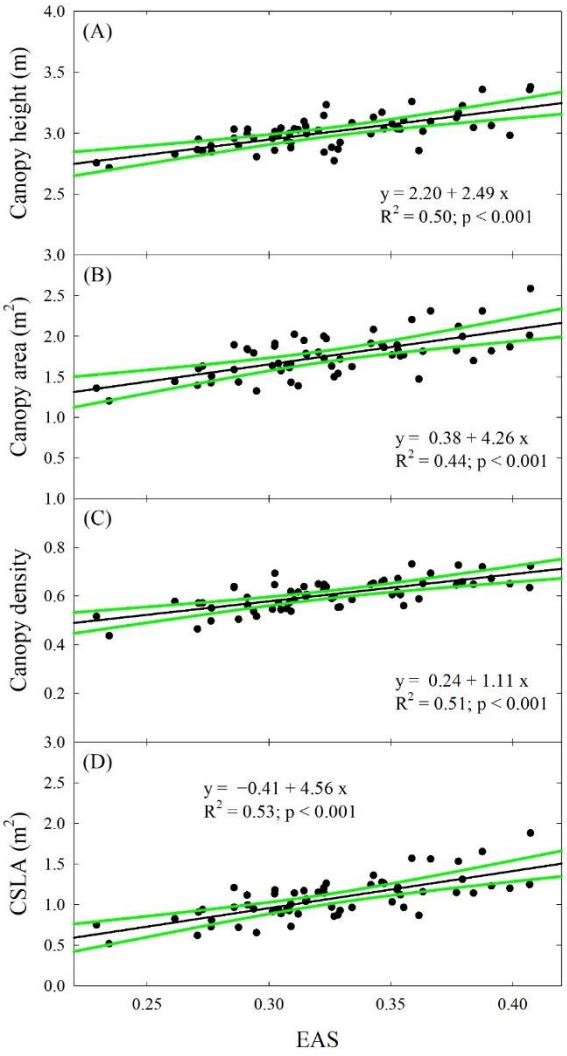

Figure 5. Scatterplots and linear regression fits of (A) canopy height, (B) canopy area, (C) canopy density, and (D) cross-sectional leaf area (CSLA) measured with Green Atlas *Cartographer* against effective area of shade (EAS) measured by a light trolley on 11 March 2022.

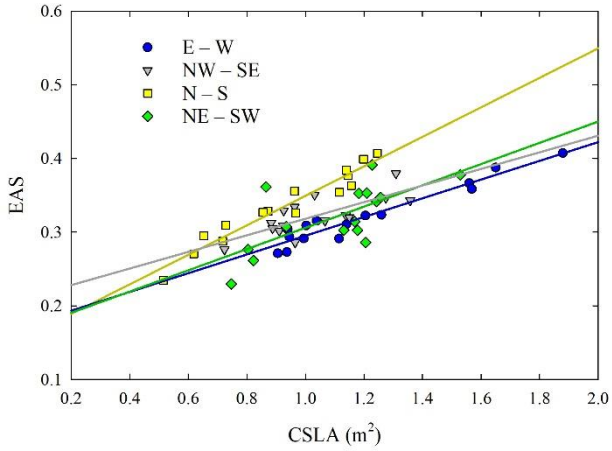

Figure 6. Linear regression models showing the effective area of shade (EAS) in response to cross-sectional leaf area (CSLA) in four different row orientations. Linear regression coefficients and statistics reported in Table 1.

Table 1. Linear regression coefficients and standard errors for the relationships between effective area of shade and cross-sectional leaf area in the four row orientations shown in Figure 6.

Row orientation	Intercept ± standard error	Slope ± standard error	Model R^2
E – W	0.17 ± 0.01	0.13 ± 0.01	0.93
NW – SE	0.21 ± 0.03	0.11 ± 0.03	0.59
N – S	0.15 ± 0.01	0.20 ± 0.01	0.94
NE – SW	0.16 ± 0.05	0.14 ± 0.04	0.47
p-value	0.551	0.108	—

EAS is an important parameter that can be utilised as a crop coefficient for irrigation management purposes. Therefore, an accurate prediction of EAS from canopy geometry data would allow to optimise canopy shape and pruning operations and to concomitantly improve irrigation efficiency. Although CSLA is the best single parameter output by *Cartographer* in terms of relationship with EAS (Figure 5), a combination of canopy geometry parameters would be beneficial to improve the prediction accuracy. Based on some geometry concepts of tree predispositions in a tree row, we attempted to predict EAS using canopy density, canopy height, and canopy width information. Row spacing in the Sundial orchard is 3.5 m and canopy width was estimated to be an average 1.6 m.

$$\text{Predicted EAS} = \text{CD} \times [\text{CH} / (\text{CW} \times \text{RS})] \qquad \text{(Equation 1)},$$

where CD, CH, CW and RS represent canopy density, canopy height, canopy width and row spacing, respectively. Predictions of EAS generated using the model in Equation 1 were plotted against EAS measured with a light trolley to assess the reliability of the estimate (Figure 7). The model demonstrated good performance, with r_c = 0.756 and root mean square error (RMSE) of 0.03. Predictions will need to be validated in more complex systems with larger 3D canopies to reassess the validity of the equation. Green Atlas is now testing a 5th canopy geometry, canopy width, directly generated from scans. This parameter will be further tested to validate its use to improve the reliability of EAS predictions from ground-based scans.

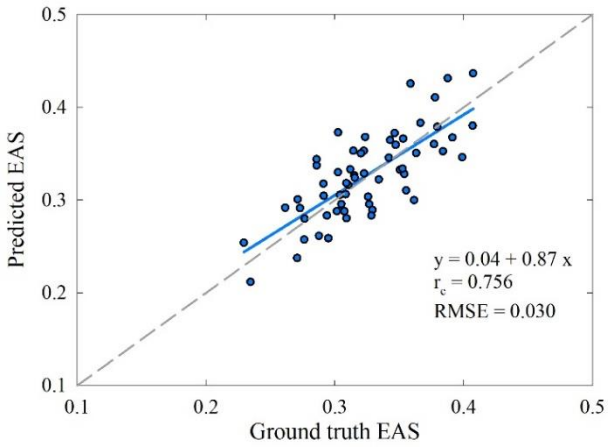

Figure 7. Scatterplot and linear fit of effective area of shade (EAS) predicted using Green Atlas *Cartographer* against EAS measured with a light trolley on 11 March 2022.

Spatial maps of CSLA extracted from *Cartographer* scans and predicted EAS (Equation 1) show the spatial variability of these two parameters. The points shown with smaller size mostly match the positions of trees grafted on B9, which had reduced vigour compared to M9 and M26.

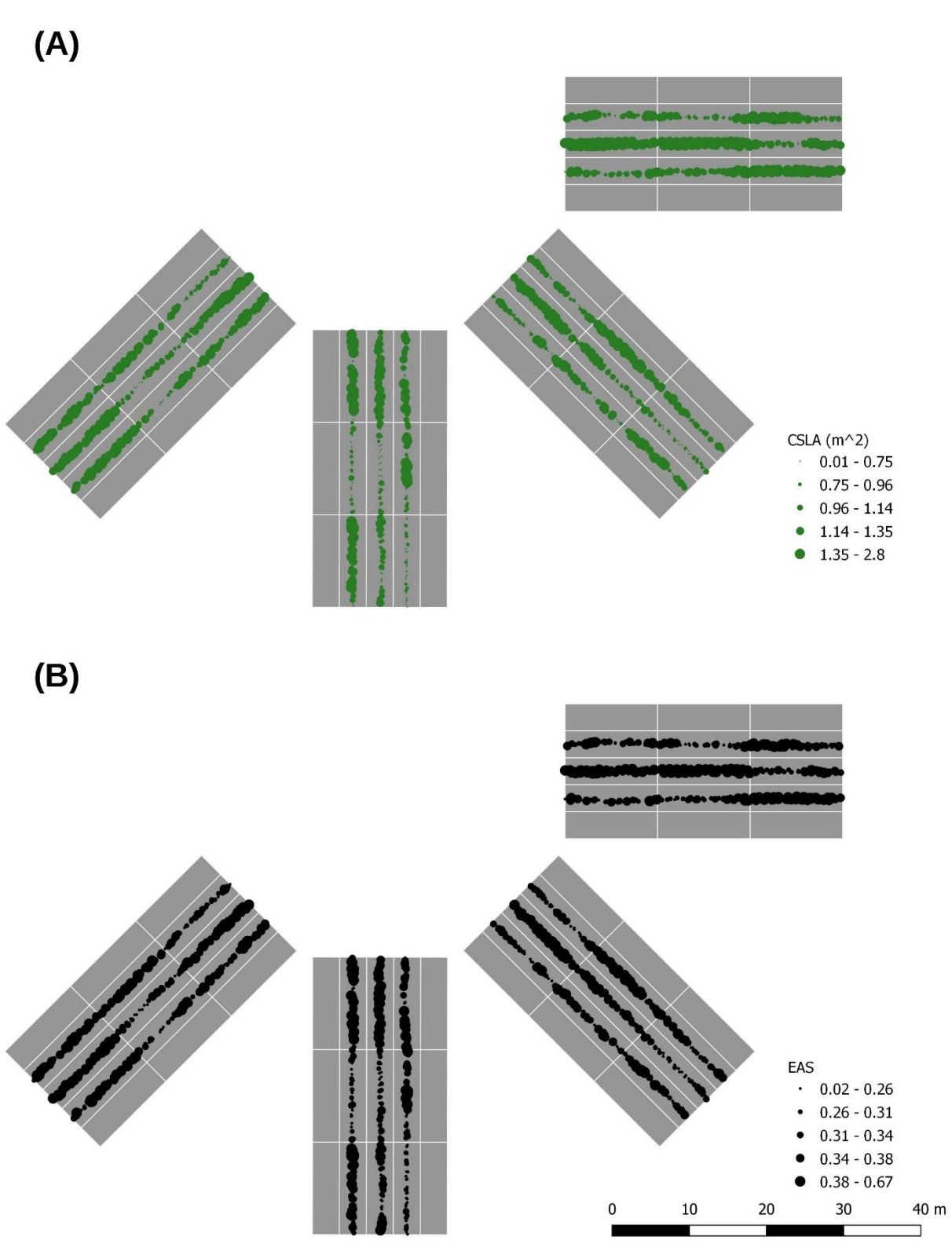

Figure 8. Heatmaps of (A) cross-sectional leaf area (CSLA) and (B) effective area of shade (EAS) predicted using the model in Figure 7 in the 36 experimental measurement plots of 'ANABP-01' apples. Data collected in March 2022.

Orchard summary

The orchard results collected in the month before harvest are summarised in Table 2. The coefficients of variation (CV) can be used to assess spatial variability and provide useful insights to growers to use objective "tolerated" thresholds of variability that orchard management should achieve every season in order to maximise profit.

Table 2. Average crop parameters and coefficients of variation (CV) obtained using Green Atlas *Cartographer* in the last month before harvest during season 2021 – 22.

Crop parameter	Mean	CV (%)
Flower clusters (n / tree)	83	24
Fruit number (n / tree)	71	34
Canopy height (m)	3.04	7
Canopy area (m^2)	1.78	24
Canopy density (0 – 1)	0.59	20
Cross-sectional leaf area (m^2)	1.09	37
Effective area of shade (0 – 1)	0.33	23

Effects of light interception on flower number, crop load and yield

In contrast to 2020 – 21, the EAS measured in 2021 – 22 did not have a significant effect ($p > 0.05$) on flower cluster number and fruit number. Nevertheless, a significant effect of EAS was observed on yield ($p = 0.018$), although this relationship was significantly affected by row orientation. No rootstock effect on the relationship was observed. The overall relationship was absent for E – W (Figure 9A) noisy for NW – SE (Figure 9B) and NE – SW (Figure 9D), and very good for N – S (Figure 9 B).

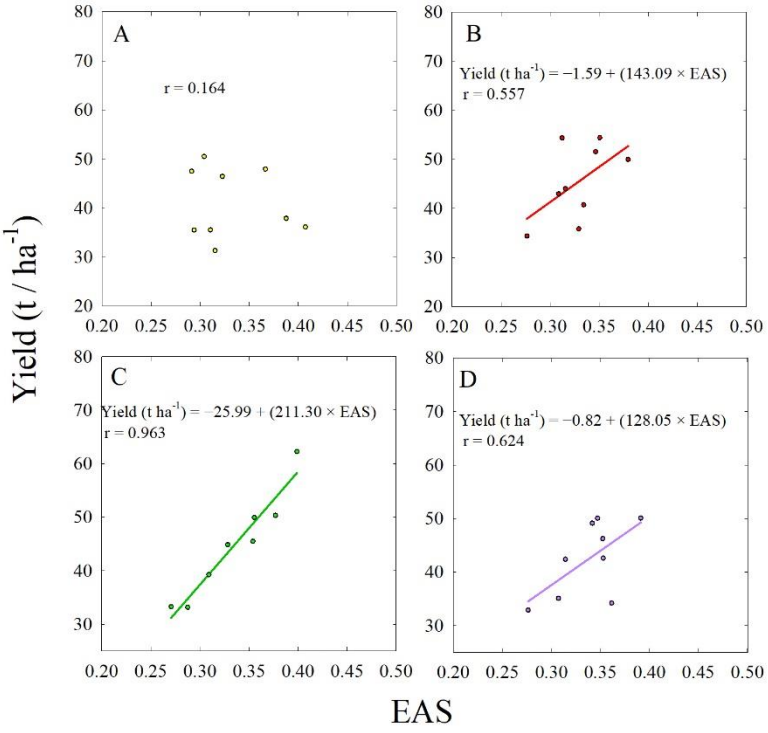

Figure 9. Correlation coefficients (Pearson's r), scatterplots and linear fits of the relationships between yield and effective area of shade in four row orientations (A: E –W; B: NW – SE; C: N – S; D: NE – SW).

Yield efficiency

Yield efficiency was expressed in terms of kg m^{-2} of CSLA, and the effects of rootstock and row orientation were tested using EAS as covariate in an analysis of covariance (ANCOVA). Both rootstock and row orientation significantly affected yield efficiency per unit of CSLA (Table 3) and EAS was correlated with CSLA as previously seen in Figure 6. No interaction between rootstock and row orientation was observed ($p > 0.05$). M9 trees showed the highest yield efficiency, in line with 2020 – 21 observations. Trees oriented N – S also yielded more efficiently compared to E – W (the least efficient) and NE – SW.

Table 3. Results of an analysis of covariance (ANCOVA) that tested the effects of rootstock and row orientation on yield efficiency per unit of cross-sectional leaf area (CSLA) using effective area of shade (EAS) as covariate. Means and standard errors (in brackets), ANCOVA's p-values and effect sizes (η^2) are reported. Different letters show significant differences based on Tukey's post hoc test ($p < 0.05$).

Factor	Level	Yield efficiency (kg m^{-2} CSLA)
Rootstock	B9	13.1 (0.7) b
	M26	13.9 (0.6) b
	M9	16.5 (0.6) a
	p-value	0.003
	η^2	0.189
Row orientation	E – W	12.0 (0.7) c
	NE – SW	13.7 (0.7) bc
	N – S	16.8 (0.7) a
	NW – SE	15.5 (0.7) ab
	p-value	< 0.001
	η^2	0.345
EAS (covariate)	p-value	0.002
	η^2	0.158

DISCUSSION

Overall, this study carried out calibrations and validations of the predictions of important crop parameters in 'ANABP-01' apple using the Green Atlas mobile platform (i.e., *Cartographer*).

The association between *Cartographer* predictions of flower cluster numbers and observations was very tight and produced small errors (Figure 2). Uncalibrated orchard maps can be produced to display areas or rows in the block where flower clusters are denser than others, to support precise chemical or mechanical thinning, such as in the case of the use of variable rate sprayers. A first calibration step is needed if actual flower cluster numbers are to be determined. Green Atlas provides calibrated or uncalibrated heatmaps to growers as part of their commercial service.

The crop load calibration had an error < 2% (Figure 5), improving the model accuracy from 2020 – 21. Yield estimates had good accuracy and the error was < 2% (an underestimation of less than 1 t ha^{-1}). Block estimates of yield were considered very accurate and similar to 2020 – 21, when an error of 1.2% was recorded.

Yield estimates presented in this study represent an improvement of our first attempt to estimate this parameter in apples. In 2020-21, we used average fruit size obtained in small, hand-picked fruit samples, whereas in 2021 – 22 the fruit weight calculated from *Cartographer* estimates of fruit diameter was used. Green Atlas is meanwhile working on improving and maximising accuracy and variability of fruit size prediction to further reduce the yield estimate error.

Using the methodology presented in this study, yield could be predicted with relatively low error any time after fruit thinning or natural fruit drop, although an estimate of harvest fruit weight is needed when yield predictions are made early in the growing season. Early predictions represent valuable informative tools to project revenues and support decision management in the logistics and post-harvest handling of the crop. Like for flowers, calibration of the crop load is only needed if absolute crop load and yield estimates are needed. In some circumstances, a simple crop load density map of the orchard may support thinning management decision (e.g., management of labour for thinning operations).

Tree height estimates needed a preliminary calibration for the ground height (Figure 10). After calibration, tree height estimates were considered accurate and in line with ground observations (Figure 10 B).

Tree geometry parameters generated by the LiDAR on the *Cartographer* were related to light interception measurements. Specifically, CSLA was confirmed (like in 2020 – 21) to be the most stable single predictor of EAS (Figure 5). However, a combination of canopy density, canopy height, row spacing and canopy width appeared to be provide the most accurate modelling of EAS (Equation 1, Figure 7). Georeferenced orchard heatmaps of canopy geometry (e.g., Figure 8) can support precise and targeted management of pruning, fertilisation and replanting. Trees in N – S rows showed the best efficiency of intercepted light per unit of foliage (CSLA, m^2, Figure 6, Table 1) and this finding substantiates the common approach from growers to plant trees in this row direction. Not only were trees in N – S more efficient in the way they use light per unit of canopy, but they also had higher yield efficiency (Table 3) compared to E – W and NE – SW. However, N – S row orientations may expose fruit to higher solar radiation that can increase sunburn. Thus, row orientation effects on fruit quality are currently being tested and will be clear after 3 years of data. E – W appeared to have the lowest efficiency (Figure 6 and Table 3). Among the rootstocks, M9 had the highest yield efficiency (Table 3).

Overall, yield was positively affected by increasing light interception, although more specifically N – S trees had the strongest relationship and E – W had no significant relationship between EAS and yield (Figure 9). The overall yield vs light interception relationship was in line with previous findings on 'Empire' (Robinson and Lakso, 1989; Wünsche et al. 1996) and 'Elstar' (Wagenmakers and Callesen, 1995). Relationships of flower clusters, crop load and yield with EAS need to be investigated at EAS > 0.5 to determine the optimal level of light intercepted to achieve the highest productivity.

CONCLUSION

In summary, this study validated the utilisation of a mobile platform for the prediction of several crop parameters in 'ANABP-01' apples. Combining predictions of several important parameters in one single platform opens the door to various possible uses of this technology. With the current push of Ag Tech into business models in the apple industry, and in other fruit industries, the availability of technology that serves multiple purposes is of pivotal importance to reduce substantial production costs such as labour and to ease growers' technology uptake in their business models and investment plans. The amount of data generated by platforms such as the Green Atlas *Cartographer* is large and can be complex to manage for unskilled workers. Currently, dedicated technical staff are needed to extract the most useful information for individual needs of growers.

RECOMMENDATIONS

We recommend using Green Atlas *Cartographer* to advise growers about flower number, fruit number, yield, canopy geometry and light interception. Relative maps can be generated quickly after scanning the orchard blocks, whereas maps with absolute numbers need additional calibration that may present some difficulties based on the experience of the staff employed to complete the task. Calibration results may be affected from both sensors' reduced precision and human errors. Typically, there is a loss of reliability in larger 3D canopy systems, whereas calibrated predictions of flower and fruit numbers in 2D systems consistently have errors below 10%, and often below 5%.

Growers should aim to obtain optimal fruit number and yield while minimising their variability in the block. The relationships developed in this project may be used to derive values of canopy geometry or EAS that improve yield and fruit quality. The maps generated by the *Cartographer* can be used to identify areas within a block that need additional management inputs (e.g., follow-up thinning) to produce high yields of quality fruit. In addition, packout yield can be forecast, irrigation requirements can be determined, and orchard automation and mechanisation can be better implemented using the *Cartographer* data. This data has great potential to be reutilised in other machines for spatially precise orchard operations (e.g., variable rate spraying, mechanical thinners, mechanical hedgers).

The next steps in this project is to improve the automation and accuracy of fruit diameter and fruit colour estimates, and to establish orchard specific relationships between tree size, fruit number, fruit size and fruit colour.

Future projects should focus on integrating spatial maps into automated systems (e.g., variable rate spraying to match spray application to canopy geometry, flower density, tree vigour control) and to convert map overlays into objective management (e.g., targeted crop load per tree to maximise profitability). Furthermore, the integration of additional sensors on *Cartographer* would improve the amount of georeferenced information of the orchard. For example, future research could focus on the integration of thermal sensors to detect canopy temperature, an important indicator of tree water status.

ACKNOWLEDGEMENTS

This technical report is part of the apple and pear industry's PIPS3 (Productivity, Irrigation, Pests and Soils) program of research and development. The project is funded by Hort Innovation, using the Hort Innovation Apple and Pear research and development levy, contributions from the Australian Government and co-investment from Agriculture Victoria. Hort Innovation is the grower-owned, not-for-profit research and development corporation for Australian horticulture.

REFERENCES

Bargoti, S., Underwood, J., 2017a. Deep fruit detection in orchards, in: Proceedings - IEEE International Conference on Robotics and Automation. Institute of Electrical and Electronics Engineers Inc., pp. 3626–3633. https://doi.org/10.1109/ICRA.2017.7989417

Bargoti, S., Underwood, J.P., 2017b. Image Segmentation for Fruit Detection and Yield Estimation in Apple Orchards. J. F. Robot. 34, 1039–1060. https://doi.org/10.1002/rob.21699

Bresilla, K., Perulli, G.D., Boini, A., Morandi, B., Corelli Grappadelli, L., Manfrini, L., 2019. Single-shot convolution neural networks for real-time fruit detection within the tree. Front. Plant Sci. 10, 611. https://doi.org/10.3389/fpls.2019.00611

Cripps, J.E., 2016. Apple tree named 'ANABP 01.' USPP27420P3.

Darbyshire, R., Goodwin, I., McClymont, L., Turpin, S., 2018. Addressing heat stress in pome fruit, in: Hermesch, S., Dominik, S. (Eds.), Breeding Focus 2018 - Reducing Heat Stress. Animal Genetics and Breeding Unit, University of New England, Armidale, NSW, Australia, pp. 81–97.

Dias, P.A., Tabb, A., Medeiros, H., 2018a. Multispecies Fruit Flower Detection Using a Refined Semantic Segmentation Network. IEEE Robot. Autom. Lett. 3, 3003–3010. https://doi.org/10.1109/LRA.2018.2849498

Dias, P.A., Tabb, A., Medeiros, H., 2018b. Apple flower detection using deep convolutional networks. Comput. Ind. 99, 17–28. https://doi.org/10.1016/j.compind.2018.03.010

Kang, H., Chen, C., 2020. Fast implementation of real-time fruit detection in apple orchards using deep learning. Comput. Electron. Agric. 168, 105108. https://doi.org/10.1016/j.compag.2019.105108

Kuznetsova, A., Maleva, T., Soloviev, V., 2020. Using YOLOv3 Algorithm with Pre- and Post-Processing for Apple Detection in Fruit-Harvesting Robot. Agronomy 10, 1016. https://doi.org/10.3390/agronomy10071016

Örn, S., 2016. Estimating Light Interception of Orchard Trees Using LiDAR and Solar Models. Master of Science Thesis, Linköping University.

Robinson, T. L. and Lakso, A.N. (1989). Light interception, yield and fruit quality of 'Empire' and 'Delicious' apple trees grown in four orchard systems. Acta Hortic. 243, 175-184. https://doi.org/10.17660/ActaHortic.1989.243.21

Scalisi, A., McClymont, L., Underwood, J., Morton, P., Scheding, S., & Goodwin, I. (2021). Reliability of a commercial platform for estimating flower cluster and fruit number, yield, tree geometry and light interception in apple trees under different rootstocks and row orientations. *Computers and Electronics in Agriculture*, *191*, 106519. https://doi.org/10.1016/j.compag.2021.106519

Underwood, J.P., Jagbrant, G., Nieto, J.I., Sukkarieh, S., 2015. Lidar-Based Tree Recognition and Platform Localization in Orchards. J. F. Robot. 32, 1056–1074. https://doi.org/10.1002/rob.21607

Underwood, J.P., Hung, C., Whelan, B., Sukkarieh, S., 2016. Mapping almond orchard canopy volume, flowers, fruit and yield using lidar and vision sensors. Comput. Electron. Agric. 130, 83–96. https://doi.org/10.1016/j.compag.2016.09.014

Wagenmakers, P. S., & Callesen, O. (1995). Light distribution in apple orchard systems in relation to production and fruit quality. Journal of Horticultural Science, 70(6), 935-948. https://doi.org/10.1080/14620316.1995.11515369

Wang, Z., Underwood, J., Walsh, K.B., 2018. Machine vision assessment of mango orchard flowering. Comput. Electron. Agric. 151, 501–511. https://doi.org/10.1016/j.compag.2018.06.040

Westling, F., Underwood, J., Örn, S., 2018. Light interception modelling using unstructured LiDAR data in avocado orchards. Comput. Electron. Agric. 153, 177–187. https://doi.org/10.1016/j.compag.2018.08.020

Wünsche, J. N., Lakso, A. N., Robinson, T. L., Lenz, F., & Denning, S. S. (1996). The bases of productivity in apple production systems: the role of light interception by different shoot types. Journal of the American Society for Horticultural Science, 121(5), 886-893. https://doi.org/10.21273/JASHS.121.5.886

Advancing sustainable and technology driven apple orchard production systems

Technical Report: Estimates of fruit number, size, colour, yield, and tree size using Green Atlas *Cartographer* and relationships with light interception in 'ANABP 01' apples

Agriculture Victoria Research

November 2022

VICTORIA State Government | Jobs, Precincts and Regions

AGRICULTURE VICTORIA

Authors: Alessio Scalisi, Maddy Peavey and Ian Goodwin

Project RDC Number: AP19003

Project RCM Number: 6472

Department of Jobs, Precincts and Regions
1 Spring Street Melbourne Victoria 3000
Telephone (03) 9651 9999

Contents

EXECUTIVE SUMMARY

Modern horticulture is moving towards increased mechanisation, automation, robotics, and non-destructive sensing and monitoring. This report describes the steps taken to validate fruit diameter and fruit colour estimates obtained with a commercial platform (Green Atlas *Cartographer*) in the Sundial Orchard at the Tatura SmartFarm planted with young 'ANABP 01' apple trees.

The study evaluated relationships between ground truth and Green Atlas *Cartographer* predictions of fruit number, size (diameter and mass), colour and yield and canopy geometry (namely, canopy height, density, area and cross-sectional leaf area) as an informative tool for apple growers. The effects of rootstock, row orientation and season on crop parameters and their relationship with the amount of radiation intercepted by canopies was investigated. The accuracy of fruit diameter and colour development index (CDI) estimates were high (> 95, and > 80% precision and accuracy). Yield prediction errors were < 3%.

Rootstock and row orientation affected tree size and geometry and the implications are discussed. An additional season of data is needed to confirm the preliminary findings.

Overall, *Cartographer* demonstrated to be a valid tool to combine new predictions of fruit diameter, CDI and yield with previously validated predictions of other significant crop parameters (e.g., cross-sectional leaf area, flower number, fruit number) using a single platform. The consistency of prediction errors over the two seasons under study suggests that the platform is reliable and its measurements are repeatable. Orchard-specific relationships between crop parameters generated by *Cartographer* across different seasons are currently under investigation. We confirm that the use of Green Atlas *Cartographer* can be beneficial for both growers and scientists to collect large amount of data and replace labour-intensive operations.

INTRODUCTION

This technical report is a deliverable for milestone 106 of the project 'Advancing sustainable and technology driven apple orchard production systems' (AP19003). The report details a study on the testing and calibration of the Green Atlas *Cartographer* (i.e., a mobile platform with multiple sensors) for estimates of fruit number, diameter, colour and yield, and the relationship of Cartographer's canopy geometry estimates to light interception in 'ANABP 01' apples. This report contributes towards meeting the project objectives by providing scientifically sound validations of mobile platform predictions of fruit number, size, colour and yield to achieve premium fruit for domestic and export markets. The results presented in this report reflect a joint effort of Agriculture Victoria and Green Atlas staff and benefited from the valuable support of Plunkett Orchards' staff.

Project outcome

The intended outcome of this project is to improve crop load management in a variable climate by providing knowledge and tools to deliver premium fruit that meets consumer expectations in domestic and export markets.

Project background

In Australia, apple production is yet to reach its full potential based on the area planted (10,000 ha) and the theoretical yield (~ 800,000 t). This is mostly due to variable crop load management, biennial bearing and inconsistent fruit quality. Australia has a unique climate characterised by relatively high temperatures and light intensity compared to other apple production areas around the world (Darbyshire et al., 2018). Light interception and carbohydrate availability play an important role not only in defining the optimal crop load to maximise consistent fruit quality for the life of the tree, but also in floral initiation and biennial bearing. While high light intensity generally leads to increasing photosynthetic rates and consequently carbohydrate availability, when excessive and/or combined with high air temperature can cause sunburn, photoinhibition (i.e., damage the leaf photosynthetic apparatus) or induce stomata closure for long periods during the day, reducing water loss but generating undesired reductions in photoassimilates. Therefore, an optimal regulation of the light harvested by tree canopies by canopy architecture, rootstock selection and planting design is paramount to minimise external inputs (e.g., water, thinning chemicals, reflective mulches, biostimulants) and maintain or even improve fruit quality characteristics such as skin colouration and fruit size.

Modern horticulture is moving toward increased mechanisation, automation, robotics, and non-destructive sensing and monitoring. The integration of technologies that are already adopted in other industries into horticulture systems aims to increase resource use efficiency — including labour — and make orchards more profitable. For this purpose, several recent studies have focused on the application of machine learning algorithms to detect tree structures (e.g., flowers, fruit, architecture) using sensorised robots or platforms. Most of the state-of-the-art research has attempted to detect apple fruit for crop load or yield determination, or for integration with automated harvesting machines using image segmentation, deep learning and different Convolutional Neural Networks (CNN) (Bargoti and Underwood, 2017a, 2017b; Bresilla et al., 2019; Kang and Chen, 2020; Kuznetsova et al., 2020) on images typically collected by RGB / RGB-D cameras. Underwood et al. (2016), Dias et al. (2018a, 2018b) and Wang et al. (2018) used similar machine vision approaches for almond, apple and mango flower recognition, respectively. In the case of almond, the machine image recognition was supported by LiDAR cloud points to reconstruct tree structure and assign tree geo-references when combined with GPS (Underwood et al., 2016). LiDAR sensors are a powerful tool to quickly determine canopy architecture parameters such as tree height, canopy size and density and have the potential to recognise tree location, alone or combined with GPS (Underwood et al., 2015). LiDAR cloud points have also been used to model light interception, as demonstrated by Örn (2016). The same idea was applied to estimate a solar-geometric model for light interception estimation in avocado trees (Westling et al., 2018).

Commercial services such as the Green Atlas Cartographer use a combination of sensors (e.g., RGB cameras, LiDAR, GPS, thermal sensors), mounted on a platform on an electric vehicle, to gather data while driving through orchard rows. The Cartographer is currently available to measure the spatial distribution of crop load in apples and to measure tree geometry parameters such as canopy area, canopy density and cross-sectional leaf area (CSLA). Canopy area (m2) represents the area of the polygon drawn around the LiDAR-generated points in the scanned transect, excluding the trunk. Canopy density represents the ratio between the number of light beams generated by the LiDAR that bounces back to the light source and the total number of emitted light beams. CSLA is the area of the points (comparable to leaves) within the canopy area polygon. The Green Atlas Cartographer is rapidly expanding its capability and aims to achieve good predictions of flower cluster number and fruit size and colour.

The results of the first year of study in the Sundial orchard are published in the high-impact factor, peer-reviewed journal Computers and Electronics in Agriculture (Scalisi et al., 2021b).

In situ fruit size estimation is paramount for determining accurate yield, forecast fruit growth and for the application of robotic harvesting. Nevertheless, to our knowledge only a few studies have investigated fruit size estimations using different machine vision systems (e.g., RGB cameras, 3D photonic mixing device cameras, thermal cameras) and artificial intelligence on aerial or ground-based platforms (Stanjko et al., 2004; Regunathan and Lee, 2005; Cheng et al., 2017; Wang et al., 2017; Gongal et al., 2018; Apolo-Apolo et al., 2020). Wang et al. (2017) recently presented good accuracy of mango fruit size estimates with low prediction errors (< 5 mm), although the authors stated that the cost-effective RGB-D cameras used in their study cannot be used under direct sunshine conditions.

Typically, fruit colour is assessed after harvest using cameras mounted in fruit grading machinery. However, orchard estimates of fruit colour can be linked to fruit maturity in some cultivars and can drive orchard management strategies to improve skin colour formation in situ, such as leaf removal, use of reflective mulch or the application of biostimulants to enhance anthocyanin pigmentation. Fruit colour estimation using non-contact sensors such as RGB or RGB-D cameras mounted on aerial and ground vehicles is difficult as it is influenced by the variable orchard light environment due to the combined effects of clouds, sun angle, netting, etc. Green Atlas *Cartographer* mounts strobe lights that continuously flash tree canopies to attenuate any potential effect of external light on colour readings by the RGB cameras.

Some of the colour parameters in the CieLAB colour space have been associated with maturity in fruit. Previous studies reported significant associations between hue angle (h°) and maturity in stone fruits (Robertson et al., 1990; Ferrer et al., 2005; Scalisi et al., 2020; 2021a). Similarly, Greer (1990) found that h° of both overcolour and background colour had a defined decreasing pattern throughout the growing season in 'Braeburn' and 'Royal Gala' apples. Using *Cartographer* proximal sensors to predict colour parameters such as h° is crucial to investigate the opportunity of fast orchard scanning for fruit colour estimations. However, an attempt to simplify the concept of h°, its interpretation and its association with maturity needs to be taken on board in order to support the broader application and use of h° as a reference parameter for colour development. Another more intuitive skin colour parameter was derived from hue angle — the colour attribute more often associated with fruit maturity and redness development (Scalisi et al., 2021a). This Colour Development Index (CDI) is expressed using a scale from 0 to 1 and represents the departure from greenness (0) around the CieLAB colour wheel, with pure red being the most distant point (1), regardless of using the bottom or the top half of the colour wheel to measure the distance from greenness (Scalisi et al., 2022; Islam et al., 2022). In other words, given that most fruit at an immature stage have greener skins as characterised by chlorophyll concentration, CDI standardises the loss of chlorophyll in any direction (i.e., departing towards blueness-redness or towards yellowness-redness). CDI is strictly correlated to hue angle but the adoption of the former has some advantages over the latter: (a) its interpretation for end-users without prior knowledge of the CieLAB / LCh colour space is much improved as its range is between 0 and 1 and it is directly related to redness development, as opposed to h° (inversely related to redness); (b) its use allows more robust colour development predictions in fruit that turn purple when ripe such as dark plums (Islam et al., 2022); (c) based on cultivar-specific fruit colour development characteristics, the 0 and 1 points can be dynamically rotated around the CieLAB colour wheel to reflect the actual colour development characteristic of the fruit.

Project objectives

The overall goal of this project was to investigate crop productivity and performance and develop management tools so that apple orchards can consistently produce high yields and fruit that meet market specifications through climate change and extreme heat events. The work presented in this report aimed to develop a rapid orchard assessment tool using proximal sensing technologies to determine fruit number, fruit size, fruit colour, yield and canopy geometry. Specifically, this work aimed to: (i) evaluate relationships between Green Atlas *Cartographer* estimates of fruit number, size and colour and tree geometry in a young multidirectional apple orchard over two seasons; and (ii) determine relationships between fruit number, size, colour, yield, canopy geometry and the amount of radiation intercepted by canopies.

METHOD

Experimental sites and apple cultivars

The study was conducted in the Sundial orchard at the Tatura SmartFarm, Victoria, Australia during 2020–21 and 2020–21. The Sundial Orchard is a high-density (~ 2857 trees / ha) circular orchard of approximately 1.3 ha. 'ANABP 01' apple trees were planted in a semicircle of the orchard following four different row orientations (i.e., northeast to southwest, north to south, northwest to southeast and east to west, henceforth referred to as NE–SW, N–S, SE–NW and E–W). Trees were grafted onto three different rootstocks — Bud.9, M.9 (T337) and M.26 — in a completely randomised design and planted in 2018 (**Figure 1**). 'ANABP 01' trees are trained to spindles on vertical trellises at 1 m spacing. The row spacing is 3.5 m and there is a total of twenty rows, five rows per row orientation, and 60 experimental plots. Each experimental plot is composed of eleven 'ANABP 01' trees and one polliniser ('Granny Smith'). The experiment was conducted on trees at their 3rd and 4th leaf.

'ANABP 01' originated from a cross-pollination between 'Cripps Red' and 'Royal Gala'. The cultivar was bred by the Department of Agriculture and Food, State of Western Australia. Fruit has dark purple colouration and consistent cropping characteristics (Cripps, 2016).

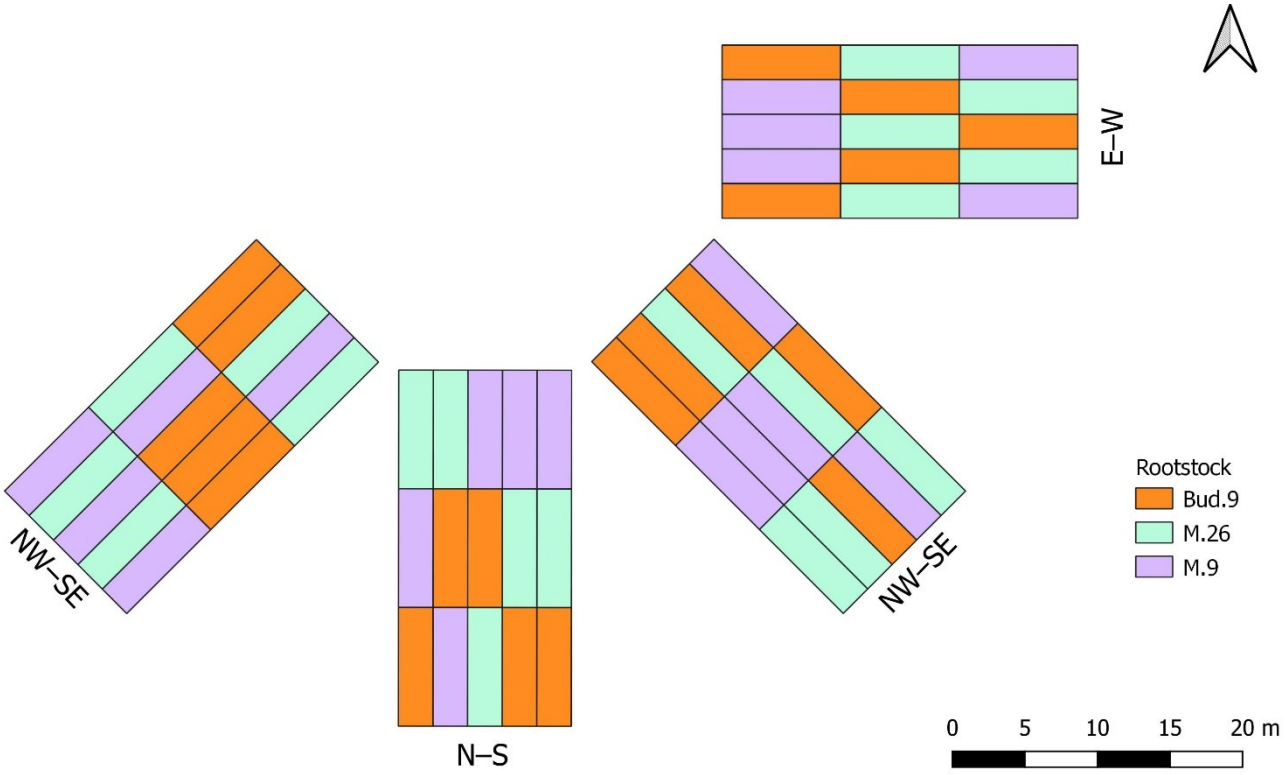

Figure 1. Layout of the sixty experimental plots of 'ANABP 01' in the Sundial orchard at the Tatura SmartFarm. Row orientations: northeast to southwest (NE–SW), north to south (N–S), northwest to southeast (NW–SE) and east to west (E–W). Each plot contains eleven 'ANABP 01' trees.

Orchard scans with *Cartographer*

Orchard scans were undertaken with Green Atlas *Cartographer*. A phone-interface was used to control logging and enter file notes to aid retrospective identification of scan locations and note relevant scan or plot issues. *Cartographer* was driven at a constant speed of approximately 10 km/h. Logging was switched on a few metres prior to the start of the measurement section and off a few metres past the end of the measurement section.

Continuous mobile scans were collected in the entire orchard block in 2020–21 and 2021–22. Data were extracted from measurement plots and data from the buffer plots (i.e., guard rows) were discarded (**Figure 2**). Data at a plot level were extracted by intersecting the points generated by the *Cartographer* with plot polygons generated with QGIS (v. 3.16, QGIS Development Team, Open-Source Geospatial Foundation, 2021). The geographic precision of plot extraction was

improved by real-time kinematic (RTK) positioning adjustments and was cross-checked on the position of posts — to mark the beginning and end of a plot — in the RGB images collected by *Cartographer*.

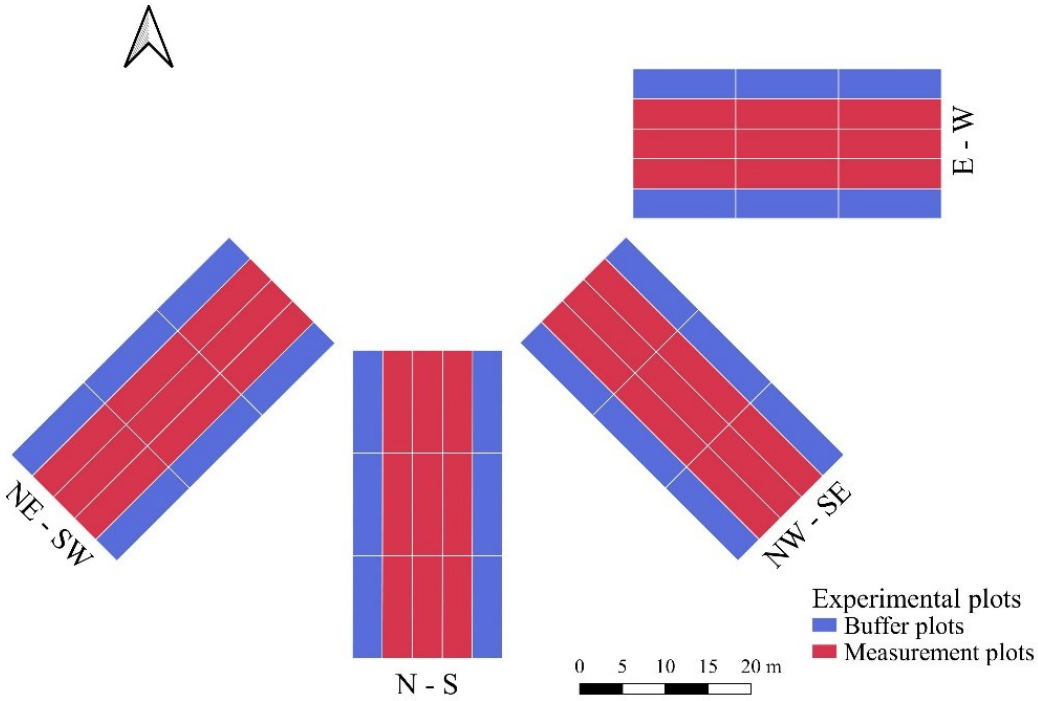

Figure 2. Layout of the 60 experimental plots (36 measurement plots) of 'ANABP-01' in the Sundial orchard at the Tatura SmartFarm. Row orientations: northeast–southwest (NE–SW), north–south (N–S), northwest–southeast (NW–SE) and east–west (E–W).

Fruit size (diameter and mass) and CDI

In 2020–21, three fruit were tagged on each central tree of 36 experimental plots, with one fruit per height zone ('Low' < 1.1 m, 'Middle' 1.1–2.1 m and 'High' > 2.1 m) in an approximately vertical line (± 25 cm horizontally) (i.e., 108 fruit). Fruit diameter (FD, mm) and fruit colour were measured at three times during the season (26 November 2020, 21 January 2021 and 15 March 2021) to increase the variability of the measures. A Bluetooth calliper (OriginCal, iGAGING, San Clemente, California, USA) was used to measure FD in tagged fruit by holding the instrument parallel to the row direction and on the same day of orchard scans. Fruit mass (FM, g) was calculated based on its exponential relationship with fruit equatorial diameter (FD) determined from data collected during the growing season (Scalisi et al., 2021b, i.e., $FM = 0.0003 \times FD^{3.04}$, S.E. = 21 g).

The ground truth colour of tagged fruit was measured with a portable tristimulus colourimeter with D50 illuminant and a 2°observer angle (Instrument & Data Tools, Rowville, Victoria, Australia), coincident with orchard scans. The instrument generated values in the CieLAB / CieLCH colour scale, and CDI was derived from hue angle values as shown by Scalisi et al. (2022).

Cartographer stationary scans were collected at the three stages in which ground truth FD and CDI data were obtained. Mobile scans in the Sundial orchard were obtained at the end of each measurement session. Fruit size and colour data corresponding to the tagged fruit was extracted from stationary images based on the longest diameter of the detection box and its 5 × 5 central pixels, respectively. Fruit diameter and colour extractions were only carried out on fruit that were completely visible from the cameras, with no leaves or other obstacles that might have affected correct measurements (n = 53). The dataset used for fruit diameter was further filtered by the uncertainty of the estimate and the final sample was 16 fruits.

Fruit number

Fruit was manually counted in plots to obtain ground truth measures per tree. Linear regression models of detected fruit counts per image against the manual counts were used to determine calibration factors to correct fruit number (FN) predictions in 2020–21 and 2021–22. The robustness of the calibrated model of FN was validated against a dataset of counts per plot obtained with a commercial grader (Compac InVision 9000, Compac Sorting Equipment Ltd, Australia) at harvest on 36 experimental plots.

Yield estimates

Cartographer predictions of yield per tree (YI) were obtained by multiplying fruit number by average FM per rootstock. Yield predictions were validated against the yield obtained with the commercial grader at harvest on 36 experimental plots in both seasons.

Canopy geometry and radiation interception

Green Atlas *Cartographer* was used to extract the following canopy geometry parameters: (i) canopy height (CH), (ii) canopy area (CA), (iii) canopy density (CD), and cross-sectional leaf area (CSLA). For a full explanation of how these indices are calculated see Scalisi et al. (2021b).

Canopy radiation interception was expressed in terms of effective area of shade (EAS, Goodwin et al., 2006) — the mean of fractional photosynthetically active radiation (PAR) interception over the tree planting square (tree x row spacing) measured at three times (solar noon, solar noon − 3.5 h and solar noon + 3.5 h) on a clear sky day. PAR was measured using a light trolley (Tranzflo, Palmerston North, New Zealand). The light trolley consisted of 24 PAR sensors at 0.125 m intervals along a 3 m bar, 0.4 m above ground level on a wheeled base. An on-board data logger (CR850, Campbell Scientific, Garbutt, Au) recorded measurements at 1 s intervals. Measurements of transmitted PAR (PARt) were made over the planting square of the central trees in each plot. The light trolley sensors were held horizontally below the canopy, perpendicular to the row direction, and moved at a slow walking speed. Unobstructed incoming PAR (PARi) was measured at 1.5 m above ground level in an open area. Measurements were carried out a month prior to harvest in both seasons.

Relationships between crop parameters, tree geometry and EAS, and effects of rootstock, row orientation and season

FN, FD, FM, CDI, YI, CH, CA, CD, and CSLA obtained with *Cartographer* were related to EAS in the two seasons and the overall effects of rootstock, row orientation, season and their interaction were analysed.

Statistical analysis

Ordinary Least Squares (OLS) linear regression procedures were carried out to determine the relationships between predicted and observed fruit diameter and fruit colour attributes. Model prediction errors were based on the root mean square errors (RMSE) or on the percent standard errors of the linear regressions. The reliability of predictions was assessed using the Lin's concordance correlation coefficient (r_c), a measure of both precision and accuracy that provides a value from 0 (no concordance) to 1 (perfect concordance) that assess the divergence of predicted data from the line of perfect concordance with observations (i.e., the line at 45 degrees on a square scatter plot, where y = x) (Lin, 1989).

The relationships between crop parameters were estimated using correlation analysis and assessed with the Spearman's rank correlation coefficient (r_s). The effects of row orientation, rootstock and season were tested using a three-way analysis of variance (ANOVA), significant differences ($p < 0.05$) were separated by Tukey's pairwise comparisons.

Regression analyses and the calculation of Lin's concordance correlation coefficient (r_c) were carried out using R (v. 4.0.2, R Core Team, 2021) and its packages "Userfriendliscience" (Peters, 2018) and "DescTools" (Signorell, 2021). Graphs were generated using SigmaPlot 12.5 (Systat software Inc., Chicago, IL, USA) and the JASP suite for Windows 10 (v. 0.15, Jasp Team, 2021).

RESULTS

FD and CDI

Stationary FD estimations with *Cartographer* were tightly associated with ground truth measurements (**Figure 3**). The RMSE was 2.5 mm and an r_c of 0.987 highlighted an optimal precision and accuracy of the prediction without further calibration. When tested on a validation dataset generated from mobile scans, the prediction had an almost identical accuracy to the stationary prediction — as suggested by the overlapping of the two lines in **Figure 3** — and observations did not significantly diverge from the line of perfect fit. Consequently, *Cartographer* predictions of fruit diameter did not need further calibration to be accurate in 'ANABP 01'.

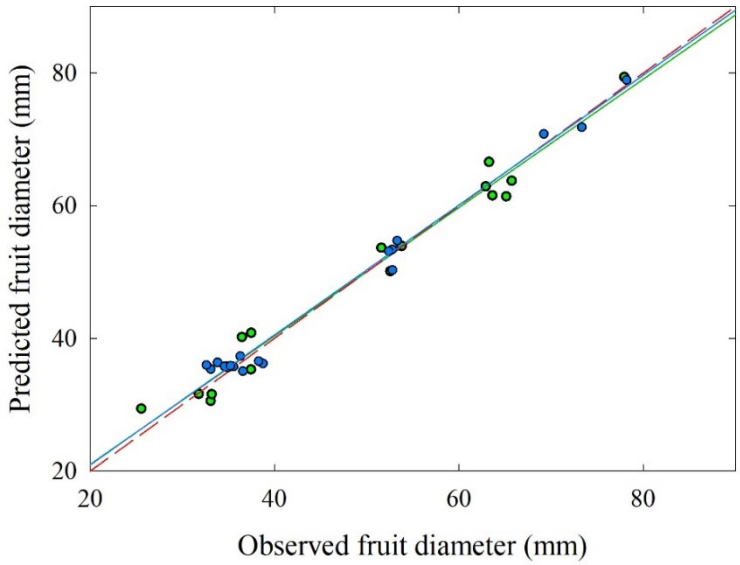

Figure 3. Predicted fruit diameter against observed fruit diameter in 16 fruits measured with stationary *Cartographer* (green points) and in 19 fruits measured with mobile *Cartographer* (blue points). Green line: linear regression fit for validation of stationary predictions; blue line: linear regression fit for validation of mobile predictions; red dashed line: perfect fit (y = x). The validation datasets included 'ANABP 01'. Stationary prediction model [y = 1.64 (2.19) + 0.97 (0.04) x; r_c = 0.987; RMSE = 2.5 mm]; mobile prediction model [y = 1.36 (1.28) + 0.98 (0.03) x; r_c = 0.993; RMSE = 1.7 mm].

The relationship between CDI predicted with stationary *Cartographer* and observed CDI measured with the portable colourimeter is shown in **Figure 4**. CDI predictions were accurate as predicted and observed values had good concordance (r_c > 0.80). Some noise was observed likely due to the different surfaces in which colour was measured — the portable colourimeter was used to measure colour in a single spot, whereas *Cartographer* colour measurements were calculated over a number of central pixels in the detection box drawn around the fruit.

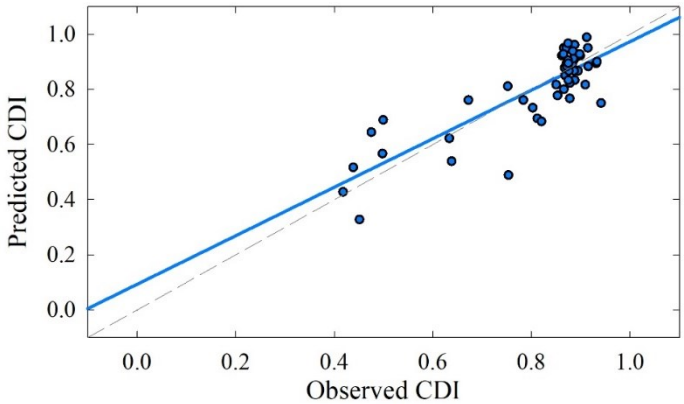

Figure 4. Predicted against observed fruit colour development index (CDI) in 53 'ANABP 01' apple fruit. Blue line: linear regression fit; grey dashed line: line of perfect fit (y = x). Linear regression model: y = 0.0929 (0.0658) + 0.880 (0.0797) x; R^2 = 0.705; r_c = 0.837; *RMSE* = 0.08.

Fruit number and yield

In 2020–21, the relationship between fruit detections per image and FN per tree yielded a RMSE = 10 fruit/image (Scalisi et al., 2021). In 2021–22, the same RMSE was obtained (**Figure 5**). The map of the calibrated FN per tree in 2021–22 (**Figure 5**) shows the position of pollenisers (white colour, no fruit) that were harvested a week prior to scanning the orchard.

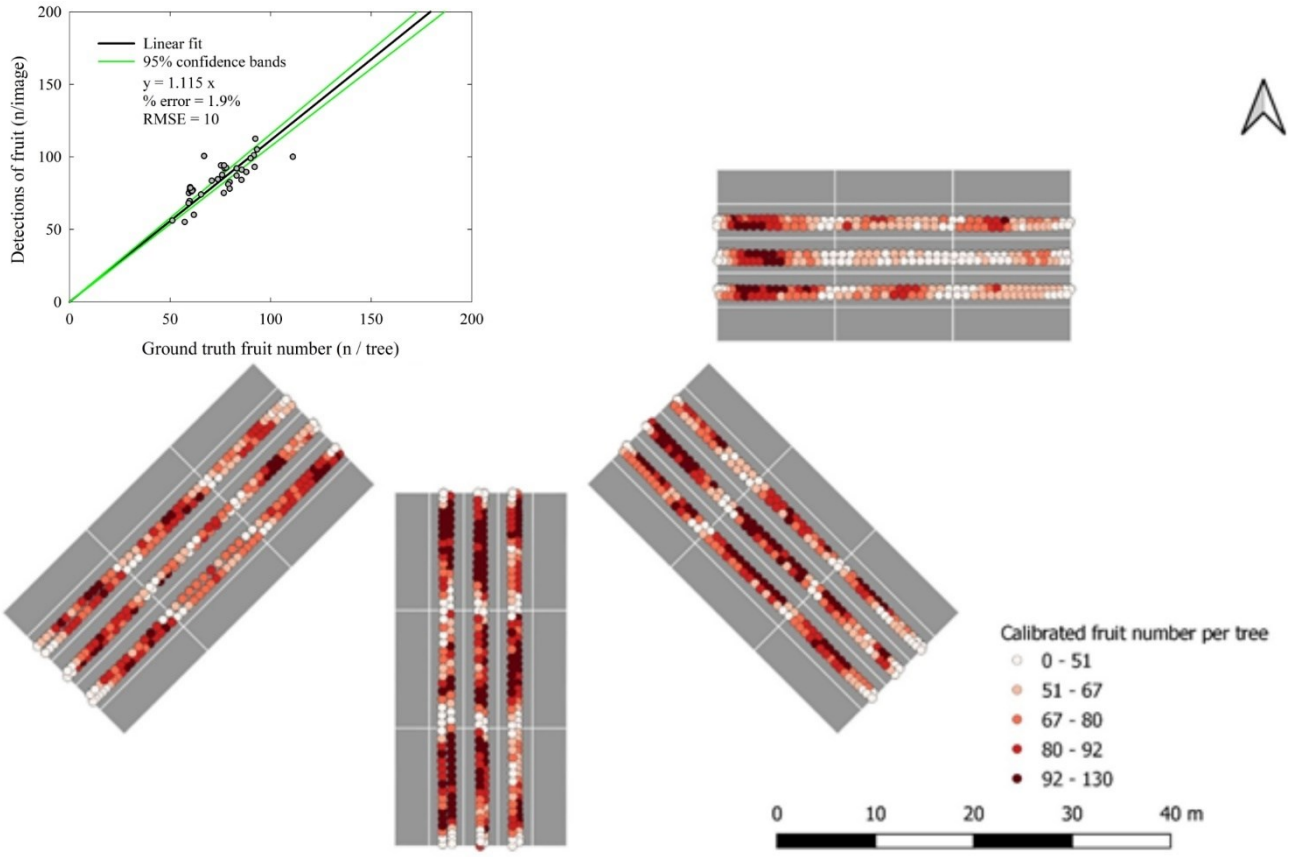

Figure 5. Heatmap of calibrated fruit number per tree in the 36 experimental measurement plots of 'ANABP-01' apples. Data collected before the 2022 harvest (1 April). The graph in the top left of the image shows calibration equation, % standard error and root mean square error (RMSE). The black and green lines represent linear regression fits and 95% confidence interval bands, respectively.

In 2021–22, estimated YI (t ha^{-1}) showed good association with the ground truth YI obtained with a commercial grader (r_c = 0.66) (**Figure 6**), although the performance of the prediction was lower than 2020–21 (r_c = 0.89; Scalisi et al., 2021b). In 2022, YI obtained with a commercial grader in the experimental plots was 43.15 t ha^{-1}. whereas *Cartographer* predicted 42.18 t ha^{-1}, which was equivalent to an overall error (underestimation) of < 1 t ha^{-1} or 2.2%. Thus, block YI estimations in 2021–22 remained below 5%, in line with 2020–21 estimates (i.e., 1.2%, Scalisi et al., 2021b).

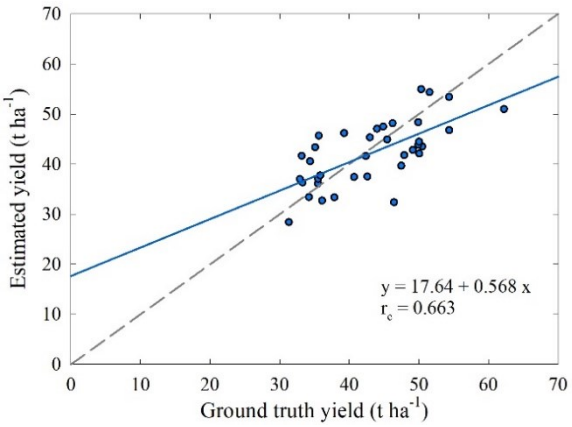

Figure 6. Validation of *Cartographer* estimated yield against yield measured by a commercial grader in 2022. Blue line: linear regression fit; grey dashed line: y = x fit. Lin's concordance correlation coefficient (r_c) reported as a measure of reliability.

Colour-coded maps of FD and CDI helped visualise spatial variability of fruit colour and size in the experimental plots two weeks prior to harvest (**Figure 7**). CDI appeared relatively uniform within the experimental site (**Figure 7a**) with no clear differences between row orientations and rootstock levels. Similarly, the spatial map of fruit diameter in **Figure 7b** showed no clear separation of fruit size across row orientations and rootstocks.

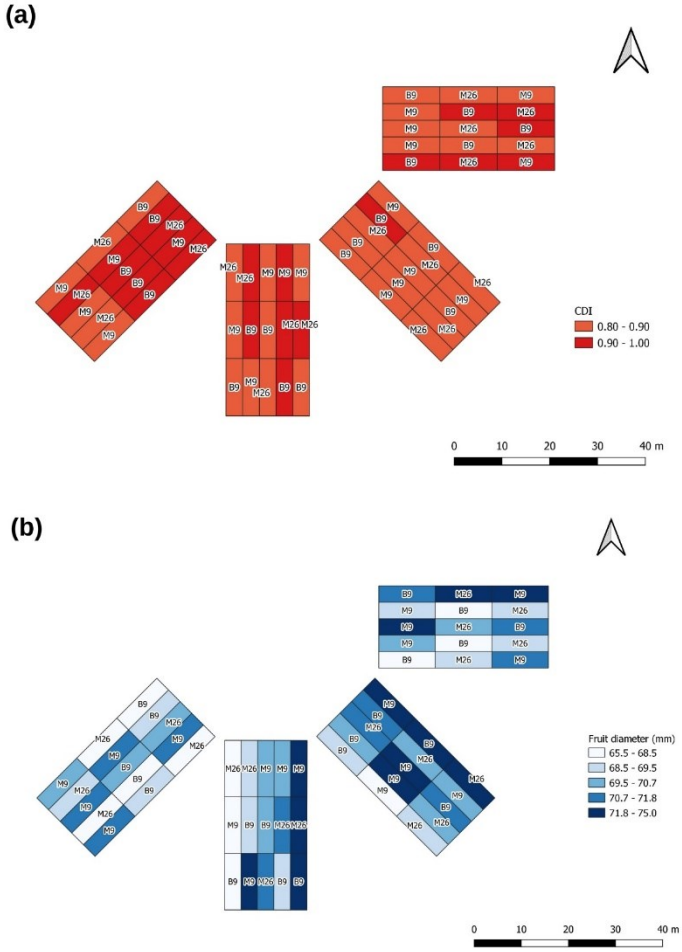

Figure 7. Spatial maps of (a) Colour Development Index (CDI) and (b) fruit diameter in the experimental plots of 'ANABP 01' in the Sundial orchard at the Tatura SmartFarm. Data collected two weeks prior the 2021–22 harvest. Fruit diameter average ± standard deviation: 70.3 ± 2.0 mm; CDI average ± standard deviation: 0.90 ± 0.05.

Canopy geometry and radiation interception

In 2020–21, we observed that the four canopy geometry parameters output by *Cartographer* (CH, CA, CD, and CSLA) were positively correlated with EAS, regardless of time of measurement, and among them, CD and CSLA had best association with EAS (Scalisi et al., 2021b). Similarly, in 2021–22, both CD and CSLA showed the best agreement with EAS (**Figure 8**).

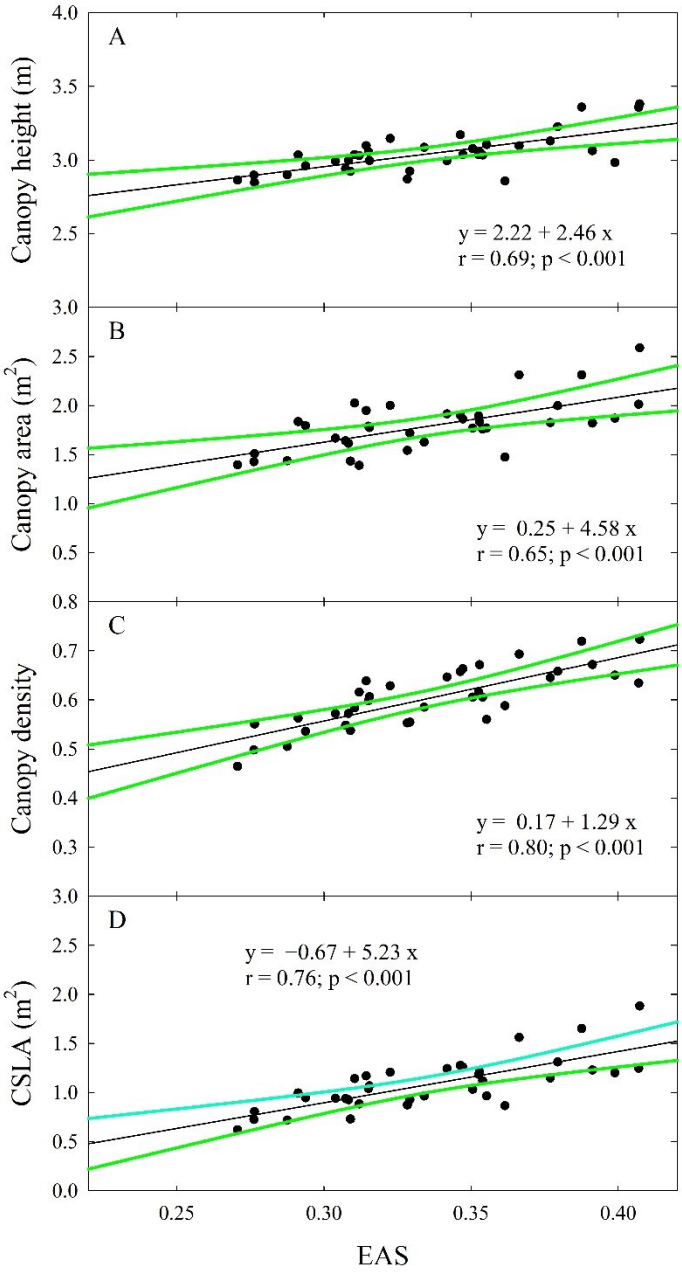

Figure 8. Scatterplots and linear regression fits of (A) canopy height, (B) canopy area, (C) canopy density, and (D) cross-sectional leaf area (CSLA) measured with Green Atlas *Cartographer* against effective area of shade (EAS) measured by a light trolley a month prior the 2022 harvest.

Relationships between crop parameters, tree geometry and EAS, and effects of rootstock, row orientation and season

In 2021–22, the EAS relationship to CSLA was separated by row orientation and the linear equations were considered independently to evaluate the efficiency of intercepted light per unit of foliage. **Figure 9** shows a visual separation of row orientations, with a steeper slope in N–S trees, suggesting an improved light use efficiency per unit of foliage in this row orientation. The visual inference was supported by statistical findings, where significant differences were detected between intercept values, and between slope coefficients in the four row orientation equations (**Table 1**). The lowest

slope of the EAS vs CSLA relationship detected in E–W trees suggest that these canopies have reduced efficiency in light interception. Rootstocks did not significantly affect the relationship between EAS and CSLA (slope and intercept coefficient p-values > 0.05).

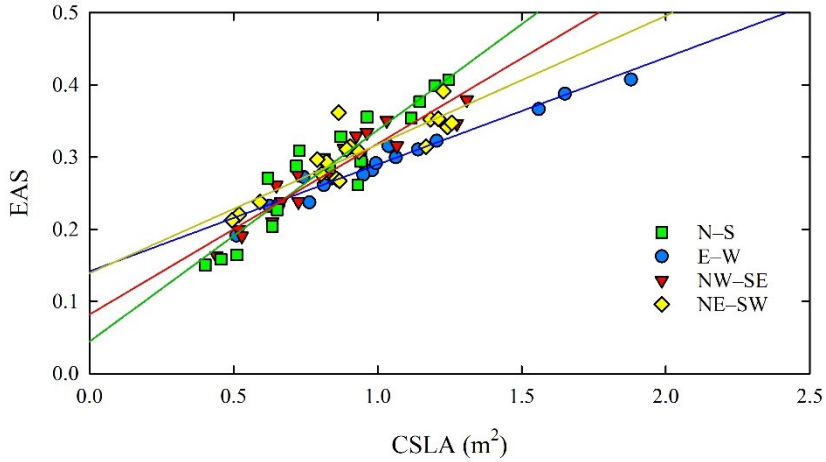

Figure 9. Linear regression models showing the effective area of shade (EAS) in response to cross-sectional leaf area (CSLA) in four different row orientations. Data from 2020–21 and 2021–22 pooled together are shown. Linear regression coefficients and statistics reported in **Table 1**.

Table 1. Linear regression coefficients and standard errors (in brackets) for the relationships between effective area of shade and cross-sectional leaf area in the four row orientations (data from 2020–21 and 2021–22 pooled together) shown in **Figure 9**. Different letters represent significant differences following Tukey's test ($p < 0.05$).

Row orientation	Intercept ± standard error	Slope ± standard error	Model R^2
N–S	0.04 (0.02) b	0.29 (0.03) a	0.87
E–W	0.14 (0.01) a	0.15 (0.01) c	0.95
NW–SE	0.08 (0.02) b	0.24 (0.02) ab	0.89
NE–SW	0.14 (0.02) a	0.18 (0.02) bc	0.77
p-value	0.0014	< 0.001	—

The relationships between crop parameters over the two seasons under study showed that FN, FD, FM and YI were only significantly affected by CH, CA, CD, CSLA and EAS in the first season (**Figure 10**). A factor that might have contributed to the non-significant relationship between canopy size and yield in 2021–22 was the reduced overall pollination. The development of peel redness (CDI) was not affected by canopy size or productivity in both seasons.

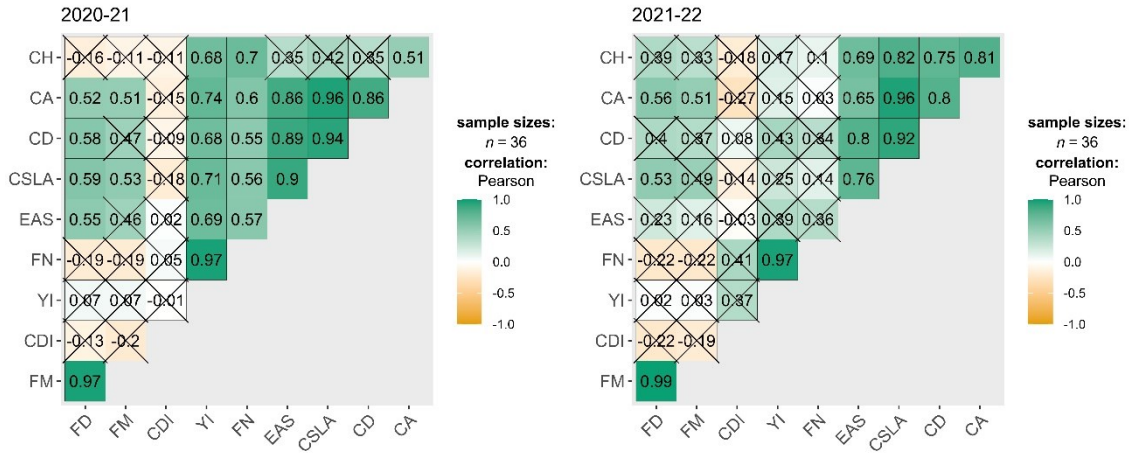

Figure 10. Correlation matrix heatmaps showing colour-coded relationships between crop parameter pairs in 2020–21 (left) and 2021–22 (right). Negative and positive correlations shown in orange and green, respectively. Pearson's correlation coefficients are reported. Crossed matrix cells represent non-significant ($p < 0.05$) correlations.

Table 2. Effects of rootstock, row orientation and season on crop parameters. Different letters represent significant differences (* p <0.05; ** p < 0.01; *** p < 0.001) based on analysis of variance followed by Tukey's pairwise comparison. Significant (p < 0.05) positive (↗) and negative (↘) changes of crop parameters between seasons are reported.

Crop parameter	Rootstock				Row orientation					Seasonal variation[1]
	Bud.9	M.9	M.26	Sig. level	N–S	E–W	NW–SE	NE–SW	Sig. level	
CH[2]	2.90 (0.08) b	2.96 (0.10) b	3.06 (0.16) a	***	2.94 (0.15) b	3.03 (0.15) a	2.98 (0.11) ab	2.93 (0.10) b	***	↗
CA[3]	1.53 (0.18) b	1.82 (0.18) a	1.89 (0.25) a	***	1.65 (0.25) b	1.95 (0.28) a	1.65 (0.18) b	1.74 (0.19) b	***	↗
CD[4]	0.45 (0.10) b	0.54 (0.10) a	0.55 (0.11) a	***	0.49 (0.10) c	0.52 (0.12) ab	0.50 (0.11) bc	0.53 (0.11) a	**	↗
CSLA[5]	0.69 (0.21) b	0.98 (0.21) a	1.03 (0.31) a	***	0.82 (0.25) b	1.03 (0.36) a	0.83 (0.25) b	0.92 (0.25) ab	***	↗
EAS[6]	0.25 (0.06) b	0.31 (0.05) a	0.31 (0.06) a	***	0.29 (0.08)	0.29 (0.06)	0.28 (0.06)	0.30 (0.05)	n.s.	↗
FN[7]	59.3 (8.9) b	72.4 (16.2) a	74.06 (10.1) a	***	66.0 (18.8)	69.6 (11.6)	68.9 (14.2)	69.8 (9.3)	n.s.	↗
YI[8]	33.3 (4.7) b	43.1 (8.4) a	42.7 (5.6) a	***	37.2 (10.1)	41.2 (6.2)	40.1 (8.3)	40.3 (5.9)	n.s.	↗
CDI[9]	0.90 (0.01)	0.90 (0.01)	0.90 (0.01)	n.s.	0.90 (0.01) ab	0.90 (0.01) b	0.90 (0.01) ab	0.91 (0.02) a	*	↘
FM[10]	197 (9) b	210 (8) a	202 (8) b	***	198 (10) b	208 (10) a	204 (7) ab	202 (9) ab	**	=
FD[11]	81.1 (1.3) c	83.1 (1.2) a	81.9 (1.1) b	***	81.5 (1.6)	82.5 (1.6)	82.0 (1.1)	82.0 (1.4)	n.s.	=

[1]from 2020–21 to 2021–22, [2]canopy height, [3]canopy area, [4]canopy density, [5]cross-sectional leaf area, [6]effective area of shade, [7]fruit number per tree, [8]yield per hectare, [9]colour development index, [10]fruit mass, [11]fruit diameter.

The effects of rootstock, row orientation and season on crop parameters are shown in **Table 2**.

The four canopy geometry parameters were affected by rootstock. Overall, M.26 trees had the tallest, denser and larger canopies, although M.9 trees were not significantly different from them, except for CH. Bud.9 trees had approximately 10% less dense canopies than M.9 and M.26. As a consequence, Bud.9 trees intercepted a reduced fraction of the incoming radiation, as shown by EAS values. This was reflected in smaller fruit numbers and overall yields. Fruit size was larger in M.9 trees. CDI was not affected by rootstock, despite Bud.9 fruit being exposed to the highest radiation due to smaller canopies (**Table 2**).

Overall, E–W-oriented trees developed the largest canopies and this likely caused the significantly lowest CDI in their fruit compared to other row orientations. However, the effect of row orientation on CDI were just measurable (± 0.01), as confirmed by the ANOVA p-value near the significance level ($p = 0.033$). FM was smallest in N–S trees, although this significant effect was not detected in the FD comparison, indicating that the effect of row orientation on fruit size need to be re-tested over more seasons.

CH, CA, CD, CSLA, EAS, FN and YI increased in the second season, as expected in a developing orchard. CDI was only slightly reduced in 2021–22, possibly because this season had increased presence of cloudy days, more frequent summer rainfall and lower average temperatures than 2020–21. CDI seasonal variations need to be re-tested over more seasons. Fruit size was not significantly affected by the season.

No significant interactions between rootstock and row orientation were observed for the crop parameters.

DISCUSSION

Overall, this study validated predictions of important crop performance parameters (i.e., FN, FD, FM, CDI, YI) in 'ANABP 01' apples using the Green Atlas mobile platform *Cartographer* over two seasons.

The *Cartographer* was demonstrated to accurately ($r_c = 0.99$) predict FD while in motion (**Figure 3**), despite potential image distortions that could have altered observations. A correct estimation of fruit diameter is important to calculate fruit volume and weight (Mitchell, 1986) and in turn generate predictions of yield (Wang et al., 2017) that can be dynamically fitted to the entire population of fruit in the orchard block rather than to relatively small samples like those used in a previous study (Scalisi et al., 2021b).

The prediction of CDI was deemed accurate ($r_c > 0.8$, **Figure 4**), although some noise existed (Figure 4) due to potential external light interference and a slightly different area on which colour was measured on the fruit surface. CDI represents a promising index of redness development, as it is more intuitive and better suits industry adoption in multiple crops.

Predictions of FN and YI in 2021–22 had errors < 10 fruit/tree (1.9%) and 1 t ha^{-1} (2.2%), respectively, which are in line with errors measured in 2020–21 (<5%, Scalisi et al., 2021b). This finding provides additional confidence on the repeatability of productive performance measurements using Green Atlas *Cartographer*.

The relationship between canopy geometry parameters generated by *Cartographer* and their radiation interception (EAS) revealed that, in 2021–22, CD and CSLA had once again the most precise linear fit (**Figure 8**). The EAS vs CSLA relationships split by row orientation revealed a possible reduced light interception efficiency in E–W trees (**Figure 9**, **Table 1**), as a larger CSLA would be needed to achieve the highest EAS. On the other hand, N–S trees performed best. Rootstocks did not significantly affect the relationship between EAS and CSLA.

Correlation analyses between crop parameters (**Figure 10**) mainly highlighted that the crop load relationships observed in 2020–21 did not stand in 2021–22 due to a possibly reduced pollination and/or the biennial bearing predisposition of apple trees. Consequently, an additional season of data will be useful to confirm the preliminary relationships determined in the first two seasons. The development of peel redness (CDI) was not affected by canopy size or productivity in both seasons.

The reduced size and density of Bud.9 trees led to smaller yields per hectare (**Table 2**). However, when fruit number is expressed as fruit/m^2 of CSLA, Bud.9 trees achieve the highest crop loads (data not shown), suggesting that this rootstock would better perform at lower tree spacings (e.g., 0.5 m) to improve light interception and overall yield per hectare. CDI was not affected by rootstock.

E–W-oriented trees developed the largest canopies but did not produce larger yields than other row orientations. The effect of row orientation on fruit size needs to be re-tested over more seasons.

Tree size and production increased in the second season, as expected. Seasonal variations of fruit size and CDI need to be re-evaluated over more seasons, as the comparison between 2020–21 and 2021–22 did not provide conclusive remarks.

CONCLUSION

Combined fruit number, size, colour and yield predictions using ground-based, fast-scanning systems are an innovative approach to assess fruit quality and productivity in apples pre-harvest. If linked to canopy geometry estimates, fruit quality and productivity predictions become a powerful tool that empowers growers to tailor precise strategies to each orchard block. With the current push of AgTech into business models in the apple industry, and in other fruit industries, the availability of technology that serves multiple purposes is of pivotal importance to reduce substantial production costs such as labour and to ease growers' technology uptake in their business models and investment plans.

RECOMMENDATIONS

Future research will focus on measuring and understanding the relationships between orchard-specific crop parameters generated by Green Atlas *Cartographer*. This will empower growers to precisely manage routine operations such as spraying, pruning, thinning, harvesting, irrigation and fertilisation.

ACKNOWLEDGEMENTS

This technical report is part of the apple and pear industry's PIPS3 (Productivity, Irrigation, Pests and Soils) program of research and development. The project is funded by Hort Innovation, using the Hort Innovation Apple and Pear research and development levy, contributions from the Australian Government and co-investment from Agriculture Victoria. Hort Innovation is the grower-owned, not-for-profit research and development corporation for Australian horticulture.

REFERENCES

Apolo-Apolo, O. E., Martínez-Guanter, J., Egea, G., Raja, P., & Pérez-Ruiz, M. (2020). Deep learning techniques for estimation of the yield and size of citrus fruits using a UAV. European Journal of Agronomy, 115, 126030.

Bargoti, S., Underwood, J., 2017a. Deep fruit detection in orchards, in: Proceedings - IEEE International Conference on Robotics and Automation. Institute of Electrical and Electronics Engineers Inc., pp. 3626–3633. https://doi.org/10.1109/ICRA.2017.7989417

Bargoti, S., Underwood, J.P., 2017b. Image Segmentation for Fruit Detection and Yield Estimation in Apple Orchards. J. F. Robot. 34, 1039–1060. https://doi.org/10.1002/rob.21699

Bresilla, K., Perulli, G.D., Boini, A., Morandi, B., Corelli Grappadelli, L., Manfrini, L., 2019. Single-shot convolution neural networks for real-time fruit detection within the tree. Front. Plant Sci. 10, 611. https://doi.org/10.3389/fpls.2019.00611

Cheng, H., Damerow, L., Sun, Y., & Blanke, M. (2017). Early yield prediction using image analysis of apple fruit and tree canopy features with neural networks. Journal of Imaging, 3(1), 6.

Cripps, J.E., 2016. Apple tree named 'ANABP 01.' USPP27420P3.

Darbyshire, R., Goodwin, I., McClymont, L., Turpin, S., 2018. Addressing heat stress in pome fruit, in: Hermesch, S., Dominik, S. (Eds.), Breeding Focus 2018 - Reducing Heat Stress. Animal Genetics and Breeding Unit, University of New England, Armidale, NSW, Australia, pp. 81–97.

Dias, P.A., Tabb, A., Medeiros, H., 2018a. Multispecies Fruit Flower Detection Using a Refined Semantic Segmentation Network. IEEE Robot. Autom. Lett. 3, 3003–3010. https://doi.org/10.1109/LRA.2018.2849498

Dias, P.A., Tabb, A., Medeiros, H., 2018b. Apple flower detection using deep convolutional networks. Comput. Ind. 99, 17–28. https://doi.org/10.1016/j.compind.2018.03.010

Ferrer, A., Remón, S., Negueruela, A. I., & Oria, R. (2005). Changes during the ripening of the very late season Spanish peach cultivar Calanda: feasibility of using CIELAB coordinates as maturity indices. Scientia Horticulturae, 105(4), 435-446.

Gongal, A., Karkee, M., & Amatya, S. (2018). Apple fruit size estimation using a 3D machine vision system. Information Processing in Agriculture, 5(4), 498-503.

Goodwin, I., Whitfield, D.M., Connor, D.J., 2006. Effects of tree size on water use of peach (Prunus persica L. Batsch). Irrig. Sci. 24, 59–68. https://doi.org/10.1007/s00271-005-0010-z

Greer, D. H. (2005). Non-destructive chlorophyll fluorescence and colour measurements of 'Braeburn'and 'Royal Gala'apple (Malus domestica) fruit development throughout the growing season. New Zealand Journal of Crop and Horticultural Science, 33(4), 413-421. https://doi.org/10.1080/01140671.2005.9514378

Islam, M. S., Scalisi, A., O'Connell, M. G., Morton, P., Scheding, S., Underwood, J., & Goodwin, I. (2022). A Ground-based Platform for Reliable Estimates of Fruit Number, Size, and Color in Stone Fruit Orchards. HortTechnology, 32(6), 510-522. https://doi.org/10.21273/HORTTECH05098-22

Kang, H., Chen, C., 2020. Fast implementation of real-time fruit detection in apple orchards using deep learning. Comput. Electron. Agric. 168, 105108. https://doi.org/10.1016/j.compag.2019.105108

Kuznetsova, A., Maleva, T., Soloviev, V., 2020. Using YOLOv3 Algorithm with Pre- and Post-Processing for Apple Detection in Fruit-Harvesting Robot. Agronomy 10, 1016. https://doi.org/10.3390/agronomy10071016

Lin, L.I.-K., 1989. A Concordance Correlation Coefficient to Evaluate Reproducibility. Biometrics 45, 255–268. https://doi.org/10.2307/2532051

Mitchell, P. D. (1986). Pear fruit growth and the use of diameter to estimate fruit volume and weight. HortScience, 21(4), 1003-1005.

Örn, S., 2016. Estimating Light Interception of Orchard Trees Using LiDAR and Solar Models. Master of Science Thesis, Linköping University.

Peters G. Userfriendlyscience: Quantitative Analysis Made Accessible. 2018. [accessed on 1 May 2021]. R Package Version 0.7.2. Available online: https://userfriendlyscience.com

R Core Team. R: A Language and Environment for Statistical Computing. R Foundation for Statistical Computing; Vienna, Austria: 2018. [accessed on 1 May 2021]. Available online: https://www.R-project.org/

Regunathan, M., & Lee, W. S. (2005). Citrus fruit identification and size determination using machine vision and ultrasonic sensors. In *2005 ASAE Annual Meeting* (p. 1). American Society of Agricultural and Biological Engineers.

Robertson, J. A., Meredith, F. I., Horvat, R. J., & Senter, S. D. (1990). Effect of cold storage and maturity on the physical and chemical characteristics and volatile constituents of peaches (cv. Cresthaven). Journal of Agricultural and Food Chemistry, 38(3), 620-624.

Scalisi, A., Pelliccia, D., & O'Connell, M. G. (2020). Maturity Prediction in Yellow Peach (*Prunus persica* L.) Cultivars Using a Fluorescence Spectrometer. Sensors, 20(22), 6555.

Scalisi, A., O'Connell, M. G., Pelliccia, D., Plozza, T., Frisina, C., Chandra, S., & Goodwin, I. (2021a). Reliability of a Handheld Bluetooth Colourimeter and Its Application to Measuring the Effects of Time from Harvest, Row Orientation and Training System on Nectarine Skin Colour. Horticulturae, 7(8), 255.

Scalisi, A., McClymont, L., Underwood, J., Morton, P., Scheding, S., & Goodwin, I. (2021b). Reliability of a commercial platform for estimating flower cluster and fruit number, yield, tree geometry and light interception in apple trees under different rootstocks and row orientations. Computers and Electronics in Agriculture, 191, 106519.

Scalisi, A., O'Connell, M. G., Islam, M. S., & Goodwin, I. (2022). A Fruit Colour Development Index (CDI) to Support Harvest Time Decisions in Peach and Nectarine Orchards. Horticulturae, 8(5), 459.

Signorell, A. DescTools: Tools for Descriptive Statistics and Exploratory Data Analysis. 2021. [accessed on 1 May 2021]. R Package Version 0.99.41. Available online: https://github.com/AndriSignorell/DescTools

Stajnko, D., Lakota, M., & Hočevar, M. (2004). Estimation of number and diameter of apple fruits in an orchard during the growing season by thermal imaging. Computers and Electronics in Agriculture, 42(1), 31-42.

Underwood, J.P., Jagbrant, G., Nieto, J.I., Sukkarieh, S., 2015. Lidar-Based Tree Recognition and Platform Localization in Orchards. J. F. Robot. 32, 1056–1074. https://doi.org/10.1002/rob.21607

Underwood, J.P., Hung, C., Whelan, B., Sukkarieh, S., 2016. Mapping almond orchard canopy volume, flowers, fruit and yield using lidar and vision sensors. Comput. Electron. Agric. 130, 83–96. https://doi.org/10.1016/j.compag.2016.09.014

Wang, Z., Walsh, K. B., & Verma, B. (2017). On-tree mango fruit size estimation using RGB-D images. Sensors, 17(12), 2738.

Wang, Z., Underwood, J., Walsh, K.B., (2018). Machine vision assessment of mango orchard flowering. Comput. Electron. Agric. 151, 501–511. https://doi.org/10.1016/j.compag.2018.06.040

Westling, F., Underwood, J., Örn, S., 2018. Light interception modelling using unstructured LiDAR data in avocado orchards. Comput. Electron. Agric. 153, 177–187. https://doi.org/10.1016/j.compag.2018.08.020

Advancing sustainable and technology driven apple orchard production systems

Technical Report:

Estimates of fruit size and colour using Green Atlas *Cartographer* and relationships with light interception

Agriculture Victoria Research

November 2021

VICTORIA State Government | Jobs, Precincts and Regions

AGRICULTURE VICTORIA

Author: Alessio Scalisi

Project RDC Number: AP19003

Project CMI Number: 106472

Department of Jobs, Precincts and Regions
1 Spring Street Melbourne Victoria 3000
Telephone (03) 9651 9999

Contents

EXECUTIVE SUMMARY

Modern horticulture is moving towards increased mechanisation, automation, robotics, and non-destructive sensing and monitoring. This report describes the steps taken to validate fruit diameter and fruit colour estimates obtained with a commercial platform (Green Atlas *Cartographer*) in the Sundial Orchard at the Tatura Smarfarm planted with young 'ANABP 01' apple trees and in a commercial 'Ruby Pink' orchard (Plunkett Orchards, Ardmona, Victoria).

The study evaluated relationships between ground truth and Green Atlas *Cartographer* predictions of fruit diameter and colour, their spatial variability as an informative tool for apple growers, the effects of rootstock and row orientation on these fruit quality parameters and their relationship with fruit number and the amount of radiation intercepted by canopies. The accuracy of fruit diameter estimates was very high (> 95 %) and overall fruit diameter prediction errors were deemed below 3 mm. Among the traditional CieLAB colour parameters tested, only hue angle was satisfactorily predicted by *Cartographer*. Hue angle is typically the best predictor of redness development in fruit. A newly developed colour parameter (Colour Development Index, CDI) was also predicted accurately by *Cartographer* and its use was intended to simplify (i) interpretation of colour estimates both in a temporal and in a spatial scale, (ii) application in a higher number of fruit crops, and (iii) large-scale adoption in fruit industries. Fruit diameter and fruit colour were associated to fruit number and amount of radiation interception by tree canopies and the direction of the correlation (positive or negative) was in line with expectations.

Overall, *Cartographer* demonstrated to be a valid tool to combine predictions of fruit diameter and fruit colour that added up to the previously validated predictions of other significant crop parameters (e.g., cross-sectional leaf area, flower number, fruit number) using a single platform. Orchard-specific relationships between crop parameters generated by *Cartographer* across different seasons are currently under investigation. We confirm that the use of Green Atlas *Cartographer* can be beneficial for both growers and scientists to collect large amount of data and replace labour-intensive operations.

INTRODUCTION

This technical report is a deliverable for milestone 104 of the project 'Advancing sustainable and technology driven apple orchard production systems' (AP19003). The report details a study on the initial testing and calibration of the Green Atlas *Cartographer* (i.e., a mobile platform with multiple sensors) for spatial distribution of fruit size and colour in relation to light interception in 'ANABP 01' apples. This report contributes towards meeting the project objectives by providing scientifically sound validations of mobile platform predictions of fruit diameter and colour to achieve premium fruit for domestic and export markets. The results presented in this report reflect a joint effort of Agriculture Victoria and Green Atlas staff and benefited from the valuable support of Plunkett Orchards' staff.

Project outcome

The intended outcome of this project is to improve crop load management in a variable climate by providing knowledge and tools to deliver premium fruit that meets consumer expectations in domestic and export markets.

Project background

In Australia, apple production is yet to reach its full potential based on the area planted (10,000 ha) and the theoretical yield (~ 800,000 t). This is mostly due to variable crop load management, biennial bearing and inconsistent fruit quality. Australia has a unique climate characterised by relatively high temperatures and light intensity compared to other apple production areas around the world (Darbyshire et al., 2018). Light interception and carbohydrate availability play an important role not only in defining the optimal crop load to maximise consistent fruit quality for the life of the tree, but also in floral initiation and biennial bearing. While high light intensity generally leads to increasing photosynthetic rates and consequently carbohydrate availability, when excessive and/or combined with high air temperature can cause sunburn, photoinhibition (i.e., damage the leaf photosynthetic apparatus) or induce stomata closure for long periods during the day, reducing water loss but generating undesired reductions in photoassimilates. Therefore, an optimal regulation of the light harvested by tree canopies by canopy architecture, rootstock selection and planting design is paramount to minimise external inputs (e.g., water, thinning chemicals, reflective mulches, biostimulants) and maintain or even improve fruit quality characteristics such as skin colouration and fruit size.

Modern horticulture is moving toward increased mechanisation, automation, robotics, and non-destructive sensing and monitoring. The integration of technologies that are already adopted in other industries into horticulture systems aims to increase resource use efficiency — including labour — and make orchards more profitable. For this purpose, several recent studies have focused on the application of machine learning algorithms to detect tree structures (e.g., flowers, fruit, architecture) using sensorised robots or platforms. Most of the state-of-the-art research has attempted to detect apple fruit for crop load or yield determination, or for integration with automated harvesting machines using image segmentation, deep learning and different Convolutional Neural Networks (CNN) (Bargoti and Underwood, 2017a, 2017b; Bresilla et al., 2019; Kang and Chen, 2020; Kuznetsova et al., 2020) on images typically collected by RGB / RGB-D cameras. Underwood et al. (2016), Dias et al. (2018a, 2018b) and Wang et al. (2018) used similar machine vision approaches for almond, apple and mango flower recognition, respectively. In the case of almond, the machine image recognition was supported by LiDAR cloud points to reconstruct tree structure and assign tree geo-references when combined with GPS (Underwood et al., 2016). LiDAR sensors are a powerful tool to quickly determine canopy architecture parameters such as tree height, canopy size and density and have the potential to recognise tree location, alone or combined with GPS (Underwood et al., 2015). LiDAR cloud points have also been used to model light interception, as demonstrated by Örn (2016). The same idea was applied to estimate a solar-geometric model for light interception estimation in avocado trees (Westling et al., 2018).

Commercial services such as Green Atlas *Cartographer* use a combination of sensors (e.g., RGB cameras, LiDAR, GPS, thermal sensors), mounted on a platform on an electric vehicle, to gather data while driving through orchard rows. *Cartographer* is currently available to measure the spatial distribution of flower cluster number, crop load in apples and to measure tree geometry parameters such as canopy area, canopy density and cross-sectional leaf area (CSLA). The first validations are reported in the MS103 of the AP19003 project.

In situ fruit size estimation is paramount for determining accurate yield, forecast fruit growth and for the application of robotic harvesting. Nevertheless, to our knowledge only a few studies have investigated fruit size estimations using different machine vision systems (e.g.,, RGB cameras, 3D photonic mixing device cameras, thermal cameras) and artificial intelligence on aerial or ground-based platforms (Stanjko et al., 2004; Regunathan and Lee, 2005; Cheng et al., 2017;

Wang et al., 2017; Gongal et al., 2018; Apolo-Apolo et al., 2020). Wang et al. (2017) recently presented good accuracy of mango fruit size estimates with low prediction errors (< 5 mm), although the authors stated that the cost-effective RGB-D cameras used in their study cannot be used under direct sunshine conditions.

Typically, fruit colour is assessed after harvest using cameras mounted in fruit grading machinery. However, orchard estimates of fruit colour can be linked to fruit maturity in some cultivars and can drive orchard management strategies to improve skin colour formation in situ, such as leaf removal, use of reflective mulch or the application of biostimulants to enhance anthocyanin pigmentation. Fruit colour estimation using non-contact sensors such as RGB or RGB-D cameras mounted on aerial and ground vehicles is difficult as it is influenced by the variable orchard light environment due to the combined effects of clouds, sun angle, netting, etc. Green Atlas *Cartographer* mounts strobe lights that continuously flash tree canopies to attenuate any potential effect of external light on colour readings by the RGB cameras.

Some of the colour parameters in the CieLAB colour space have been associated with maturity in fruit. Previous studies reported significant associations between hue angle (h°) and maturity in stone fruits (Robertson et al., 1990; Ferrer et al., 2005; Scalisi et al., 2020; 2021a). Similarly, Greer (1990) found that h° of both overcolour and background colour had a defined decreasing pattern throughout the growing season in 'Braeburn' and 'Royal Gala' apples. Using *Cartographer* proximal sensors to predict colour parameters such as h° is crucial to investigate the opportunity of fast orchard scanning for fruit colour estimations. In addition, an attempt to simplify the concept of h°, its interpretation and its association with maturity needs to be taken on board in order to support the broader application and use of h° as a reference parameter for colour development.

Project objectives

The overall goal of this project was to investigate physiological mechanisms and develop management tools so that apple orchards can consistently produce high yields and fruit that meet market specifications through climate change and extreme heat events. The work presented in this report aimed to develop a rapid orchard assessment tool using proximal sensing technologies to determine fruit diameter and colour. Specifically, this work aimed to: (i) evaluate relationships between ground truth and Green Atlas *Cartographer* predictions of fruit size and colour in apple trees; (ii) evaluate spatial variability of fruit size and colour as an informative tool for apple growers; (iii) determine the effects of rootstock and row orientation on fruit size and colour; (iv) determine relationships between fruit size, fruit colour and fruit number, and the amount of radiation intercepted by canopies.

METHOD

Experimental sites and apple cultivars

The study was conducted in the Sundial Orchard at the Tatura SmartFarm, Victoria, Australia during 2020-21. The Sundial Orchard is a high-density (~ 2857 trees / ha) circular orchard of approximately 1.3 ha. 'ANABP 01' apple trees were planted in a semicircle of the orchard following four different row orientations (i.e., northeast to southwest, north to south, northwest to southeast and east to west, henceforth referred to as NE-SW, N-S, SE-NW and E-W). Trees were grafted onto three different rootstocks — Bud.9, M9 (T337) and M26 — in a completely randomised design and planted in 2018 (Figure 1). 'ANABP 01' trees are trained to spindles on vertical trellises at 1 m spacing. The row spacing is 3.5 m and there is a total of twenty rows, five rows per row orientation, and 60 experimental plots. Each experimental plot is composed of eleven 'ANABP 01' trees and one polliniser ('Granny Smith'). The experiment was conducted on trees at their 3rd leaf.

'ANABP 01' originated from a cross-pollination between 'Cripps Red' and 'Royal Gala'. The cultivar was bred by the Department of Agriculture and Food, State of Western Australia. Fruit has dark purple colouration and consistent cropping characteristics (Cripps, 2016).

Additional data collection and measurements were undertaken in a commercial 'Ruby Pink' orchard (Plunkett Orchards, Ardmona, Victoria, Australia).

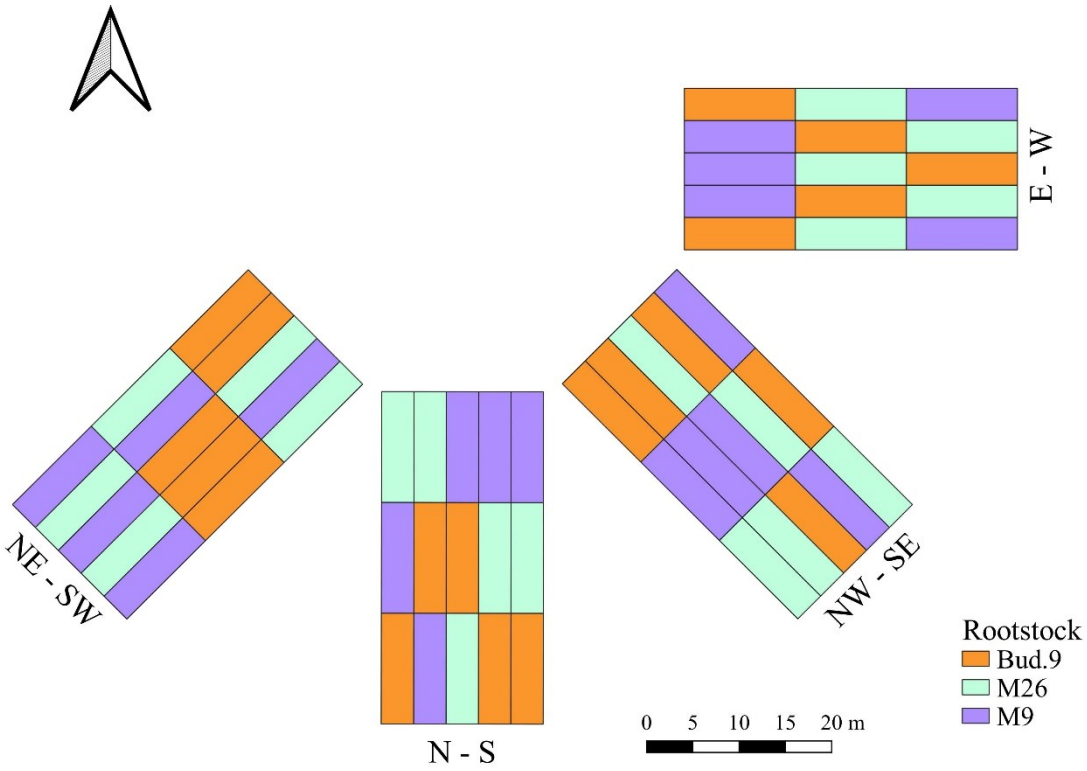

Figure 1. Layout of the sixty experimental plots of 'ANABP 01' in the Sundial Orchard at the Tatura SmartFarm. Row orientations: northeast to southwest (NE-SW), north to south (N-S), northwest to southeast (NW-SE) and east to west (E-W). Each plot contains 11 'ANABP 01' trees.

Orchard scans with *Cartographer*

Orchard scans were undertaken with Green Atlas *Cartographer*. A phone-interface was used to control logging and enter file notes to aid retrospective identification of scan locations and note relevant scan or plot issues. *Cartographer* was driven at a constant speed of approximately 10 km/h. Logging was switched on a few metres prior to the start of the measurement section and off a few metres past the end of the measurement section.

Stationary scans were conducted to compare predicted fruit diameter and colour with ground truth data. Images were collected while *Cartographer* was stationary with cameras positioned directly in front of tagged fruit. Mobile scans of three validation zones were conducted in the commercial 'Ruby Pink' orchard on 30 April 2021 — a few weeks prior to

harvest. Predictions of fruit diameter in the validation zones were computed to validate the accuracy of mobile predictions as opposed to the stationary estimations previously obtained, as motion may potentially cause a shape distortion of detected objects in images.

Continuous mobile scans were collected in the entire orchard block to spatial variability of fruit diameter and colour.

Data at a plot level was extracted by intersecting the points generated by the *Cartographer* with plot polygons generated with QGIS (v. 3.16, QGIS Development Team, Open Source Geospatial Foundation, 2021). The geographic precision of plot extraction was improved by real-time kinematic (RTK) positioning adjustments and was cross-checked on the position of posts — to mark the beginning and end of a plot — in the RGB images collected by the *Cartographer*.

Fruit diameter and colour predictions

An exploratory analysis was conducted to verify the ability of *Cartographer* to predict fruit diameter (FD) and skin colour attributes.

Three fruits were tagged on each central tree of 36 experimental plots, with one fruit per height zone ('Low' < 1.1 m, 'Middle' 1.1 – 2.1 m and 'High' > 2.1 m) in an approximately vertical line (+/− 25 cm horizontally) (i.e., 108 fruit). FD and fruit colour were measured at three times during the season (26 November 2020, 21 January 2021 and 15 March 2021) to increase the variability of the measures. FD of tagged fruit was measured with a Bluetooth calliper (OriginCal, iGAGING, San Clemente, California, USA) held parallel to the row direction and on the same day of orchard scans. The colour of tagged fruit was measured with a portable colourimeter (Rubens Technologies Ltd) with D50 illuminant and a 2°observer angle, coincident with orchard scans. The portable colourimeter generated values in the CieLAB / CieLCH colour scale (i.e., L*, a*, b*, C* and h°). For a full description of the meaning of each of these colour attributes see Scalisi et al. (2021a).

Another more intuitive skin colour parameter was derived from hue angle — the colour attribute more often associated with fruit maturity and redness development (Scalisi et al., 2021a). This Colour Development Index (CDI) is expressed using a scale from 0 to 1 and represents the departure from greenness (0) around the CieLAB colour wheel, with pure red being the most distant point (1), regardless of using the bottom or the top half of the colour wheel to measure the distance from greenness. In other words, given that most fruit at an immature stage have greener skins as characterised by chlorophyll concentration, CDI standardises the loss of chlorophyll in any direction (i.e., departing towards blueness-redness or towards yellowness-redness). CDI is strictly correlated to hue angle but the adoption of the former has some advantages over the latter: (a) its interpretation for end-users without prior knowledge of the CieLAB / LCh colour space is much improved as its range is between 0 and 1 and it is directly related to redness development, as opposed to h° (inversely related to redness); (b) its use allows more robust colour development predictions in fruit that turn purple when ripe such as dark plums (Islam et al., 2021); (c) based on cultivar-specific fruit colour development characteristics, the 0 and 1 points can be dynamically rotated around the CieLAB colour wheel to reflect the actual colour development characteristic of the fruit. In this study, CDI was calculated as shown in Table 1.

Table 1. Calculations of fruit skin Colour Development Index (CDI) from hue angle (h°) on a 0 – 360° scale using an *if* statement.

***if* statement**	**Equation**
h° > 180	CDI = (180 − |h° − 360|) / 180
h° ≤ 180	CDI = (180 − h°) / 180

Cartographer stationary scans were collected at the three stages in which ground truth fruit size and colour data were collected. Mobile scans in the Sundial Orchard were obtained at the end of each measurement session. Fruit size and colour data corresponding to the tagged fruit was extracted from stationary images based on the longest diameter of the detection box and its 5×5 central pixels, respectively. Fruit diameter and colour extractions were only carried out on fruit that were completely visible from the cameras, with no leaves or other obstacles that might have affected correct measurements (n fruit = 53). The dataset used for fruit diameter was further filtered by the uncertainty of the estimate and the final sample was 16 fruits.

Spatial variability of fruit diameter and colour

Spatial maps of predicted fruit diameter and fruit colour were generated for 'ANABP 01' apples in the Sundial Orchard and for 'Ruby Pink' apples in a commercial orchard during the 2020-21 season. Maps were produced using a combination of the Atlas tool provided by the Green Atlas User Interface and by elaborating data generated by *Cartographer* using QGIS (v. 3.16, QGIS Development Team, Open Source Geospatial Foundation, 2021).

Effects of rootstock and row orientation on fruit size and colour

The overall effects of rootstock and row orientation, and their interaction, on fruit diameter and colour were investigated. Fruit diameter and colour were measured using *Cartographer* in the Sundial Orchard of the Tatura SmartFarm and two weeks prior to harvest.

Relationships of fruit size, fruit colour and fruit number with canopy radiation interception

Fruit diameter, fruit colour and fruit number obtained with *Cartographer* in the commercial 'Ruby Pink' orchard were related to the effective area of shade (EAS) — a proxy of light interception (Goodwin et al., 2021) — to determine whether the fraction of photosynthetically active radiation intercepted by trees played a role in the regulation of these two important crop parameters. EAS was estimated from cross-sectional leaf area obtained with *Cartographer*'s LiDAR using the equation reported in one of our previous publications (Scalisi et al., 2021b). A grid was overlaid onto the orchard spatial map and crop parameters estimated by *Cartographer* were grouped and averaged in grid rectangles — defined as plots and measuring 12 × 10 m — that encompassed ~ 24 trees each.

Statistical analysis

Ordinary Least Squares Linear regression procedures were carried out to determine the relationships between predicted and observed fruit diameter and fruit colour attributes. Model prediction errors were based on root mean square errors (RMSE) of the linear regressions. The reliability of predictions was assessed using the Lin's concordance correlation coefficient (r_c), a measure of both precision and accuracy that provides a value from 0 (no concordance) to 1 (perfect concordance) that assess the divergence of predicted data from the line of perfect concordance with observations (i.e., the line at 45 degrees on a square scatter plot, where y = x) (Lin, 1989).

The relationships between EAS and fruit diameter and colour were estimated using correlation analysis and assessed with the Spearman's rank correlation coefficient (r_s). The effects of row orientation and rootstock were tested using a two-way analysis of variance (ANOVA), significant differences ($p < 0.05$) were separated by Tukey's Honestly Significant difference (HSD) and results were displayed using raincloud plots.

Regression analyses and the calculation of Lin's concordance correlation coefficient (r_c) were carried out using R (v. 4.0.2, R Core Team, 2021) and its packages "Userfriendliscience" (Peters, 2018) and "DescTools" (Signorell, 2021). Graphs were generated using SigmaPlot 12.5 (Systat software Inc., Chicago, IL, USA) and the JASP suite for Windows 10 (v. 0.15, Jasp Team, 2021).

RESULTS

Fruit diameter and colour predictions

Stationary fruit diameter estimations with *Cartographer* were tightly associated with ground truth measurements (Figure 2). The estimation error was only 2.5 mm and an r_c of 0.987 highlighted an optimal precision and accuracy of the prediction without further calibration. When tested on a validation dataset generated from mobile scans, the prediction had an almost identical accuracy to the stationary prediction — as suggested by the overlapping of the two lines in Figure 2 — and observations did not significantly diverge from the line of perfect fit. Consequently, *Cartographer* predictions of fruit diameter did not need further calibration to be accurate in both 'ANABP 01' and 'Ruby Pink' trees.

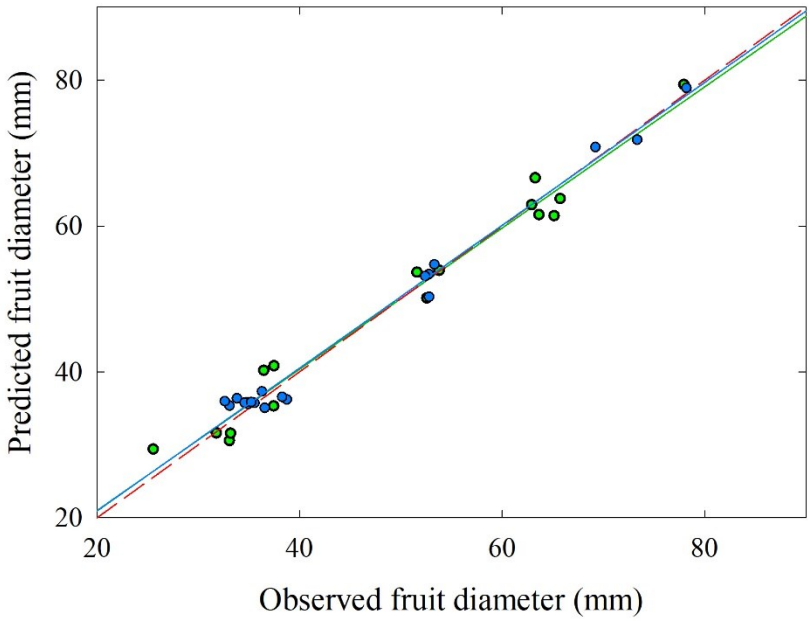

Figure 2. Predicted fruit diameter against observed fruit diameter in 16 fruits measured with stationary *Cartographer* (green points) and in 19 fruits measured with mobile *Cartographer*. Green line: linear regression fit for validation of stationary predictions; blue line: linear regression fit for validation of mobile predictions; red dashed line: perfect fit (y = 0). The validation datasets included 'ANABP 01' and 'Ruby Pink' fruit. Stationary prediction model: [y = 1.64 (2.19) + 0.97 (0.04) x; r_c = 0.987; RMSE = 2.5 mm]; mobile prediction model [y = 1.36 (1.28) + 0.98 (0.03) x; r_c = 0.993; RMSE = 1.7 mm].

The relationship between colour attributes (L*, a*, b*, C* and h°) predicted with stationary *Cartographer* and measurements collected with the Rubens colourimeter are shown in Figure 3 and Table 2. Significant relationships (p < 0.001) were obtained for L*, a*, b* and h° (Figure 3 A, B, C and E, respectively). No significant association (p = 0.088) was obtained between predicted and observed C* (Figure 3 D). Although significant, the predictions of L*, a* and b* were very weak (R^2 < 0.3). The only parameter that was satisfactorily predicted was h° (R^2 > 0.7, Table 4). Not only did hue angle have good precision, but it was also relatively accurate. CDI predictions were accurate (Figure 4) as predicted and observed values had good concordance (r_c > 0.80). Some noise was observed likely due to the different surfaces in which colour was measured — the portable colourimeter was used to measure colour in a single spot, whereas *Cartographer* colour measurements were calculated over a number of central pixels in the detection box drawn around the fruit.

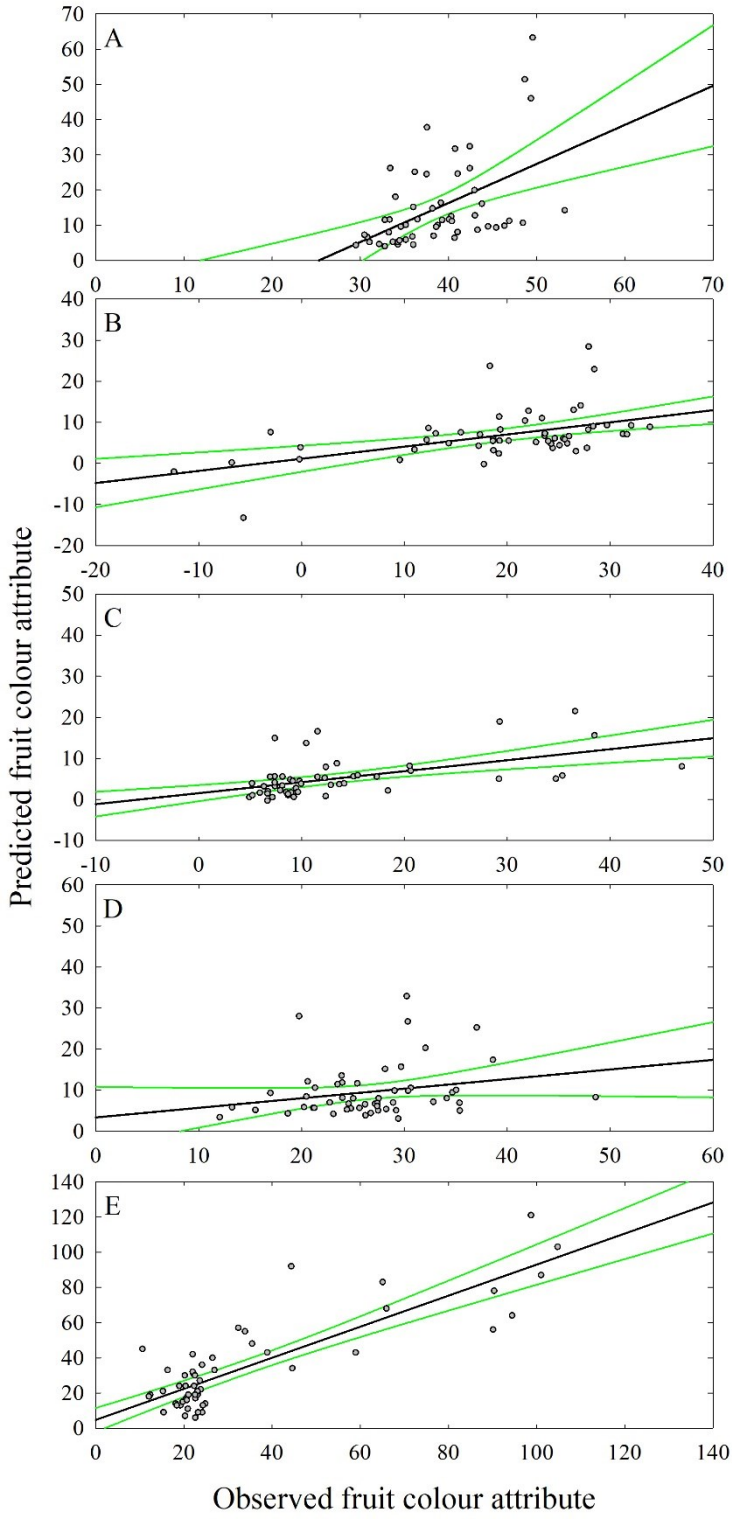

Figure 3. Predicted against observed fruit CieLab-CieLCh colour attributes in 53 'ANABP 01' apple fruit. (A) L*, (B) a*, (C) b*, (D) C* and (E) h°. Black lines: linear regression fits; green lines: 95% confidence interval bands. Equations and statistics reported in Table 2.

Table 2. Linear regression equations for the relationships between fruit colour attributes predicted by *Cartographer* (y) and the same fruit colour attributes measured with a portable reference colourimeter (x).

Colour attribute	Equation	$R^{2\,x}$	r_c [y]	p [z]
L*	y = − 28.08 (10.60) + 1.11 (0.27) x	0.249	0.091	< 0.001
a*	y = 1.13 (1.58) + 0.30 (0.07) x	0.248	0.209	< 0.001
b*	y = 1.50 (0.98) + 0.27 (0.06) x	0.289	0.267	< 0.001
C*	y = 3.37 (3.70) + 0.23 (0.13) x	0.056	0.053	0.088
h°	y = 4.73 (3.38) + 0.88 (0.08) x	0.703	0.837	< 0.001

[x] coefficient of determination; [y] Lin's concordance correlation coefficient; [z] linear regression p-value.

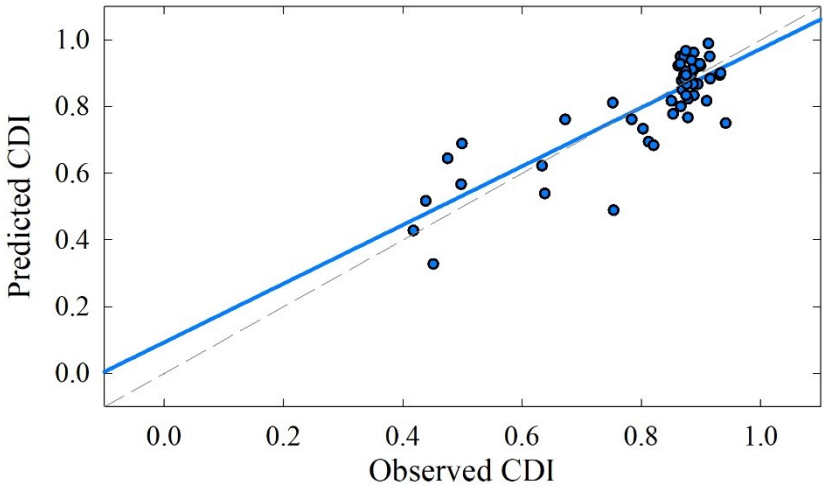

Figure 4. Predicted against observed fruit colour development index (CDI) in 53 'ANABP 01' apple fruit. Blue line: linear regression fit; grey dashed line: line of perfect fit (y = x). Linear regression model: y = 0.0929 (0.0658) + 0.880 (0.0797) x; R^2 = 0.705; r_c = 0.837; *RMSE* = 0.08.

Spatial variability of fruit diameter and colour

Colour-coded maps of CDI and fruit diameter in the Sundial Orchard helped visualise spatial variability of fruit colour and size in the experimental plots two weeks prior to harvest (Figure 5). CDI appeared relatively uniform within the experimental site (Figure 5a) with no clear differences between row orientations and rootstock levels. Similarly, the spatial map of fruit diameter in Figure 5b showed no clear separation of fruit size across row orientations and rootstocks.

Spatial maps of 'Ruby Pink' fruit diameter on 13 January (Figure 6a) and 30 April (Figure 6b) visibly highlighted the growth of fruit between the two scanning periods and revealed irregular locations of the orchard where trees had a lower average fruit size. Likewise, CDI maps in January (Figure 7a) and April (Figure 7b) portrayed both chronological and spatial variation of fruit colour. Most of the green-yellow light spots in Figure 7b represented the average fruit colour in 'Granny Smith' trees used as pollinisers in the block.

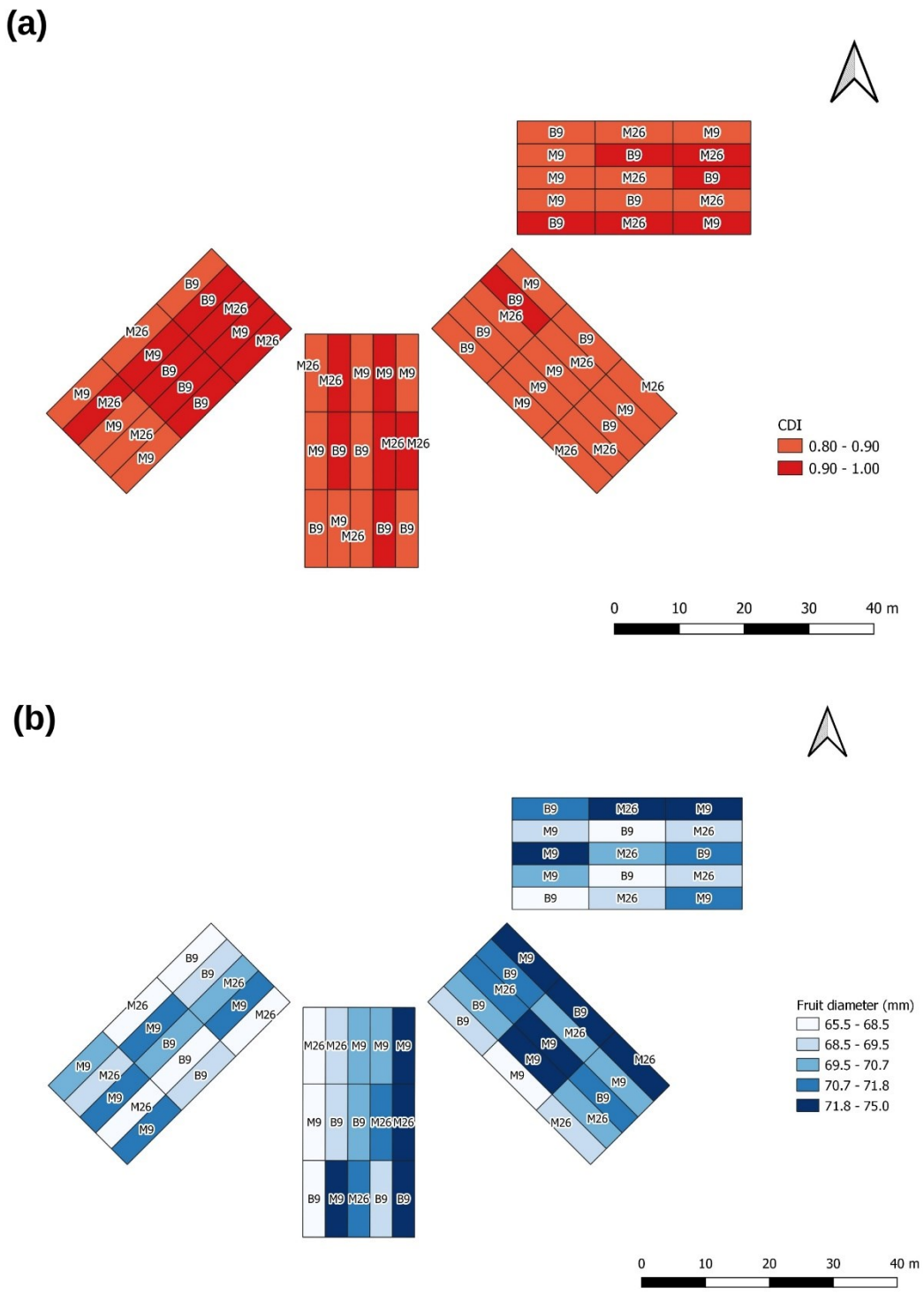

Figure 5. Spatial maps of (a) Colour Development Index (CDI) and (b) fruit diameter in the experimental plots of 'ANABP 01' in the Sundial Orchard at the Tatura SmartFarm. Data collected two weeks prior to harvest. Fruit diameter average ± standard deviation: 70.3 ± 2.0 mm; CDI average ± standard deviation: 0.90 ± 0.05.

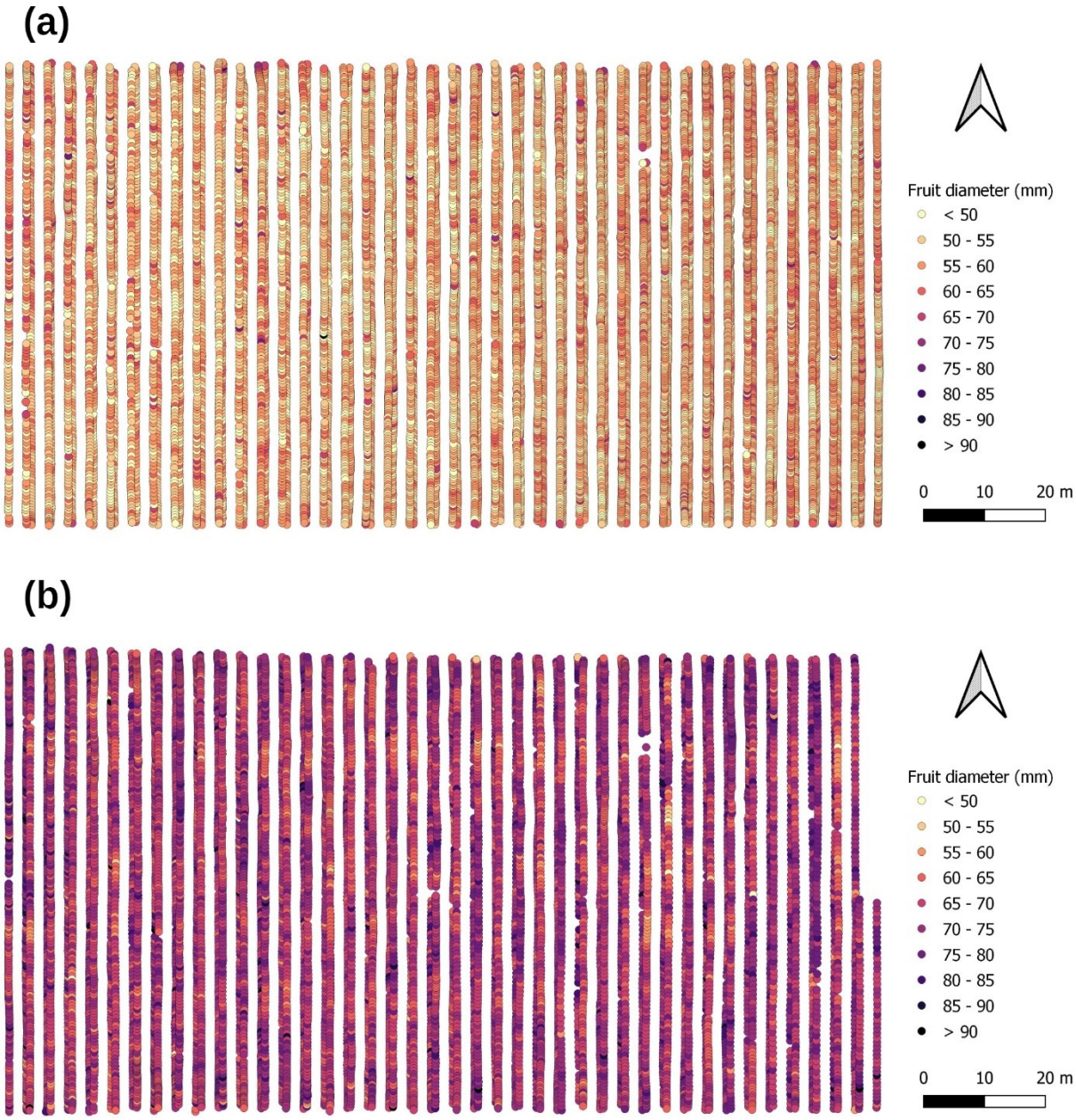

Figure 6. Spatial maps of fruit diameter on (a) 13 January 2021 and on (b) 30 April 2021 at the commercial 'Ruby Pink' orchard (Plunkett Orchards, Ardmona, Victoria, Australia). Fruit diameter average ± standard deviation: (a) 54.9 ± 4.4 mm; (b) 70.4 ± 5.1 mm.

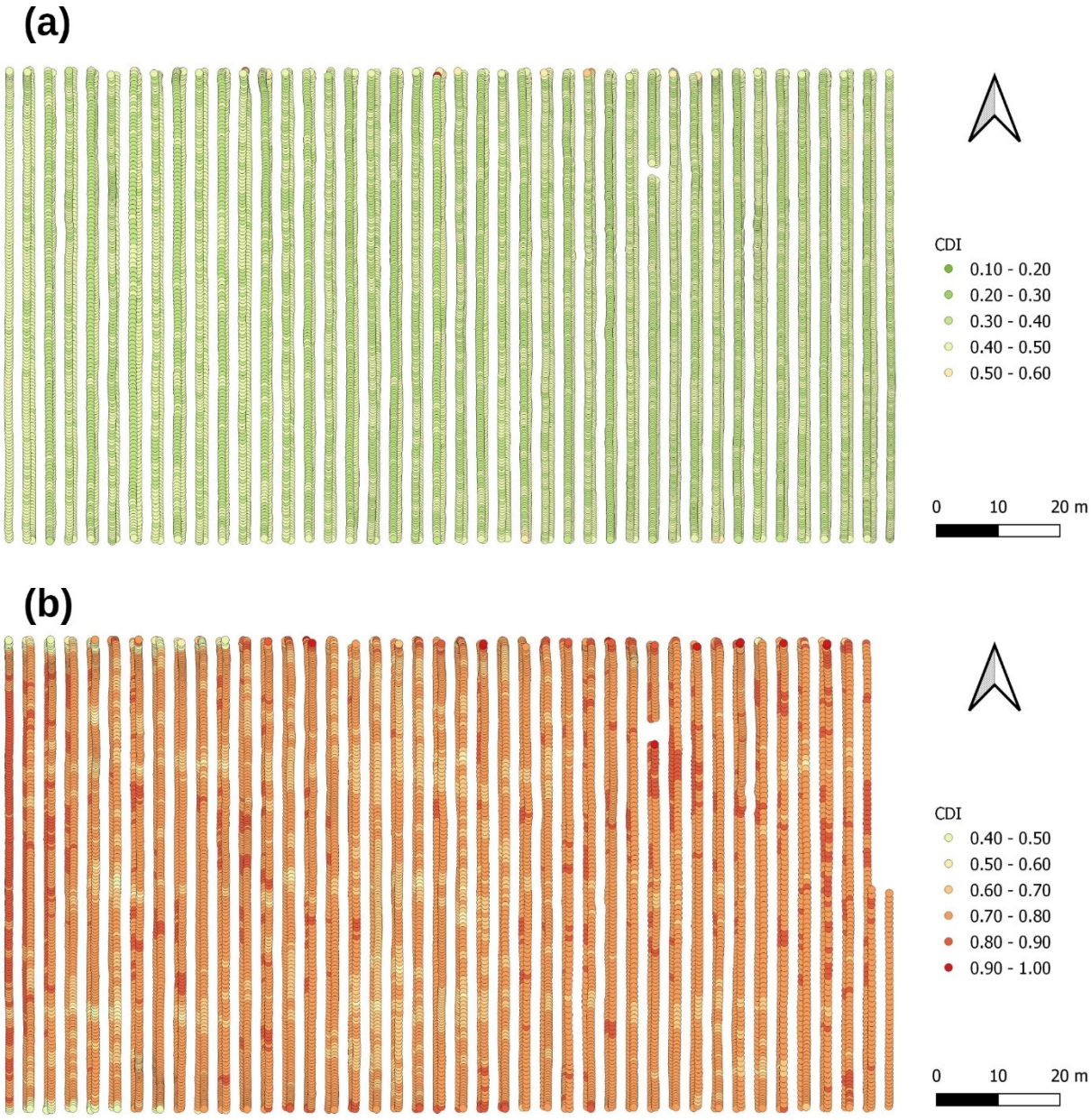

Figure 7. Spatial maps of Colour Development Index (CDI) on (a) 13 January 2021 and on (b) 30 April 2021 at the commercial 'Ruby Pink' orchard (Plunkett Orchards, Ardmona, Victoria, Australia). CDI Average ± standard deviation: (a) 0.41 ± 0.02; (b) 0.76 ± 0.05.

Effects of rootstock and row orientation on fruit size and colour

As suggested by Figure 5a, no significant differences in CDI of 'ANABP 01' apples were observed between row orientations and rootstocks ($p > 0.05$; Table 3). This might have been due to the fact that fruit of this cultivar turn dark burgundy at harvest time and CDI might plateau around 0.90, regardless of physiological maturity.

Fruit diameter differences were only observed in different rootstocks, with M9 trees yielding the significantly largest fruit ($p = 0.029$; Table 3) although differences were small. No significant interaction between rootstock and row orientation was observed.

Table 3. Effects of row orientation, rootstock and their interaction on fruit diameter and Colour Development Index (CDI) obtained with *Cartographer* two weeks prior to harvest. Means ± standard errors (S.E.), ANOVA's *p*-values and effect size (η^2) are reported. Different letters represent significant differences according to the Tukey's post hoc test and significant comparisons are shown with underlined text.

Effect	Level	CDI ± S.E.	Fruit diameter (mm) ± S.E.
Row orientation	E – W	0.898 ± 0.004	70.3 ± 0.5
	NE – SW	0.907 ± 0.006	69.3 ± 0.5
	N – S	0.899 ± 0.002	70.2 ± 0.6
	NW – SE	0.896 ± 0.001	70.8 ± 0.4
	p	0.256	0.212
	η^2	0.077	0.073
Rootstock	Bud.9	0.902 ± 0.003	69.4 ± 0.4 b
	M26	0.901 ± 0.004	70.0 ± 0.4 b
	M9	0.896 ± 0.003	71.1 ± 0.4 a
	p	0.486	0.029
	η^2	0.027	0.120
Row orientation × Rootstock	*p*	0.992	0.735
	η^2	0.014	0.056

Relationships between fruit size, fruit colour and fruit number, and canopy radiation interception

Significant correlations were obtained between all the pairwise comparisons of EAS, fruit diameter, CDI and fruit number at the commercial 'Ruby Pink' orchard (Table 4). Increasing EAS caused a reduction of fruit diameter and CDI, but also had a weak positive correlation with fruit number.

Table 4. Correlation matrix for effective area of shade (EAS), fruit diameter, Crop Development Index (CDI) and fruit number measured on 30 April 2021 at the commercial 'Ruby Pink' orchard (Plunkett Orchards, Ardmona, Victoria, Australia). Spearman's rank correlation coefficients (r_s) and significance levels reported.

	EAS	Fruit diameter	CDI	Fruit number
EAS	—			
Fruit diameter	− 0.442 ***	—		
CDI	− 0.353 ***	0.596 ***	—	
Fruit number	0.298 **	− 0.499 ***	− 0.659 ***	—

$^{*}p < 0.05$; $^{**}p < 0.01$; $^{***}p < 0.001$

DISCUSSION

Overall, this study validated predictions of fruit diameter and fruit colour in 'ANABP 01' and 'Ruby Pink' apples using the Green Atlas mobile platform *Cartographer*.

The *Cartographer* was demonstrated to accurately ($r_c = 0.99$) predict fruit diameter while in motion (Figure 2), despite potential image distortions that could have altered observations. A correct estimation of fruit diameter is important to calculate fruit volume and weight (Mitchell, 1986) and in turn generate predictions of yield (Wang et al., 2017) that can

be dynamically fitted to the entire population of fruit in the orchard block rather than to relatively small samples like those used in a previous study (Scalisi et al., 2021b).

Spatial variation in fruit diameter did not reveal clear effects of rootstock and row orientation on 'ANABP 01' fruit size in the Sundial Orchard at the Tatura SmartFarm (Figure 5b), although a significant effect of rootstock was statistically obtained, showing that M9 trees had slightly larger fruit than M26 and Bud.9 trees (Table 3). No effects of row orientation or a combination of row orientation and rootstocks on fruit diameter were observed (Table 3). However, size predictions were obtained two weeks prior to harvest and harvest results might have differed.

Spatial maps of 'Ruby Pink' fruit diameters at different fruit growth stages (i.e., after thinning and a few days prior to harvest) allowed a time-scale comparison of fruit size (Figure 6). At harvest, fruit had an average diameter of 70.4 mm with a standard deviation of 5.1 mm. The location of trees with lowest fruit diameter was irregular and possibly not associated to irregular thinning being carried out by different operators. Spatial variation of accurate fruit size estimates may help forecast yield and drive orchard management to improve or reduce fruit size to meet the most profitable fruit grade.

The prediction of an important fruit skin colour parameter such as h° was also deemed accurate, although some noise existed (Figure 3e) due to potential external light interference and a slightly different area on which colour was measured on the fruit surface. A similar accuracy (> 80 %) was obtained for CDI, a colour parameter that is more dynamic, intuitive and better suits industry adoption in multiple crops. CDI predictions in the 'Ruby Pink' commercial orchard showed the development of colour over time and unveiled a better redness development in fruit in the westernmost row at harvest (figure 7b).

No effects of row orientation, rootstock or their interaction were observed on CDI in young 'ANABP 01' trees (Table 3). CDI may not be the best descriptor of colour in 'ANABP 01' due to the characteristic skin darkening that cause a reduction of both C* and L*. When measured over the last weeks prior to harvest, CDI in 'ANABP 01' may have a peak at ~ 0.90 in which fruit reach maximum redness followed by a slight decrease of its value due to the darkening of the skin. It is possible that a parameter that dynamically combines hue angle with C* and L* after reaching the CDI peak will need to be used to directly link colour development to maturity in 'ANABP 01'. However, using proximal cameras for the measurements of C* and L* is not ideal, as these indices are more affected by the influence of external light compared to h° and CDI. Ad-hoc studies will be conducted to quantify the effects of sunlight on *Cartographer* colour measurements at different times of the day (e.g., solar noon, solar noon − 2h, solar noon + 2 h, and after dusk). In addition, in 2021-22, relationships of the colour attributes used in this study with maturity indices (e.g., starch index, flesh firmness and soluble solids concentration) in 'ANABP 01' apples will be explored.

Relationships between crop parameters and canopy light interception in the 'Ruby Pink' orchard revealed a decrease in fruit colour and size in response to increasing intercepted canopy radiation. These responses are expected when canopies are larger (i.e., higher light interception) as vegetative growth compete with fruit growth and higher EAS can cause some degree of shading on fruit which in turn do not accumulate as much anthocyanins responsible for skin redness. The positive correlation between EAS and fruit diameter was likely to be driven by the fact that larger trees might have born a higher number of fruit or that manual thinning in these trees was not as efficient due to a higher proportion of fruit hiding behind foliage. The significant positive correlation between fruit diameter and CDI is probably only a consequence of the negative effect of fruit number on fruit size and colour. In fact, our results highlighted the robust negative effect of increasing fruit number on fruit diameter and CDI, which is in line with previous findings (Stopar et al., 2002; Serra et al., 2016; Stefanelli et al., 2019).

CONCLUSION

Combined fruit diameter and fruit colour predictions using ground-based, fast-scanning systems are an innovative approach to assess fruit quality and maturity in apples in situ. This report is a pioneer study that validated the capability of a commercially available platform to assess fruit colour development variability in a spatial and in a time scale in apple cultivars of relevant commercial interest.

Combining predictions of several important parameters in one single platform opens the door to various possible uses of this technology. With the current push of AgTech into business models in the apple industry, and in other fruit industries, the availability of technology that serves multiple purposes is of pivotal importance to reduce substantial production costs such as labour and to ease growers' technology uptake in their business models and investment plans.

RECOMMENDATIONS

Future research will focus on measuring and understanding the relationships between orchard-specific crop parameters generated by Green Atlas *Cartographer*. This will empower growers to precisely manage routine operations such as spraying, pruning, thinning, harvesting, irrigation and fertilisation. Green Atlas is currently investigating opportunities to use *Cartographer* for missing or dead tree localisation in orchards and to integrate *Cartographer* with commercial spraying units.

REFERENCES

Apolo-Apolo, O. E., Martínez-Guanter, J., Egea, G., Raja, P., & Pérez-Ruiz, M. (2020). Deep learning techniques for estimation of the yield and size of citrus fruits using a UAV. European Journal of Agronomy, 115, 126030.

Bargoti, S., Underwood, J., 2017a. Deep fruit detection in orchards, in: Proceedings - IEEE International Conference on Robotics and Automation. Institute of Electrical and Electronics Engineers Inc., pp. 3626–3633. https://doi.org/10.1109/ICRA.2017.7989417

Bargoti, S., Underwood, J.P., 2017b. Image Segmentation for Fruit Detection and Yield Estimation in Apple Orchards. J. F. Robot. 34, 1039–1060. https://doi.org/10.1002/rob.21699

Bresilla, K., Perulli, G.D., Boini, A., Morandi, B., Corelli Grappadelli, L., Manfrini, L., 2019. Single-shot convolution neural networks for real-time fruit detection within the tree. Front. Plant Sci. 10, 611. https://doi.org/10.3389/fpls.2019.00611

Cheng, H., Damerow, L., Sun, Y., & Blanke, M. (2017). Early yield prediction using image analysis of apple fruit and tree canopy features with neural networks. Journal of Imaging, 3(1), 6.

Cripps, J.E., 2016. Apple tree named 'ANABP 01.' USPP27420P3.

Darbyshire, R., Goodwin, I., McClymont, L., Turpin, S., 2018. Addressing heat stress in pome fruit, in: Hermesch, S., Dominik, S. (Eds.), Breeding Focus 2018 - Reducing Heat Stress. Animal Genetics and Breeding Unit, University of New England, Armidale, NSW, Australia, pp. 81–97.

Dias, P.A., Tabb, A., Medeiros, H., 2018a. Multispecies Fruit Flower Detection Using a Refined Semantic Segmentation Network. IEEE Robot. Autom. Lett. 3, 3003–3010. https://doi.org/10.1109/LRA.2018.2849498

Dias, P.A., Tabb, A., Medeiros, H., 2018b. Apple flower detection using deep convolutional networks. Comput. Ind. 99, 17–28. https://doi.org/10.1016/j.compind.2018.03.010

Ferrer, A., Remón, S., Negueruela, A. I., & Oria, R. (2005). Changes during the ripening of the very late season Spanish peach cultivar Calanda: feasibility of using CIELAB coordinates as maturity indices. Scientia Horticulturae, 105(4), 435-446.

Gongal, A., Karkee, M., & Amatya, S. (2018). Apple fruit size estimation using a 3D machine vision system. Information Processing in Agriculture, 5(4), 498-503.

Goodwin, I., Whitfield, D.M., Connor, D.J., 2006. Effects of tree size on water use of peach (Prunus persica L. Batsch). Irrig. Sci. 24, 59–68. https://doi.org/10.1007/s00271-005-0010-z

Islam, M.S., Scalisi, A., O'Connell, M.G., Morton, P., SScheding, S., Underwood, J., and Goodwin, I. (2021). Reliability of Green Atlas Cartographer for fast spatial estimates of fruit number, fruit size and fruit colour in stone fruit orchards. Draft.

Kang, H., Chen, C., 2020. Fast implementation of real-time fruit detection in apple orchards using deep learning. Comput. Electron. Agric. 168, 105108. https://doi.org/10.1016/j.compag.2019.105108

Kuznetsova, A., Maleva, T., Soloviev, V., 2020. Using YOLOv3 Algorithm with Pre- and Post-Processing for Apple Detection in Fruit-Harvesting Robot. Agronomy 10, 1016. https://doi.org/10.3390/agronomy10071016

Lin, L.I.-K., 1989. A Concordance Correlation Coefficient to Evaluate Reproducibility. Biometrics 45, 255–268. https://doi.org/10.2307/2532051

Mitchell, P. D. (1986). Pear fruit growth and the use of diameter to estimate fruit volume and weight. HortScience, 21(4), 1003-1005.

Örn, S., 2016. Estimating Light Interception of Orchard Trees Using LiDAR and Solar Models. Master of Science Thesis, Linköping University.

Peters G. Userfriendlyscience: Quantitative Analysis Made Accessible. 2018. [accessed on 1 May 2021]. R Package Version 0.7.2. Available online: https://userfriendlyscience.com

R Core Team. R: A Language and Environment for Statistical Computing. R Foundation for Statistical Computing; Vienna, Austria: 2018. [accessed on 1 May 2021]. Available online: https://www.R-project.org/

Regunathan, M., & Lee, W. S. (2005). Citrus fruit identification and size determination using machine vision and ultrasonic sensors. In *2005 ASAE Annual Meeting* (p. 1). American Society of Agricultural and Biological Engineers.

Robertson, J. A., Meredith, F. I., Horvat, R. J., & Senter, S. D. (1990). Effect of cold storage and maturity on the physical and chemical characteristics and volatile constituents of peaches (cv. Cresthaven). Journal of Agricultural and Food Chemistry, 38(3), 620-624.

Scalisi, A., Pelliccia, D., & O'Connell, M. G. (2020). Maturity Prediction in Yellow Peach (*Prunus persica* L.) Cultivars Using a Fluorescence Spectrometer. Sensors, 20(22), 6555.

Scalisi, A., O'Connell, M. G., Pelliccia, D., Plozza, T., Frisina, C., Chandra, S., & Goodwin, I. (2021a). Reliability of a Handheld Bluetooth Colourimeter and Its Application to Measuring the Effects of Time from Harvest, Row Orientation and Training System on Nectarine Skin Colour. Horticulturae, 7(8), 255.

Scalisi, A., McClymont, L., Underwood, J., Morton, P., Scheding, S., & Goodwin, I. (2021b). Reliability of a commercial platform for estimating flower cluster and fruit number, yield, tree geometry and light interception in apple trees under different rootstocks and row orientations. Computers and Electronics in Agriculture, 191, 106519.

Serra, S., Leisso, R., Giordani, L., Kalcsits, L., & Musacchi, S. (2016). Crop load influences fruit quality, nutritional balance, and return bloom in 'Honeycrisp'apple. *HortScience*, *51*(3), 236-244.

Signorell, A. DescTools: Tools for Descriptive Statistics and Exploratory Data Analysis. 2021. [accessed on 1 May 2021]. R Package Version 0.99.41. Available online: https://github.com/AndriSignorell/DescTools

Stajnko, D., Lakota, M., & Hočevar, M. (2004). Estimation of number and diameter of apple fruits in an orchard during the growing season by thermal imaging. Computers and Electronics in Agriculture, 42(1), 31-42.

Stefanelli, D., Plozza, T., Flachowsky, H., & Wünsche, J. N. (2017, June). Young apple tree responses to crop load. In *International Symposium on Flowering, Fruit Set and Alternate Bearing 1229* (pp. 221-228).

Stopar, M., Bolcina, U., Vanzo, A., & Vrhovsek, U. (2002). Lower crop load for cv. Jonagold apples (Malus× domestica Borkh.) increases polyphenol content and fruit quality. *Journal of agricultural and food chemistry*, *50*(6), 1643-1646.

Underwood, J.P., Jagbrant, G., Nieto, J.I., Sukkarieh, S., 2015. Lidar-Based Tree Recognition and Platform Localization in Orchards. J. F. Robot. 32, 1056–1074. https://doi.org/10.1002/rob.21607

Underwood, J.P., Hung, C., Whelan, B., Sukkarieh, S., 2016. Mapping almond orchard canopy volume, flowers, fruit and yield using lidar and vision sensors. Comput. Electron. Agric. 130, 83–96. https://doi.org/10.1016/j.compag.2016.09.014

Wang, Z., Walsh, K. B., & Verma, B. (2017). On-tree mango fruit size estimation using RGB-D images. Sensors, 17(12), 2738.

Wang, Z., Underwood, J., Walsh, K.B., (2018). Machine vision assessment of mango orchard flowering. Comput. Electron. Agric. 151, 501–511. https://doi.org/10.1016/j.compag.2018.06.040

Westling, F., Underwood, J., Örn, S., 2018. Light interception modelling using unstructured LiDAR data in avocado orchards. Comput. Electron. Agric. 153, 177–187. https://doi.org/10.1016/j.compag.2018.08.020

PIPS3: AP19003 Advancing sustainable and technology driven apple orchard production systems

Report Summary

Light interception and rootstock experiments

Agriculture Victoria Research

May 2023

VICTORIA State Government | Jobs, Precincts and Regions

AGRICULTURE VICTORIA

Authors: Madeleine Peavey

Project RDC Number: AP19003

Project RCM Number: 6472

Department of Environment, Energy and Climate Action
8 Nicholson Street Melbourne Victoria 3000
Telephone 136 186

EXECUTIVE SUMMARY

The overall goal of this project was to investigate crop productivity and performance and develop management tools so that apple orchards can consistently produce high yields and fruit that meet market specifications through climate change and extreme heat events. The work presented in this summary aimed to investigate the influence that choice of rootstock had on light interception (LI). Canopy LI of 'ANABP 01' apple trees grown on three dwarfing rootstocks — Bud.9, M.26 and M.9 — was measured during the 2020–21. 2021–22 and 2022–23 growing seasons. Among the studied dwarfing rootstocks, 'ANABP 01' scions grown on M.26 and M.9 achieved better levels of light interception compared to Bud.9. The canopy vigour of trees grown on Bud.9 rootstock may not be suitable to support higher crop loads and its sparseness may increase the risk of sunburn damage.

INTRODUCTION

This report summary is a deliverable for milestone 107 of the project 'Advancing sustainable and technology driven apple orchard production systems' (AP19003). The report summarises the data collected on canopy light interception (LI) of apple trees as affected by three dwarfing rootstocks. This report contributes towards meeting the project objectives by providing scientifically sound data on LI to achieve premium fruit for domestic and export markets.

Project outcome

The intended outcome of this project is to improve crop load management in a variable climate by providing knowledge and tools to deliver premium fruit that meets consumer expectations in domestic and export markets.

Project background

In Australia, apple production is yet to reach its full potential based on the area planted (10,000 ha) and the theoretical yield (~ 800,000 t). This is mostly due to variable crop load management, biennial bearing and inconsistent fruit quality. Australia has a unique climate characterised by relatively high temperatures and light intensity compared to other apple production areas around the world (Darbyshire et al., 2018). LI and carbohydrate availability play an important role not only in defining the optimal crop load to maximise consistent fruit quality for the life of the tree, but also in floral initiation and biennial bearing. While high light intensity generally leads to increasing photosynthetic rates and consequently carbohydrate availability, when excessive and/or combined with high air temperature can cause sunburn, photoinhibition (i.e., damage the leaf photosynthetic apparatus) or induce stomata closure for long periods during the day, reducing water loss but generating undesired reductions in photoassimilates. Therefore, an optimal regulation of the light harvested by tree canopies by canopy architecture, rootstock selection and planting design is paramount to minimise external inputs (e.g., water, thinning chemicals, reflective mulches, biostimulants) and maintain or even improve fruit quality characteristics such as skin colouration and fruit size.

Apple orchard design has evolved substantially in recent years with modern high-density 2D planting systems striving to optimise the use of space and resources, particularly sunlight. The quantity and quality of sunlight exposure of apple leaves and fruit plays one of the most important roles in tree and fruit growth (Jackson et al., 1977; Monteith, 1981; Robinson & Lakso, 1991) and harvest fruit quality (Hamadziripi et al., 2014). Sunlight is a key influence in the productive performance of an orchard, comprising fruit yield and quality, and is dependent largely on LI and distribution within the tree canopy. Achieving good levels of LI is important for making efficient use of the available canopy space and incoming sunlight. LI is directly linked to the yield potential of apple orchards (Jackson, 1978; Jackson et al., 1977; Palmer et al., 2002; Robinson & Lakso, 1991). However, overcrowding of trees with excessive vigour in order to obtain higher levels of LI leads to more shading of the canopy on the interior and at the base of the tree, particularly if tree height and row spacing are not optimised.

Reduction of vegetative vigour by dwarfing rootstocks allows orchards to be planted with higher tree densities that result in increased LI and yields in young orchards and better distribution of sunlight to leaves and fruits throughout the canopy. Attempting to grow a high-density planting of apple scions on more vigorous rootstocks would undoubtedly result in an increased need for manual labour to manage pruning and tree training requirements. While many studies have investigated the influence of rootstocks on fruit growth and quality, the interactions of sunlight and crop load were often not reported (Autio, 1991; Barritt et al., 1997; Musacchi & Serra, 2018).

Project objectives

The overall goal of this project was to investigate crop productivity and performance and develop management tools so that apple orchards can consistently produce high yields and fruit that meet market specifications through climate change and extreme heat events. The work presented in this summary aimed to investigate the influence that choice of rootstock had on LI.

METHOD

Study site and experimental plots

The Sundial Orchard at the Tatura SmartFarm (Agriculture Victoria, Australia; 36.437 °S, 145.268 °E, 114 m above mean sea level; **Figure 1**) is a multidirectional orchard with a high-density (HD) planting of 'ANABP 01' trees. 'ANABP 01'originated from a cross-pollination between 'Cripps Red' and 'Royal Gala'. The cultivar was bred by the Department of Agriculture and Food, State of Western Australia. Fruit has dark burgundy colouration and consistent cropping characteristics (Cripps, 2016). The trees are planted in four row orientations (E–W, NW–SE, N–S, NE–SW) organised as a semicircle (half of the orchard). Scions were grafted onto three dwarfing rootstocks — Budagovsky 9 (Bud.9), Malling 9 T337 (M.9) and Malling 26 (M.26) — and planted as one-year-old bare-rooted trees on the site in the winter of 2018 in a complete randomised block design. **Figure 2** shows examples of 'ANABP-01' trees on the three rootstocks. The trees are trained as slender spindles on a vertical trellis with 1 m and 3.5 m tree and row spacings, respectively (2857 trees per hectare). Each row orientation arm is comprised of five rows measuring 36 m in length, with the two outer rows serving as guard rows. Each row is divided into three 12 m panels containing 11 'ANABP 01' trees and one 'Granny Smith' polleniser. Each panel represents an experimental plot (n = 36). The 2020–21 southern hemisphere growing season produced the first crop for this orchard. Irrigation, nutrition and pest management was the same for all trees.

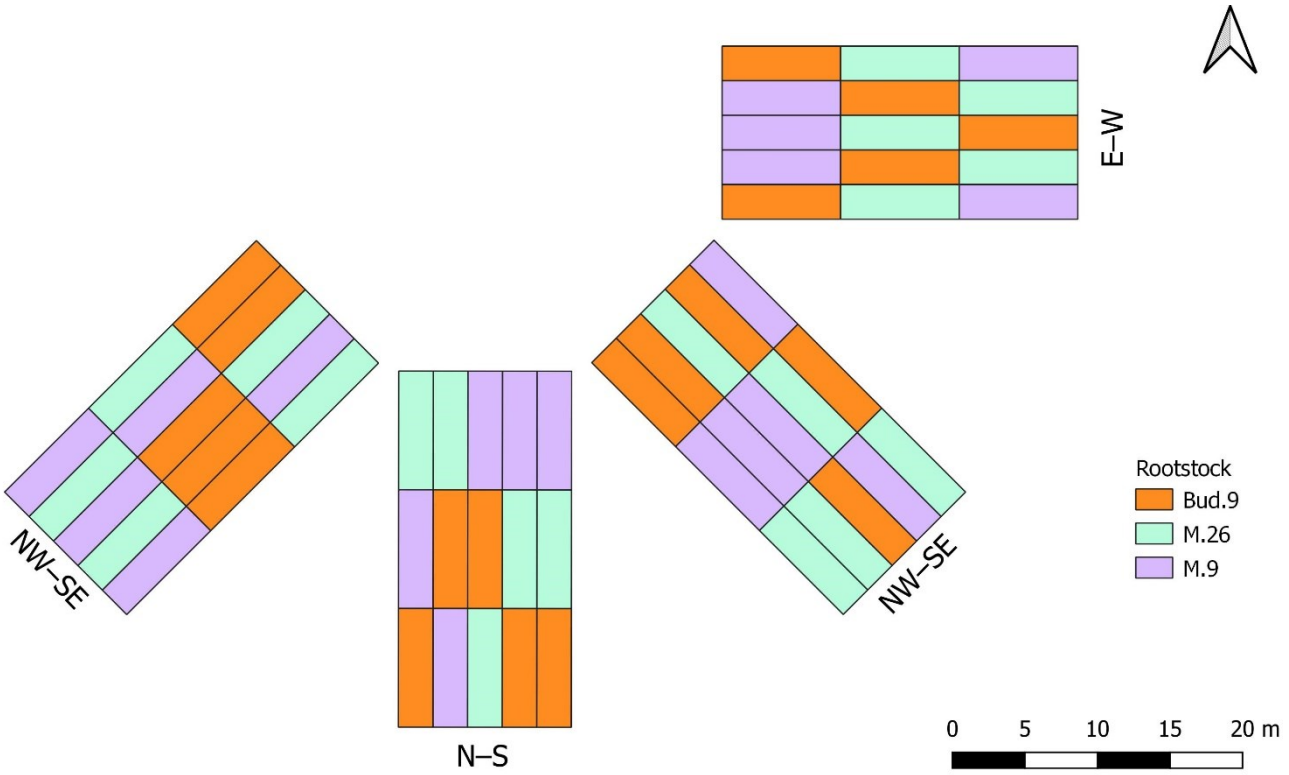

Figure 1. Layout of the sixty experimental plots of 'ANABP 01' in the Sundial orchard at the Tatura SmartFarm. Rootstocks: Bud.9, M.26 and M.9. Row orientations: northeast to southwest (NE–SW), north to south (N–S), northwest to southeast (NW–SE) and east to west (E–W). Each plot contains eleven 'ANABP 01' trees.

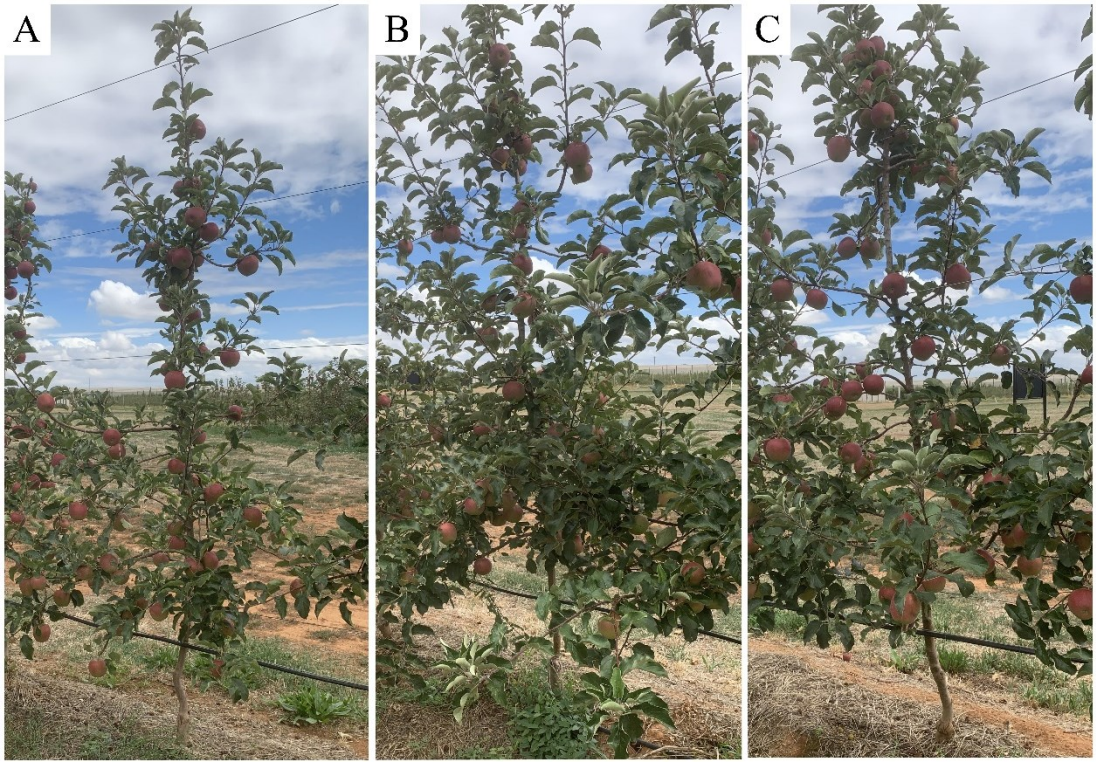

Figure 2. 'ANABP 01' scions grown on Bud.9 (A), M.9 (B) and M.26 (C) rootstocks. Photos taken on 8 April 2022 during the trees' third leaf.

Canopy light interception (LI)

Canopy LI was measured during the 2020–21, 2021–22 and 2022–23 growing seasons. Measurements occurred in November and February in 2020–21, in October and March in 2021–22, and monthly from November to March in 2022–23. Measurements were performed three times per day on clear sky days for the first two seasons and five times per day during the 2022–23 season. The first and last measurements of the day occurred when the shadow length did not exceed the row width and consequently shade the adjacent row. The sun elevation angle in relation to the tree shadow length was calculated with the equation: $\alpha = \tan^{-1}(h/L)$, where α represented the angle of elevation of the sun (rads), h was the object height (tree/row height in this instance) and L was the length of the shadow. Measurements were also performed at solar noon. Two additional measurements were done in 2022–23—one midway between the first morning measurement and solar noon, and the other between solar noon and the last afternoon measurement. On measurement days, the time of measurement and solar elevation angles was cross-checked with historical data files and noted for posterity.

LI was measured with a three-meter length, custom-built mobile light bar equipped with 24 quantum PAR sensors (QPAR, Tranzflo NZ Ltd., Palmerston North, New Zealand; Fielder & Comeau, 2000) mounted at 12.5 cm spacing, situated at approximately 15 cm above ground level and wired to a data logger (CR850, Campbell Scientific, Inc., Logan, UT, United States). Data was collected as an average absolute value of photosynthetic photon flux density (PPFD; µmol m^{-2} s^{-1}) for each experimental plot as well as a reference solar measurement in full direct sunlight at the beginning of each row orientation.

Data was expressed as the fraction of intercepted PAR with the equation: $fPAR_i = 1 - PAR_m/PAR_s$, where PAR_m is the measured PAR, and PAR_s is the solar reference measurement. The mean daily $fPAR_i$ was calculated as the mean of the three/five daily $fPAR_i$ values.

Statistical analysis

The seasonal progression of LI data was analysed using One-Way Analysis of Variance (ANOVA) to determine significant differences ($p < 0.05$) between rootstocks. The post-hoc test Tukey's pairwise comparison was used to separate groups.

RESULTS

The $fPAR_i$ results show the seasonal progressions of vegetative growth for each rootstock in 2020–21 (**Table 1**), 2021–22 (**Table 2**), and 2022–23 (**Table 3**). The lower values of $fPAR_i$ across all rootstocks in January 2023 compared to November/December 2022 was likely due to extensive foliar damage resulting from a severe hailstorm which occurred on 22 December 2022 (**Figure 2**). The damage shown in the picture was evident across the entire apple block in the Sundial Orchard.

The canopies of trees grown on Bud.9 rootstock consistently intercepted the least amount of light and displayed significantly lower $fPAR_i$ than M.26 at every time point measured during the three seasons ($p < 0.001$; **Tables 1, 2 and 3**). M.26 and M.9 rootstocks both achieved similar $fPAR_i$ values during their growth, although M.26 was significantly higher than M.9 in March 2023 ($p < 0.001$; **Table 3**). Previously published work from this experimental site showed marked differences in aspects of tree geometry (i.e., tree height, canopy area, canopy density and canopy cross-sectional area) between 'ANABP 01' trees grown on these rootstocks (Scalisi et al., 2021).

Although it was expected to measure an increase in $fPAR_i$ between 2021–22 and 2022–23, this was not achieved likely due to the hailstorm event in late December 2022 that caused foliage shredding and leaf area reduction.

Table 1. Estimated marginal means of $fPAR_i$ of 'ANABP 01' apple trees grown on three dwarfing rootstocks (Bud.9, M.26 and M.9) during the 2020–21 season. Measurements were performed on clear sky days in November and February. The standard error of the means (SE) is reported. Letter separation by Tukey's Honestly Significant Differences.

Rootstock	November		February	
	Mean daily $fPAR_i$	SE	Mean daily $fPAR_i$	SE
Bud.9	0.20 b	0.007	0.22 b	0.008
M.26	0.26 a	0.007	0.30 a	0.008
M.9	0.27 a	0.005	0.31 a	0.009
p	< 0.001		< 0.001	

Table 2. Estimated marginal means of $fPAR_i$ of 'ANABP 01' apple trees grown on three dwarfing rootstocks (Bud.9, M.26 and M.9) during the 2021–22 season. Measurements were performed on clear sky days in October and March. The standard error of the means (SE) is reported. Letter separation by Tukey's Honestly Significant Differences.

Rootstock	October		March	
	Mean daily $fPAR_i$	SE	Mean daily $fPAR_i$	SE
Bud.9	0.22 b	0.004	0.30 b	0.007
M.26	0.25 a	0.005	0.36 a	0.010
M.9	0.24 ab	0.007	0.35 a	0.010
p	< 0.001		< 0.001	

Table 3. Estimated marginal means of $fPAR_i$ of 'ANABP 01' apple trees grown on three dwarfing rootstocks (Bud.9, M.26 and M.9) during the 2022–23 season. Measurements were performed approximately monthly. The standard error of the means (SE) is reported. Letter separation by Tukey's Honestly Significant Differences.

Rootstock	November/December		January		February		March	
	Mean daily $fPAR_i$	SE	Mean daily $fPAR_i$	SE	Mean daily $fPAR_i$	SE	Mean daily $fPAR_i$	SE
Bud.9	0.27 b	0.014	0.25 b	0.011	0.31 b	0.011	0.30 c	0.018
M.26	0.31 a	0.018	0.30 a	0.012	0.36 a	0.009	0.38 a	0.011
M.9	0.32 a	0.019	0.30 a	0.013	0.35 a	0.013	0.35 b	0.014
p	< 0.001		< 0.001		< 0.001		< 0.001	

Figure 3. Foliage damage to 'ANABP 01' tree in the Sundial Orchard after a hailstorm in Tatura on 22 December 2022. Picture taken on 28 December 2022.

CONCLUSION

Among the studied dwarfing rootstocks, 'ANABP 01' scions grown on M.26 and M.9 achieved better levels of light interception compared to Bud.9. The canopy vigour of trees grown on Bud.9 rootstock may not be suitable to support higher crop loads and its sparseness may increase the risk of sunburn damage.

ACKNOWLEDGEMENTS

This report summary is part of the apple and pear industry's PIPS3 (Productivity, Irrigation, Pests and Soils) program of research and development. The project is funded by Hort Innovation, using the Hort Innovation Apple and Pear research and development levy, contributions from the Australian Government and co-investment from Agriculture Victoria. Hort Innovation is the grower-owned, not-for-profit research and development corporation for Australian horticulture.

REFERENCES

Autio, W. R. (1991). Rootstock Affect Ripening and Other Qualities of “Delicious” Apples. *Journal of the American Society for Horticultural Science*, *116*(3), 378–382. https://doi.org/10.21273/jashs.116.3.378

Barritt, B. H., Konishi, B. S., Drake, S. R., & Rom, C. R. (1997). Influence of sunlight level and rootstock on apple fruit quality. In Barritt, Kappel, Elfving, Flore, Lang, Quamme, & Webster (Eds.), *Poceedings of the 6th International Symposium on Integrating Canopy, Rootstocks and Environmental Physiology in Orchard Systems* (pp. 569–577). Acta Hort, 451, ISHS. https://doi.org/10.17660/ActaHortic.1997.451.66

Darbyshire, R., Goodwin, I., McClymont, L., & Turpin, S. (2018). Addressing heat stress in pome fruit. In S. Hermesch & S. Dominik (Eds.), *Breeding Focus 2018 - Reducing Heat Stress* (pp. 81–97). Animal Genetics and Breeding Unit, University of New England.

Fielder, P., & Comeau, P. (2000). Construction and Testing of an Inexpensive PAR Sensor. *Res. Br., Min. For., Work.-Pap*, 53/2000. https://www.for.gov.bc.ca/hfd/pubs/Docs/Wp/Wp53.htm

Hamadziripi, E. T., Theron, K. I., Muller, M., & Steyn, W. J. (2014). Apple Compositional and Peel Color Differences Resulting from Canopy Microclimate Affect Consumer Preference for Eating Quality and Appearance. *HortScience*, *49*(3), 384–392.

Jackson, J. E. (1978). Utilization of Light Resources by HDP Systems. *Acta Horticulturae*, *65*, 61–70. https://doi.org/10.17660/ActaHortic.1978.65.7

Jackson, J. E., Palmer, J. W., Perring, M. A., & Sharples, R. O. (1977). Effects of Shade on the Growth and Cropping of Apple Trees. III. Effects on Fruit Growth, Chemical Composition and Quality at Harvest and After Storage. *Journal of Horticultural Science*, *52*(2), 267–282. https://doi.org/10.1080/00221589.1977.11514755

Monteith, J. L. (1981). Climatic variation and the growth of crops. *Quarterly Journal of the Royal Meteorological Society*, *107*, 749–774.

Musacchi, S., & Serra, S. (2018). Apple fruit quality: Overview on pre-harvest factors. *Scientia Horticulturae*, *234*(2018), 409–430. https://doi.org/10.1016/j.scienta.2017.12.057

Palmer, J. W., Wünsche, J. N., Meland, M., & Hann, A. (2002). Annual dry-matter production by three apple cultivars at four within-row spacings in New Zealand. *Journal of Horticultural Science and Biotechnology*, *77*(6), 712–717. https://doi.org/10.1080/14620316.2002.11511561

Robinson, T. L., & Lakso, A. N. (1991). Bases of Yield and Production Efficiency in Apple Orchard Systems. *Journal of the American Society for Horticultural Science*, *116*(2), 188–194. https://doi.org/10.21273/jashs.116.2.188

Scalisi, A., McClymont, L., Underwood, J., Morton, P., Scheding, S., & Goodwin, I. (2021). Reliability of a commercial platform for estimating flower cluster and fruit number, yield, tree geometry and light interception in apple trees under different rootstocks and row orientations. *Computers and Electronics in Agriculture*, *191*, 106519. https://doi.org/10.1016/J.COMPAG.2021.106519

Rootstocks, canopy architecture and fruit quality of 'ANABP 01' apples

MADELEINE PEAVEY

Scientists at Agriculture Victoria's (AgVic) Tatura SmartFarm have been exploring the influence of different rootstocks on the quality of 'ANABP 01' apples (marketed as Bravo™).

The *Advancing sustainable and technology driven apple orchard production systems* (AP19003) project is part of the industry's PIPS3 Program. Now in its second year of research activity, the project is aiming to determine adaptions and improvements growers may potentially consider in orchard design and management to combat the impact of increasing climate variability. In this experiment, the Tatura AgVic research team is investigating whether different rootstocks that alter tree canopy architecture, and consequently interception of sunlight, may inhibit or advance fruit ripening and cause variations in fruit quality.

The Bravo™ apple, originating from Western Australia and known for its deep purple-burgundy overcolour, has no published research on its fruit quality response to different rootstocks. The study at the Tatura SmartFarm is being conducted in the Sundial Orchard, a unique multidirectional research orchard, on three dwarfing rootstocks: Bud.9, M9 and M26. Trees are grown at 1 m and 3.5 m tree and row spacing, respectively, and trained to spindles on vertical trellises.

> The variation in scion vigour between the three rootstocks was visually evident from the kickoff of orchard planting and early growth.

About the author:
Madeleine Peavey

Tatura SmartFarm,
Agriculture Victoria

E: maddy.peavey@agriculture.vic.gov.au

Canopy architecture

The variation in scion vigour between the three rootstocks was visually evident from the kickoff of orchard planting and early growth. Bare-rooted Bud.9 trees were notably "weaker" in appearance. Figure 1 shows the 'ANABP 01' scions in their third leaf and demonstrates the fuller canopies of the scions grown on M9 and M26 rootstocks. To quantify this, canopy radiation interception was measured with a custom-built three-metre-wide trolley equipped with light sensors. As expected, trees grown on Bud.9 intercepted significantly less light when compared to trees grown on M9 and M26 (see Table 1).

Fruit quality

Fruit was harvested on 4 April 2022 at optimum storage maturity (i.e. 3–4 starch index). Between rootstocks, significant differences were found for background colour and overcolour, index of absorbance difference (IAD) and starch index (see Table 1). The classes for background colour and overcolour of 'ANABP 01' are depicted in Figure 2. Specifically, Bud.9 rootstock displayed advanced maturity in comparison to the other two rootstocks, with less green background colour, darker overcolour, lower IAD and higher starch index values. No significant effect of rootstock was evident for sunburn susceptibility, individual fruit weight, flesh firmness, soluble solids concentration and dry matter content.

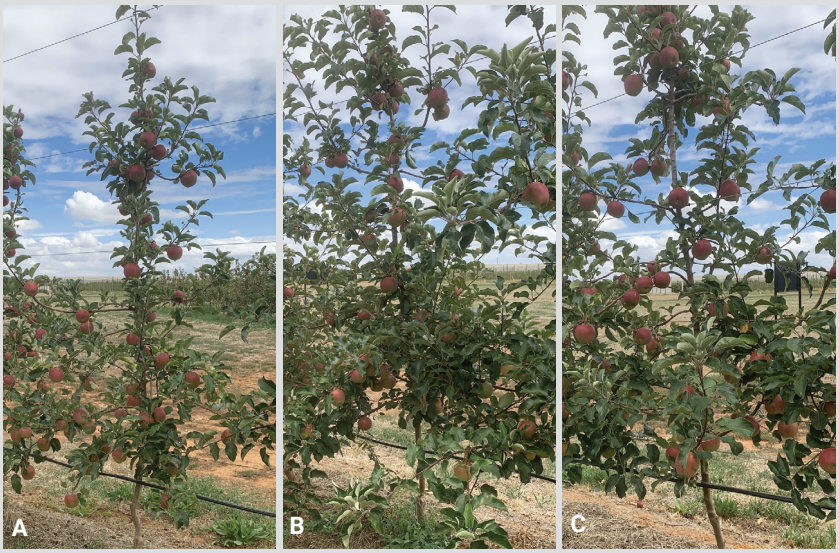

Figure 1: 'ANABP 01' trees at the Tatura SmartFarm in their third leaf grown on Bud.9 (A), M9 (B) and M26 (C) rootstocks.

Table 1: Mean values of significantly different (Analysis of variance $p < 0.05$) parameters of 'ANABP 01' apple fruit grouped by rootstock in a randomised block design. Data represents combined 2020–21 and 2021–22 seasons.

Rootstock	Effective area of shade (%)	Background colour	Overcolour	IAD	Starch index
Bud.9	30.4	2.5	3.1	0.99	3.6
M9	34.8	2.2	2.9	1.08	3.3
M26	35.5	2.0	2.8	1.06	3.2

What it means for growers

'ANABP 01' is performing well on all trialed rootstocks. The fruit grown on Bud.9 developed deeper overcolour and were advanced in their maturity, caused by a more open canopy allowing for increased sunlight penetration. A negative correlation (Pearson's $r = -0.271$; $p < 0.05$) was discovered between effective area of shade (EAS) and overcolour, indicating that trees that fill more of the available space achieve less purple-burgundy colour development. The time taken by trees grown on Bud.9 to reach desired tree height and to fill out would be a drawback and could sacrifice early yields; however, the open canopy would be beneficial if growing 'ANABP 01' apples under netting. M26 has also demonstrated good performance in Western Australian trials (Steele et al., 2017)[1]. Long-term effects of rootstock on fruit quality and yield parameters will be investigated in the following seasons. AFG

[1] Steele, J., Lacey, K., Sutton, J., 2017. *Technical Information Dossier for Australia Apple Variety: ANABP 01.*

Acknowledgements:
The PIPS3 *Advancing sustainable and technology driven apple orchard production systems* (AP19003) project has been funded by Hort Innovation, using the apple and pear research and development levy, contributions from the Australian Government and co-investment from Agriculture Victoria. Hort Innovation is the grower-owned, not-for-profit research and development corporation for Australian horticulture.

> 'ANABP 01' is performing well on all trialed rootstocks.

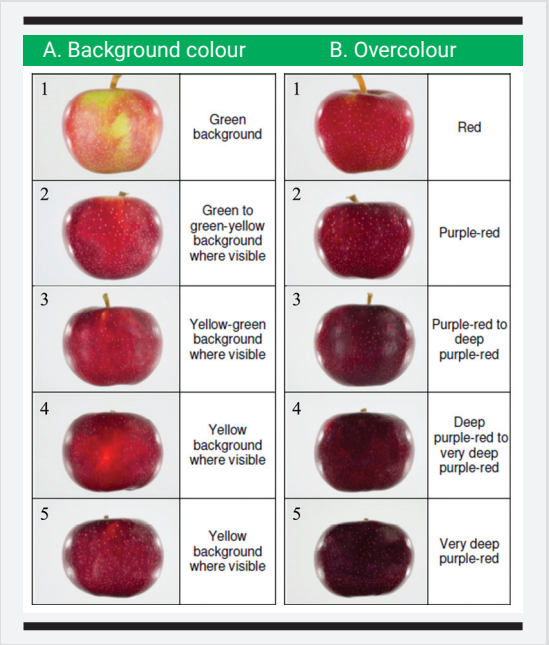

Figure 2: 'ANABP 01' colour classes (1–5) for (A) background colour and (B) overcolour. Adapted from Steele, J., Lacey, K., Sutton, J., 2017. *Technical Information Dossier for Australia Apple Variety: ANABP 01.*

Effects of crop load on fruit quality in 'Rosy Glow' apples

TIM PLOZZA AND CHRISTINE FRISINA

Higher crop loads have an adverse effect on fruit quality, a five year research experiment has shown.

Varying the crop load of apple trees is a tool that can be used by growers to produce fruit of a particular size range to suit market requirements. For example, leaving a larger number of fruit on the trees will result in smaller fruit since the limited amount of photo assimilates produced by the trees must be distributed amongst a greater number of fruit.

Care needs to be taken, however, since there are limits to the crop load — number of fruit per unit of trunk cross-sectional area (TCSA) — some cultivars can sustain before they tip into a biennial bearing cropping pattern, where excessive numbers of fruit one season cause a reduced number of flowers the following season, potentially resulting in a lower crop load, yield, and income for the farmer.

Similar to the effect on fruit size, crop load also affects the quality of the fruit, and a recent experiment conducted by Agriculture Victoria at Sanders Apples, a commercial orchard at Three Bridges in the Yarra Valley, has highlighted these effects.

The experiment studied the effect of crop load on return bloom and fruit quality in 'Rosy Glow' (marketed as Pink Lady) apples and showed that as well as reducing return bloom, particularly after prolonged high crop loads over several seasons, higher crop loads also have negative effects on fruit quality.

The experiment ran for five seasons. Thirty trees in their 3rd leaf had one of five crop load treatments applied: 10, 50, 100, 150 or 200 per cent of the normal grower practice of eight fruit/cm^2 trunk cross sectional area (TCSA). This was done either on a constant crop load regime (same crop load each year), or a variable crop load regime (alternating high-low year-to-year, e.g., 10 per cent became 200 per cent; 150 per cent became 50 per cent. The number of flower clusters on each tree was counted manually each season at full bloom to determine return bloom, and the clusters thinned by hand to leave the required number of fruit per tree.

From approximately 28 days before harvest, a random sample of fruit on each tree was tagged and measured weekly with a DA-meter. These non-destructive measurements of Index of Absorbance Difference (I_{AD}) were used to determine the effects of crop load on changes in fruit maturity and to predict ideal harvest times. Two fruit harvests were conducted each season, the first occurring when the average maturity of the '100 per cent' treatment (i.e., grower practice) reached the target I_{AD} value (I_{AD} = 1.1).

At this harvest, all fruit perceived to have similar or less green background colour than fruit at the target I_{AD} value were picked, or a minimum of 20 fruit per tree for comparative purposes. The second harvest occurred approximately two weeks later. All harvested fruit were counted and weighed to obtain total yield and average fruit weight, and a range of fruit measurements (fruit weight, colour, flesh firmness and soluble solids concentration) were conducted on a random subsample of 20 fruit per tree.

The results showed that, on average, fruit from the higher crop load treatments developed less colour intensity and matured approximately one week later than fruit from trees with a normal crop load, whereas fruit from the lowest crop load trees developed more colour intensity, as shown in Figure 1, and reached maturity almost two weeks earlier. The differences in colour intensity could be due to a number of factors such as the greater competition for assimilates in high crop load trees.

There was a consistent strong negative correlation of soluble solids concentration with crop load, as shown in Figure 2. This effect was not significantly different for constant and variable crop load trees, indicating that the effect was a function of the carbon balance in the trees during the growing season. Although soluble solids concentration values varied year-to-year, fruit from the highest crop load trees were generally 2.5–3 °Brix lower than those from trees with the lowest crop loads.

The effect of crop load on flesh firmness varied depending on whether the trees had a constant

About the authors:
Tim Plozza and Christine Frisina

Agriculture Victoria, AgriBio, Bundoora

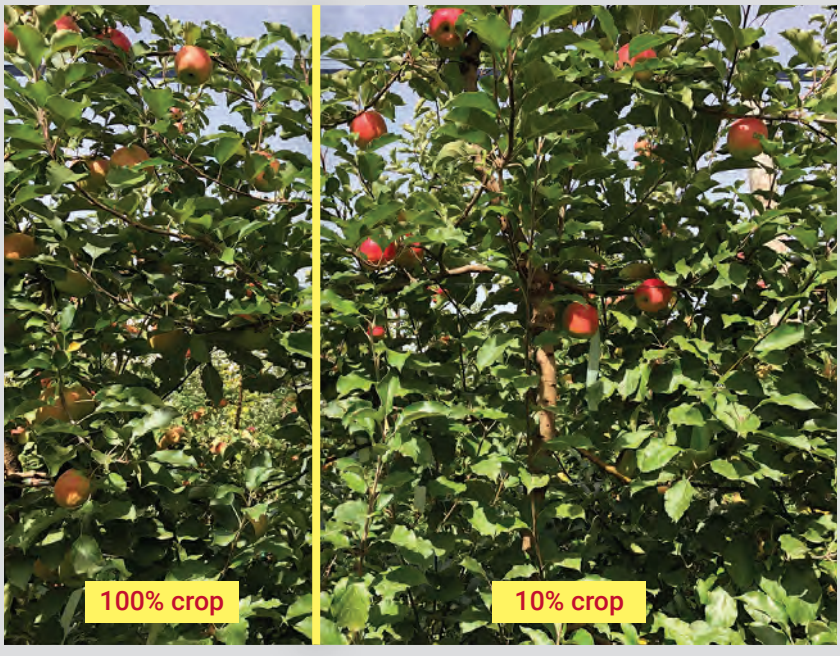

Figure 1: Comparison of 'Rosy Glow' fruit colour from a tree with a normal crop (far left) and a tree with 10% of the normal crop load (centre-right). Photo taken late March 2019.

or variable crop load treatment. Flesh firmness was not affected by crop load for the constant crop load treatments, whereas there was a strong negative correlation of firmness and crop load for variable crop load trees. This indicates there may be a carry-over effect of the previous season's crop load, and that consistent crop loads year to year are more likely to yield consistent flesh firmness.

Comparison of data from the final two seasons of the experiment, when tree canopy was approaching full size and the crop load treatments had taken effect, showed that target constant crop loads of 100 per cent and 150 per cent of normal grower practice produced the highest yields overall.

However, the 150 per cent treatment trees were not able to achieve their target crop loads in these seasons due to reduced flowering and fruit drop during the growing season, which is indicative of stressed trees due to an overly high crop load. These trees also produced fruit with soluble solids content below 13 °Brix in these seasons, which is below the quality specifications of Pink Lady. These results indicate that the normal grower practice of eight fruit/cm^2 TCSA was the best crop load for consistent high yields year-to-year, and better fruit quality than higher crop loads.

In summary, the experiment showed that higher crop loads resulted in smaller, later maturing fruit, which had less colour and soluble sugars.

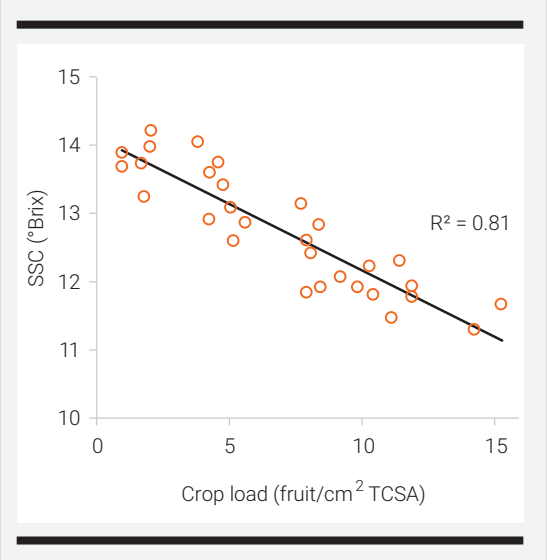

These results show that while higher crop loads are an effective means of producing smaller fruit, which may be appealing for some markets and may also increase yields in the short term, this practice will have an adverse effect on fruit quality, which may affect consumer acceptance, as well as potentially limiting crop load and yield in the following season due to biennial bearing. AFG

Figure 2: Relationship between soluble solids concentration (SSC) and actual crop load [fruit/cm^2 TCSA] of each 'Rosy Glow' plot tree for the 2019–20 season.

Acknowledgements:
This article is a component of the apple and pear industry's PIPS3 (Productivity, Irrigation, Pests and Soils) program of research and development funded by Hort Innovation, using the Hort Innovation Apple and Pear research and development levy, contributions from the Australian Government and co-investment from Agriculture Victoria. Hort Innovation is the grower-owned, not-for-profit research and development corporation for Australian horticulture.

Unveiling apple block variability using Green Atlas Cartographer

ALESSIO SCALISI

New scanning and mapping technology has insights for managing crop load variability and fruit quality in apple orchards.

Excessive variability of crop load, fruit size and skin colour in apple orchards can cause loss of profit for growers. Currently there are no well-established methods to quantify crop load, fruit size and fruit colour variability objectively and accurately within orchard blocks or to inform and automate precision orchard management strategies. The apple cultivars sold domestically under the name Pink Lady can have variable fruit quality, with some fruit not meeting marketing specifications. An adequate level of fruit redness is one of the key factors that determines premium price for the produce.

Pioneering research at Agriculture Victoria's Tatura SmartFarm, and in Goulburn Valley commercial orchards, is validating new technology to measure yield and fruit quality variability. The benefit of exploring this technology is its potential to inform more efficient management options. The current work is part of the PIPS3 Program's *Advancing sustainable and technology driven apple orchard production systems* (AP19003) project led by Agriculture Victoria.

About the author:
Alessio Scalisi

Tatura SmartFarm, Agriculture Victoria

E: alessio.scalisi@agriculture.vic.gov.au

Measuring and mapping fruit number, fruit size and skin colour

The Australian company, Green Atlas, has commercialised the Cartographer, a ground-based platform that is equipped with a number of sensors – RGB cameras, LiDAR, GPS – used to estimate crop parameters such as flower and fruit number, and tree geometry attributes such as canopy height, area and density. The collaboration between Green Atlas and Agriculture Victoria aimed to validate the capability of the technology to accurately detect flower and fruit, after calibration against manual counts, and to test the accuracy and precision of fruit diameter and colour estimates from the detections.

In a recent study of ANABP 01 apples (marketed as Bravo™, the Cartographer was capable of predicting flower number, fruit number and yield with errors below 5 per cent. Accurate detections of fruit are a prerequisite for accurate estimates of fruit size and colour with machine vision, as AI-derived detection boxes are used for the extraction of fruit diameter and colour attributes. Fruit skin colour was assessed using an intuitive colour development index (CDI) – a colour attribute derived from hue angle that ranges from 0 (pure green) to 1 (pure red). ANABP 01 fruit diameter and CDI were predicted with an accuracy higher than 95 and 80 per cent, respectively.

During the 2021–22 season, Agriculture Victoria scanned a commercial orchard of Ruby Pink apples (Plunkett Orchards, Ardmona) for detections of fruit number, fruit diameter, CDI and tree geometry (canopy height, canopy area, canopy density and cross-sectional leaf area).

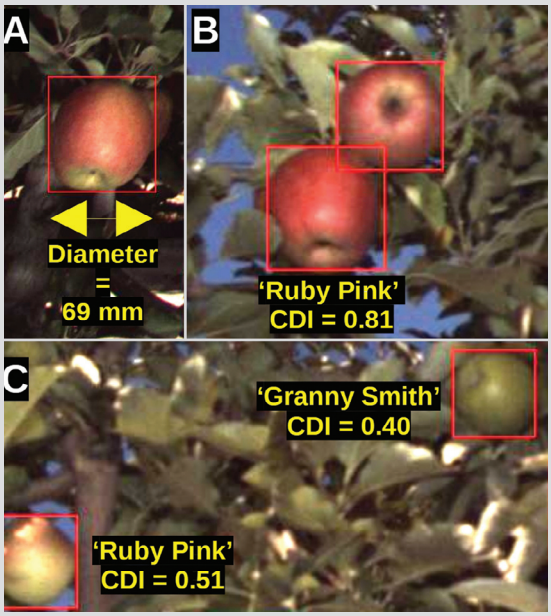

Examples of size and colour estimates of fruit detected by Green Atlas Cartographer: (A) Ruby Pink fruit diameter, (B) Ruby Pink colour development index (CDI) and (C) green Ruby Pink (left) and Granny Smith (right) CDI.

Measurement time	Cartographer output	Average in the block	Coefficient of variation (%)
Pre-thinning (December 2021)	Calibrated fruit number (n/tree)	173	49
	Fruit diameter (mm)	45	8.8
	Colour development index (CDI, 0–1)	0.41	8.8
Pre-harvest (April 2022)	Canopy height (m)	4.35	8.5
	Canopy area (m^2)	3.18	19
	Canopy density (0–1)	0.72	20
	Cross-sectional leaf area (m^2)	2.35	29
	Calibrated fruit number (n/tree)	101	42
	CDI (0–1)	0.72	8.9
	Fruit diameter (mm)	74	8.7

Average crop parameters and their variability (coefficient of variation) estimated using Green Atlas Cartographer in a commercial Ruby Pink block (Plunkett Orchards, Ardmona) during 2021–22.

The block was scanned in December (before thinning) and in April (before harvest). Fruit numbers per images were calibrated to generate estimates of fruit number per tree, with errors of 7 and 6 per cent respectively, for the two dates. Spatial maps of crop parameters were generated and block averages and relative measures of spatial variability (coefficient of variation, percentage) were estimated. The relatively high variability of fruit number (> 40 per cent) observed in the block, on both measurement dates, was mainly attributed to the very low crop load on Granny Smith pollenisers that likely drove low pollination and crop load in Ruby Pink.

At harvest, fruit diameter and CDI had an average of 74mm and 0.72 respectively, and relatively low spatial variability (coefficient of variation < 10 per cent).

The fruit number map helped identify orchard hotspots with low crop load, mostly corresponding to pollenisers. There was a tendency for higher yields in the westernmost rows of the block. CDI was significantly reduced ($p < 0.001$) with higher canopy height, canopy area, canopy density, cross-sectional leaf area and fruit number per tree, and it was directly correlated with increasing fruit size. Interestingly, the CDI map unveiled a row in the block (thirteenth row from west to east) with greener fruit in which pruning and thinning were not managed following the standards utilised in the rest of the block. This was due to an ongoing crop load experiment as part of the AP19003 project.

> The maps generated by the Cartographer can be used to identify areas within a block that need additional management inputs ...

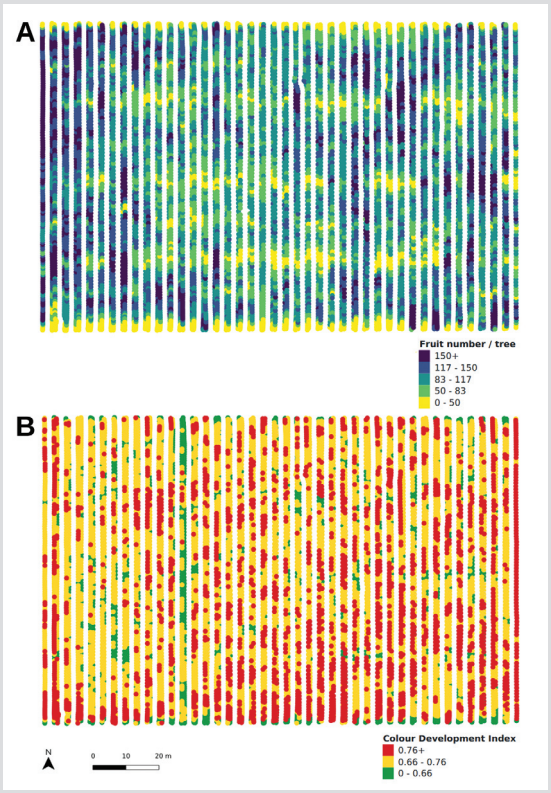

Spatial maps of (A) calibrated fruit number per tree and (B) colour development index (CDI) in a commercial Ruby Pink block (Plunkett Orchards, Ardmona) scanned in April 2022.

Further information:
Find out more about the utilisation of the Green Atlas Cartographer at https://greenatlas.com.au/.

For videos on the research and outcomes to date of the Green Atlas Cartographer, head to the PIPS3 Program resources webpage: https://apal.org.au/programs/more-industry-programs/pips3program/ap19003/

Acknowledgements:
The PIPS3 Program's *Advancing sustainable and technology driven apple orchard production systems* (AP19003) project is funded by Hort Innovation, using the apple and pear research and development levy, contributions from the Australian Government and co-investment from Agriculture Victoria. Hort Innovation is the grower-owned, not-for-profit research and development corporation for Australian horticulture.

Growers should aim to obtain optimal fruit number, fruit size and colour while minimising the variability in the block. The maps generated by the Cartographer can be used to identify areas within a block that need additional management inputs (e.g. follow-up thinning) to produce high yields of quality fruit. In addition, packout yield can be forecast, irrigation requirements can be determined, and orchard automation and mechanisation can be better implemented using the Cartographer data. This data has great potential to be reutilised in other machines for spatially precise orchard operations (e.g. variable rate spraying, mechanical thinners, mechanical hedgers).

Agriculture Victoria is currently conducting research on extracting zonal data generated from the Cartographer to determine relationships between yield and fruit quality, and tree geometry parameters that can drive precision management strategies. AFG

Advancing sustainable and technology driven apple orchard production systems

Technical Report: New technology and advanced management system for apple

Agriculture Victoria Research

May 2023

VICTORIA State Government | Jobs, Precincts and Regions

AGRICULTURE VICTORIA

Author: Alessio Scalisi

Project RDC Number: AP19003

Project RCM Number: 6472

Department of Jobs, Precincts and Regions
1 Spring Street Melbourne Victoria 3000
Telephone (03) 9651 9999

Contents

EXECUTIVE SUMMARY

The Green Atlas Cartographer uses a combination of sensors (e.g., RGB cameras, LiDAR, GPS, thermal sensors) mounted on a platform on an electric vehicle, to gather data while driving through orchard rows. The Cartographer is currently available to measure the spatial distribution of fruit number, fruit size and colour in apples. A protocol for machine operation outdoor is described. Calibration is required for fruit number estimates, but unnecessary for fruit size and colour. Once the desired output is obtained, it is presented in geo-referenced points that can be colour-coded to provide an orchard map of important crop variables. These maps can be overlaid to understand how different variables relate to each other. For management purposes, it is recommended to create spatial zones from data points, in order to simplify operations. At least three main zoning approaches are described—contouring, interpolation and gridding with pseudo-plots. Data can be summarised into management zones such as the pseudo-plots, and then extracted for each block to model relationships between fruit number, size and colour that are specific for that block. These provide valuable support for determining the most appropriate crop load that is needed to achieve harvest targets. The availability of technology that serves multiple purposes is of pivotal importance for industry growth, as it may potentially reduce production costs such as labour, and provide long-term benefits such as the creation of historical databases that can help measure performance over many years and support business decisions.

INTRODUCTION

This technical report is a deliverable for milestone 107 of the project 'Advancing sustainable and technology driven apple orchard production systems' (AP19003).

The report details a protocol on the use of the Green Atlas *Cartographer* (i.e., a mobile platform with multiple sensors) for estimates of fruit number, diameter and colour in apples, and recommends two advanced uses of data—spatial zoning for management purposes and block-specific relationships to define crop load and fruit quality targets. This report contributes towards meeting the project objectives by providing instructions to operate the platform and scientifically sound guidelines for orchard best-practices. The results presented in this report reflect a joint effort of Agriculture Victoria and Green Atlas staff and benefited from the valuable support of Plunkett Orchards' staff.

Background

Modern horticulture is moving toward increased mechanisation, automation, robotics, and non-destructive sensing and monitoring. The integration of technologies that are already adopted in other industries into horticulture systems aims to increase resource use efficiency — including labour — and make orchards more profitable. For this purpose, several recent studies have focused on the application of machine learning algorithms to detect tree structures (e.g., flowers, fruit, architecture) using sensorised robots or platforms.

Commercial services such as the Green Atlas Cartographer use a combination of sensors (e.g., RGB cameras, LiDAR, GPS, thermal sensors), mounted on an electric vehicle platform, to gather data while driving through orchard rows. The Cartographer is currently available to measure the spatial distribution of fruit number, fruit size and colour in apples and to measure tree geometry parameters such as canopy area, canopy density and cross-sectional leaf area (CSLA). Canopy area (m^2) represents the area of the polygon drawn around the LiDAR-generated points in the scanned transect, excluding the trunk. Canopy density represents the ratio between the number of light beams generated by the LiDAR that bounces back to the light source and the total number of emitted light beams. CSLA is the area of the points (comparable to leaves) within the canopy area polygon. The Green Atlas Cartographer is rapidly expanding its capability and is currently offering flower cluster and fruitlet cluster number predictions, although a scientific calibration-validation process should be carried out.

Typically, fruit colour is assessed after harvest using cameras mounted in fruit grading machinery. However, orchard estimates of fruit colour can be linked to fruit maturity in some cultivars and can drive orchard management strategies to improve skin colour formation in situ, such as leaf removal, use of reflective mulch or the application of biostimulants to enhance anthocyanin pigmentation. Fruit colour estimation using non-contact sensors such as RGB or RGB-D cameras mounted on aerial and ground vehicles is difficult as it is influenced by the variable orchard light environment due to the combined effects of clouds, sun angle, netting, etc. Green Atlas *Cartographer* mounts strobe lights that continuously flash tree canopies to attenuate any potential effect of external light on colour measurements by the RGB cameras.

Objectives

The objective of this report is to describe the Green Atlas Cartographer technology and its use, and to elaborate on potential usage of data for management purposes. This report can serve as a guideline for apple growers and scientists to answer agronomical and tree productivity questions in complex scenarios affected by multiple environmental variables and management strategies.

OPERATING GREEN ATLAS CARTOGRAPHER

The mobile platform *Cartographer* (Green Atlas, Alexandria, NSW, Australia) is used by Agriculture Victoria Research (AVR) to identify fruit, measure fruit size and colour, and predict yield in fruit and nut tree crops (Figure 1). The *Cartographer* owned by AVR is a combination of hardware and software installed on an electric all-terrain vehicle (ATV) (Ranger EV, Polaris Industries Inc). The *Cartographer* requires independent charging operated through a smart Bluetooth charger. The plug for charging is separate from the ATV's charging system. It's good practice to regularly charge both systems.

Figure 1. Cartographer (Green Atlas, Alexandria, NSW, Australia) used by Agriculture Victoria Research.

Data is logged in a removable disk provided by Green Atlas. The disk is plugged into the main unit through a USB port. It is important to go through the following steps prior to initialising the scanner:

- Check sensors, cameras and batteries for dirt, dust, water or signs of damage. Clean if dirty using a soft cloth.
- Ensure connections and sensors are firmly mounted on the frame (no connections or bolts have become loose).
- If damage is observed contact Green Atlas.
- Avoid scanning in rain or fog.
- Remove mains charging cable if system is on charge.
- Drive to an outdoor location for GPS signal.

For fruit colour measurements, it is advised to scan the orchard block at solar noon, early in the morning, late in the afternoon or at night. It is best to avoid scans done in the middle of the morning or afternoon if accurate colour estimation is desired. The scanner is powered on using a yellow button on the circuit breaker (Figure 2. Circuit breaker with yellow and red buttons.Figure 2). The strobe cameras will flash once and will start to warm up. After approximately 5 minutes, the strobe lights will start flashing intermittently. At this stage is important to check that all strobe lights are flashing evenly. This step requires approximately 5 more minutes. When strobe lights stop flashing the system is ready for orchard scans. Next, the vehicle can be positioned at the start of the block rows that need to be scanned. Logging is started and stopped either via a physical logging switch or via a smartphone connection (via WiFi). AVR uses the smartphone connection, as the user interface allows additional checks on the sensors and enables metadata to be entered on the scan. The user interface to enter metadata and start and stop each log is shown in Figure 3. Once ready for logging a scan, the **Start** button is pressed and when the scan is completed logging is terminated using the **Stop** button. If another orchard block scan is required, the process can be repeated using the start and stop routine. It is advised to do individual logs for different orchard blocks rather than leaving the logging on while moving from one block to the other.

When scanning is completed for all the orchard blocks, the *Cartographer* scanner is shut down by turning off the power using the red button in the circuit breaker (Figure 2).

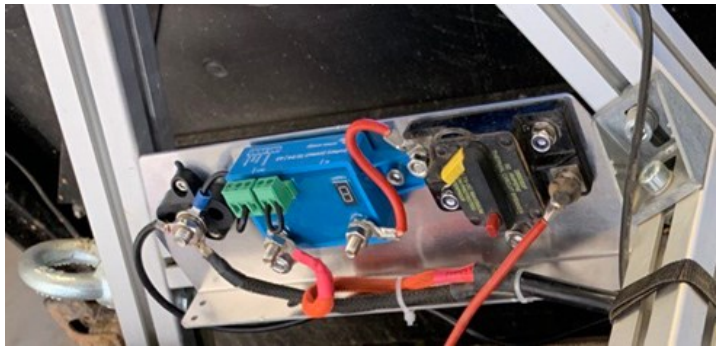

Figure 2. Circuit breaker with yellow and red buttons.

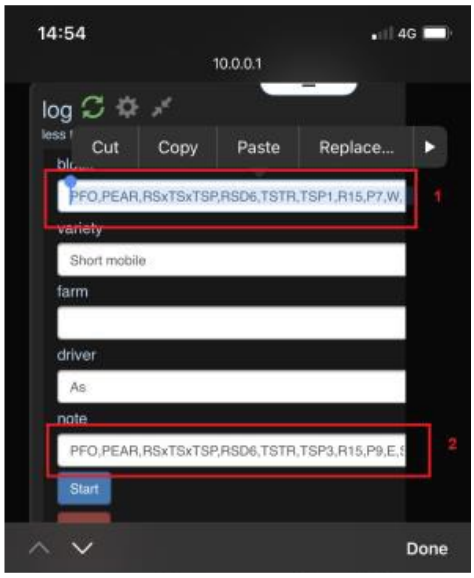

Figure 3. Smartphone application interface to operate Cartographer.

The vehicle should then be parked in a secure, dry and covered area where it can be plugged in for charging. Subsequently, the portable disk needs to be unplugged from the *Cartographer* scanner and plugged into one of the USB ports on the Green Atlas processor (Figure 4).

Figure 4. Green Atlas processor with two portable disks.

When fruit are on the trees and the appropriate crop-specific processing model is applied, *Cartographer*'s settings automatically produce data for fruit number, fruit diameter and colour development index (CDI). Data will start to be processed as soon as the disks are plugged into the processor and the crop-specific model is applied. Results will be remotely available on request. Green Atlas estimated that the time utilised to process the raw data is typically 1.5-fold the time used for scanning (for example: if scanning is 1 hour, processing will need 1.5 hours). The Green Atlas software interface (Figure 5) allows (i) visualisation of orchard maps, (ii) data extraction, (iii) creation of pdf summaries and statistics, (iv) and zoning to identify management zones and produce georeferenced data to feed to orchard management machines such as sprayers, weeders and hedgers.

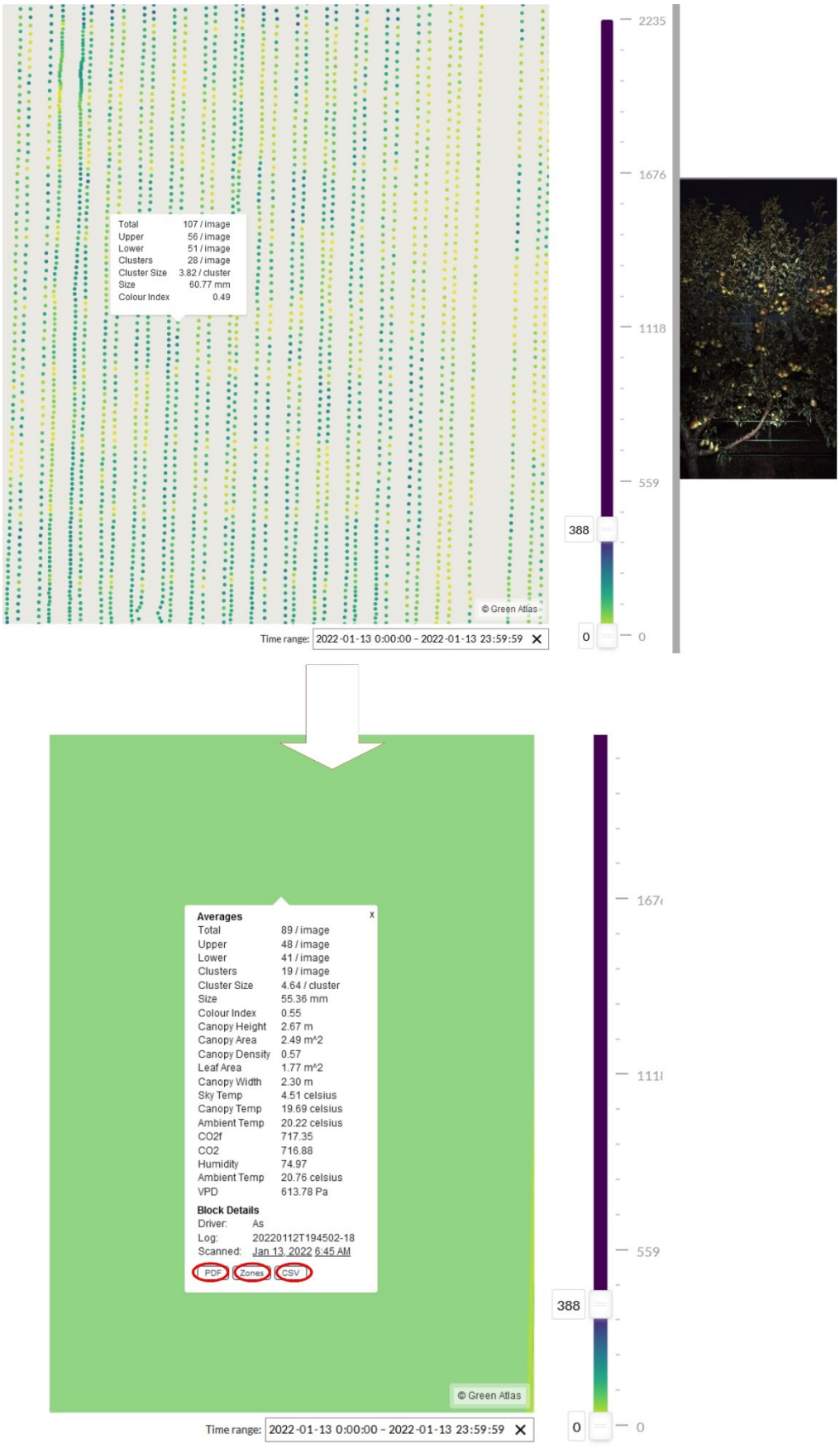

Figure 5. Green Atlas software interface.

CALIBRATION REQUIREMENTS

A process of field calibration is required to convert uncalibrated relative estimates of fruit number per image to calibrated estimates of the number of fruit per tree (or per metre of row) and per block. Green Atlas provides a hand count template sheet (Figure 6) to be completed for each orchard block that requires calibration. It is important to note that after scientific testing and validation carried out by AVR, calibration is not a requirement for fruit diameter and CDI data.

	A	B	C	D	E	F	G	H	I
1	Where / When				Crop Information				
2	Client		Crop		Row Spacing	e.g. 3.7 m			
3	Orchard		Variety		Tree Spacing				
4	Block		Rootstock		Block Area / Size	e.g. 11.32 ha			
5	Scan Date		Architecture		# of Trees				
6	Count Date								
7									
8	Zone A		Zone B		Zone C		Zone D		
9	Scan Time		Scan Time		Scan Time		Scan Time		
10	Row		Row	e.g. 7 from west	Row	e.g. 26 from E	Row	e.g. 10 from N	
11	Zone Length		Zone Length		Zone Length		Zone Length		
12	Fruit Size		Fruit Size		Fruit Size		Fruit Size		
13	Hand Counts		Hand Counts		Hand Counts		Hand Counts		
14	Tree 1		Tree 1		Tree 1		Tree 1		
15	Tree 2		Tree 2		Tree 2		Tree 2		
16	... 3		... 3		... 3		... 3		
17	4		4		4		4		
18	5		5		5		5		
19	6		6		6		6		
20	7		7		7		7		
21	8		8		8		8		
22	9		9		9		9		
23	10		10		10		10		
24	mean	computed	mean	computed	mean	computed	mean	computed	
25	total	0	total	0	total	0	total	0	
26	n	0	n	0	n	0	n	0	
27									

Figure 6. Hand Count Template provided by Green Atlas for field calibrations visualized in a Microsoft Excel spreadsheet.

Field calibration for fruit counts require the selection of calibration zones (7–15 m sections along a row for trellises, or a set of adjacent trees for non-trellises) that are representative of the variability across the orchard block. The more calibration zones are manually counted, the most accurate orchard predictions are generated. It is advised to select at least three zones with low, medium and high yield within the block to be calibrated. Next, fruit need to be counted within the zones. It is preferrable to have counts for individual trees and record all the information required to fill the hand count template sheet (Figure 6). The same calibration zones manually counted need to be scanned by starting and stopping the *Cartographer* logging for each zone, rather than leaving it logging while driving from zone to zone. To scan, the following steps need to be followed:

- Position and drive the ATV such that the left camera will view the zone.
- Position the ATV approximately 10 m before the start of the zone.
- For your own reference later, note a zone designation (e.g., A, B,C or D) and the corresponding time of day, the block and the location in the block — whatever may be needed to help identify this zone in the map later.
- Turn the logging switch on and wait for audible or visible confirmation that the strobes are firing.
- Drive at a constant and slower than normal scan speed until you have certainly passed the end of the zone.
- Stop the log.
- Drive to the other side of the zone (next interrow) and repeat the steps above.
- Once finished, submit the data using the calibration user interface in the Green Atlas Software (Figure 7).

The note keeping requires attention to detail and effort to avoid sources of ambiguity. Doing the count accurately is critical to getting the most accurate calibration and yield estimation results — the machine vision process cannot compensate for a bias in manual counting errors. Similarly, if ambiguity in note keeping results in a perfectly accurate count being associated to the wrong tree, the resulting yield estimation error can be significant.

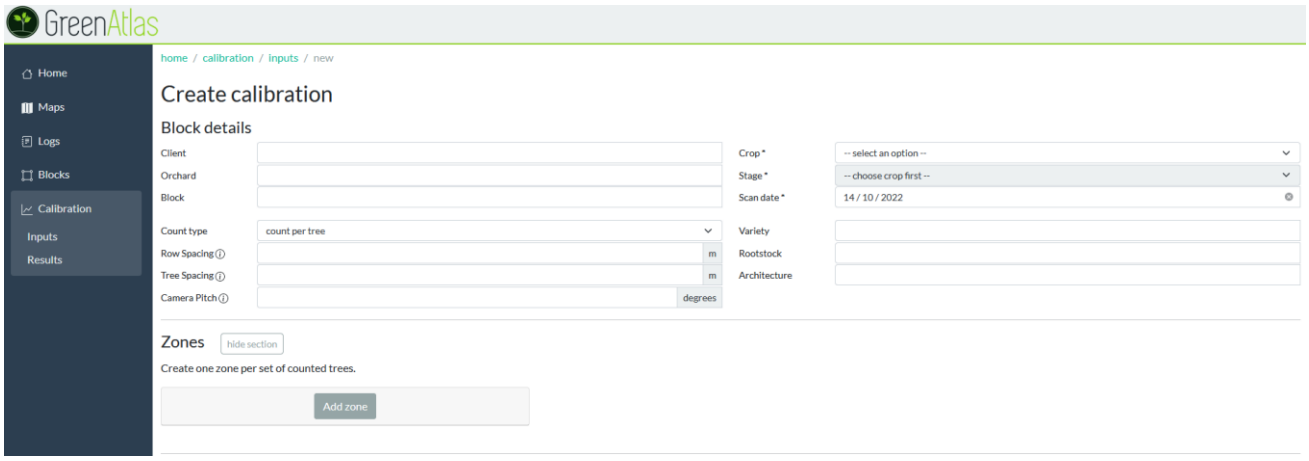

Figure 7. Calibration user interface in the Green Atlas software.

Applications that require relative spatial data do not require calibration. For example, if it is sufficient to know where there is more and less yield, including how much more or less in a relative sense (e.g., 1.2 times as much yield in location A compared to location B), then calibration is not required at all. In this case, the uncalibrated maps produced by *Cartographer* represent "detected fruit per image" as opposed to fruit per tree and the step of field calibration can be skipped entirely.

Field calibration is required to translate the scale in *Cartographer* maps from "detections per image" to an estimate of "count per tree" or "count per metre of row". This is also required to estimate the total count for any given region, including a whole block or set of blocks, a whole row, or some arbitrary region within a block.

One calibration result may be used for multiple blocks, if those blocks have similar properties such as rootstock and cultivar, planting density, tree and row spacing, canopy architecture and pruning style, age of trees, terrain slope, over-canopy netting, and management practices. For blocks that differ in these properties, the field calibration process should be done for each different style of block. For example, if a farm features 10 blocks of mature 'Gala' apples on 3.6 m row spacing with a V-trellis, and 5 blocks of 'Rosy Glow' apples on a 4 m row spacing with a vertical trellis, then at least two independent field calibrations must be done. Amongst similar blocks, a minimum of only one field calibration process should be done; performing this for more than one block will lead to greater accuracy.

SPATIAL ZONING FOR MANAGEMENT PURPOSES

Once data on fruit number per tree are calibrated and accurate estimates are produced, it is possible to extract geo-referenced data points as shown in Figure 8 (generated in April 2022). Although the calibrated fruit number points can be used to understand and navigate within-block spatial variability, it is practically challenging to modulate and implement a mechanical and/or automated management strategy (e.g., Darwin thinning, Waatic spraying) at a point level. Therefore, these data points can be used to create orchard zones to simplify orchard operations such as spraying, thinning and picking. The main zoning approaches that are believed to be valuable for orchards are: (I) contouring, (II) interpolation, (III) grids and pseudo-plots.

I. Contouring

Green Atlas offers a zoning creation approach that is defined 'contouring'. Contours are lines that connect locations of equal value. The line features connect cells of a constant value in the input. Contour lines are often generally referred to as isolines but can also have specific terms depending on what is being measured. Some examples are isobars for pressure, isotherms for temperature, and isohyets for precipitation. Green Atlas zoning works similarly to the method utilised by the QGIS 'Contour' plugin that generates a contour layer from a point vector layer. To generate zones from a heatmap in the Green Atlas software, the user will need to click on the zone button shown in Figure 5 (bottom). There, the user can decide the number of bands to visualise and whether to generate a simple zone map or a zone map that is compatible with management technologies such as the Darwin thinner or the Waatic sprayer, as shown in Figure 9.

When the user selects one of the management technologies from the drop-down menu, the graphic interface allows to input user-defined thresholds for additional variables, such as rates of spray (L/ha) for the Waatic sprayer, or revolutions per minute (RPM) for the Darwin thinner. This is beneficial, as if the orchard manager uses this method, the operator will not need to convert from, for instance, flower density to intensity of chemical or mechanical thinning.

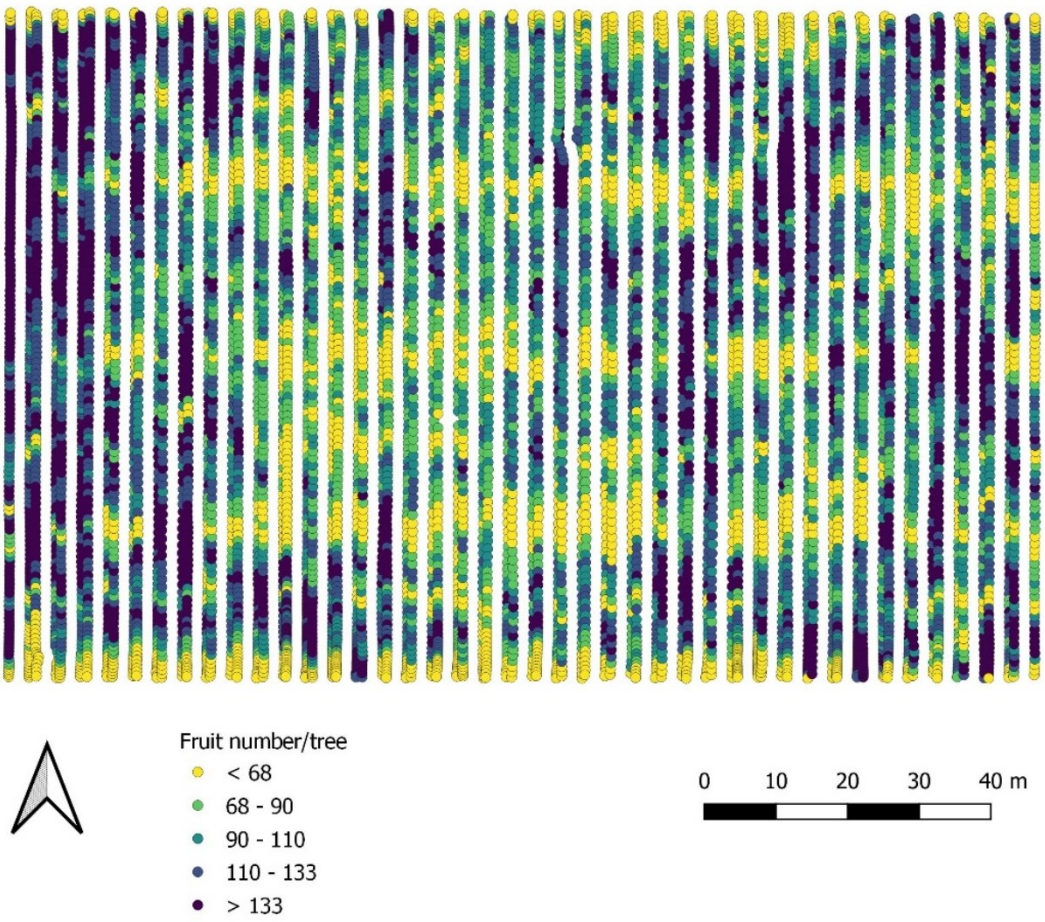

Figure 8. Heatmap of fruit number per tree obtained by subdividing data into 5-quantile classes, colour-coded with five Viridis colour palettes.

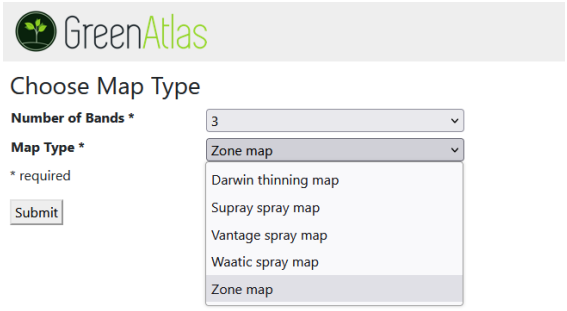

Figure 9. Zoning options offered by Green Atlas.

An example of a contoured map derived from calibrated points is shown in Figure 10. In this case, we classified contours into Low, Medium and High crop loads based on subjective fruit number thresholds. A map generated for use with a Waatic sprayer or a Darwin thinner would appear identical to the one shown in Figure 10, except for the classification into spray rates or RPM.

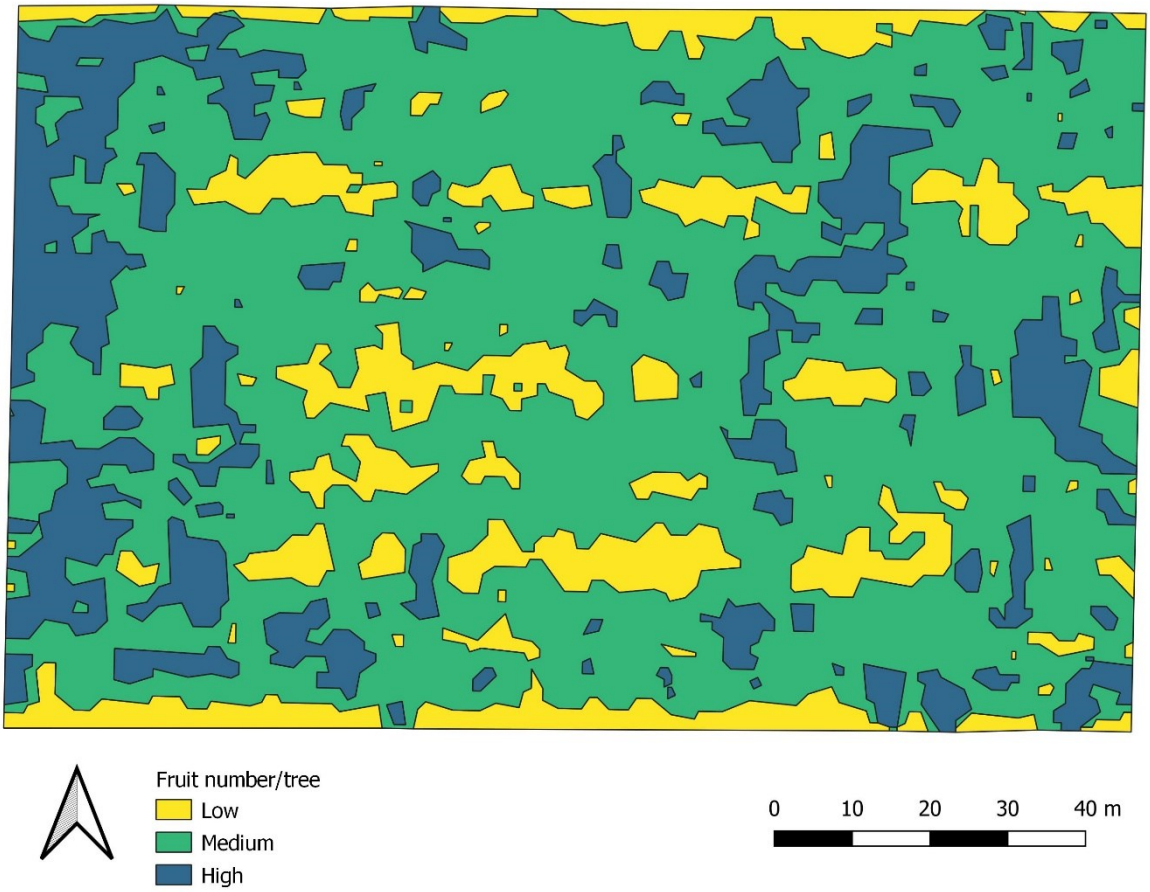

Figure 8. Three-zone (low, medium and high) contour map obtained from calibrated data points of fruit number per tree. Map colour-coded with five Viridis colour palettes.

II. Interpolation

Spatial interpolation uses points with known values to estimate values at other unknown points in between. Different spatial interpolation approaches are available via GIS software, such as the Triangulated Irregular Network (TIN), Inverse Distance Weighting (IDW), Spline interpolation, and Kriging interpolation. Each triangulation algorithm has its own advantages. As an example, we used IDW to show how management zones can be classified via interpolation approaches. An IDW-generated zone map is shown in Figure 11 for the data previously presented in Figure 8.

III. Grids and pseudo-plots

Overlaying a grid to data points to generate pseudo-plots—a concept that recalls experimental design plotting—is another possibility to summarise data in a customised number of zones. For example, if we used a grid with rectangles measuring 8 and 7 m vertically and horizontally, respectively, and we overlaid to the data points in Figure 8, we can obtain a spatial grid as shown in red in Figure 12.

In such a grid, means of fruit number per tree can be calculated and other statistics summarised, and then pseudo-plots can be colour-coded as shown for previous zoning approaches. An example of a map obtained with grids of pseudo-plots is shown in Figure 13.

Contouring, interpolation and grids with pseudo-plots are alternative methods that need to be further tested and validated for their suitability to generate reliable management units.

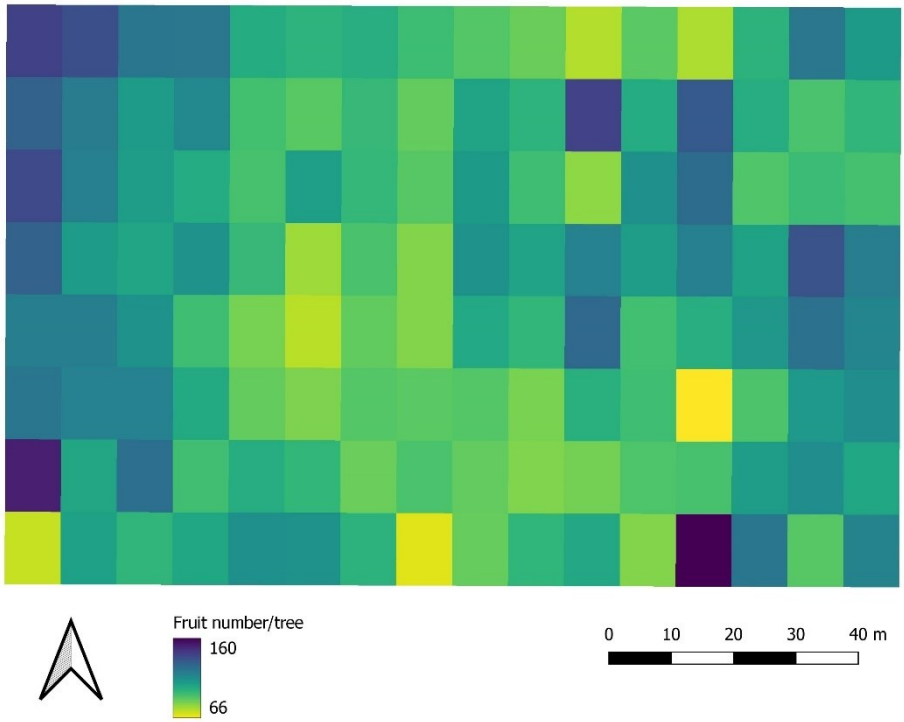

Figure 9. Map obtained from calibrated data points of fruit number per tree using an Inverse Distance Weighting (IDW) interpolation. Map colour-coded with the Viridis colour palette.

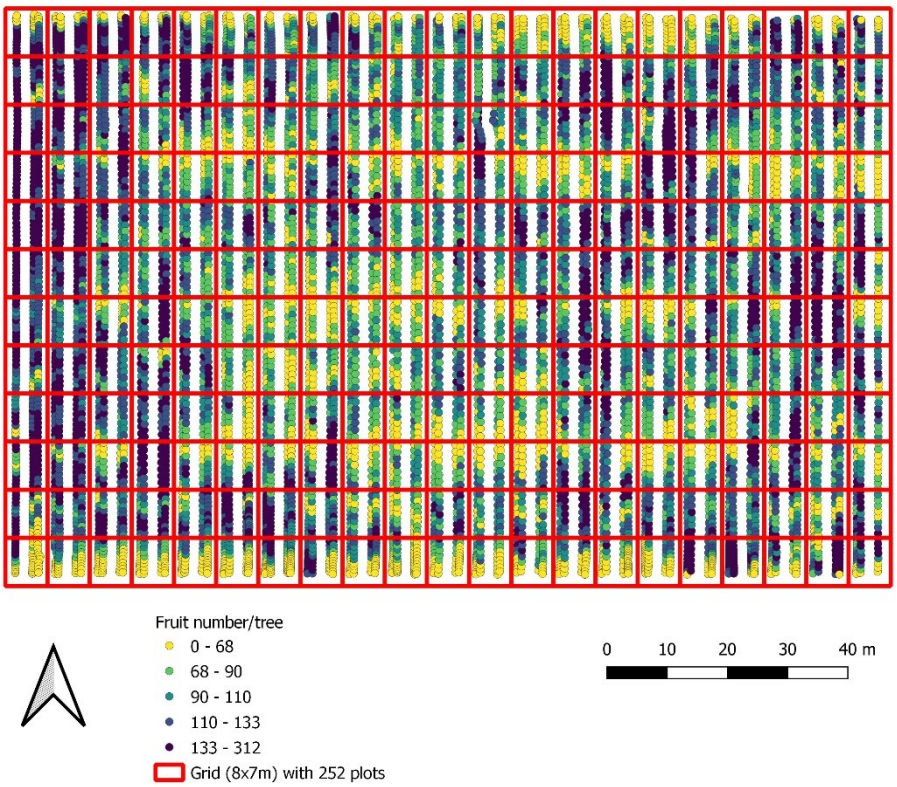

Figure 10. Example of a grid of 8 × 7 m pseudo-plots overlaid to calibrated fruit number data points.

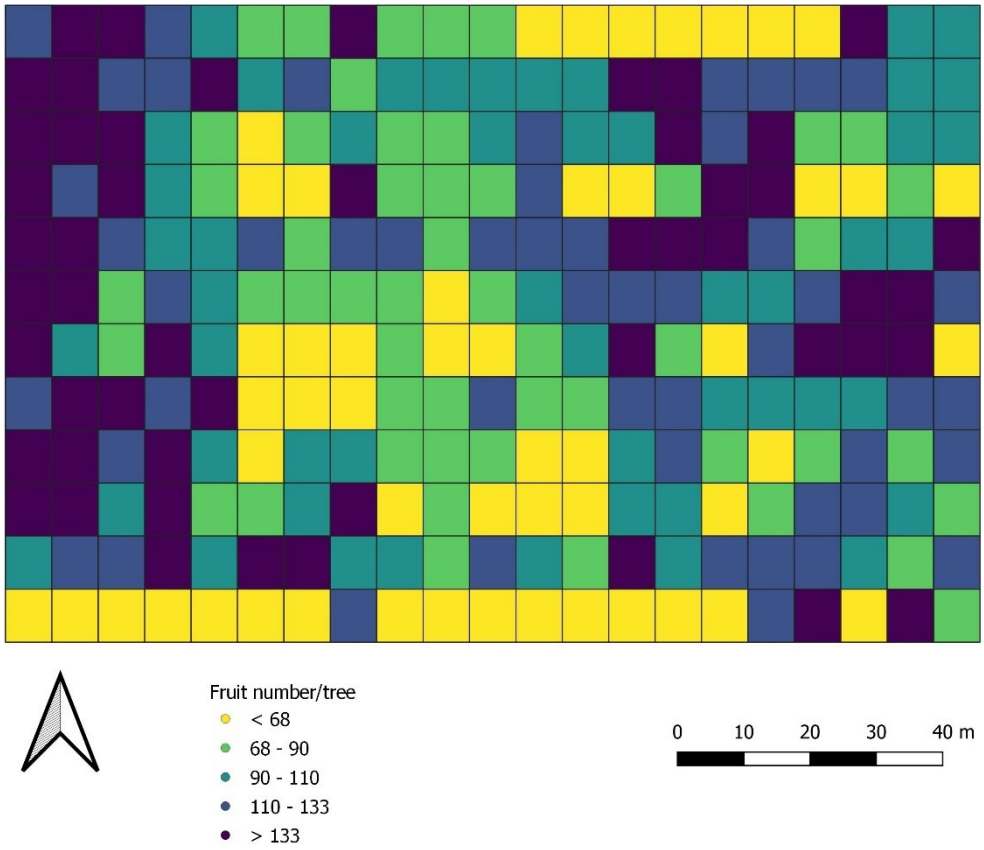

Figure 11. Map obtained from calibrated data points of fruit number per tree using a grid with pseudo-plots with means summarised. Map colour-coded with the Viridis colour palette.

BLOCK-SPECIFIC RELATIONSHIPS TO DEFINE FRUIT NUMBER AND FRUIT QUALITY TARGETS

Fruit number relationships between parameters predicted with Green Atlas Cartographer could be extracted from management units such as the pseudo-plots in Figure 13. However, our preference is to remove pseudo-plots at the edges of the block, as those shown in yellow in Figure 14, to avoid the confounding buffer effects from external factors (e.g., non-representative light environments, proximity to beehives, labour efficiency). Thus, we proceed with extracting means from the pseudo-plots shown in red in Figure 14. These pseudo-plot means are used for multiple regression analysis purposes to identify the ideal fruit number per tree (FN) to achieve target CDI and fruit diameter (FD).

In 2022, fruit numbers were lower than usual, as the year was an 'off' season in the biennial bearing cycle of the block. In addition, the relationships in 2022 were obtained from a scan > 20 days before harvest, and some peel colour and fruit diameter would have changed in this time interval. Nevertheless, the relationships of both CDI and FD with FN were significantly negative ($p < 0.001$, Pearson's r for CDI vs fruit number = −0.383; Pearson's r for FD vs fruit number = −0.432).

Pre-harvest data in 2021 were obtained closer to harvest time, and they included a good range of fruit numbers. Therefore, using the gridding approach shown in Figure 14, means of fruit number, CDI and FD were extracted for pseudo-plots (n = 190). Next, we built a multiple regression model where CDI and FD were the two dependent variables and FN was the independent variable. The model to estimate fruit number from CDI and FD was significant ($p < 0.001$; $R^2 = 0.452$) and is shown in equation 1.

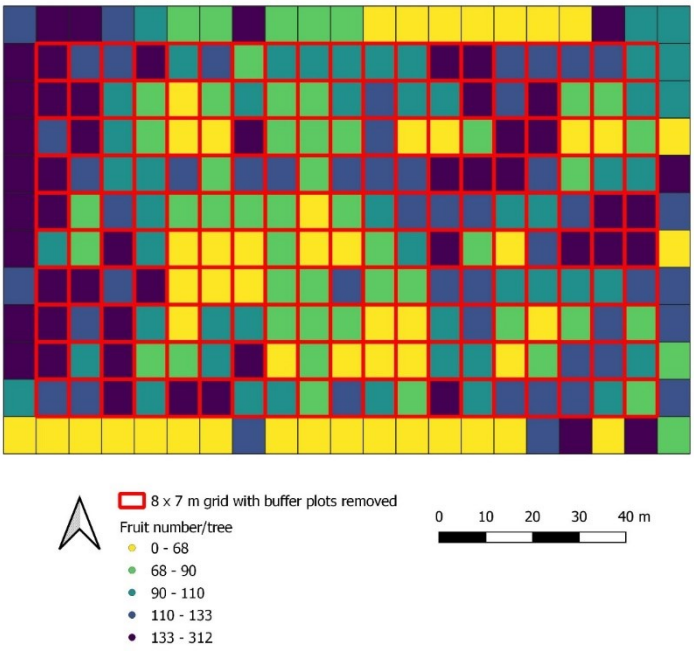

Figure 12. Pseudo-plots selected (in red) for extraction of data for multiple regression analysis.

$$FN = 1179 - (814.3 \times CDI) - (3.531 \times FD) \qquad \text{Equation 1}$$

Single linear regression fits of the FN vs FD and vs CDI relationships are shown in Figure 15 to visualise the negative trends of the associations.

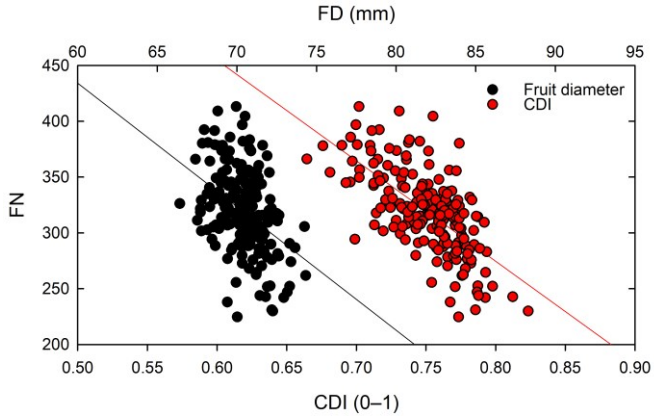

Figure 13. Linear regression fits for the relationships between fruit diameter and fruit number per tree (black circles) and colour development index (CDI) and fruit number per tree (red circles).

CONCLUSION

Combined fruit number, size, colour and yield predictions using ground-based, fast-scanning systems are an innovative approach to assess fruit quality and productivity in apples pre-harvest. The Green Atlas Cartographer platform is relatively easy to operate for unskilled staff and, through AI, can generate accurate results of fruit number, fruit size and colour, while concomitantly measuring tree size and geometry features. If linked to canopy geometry estimates, fruit quality and productivity predictions become a powerful tool that empowers growers to tailor precise strategies to each orchard block. Additional spatial zoning within blocks is recommended to establish management zones that can simplify orchard

operations. Multiple zoning approaches can be applied to data points and the efficiency of management should be measured in zones generated with the different methods described in this study for comparison purposes. Block-specific relationships can help identify the ideal fruit number based on important fruit quality parameters like peel colour and fruit size. This could be linked to the leaf area output obtained on-board to determine the optimal crop load that a tree can bear in a given season, without affecting fruit quality and return bloom. With the current push of Ag Tech into business models in the apple industry, and in other fruit industries, the availability of technology that serves multiple purposes is of pivotal importance as it may potentially reduce production costs such as labour.

RECOMMENDATIONS

Future research will focus on measuring the efficiency of orchard operations managed through data generated by the Cartographer against the current standard practices. Efficiency will be measured both in terms of accuracy of operations, and in terms of economic efficiency. Profitability will be the focus of PIPS 4 Profit activities in apples and pears.

ACKNOWLEDGEMENTS

This technical report is part of the apple and pear industry's PIPS3 (Productivity, Irrigation, Pests and Soils) program of research and development. The project is funded by Hort Innovation, using the Hort Innovation Apple and Pear research and development levy, contributions from the Australian Government and co-investment from Agriculture Victoria. Hort Innovation is the grower-owned, not-for-profit research and development corporation for Australian horticulture.